FOSSIL

DOE/MC/26044-3054
(DE92001136)

WEAR MECHANISM AND WEAR PREVENTION IN COAL-FUELED DIESEL ENGINES

Final Report

By
J. A. Schwalb
T. W. Ryan

October 1991

Work Performed Under Contract No. AC21-89MC26044

For
U.S. Department of Energy
Morgantown Energy Technology Center
Morgantown, West Virginia

By
Southwest Research Institute
San Antonio, Texas

DISCLAIMER

Printed in the United States of America, Office of Scientific and Technical Information, Oak Ridge , Tennessee

DOE/MC/26044--3054

DE92 001136

Wear Mechanism and Wear Prevention in Coal-Fueled Diesel Engines

Final Report

J.A.Schwalb
T.W.Ryan

Work Performed Under Contract No.: DE-AC21-89MC26044

For
U.S. Department of Energy
Office of Fossil Energy
Morgantown Energy Technology Center
P.O. Box 880
Morgantown, West Virginia 26507-0880

By
Southwest Research Institute
Engine, Fuel, and Vehicle Research Division
6220 Culebra Road
San Antonio, Texas 78228-0510

October 1991

EXECUTIVE SUMMARY

Piston ring/cylinder liner wear in coal/water slurry fueled engines involves soft abrasive polishing wear and a hard-abrasive three-body wear process. The hard abrasive process is of primary concern. The magnitude of wear rate is highly dependent on whether contaminant particles are in a critical size range where they are small enough to enter the wear zone, but large enough to contact both wearing surfaces. Because of this dependency, the size of particles relative to surface roughness and hydrodynamic film thickness are the critical parameters determining wear magnitude. There was little apparent advantage of putting various configurations of slots in the cylinder surface, but the wear process seemed to be highly sensitive to lubricant formulation. A mixture of baseline oil and a calcium sulfonate detergent additive resulted in the lowest wear when the lubricant was contaminated with a coal ash.

The conclusions stated above were reached through the completion of the multi-task program outlined in this report. The program involved bench scale wear tests and detailed analysis of wear specimens with the intent of defining the wear mechanism, and investigating traditional approaches to wear prevention. Included in the test matrices were variations of contaminant particle size, contaminant composition, cylinder specimen surface roughness, orientation of grooves in the surface finish, slot configurations cut into the cylinder surface, and lubricant formulations. Analyses were performed using weight loss and dimensional measurements to determine the wear magnitude, and photomicroscopic and profilometric analyses to study details of the wear scar profiles. Ferrographic techniques were also used to separate out and analyze wear particles.

In addition to the coal/water slurry work described above, this program also included a task devoted to Locomotive Engine Testing using a mixture of diesel fuel with a coal-derived liquid fuel. A 500 hour endurance test was completed, and wear evaluations were made based on measurements of engine components before and after the test. Engine performance and emissions were also evaluated before and after the endurance test to further test the effects of the coal-derived fuel. No significant increase in wear was observed, nor was there any significant change in engine performance. Somewhat more than normal varnish deposits were observed on the injection nozzles. Emissions were not affected by the coal-liquid fuel other than an increase in SO_2 emissions corresponding to the higher sulfur content in the coal-liquid fuel.

ACKNOWLEDGEMENTS

The U.S. Department of Energy, Morgantown Energy Technology Center is gratefully acknowledged for their sponsorship of this program. In particular Mr. William C. Smith of Morgantown Energy Technology Center is acknowledged for his assistance as the DOE Project Monitor. Thanks also go to Mr. Jack Dozier who conducted the Cameron-Plint tests, Mr Floyd Bradely who conducted the Engine Friction and Wear Rig tests, Mr. Michael Crane and Mr. Steve Fritz who helped in setting up the radioactive measurement techniques and in managing the Engine Friction and Wear Rig experiments. Mr. Ping Sui and Dr. Paul Lacey of SwRI and Dr. Ron Mayville of A.D. Little are gratefully acknowledged for their helpful advice and discussions on various aspects of the wear problem. The Cameron-Plint tests were conducted at the Belvoir Fuels and Lubricants Research Facility/SwRI with authorization from the U.S. Army Belvoir Research, Development and Engineering Center, Fuels and Lubricants Division (STRBE-VF).

TABLE OF CONTENTS

INTRODUCTION

Coal fueled diesel engines present unique wear problems in the piston ring/cylinder liner area because of their tendency to contaminate the lube-oil with high concentrations of highly abrasive particles. This program involved a series of bench-scale wear tests and engine tests designed to investigate various aspects of the ring/liner wear problem and to make specific recommendations to engine manufacturers as to how to alleviate these problems. The program was organized into tasks, designed to accomplish the following objectives.

- Task 1 - Define the predominant wear mechanisms causing accelerated wear in the ring/liner area.
- Task 3 - Investigate the effectiveness of traditional approaches to wear prevention to prevent wear in coal-fueled engines.
- Task 4 - Further refine information on the most promising approaches to wear prevention.
- Task 5 - Present detailed information and recommendations to engine manufacturers on the most promising approach to wear prevention.
- Task 6 - Present a final report covering the entire program
- Task 7 - Complete engine tests with a coal-derived liquid fuel, and investigate the effects of the fuel on engine wear and emissions.

Tasks 1 - 6 were the original plan, and primarily focussed on wear in coal/water slurry fueled engines. The original plan also included Task 2, an investigation of novel piston and ring designs, but that was dropped from the program in favor of more extensive investigation in the remaining tasks. Task 7 was added at a later date, as a parallel study of wear in an engine fueled by a mixture of diesel fuel, and a coal-derived liquid fuel.

This "final" report is intended to meet the requirements of Task 6 and to conclude the program. Subsequent sections of this report summarize the results of each of the tasks described above, and discuss the most important conclusions. For each task, a topical report was also written which contains a detailed accounting of the test conditions, apparatuses, results and conclusions reached. Those reports are included in appendices A - E.

RESULTS

Task 1 - Definition of the Wear Mechanism

Task 1 involved bench scale experiments with two different apparatuses, the Cameron-Plint High Frequency Friction Machine, and the Engine Friction and Wear Rig.

The Cameron-Plint Machine is a small scale apparatus that uses pieces of the ring and cylinder liner as wear specimens. The ring specimen is attached to a reciprocating arm, and a load is applied normal to the direction of travel. The two wear specimens are immersed in a bath containing a baseline lubricant that has been contaminated by various coal-related solids. For the tests in Task 1, the goal was to determine the wear mechanism and the relative roles that soft carbon and hard abrasive particles play. With that in mind, wear tests were conducted with several different contaminants ranging from pure carbon-black to coal ash. Concentrations tested varied from 5 to 15 percent contaminant (by weight) in the lube oil. Four-hour wear tests were completed during which averaged friction force and electrical resistances between the wearing specimens (a measure of the presence and thickness of a hydrodynamic film) were continuously recorded on a strip-chart recorder. Following each test, specimens were analyzed for weight-loss, and using a photomicroscope, and profilometer.

The Engine Friction and Wear Rig is a complete Labeco cylinder liner that is reciprocated against a stationary ring. Ring load is applied by constant gas pressure in the compression zone. Wear is determined continuously by the measurement of relative radioactivity of a previously irradiated piston ring. Tests were completed using the same coal ash contaminant used in the Cameron-Plint tests and at equivalent concentrations. The Engine Friction and Wear Rig is one step closer to the actual engine conditions, and was used to test the Cameron-Plint's ability to simulate real engine wear.

Conclusions from Task 1 are listed below.

- Primarily, two wear mechanisms were observed:
    - Soft abrasive "polishing" wear was caused by carbon particles. The wear tended to remove the original surface finish and leave a highly polished surface.
    - Hard abrasive wear was caused by hard (mostly quartz and alumina) particles found in the coal ash. The hard abrasive wear continued to increase as ash concentration in the lube-oil was increased.

- Wear scars consisted primarily of long straight grooves, and it appeared that the two wear scar patterns conformed to one another (the ring wear scar pattern was a mirror image of the cylinder pattern).

- The hard abrasive wear mechanism was primarily three-body abrasion. This was confirmed by photomicroscopic and profilometric analysis that indicated there was no evidence of embedded particles in either of the wear specimens. Later ferrographic analysis (presented in the Task 3 topical report) confirmed that the wear particles were consistent with three-body abrasive processes, and there was no evidence of the cutting-wear particles expected with a two-body process.

- Evidence was presented that there is a significant affect of contaminant particle size on wear with the smaller particle size distribution causing more wear than a larger size distribution.

- Wear trends observed in Engine Friction and Wear Rig tests were consistent with trends observed in the Cameron-Plint tests.

Task 3 - Traditional Approaches to Wear Prevention

Task 3 was a continuation of Cameron-Plint tests using one of the coal ash contaminants from Task 1. The tests in Task 3 were designed to investigate various approaches to wear prevention, and to determine how engine manufacturers should use each approach to help mitigate the wear process. The three items studied in Task 3 were as follows.

- Investigation of the Effects of Cylinder Surface Finish Conditions (including the effects of asperity height, and predominant orientation of the asperities)

- Investigation of Various Configurations of Slots in the Cylinder Surface

- Investigation of Various Types of Lube-Oil Additives Added to the Baseline Lubricant

Surface finish investigations involved Cameron-Plint tests with cylinder specimens honed with various surface roughnesses and cross-hatch angles. Surface finish has always played a role in diesel engine design because of its effect on the engine break-in process, and the need for sufficient oil retention on cylinder surfaces. It was felt that, in coal/water slurry fueled engines, cylinder surface features might also play a role in enhancing hydrodynamic film thickness and/or allowing avenues of escape for abrasive contaminant particles. Roughnesses in the range from 0.15 to 2.1 Ra micrometers (Ra is an arithmetic average of the height of surface asperities) and cross-hatch angles from 0 to 90 degrees were evaluated in terms of the resulting wear magnitude, any changes they might have made in

the wear mechanism, and their effects on the hydrodynamic film thickness (film thickness is evaluated using the electrical resistance strip-chart data).

Investigations of slot configurations were carried out using cylinder specimens in which slots of various widths, spacings, and orientations were cut. The idea of slots in the cylinder surface was to provide some means for contaminant particles trapped in the wear zone to escape, and/or to enhance the flow of clean oil from the bottom side of the ring to dilute the high concentrations of contaminant on the combustion side of the ring. The slot widths and spacings ranged from 0.15 to 0.35 mm wide, and the test matrix was designed so that tests were conducted with different widths at equivalent spacings, and vice versa. Each width/spacing combination in the test matrix was done in a circumferential orientation (normal to the direction of ring travel) and a longitudinal orientation (parallel to the direction of ring travel). Once again the tests were designed to investigate the effects of slots on wear magnitude, wear mechanism, and hydrodynamic film thickness.

Lube-oil additive investigations were conducted by choosing representative additives from some of the general classes, adding them to the baseline lube-oil in their maximum recommended concentrations, and conducting wear evaluations in the Cameron-Plint machine. The hope was to find some additive that was effective in coating the wearing surfaces, excluding contaminant particles from the wear zone, and/or coating the contaminant particles to make them less abrasive. A detergent, a dispersant, zinc aryl and zinc alkyl dithiophosphate additives, a VI improver, and a thickener were chosen, and each was mixed with the baseline oil (no combinations of additives were used in this program). The tests evaluated wear magnitude, the appearance of the worn specimens and the presence of any chemical or hydrodynamically generated films.

Conclusions from the Task 3 investigations can be summarized as follows.

- Wear increased slightly with increased surface roughness, but cross-hatch angle did not have any discernible effect on wear magnitude.
- Hydrodynamic film thickness increased with surface roughness.
- Hydrodynamic film thickness was also enhanced by orienting the surface finish grooves normal to the direction of ring travel (0 degree cross-hatch angle).
- All the slotted specimen configurations resulted in at least as much, if not more wear than an unslotted specimen.
- In many cases, there was evidence the presence of slots enhanced the hydrodynamic film thickness. Slots oriented normal to the ring travel direction were most effective at enhancing hydrodynamic film thickness.

- The use of a constant concentration bath in which wear specimens are immersed does not allow for a fair evaluation of the effectiveness of slots in diluting and channeling contaminant particles away from the wear zone.

- In surface finish and slotted specimen tests, there was not a clear indication of the effect of hydrodynamic film thickness on wear.

- A calcium sulfonate detergent additive was effective in reducing wear almost to the level achieved with an uncontaminated lube-oil test.

- There was evidence that the detergent additive created a chemical or hydrodynamic film that was much thicker than films created with any of the other configurations tested in this program.

- An ashless dispersant increased wear substantially above the level achieved with no additive in the lube-oil.

- Wear seemed to be much more sensitive to lubricant additive formulation than to surface finish or slot configurations.

Task 4 - Refinement of the Most Promising Approach to Wear Prevention

The results of Tasks 1 and 3 left some unanswered questions, which were investigated in Task 4. The major issues dealt with in Task 4 were as follows.

- All of the Cameron-Plint wear tests evaluated in previous Tasks were for test durations of four hours. Questions remained as to whether the entire wear process proceeded at a constant rate over those four hours, or whether there were accelerated wear periods.

- The Cameron-Plint tests in previous tasks were completed using a 100 MPa contact pressure between the wearing specimens. While this loading is low relative to loads typically used in the pin-on-disk or four-ball wear tests, it is still an order of magnitude higher than the typical load at Top Dead Center in the engine. Questions remained as to whether the same wear modes applied at the higher load conditions.

- The conclusions in Task 3 above indicated that the use of a constant concentration bath lubricant supply was not a fair means of evaluating the effectiveness of slotted specimens. Dripped oil supplies that supply clean oil to one side of the ring and contaminated oil to the other would be a more accurate simulation of the actual engine situation.

In response to these issues, three test matrices were formulated involving continued Cameron-Plint testing with various test durations, under lower load conditions than were used in previous tests, and using the double dripped oil supply configuration described above. Once again wear evaluations were made based on weight loss, photomicroscopic observations, and profilometric measurements. Micrometer measurements of the depth of the ring specimen wear scar were also added in an attempt to obtain a more accurate measurement at the lower wear conditions expected.

Also, after completing the low-load wear test matrix, it became apparent that a simple wear calculation might be a useful tool in explaining the trends observed. The model was developed, based on the supposition that abrasive wear is proportional to the concentration of particles that are in the right size range to enter the wear zone. Various coefficients were adjusted to fit the calculation to the data obtained. Calculations were then extrapolated to predict the effects of surface finishes, hydrodynamic film thicknesses, and contaminant particle sizes not specifically tested in the program.

The conclusions from Task 4 work can be summarized as follows:

- There appears to be a short region of accelerated wear at the beginning of the Cameron-Plint tests (within the first 15 minutes) which is associated with a "break-in" period. The "break-in" wear, however, is much smaller in magnitude than the total wear for two or four hour duration tests.

- There is a significant effect of load on the wear magnitude and on the trends observed in Task 3. In particular, it was found that wear is much more sensitive to surface finish at the lower load conditions than it was at the higher load conditions used in Task 3.

- The wear model, which assumed the abrasive wear was proportional to the number of contaminant particles that could enter the wear zone, was successful in fitting the Cameron-Plint data obtained at low-load conditions.

- Based on the wear model assumptions, the parameters determining abrasive wear characteristics are the mean contaminant particle size relative to the size of surface finish asperities, and the hydrodynamic film thickness (these interactions are discussed in detail in the Task 4 and Task 5 topical reports).

- Profilometer traces indicated that the cylinder specimens with longitudinal slots were effective in promoting mixing of clean and contaminated oil supplies separated by the ring. There was not, however, any significant wear reduction with the longitudinal slots.

- Data with the slotted specimens indicates that longitudinal slots with relatively wide spacing and relatively narrow width (although the slot width should still

be much larger than the contaminant particle size) resulted in the lowest wear.

Task 5 - Presentation of the Most Promising Approach to Wear Prevention

Task 5 involved a discussion and representation of the Task 1 - 4 conclusions in a format that could be easily used by engine manufacturers looking for specific recommendations on wear reduction strategies. The Task 5 topical report discusses contaminant particle size, cylinder surface finish, and hydrodynamic film thickness as separate issues, and makes specific recommendations on the ideal values of each of these parameters, and the tradeoffs that result if those ideal values cannot be attained. The report also discusses the effects of lube-oil additives and cylinder surface slots, although specific recommendations could not be made in these areas because of the inconclusive results.

Conclusions presented in the Task 5 report can be summarized as follows.

- Cylinder surface finish should be held as smooth as possible, and everything possible should be done to promote a tight clearance between the ring and cylinder liner. It is especially critical that the liner asperities be at least an order of magnitude smaller than the contaminant particles.

- If contaminant particle size can be controlled, it would be best to maintain it at a moderate size (at least 3 micrometers). As indicated above, this allows for a surface finish much smaller than the particle size using conventional honing techniques. The model predicts that wear will continue to decrease as particle size increases, however, common sense dictates that there must be a limit at which large particles would begin to cause problems somewhere else in the system.

- The model also predicts that wear can be reduced if the contaminant consists of extremely small particles (much smaller than the hydrodynamic film thickness). This suggests an alternate strategy of attempting to reduce particle size while at the same time increasing hydrodynamic film thickness. In either the case, the idea is to avoid a situation where the film thickness + surface roughness is approximately the same as the mean contaminant particle size.

- If hydrodynamic film thickness can be controlled, it is not obvious how it will affect the wear. In a situation where most of the contaminant particles are much larger than the film thickness + surface finish, a thicker film could allow more abrasive particles into the wear zone. On the other hand, a real engine depends on having some hydrodynamic lubrication at the mid-stroke of the ring.

- Despite Cameron-Plint data indicating there is little advantage to using slots in the cylinder surface, it is still felt that slots in a real engine might play a constructive role in diluting and channeling contaminants away from the wear zone. If slots are to be used, they should be oriented longitudinally, at a relatively wide spacing (at least 0.5 mm) and using a slot width of 0.15 mm.

- Data presented in this program indicates the wear process can be extremely sensitive to lube-oil additive formulation. Because of unknown additive interactions, it cannot be predicted what would happen if similar additives are added to a fully formulated oil, but it seems that the magnitude of wear reductions experienced here warrant some further experimentation. It should be possible to tailor the oil formulation to the coal/water slurry fueled engine application.

Task 7 - Extended Wear Testing

As discussed earlier, Task 7 was a parallel program added after the initial program was started. The intent of Task 7 was to test a mixture of diesel fuel and a coal-derived liquid fuel in a locomotive engine. The test followed standard procedures including engine part measurements and load curve determinations before and after a 500 hour endurance test. In addition, emissions measurements were also recorded both on pure diesel fuel and on the diesel/coal fuel mixture before and after the endurance test. Conclusions following the completion of locomotive engine testing can be summarized as follows.

- The coal-derived liquid fuel did not cause any catastrophic increase in engine wear.

- There was more than the usual amount of varnish deposits on the fuel injectors following the endurance test. These deposit levels should be closely monitored in any future engine tests with the coal-derived fuel.

- Emissions measurements were not significantly affected by the coal-liquid fuel with the exception of a higher SO2 level. The higher SO2 corresponds directly with the higher sulfur content in the coal-liquid fuel.

CONCLUSIONS

The most important results from the tasks discussed above can be summarized as follows.

- The mechanism causing accelerated piston ring and cylinder liner wear in coal/water slurry fueled engines is a three-body process involving both soft abrasive "polishing" wear, and a hard abrasive scratching and gouging type wear. The hard abrasive process is of primary concern.

- Surface finish was found to have a significant affect on wear, especially under low load conditions typically seen in the diesel engine combustion chamber. It is always to the advantage to have as smooth a surface finish as possible.

- The abrasive wear process is primarily governed by the size of contaminant particles relative to the clearance between the wearing surfaces. If particles are substantially larger than the clearance, they will not be able to enter the wear zone and will not accelerate wear. On the other hand, if particles are sufficiently smaller than the hydrodynamic film thickness, they will not be able to participate in the three-body mechanism either. If possible, parameters should be adjusted so that the particles are either much larger, or much smaller than the critical size range.

- Tests with various slot configurations in the cylinder surface did not determine any clear advantages to having slots. However, if attempts are made to test slotted cylinders in the future, the longitudinally oriented, 0.15 mm wide, 0.25 mm spaced slots seemed to have the best chance at succeeding.

- The abrasive wear process was extremely sensitive to additive formulation. A fundamental explanation for this behavior is difficult to attain, but it does seem apparent that future experimentation aimed at tailoring the lube-oil formulation to coal/water slurry fueled engines might lead to significant wear reductions.

- The coal-derived liquid fuel tested in this program did not cause any obvious detrimental effects on engine wear or engine performance.

RECOMMENDATIONS

The multi-tasked program described here was successful in defining some aspects of the wear mechanism in the piston rings and cylinder liners of coal/water slurry fueled engines. A large number of parameters were investigated in bench-scale wear experiments, and from the results some specific recommendations to coal/water slurry engine manufacturers were made. It has become apparent, however, that there are still numerous issues to be addressed before a full explanation of coal/water slurry fueled-engine wear can be made. Foremost among the issues still outstanding are the following.

- How should the Task 4 wear model, which was developed for a constant contaminant concentration and constant applied load, be applied to the real engine situation where concentration and load are continuously varying?

- What is the effect of contaminant on the adhesive and/or abrasive wear mechanism at high load conditions?

- What is the fundamental explanation for the reduction in wear observed when a calcium sulfonate detergent was added to the lube-oil?

- How do the temperature variations present in the engine affect the wear process?

The most direct approach to dealing with these issues would involve using the same ring and cylinder materials and the same lube-oil formulation used in the present coal/water slurry fueled engines. Wear tests would then be completed in an apparatus as close to an actual engine configuration as possible. A few data points under these relatively expensive, but accurate wear test conditions could be used to refine the wear model presented above and to extend its application to varying concentration, load and temperature conditions. It is doubtful that the model would ever be accurate enough to predict wear in a un-tried engine design. If properly developed, however, the model could be a useful tool to an engine manufacturer who wants to predict the effects of varying slurry properties, varying lubricant properties, and varying cylinder surface conditions based on only a small amount of wear data.

APPENDIX A

Task I - Definition of the Wear Mechanism

TOPICAL REPORT

WEAR MECHANISM AND WEAR PREVENTION IN COAL-FUELED DIESEL ENGINES

TASK I: DEFINITION OF THE WEAR MECHANISM

U.S. DOE Contract DE-AC21-88MC26044
SwRI Project No. 02-2681

Submitted to
U.S. Department of Energy
Morgantown Energy Technology Center
P.O. Box 880
Morgantown, WV 26507-0880

Submitted by
Southwest Research Institute
6220 Culebra Road
San Antonio, Texas 78228-0510

March 1, 1990

TABLE OF CONTENTS

LIST OF TABLES

LIST OF FIGURES

LIST OF FIGURES (Continued)

I. Introduction

Considerable interest has arisen recently in the development of coal-fired diesel engines which could efficiently utilize the large coal reserves of the United States and reduce dependence on foreign oil. The idea is not new, but development of such engines has proved elusive for several reasons. One of the major obstacles is the inevitable contamination of the lube oil by unburned coal particles, ash, and combustion products. The contaminated oil is then responsible for extremely large increases in the wear rates of cylinder liners and rings. Tests in experimental engines reported by Kamo and Valdmanis (1988), Clingenpeel, et al. (1984), Prater and Courtright (1985), Nydick, et al. (1987), Hsu (1988), Leonard, et al. (1989), Rao, et al. (1988), Kahwani and Kamo (1988) and Pratt (1982) indicate an increase in wear of up to 150 times when fired with coal/water slurry instead of diesel fuel. This trend is consistent with the experience of Southwest Research Institute on previous coal/water slurry studies.(Urban, et al., 1988; Likos and Ryan, 1988; Mecredy and Jett, 1987) In addition, some tribological studies have been carried out by Odi-Owei and Roylance (1986) using the four ball machine and by Mehan (1988) and Fusaro and Schrubens (1987) using the pin on disk tribometer. These tests confirm that even a small amount of contaminant can have a significant effect on the wear characteristics of sliding surfaces.

What can be done to reduce the wear rate to an acceptable level? That question is difficult to answer because of the general lack of understanding of the wear mechanism and how contaminants in the lube oil participate in it. So far, the approach by many researchers (Kamo and Valdmanis, 1988; Prater and Courtright, 1985; Mehan, 1988; Flynn, et al., 1989) has been to develop various metallic and ceramic coatings which would provide the hardest ring and cylinder surfaces possible. The presumption was that most of the wear was caused by ash from the coal getting into the lube oil, and the only way to stop it would be to develop a ring and cylinder surface that is harder than the ash itself. The harder rings and cylinders did in fact reduce wear, but so far have not proved economical because of the cost of materials and application processes. It is also noted in the literature that surface finish has a significant effect on wear rate. Richez, et al. (1983) and Janczak and Wisniewski (1987) observed a slight increase in hydrodynamic film thickness with surface roughness when an uncontaminated lubricant was used. The effect of adding contaminant, however, probably depends on the relative size of the contaminant and the asperities. Under conditions where the asperity size was much smaller than particle size (approximately 0.13 micrometer size asperities were used where the particle size was 2 micrometer), Mehan (1988) reports an increase in wear with surface roughness. When the asperity size is larger than the particle size, however, the trends

may be reversed. It is possible that the large asperities provide avenues of escape for particles which would otherwise be trapped between the sliding surfaces. If this is true, it may be possible to engineer the size, spacing and shape of asperities to enhance this effect.

The properties of the contaminated lube oil have also been studied in the literature. The typical average particle size seems to be approximately 3 micrometers with the majority being unburned coal or char in agglomerates with metallic wear particles (Gaydos, 1989). During combustion, some fragmentation of the ash particles takes place and they tend to fuse into a spherical shape. Although there is little change in the size distribution, Flynn, et al. (1989), Gaydos (1989), and Dunn-Rankin and Kerstein (1988) report that only the smaller ash particles tend to be trapped in the lube oil, resulting in an average ash size of approximately one micrometer. How these properties affect wear is somewhat uncertain. In general, the literature indicates that wear increases with particle size, particle hardness, and concentration of particles in the lube oil, however, the effects are somewhat complex. The particle size seems to cause increased wear as it gets larger, and is especially critical when it is approximately the same as the thickness of the hydrodynamic film (Mehan, 1988) (although studies by Perrotto, et al. (1979) on bearings indicate that significant wear still occurs when the particles are smaller than the film thickness). While this was true in standard tribological tests, Nydick, et al. (1979) indicate that in an engine a minimum wear rate was found when particles in the 6 - 10 micrometer range were used. These wear characteristics are most likely dependent on the ratio of particle size to hydrodynamic film thickness, but confirming that correlation has been difficult because of the difficulties in measuring film thickness in an operating engine. Particle hardness was expected to play a role in determining wear rate and, in fact, slightly higher wear rates were observed when higher ash concentrations were used. The effect, however, was not as large or as predictable as one might expect. Clingenpeel, et al. (1984) report that under some conditions, even clean (ash-free) char caused significant increases in wear rate. Finally, increasing particle concentration in the lube oil was expected to increase wear rate, and the literature seems to bear this out. There is, however, a tendency for wear to level off at a certain saturating concentration (Mehan, 1988).

The above paragraphs indicate that a significant amount of work has been done on this problem. Much has been learned about hardened coatings, and a general understanding of the effects of contaminated lubricant has been obtained, but there are still complex interactions occurring in the engine tests that are not accurately accounted for in the standard pin on disk or four ball tribological tests. A detailed understanding of the wear mechanism would go a long way towards explaining these complex effects. If, for example, the presence of contaminant in the lubricant causes significant changes in its rheological properties (studies by Sekar, et al. (1988) and Ryan et

al. (1989) of the rheological properties of slurries indicate they have a highly complex, non-Newtonian behavior which can be either shear thickening, or shear thinning at high shear rates) it would affect the formation of a hydrodynamic film. Breakdown of the film might be characterized by adhesive wear in the engine, especially at TDC, and would not be highly dependent on the hardness of the particles. Such a situation might be remedied by introducing chemically reactive lube oil additives which aid lubrication under mixed boundary, or boundary lubrication conditions (Kanakia and Lestz, 1989). If, on the other hand, the wear mechanism is an abrasive two-body or three-body process, the wear characteristics would be different, and particle hardness and size would play a more important role (their effect on wear rate is approximately the same for two-body and three-body mechanisms)(Misra and Finnie, 1981). Such wear is usually characterized by straight clean furrows as opposed to the rough torn surfaces and plastic deformation seen in adhesive wear (Nydick, et al., 1979). Two body abrasion tends to remove material by scratching or cutting leaving sharp clean edges, whereas three-body abrasion involves some plastic deformation and smoothing of the edges (Misra and Finnie, 1981). In either case it is also possible that the metal is being work-hardened, making it more susceptible to cutting processes (Gahr, 1988; Torrance and d'Art, 1986; Buckley, 1981). Abrasive wear of either of these types might be dealt with by the use of lube oil additives (dispersants, lube enhancers, viscosity enhancers, etc.) which coat the particles and change their surface characteristics and flow properties. If these changes inhibit the ability of particles to enter the wear zone, or allow them to slide through the wear zone with less abrasive interaction, then they would be beneficial in reducing wear. Engineering the asperity size, spacing and shape may also be effective in reducing this type of wear, especially if it is a three body mechanism. Finally, specifications on the fuel ash content, ash particle size, and overall particle size should be effective in dealing with abrasive type wear also.

The above paragraphs have established the need for a detailed understanding of the wear mechanism. Mayville (1989) attempted to address that need by conducting wear experiments with coal product contaminated lubricants in a reciprocating wear device. His results indicated a linear increase in wear with contaminant concentration and hardness of the contaminant. The approach of this study was similar to that of Mayville. Wear was simulated in a laboratory apparatus called the Cameron-Plint high -frequency friction machine. It was intended to be as close to actual engine conditions as possible, but still allowed for detailed control of the lubricant, its contaminants, and the load conditions. In this way, the attempt was made to bridge the gap between the tribological studies and the actual engine tests. The basic outline of the project was to conduct these wear tests on sample specimen made of typical ring and cylinder materials, and then analyze each piece for

its wear characteristics. The lubricant would be contaminated with various concentrations of unburned coal, pure carbon (carbon black), and pure ash so that an understanding could be obtained of the effects of concentration and composition of the contaminant.

In parallel with the Cameron-Plint tests, a second set of tests was also conducted in an apparatus called the Engione Friction and Wear Rig. This apparatus included actual rings on a piston inside a reciprocating cylinder. It is one step closer to the actual engine, and was intended to provide confirmation of the Cameron-Plint machine's ability to recreate actual ring/cylinder liner wear.

II. Experimental Apparatus and Procedures

A. Cameron-Plint Tests

The apparatus chosen for these tests is the commercially available Cameron-Plint high frequency friction machine; a schematic of which is shown in Figure 1. (Detailed descriptions of the machine are included in the paper by Cameron and Pumphrey (1983).) The machine provides reciprocating motion through a scotch yoke drive mechanism which simulates the relative motion of the piston ring and cylinder in a diesel engine. The ring specimen is mounted to the bottom of the reciprocating arm where it can rub against a rigidly mounted cylinder specimen beneath it. The entire cylinder piece is immersed in a temperature controlled bath of the lubricant/contaminant combination which is being tested. Above the reciprocating arm is a spring tensioned bar which applies a force normal to the direction of arm travel. Also, the reciprocating arm is instrumented to measure friction force (force in the direction of ring travel) and electrical resistance between the ring and cylinder specimen. Typically the electrical resistance is used as a measure of hydrodynamic film thickness, but it must be viewed with some caution in this case because of the electrically conductive properties of the contaminants in the lube oil. The friction force and resistance signals could be read continuously on a real time basis, however, in this case, the circuitry was arranged so that a time averaged signal was transmitted to the strip chart recorder. In this way, one can observe the overall changes in wear characteristics without having to sort out the variations within a single cycle. Details of how the Cameron-Plint machine was configured for the majority of these tests are contained in Table 1.

The test specimens were chosen to represent typical materials used in diesel engines. Cylinder pieces were cut from the 96.5 mm I.D. cylinder liners of a Labeco CLR engine. The

EXPERIMENTAL APPARATUS

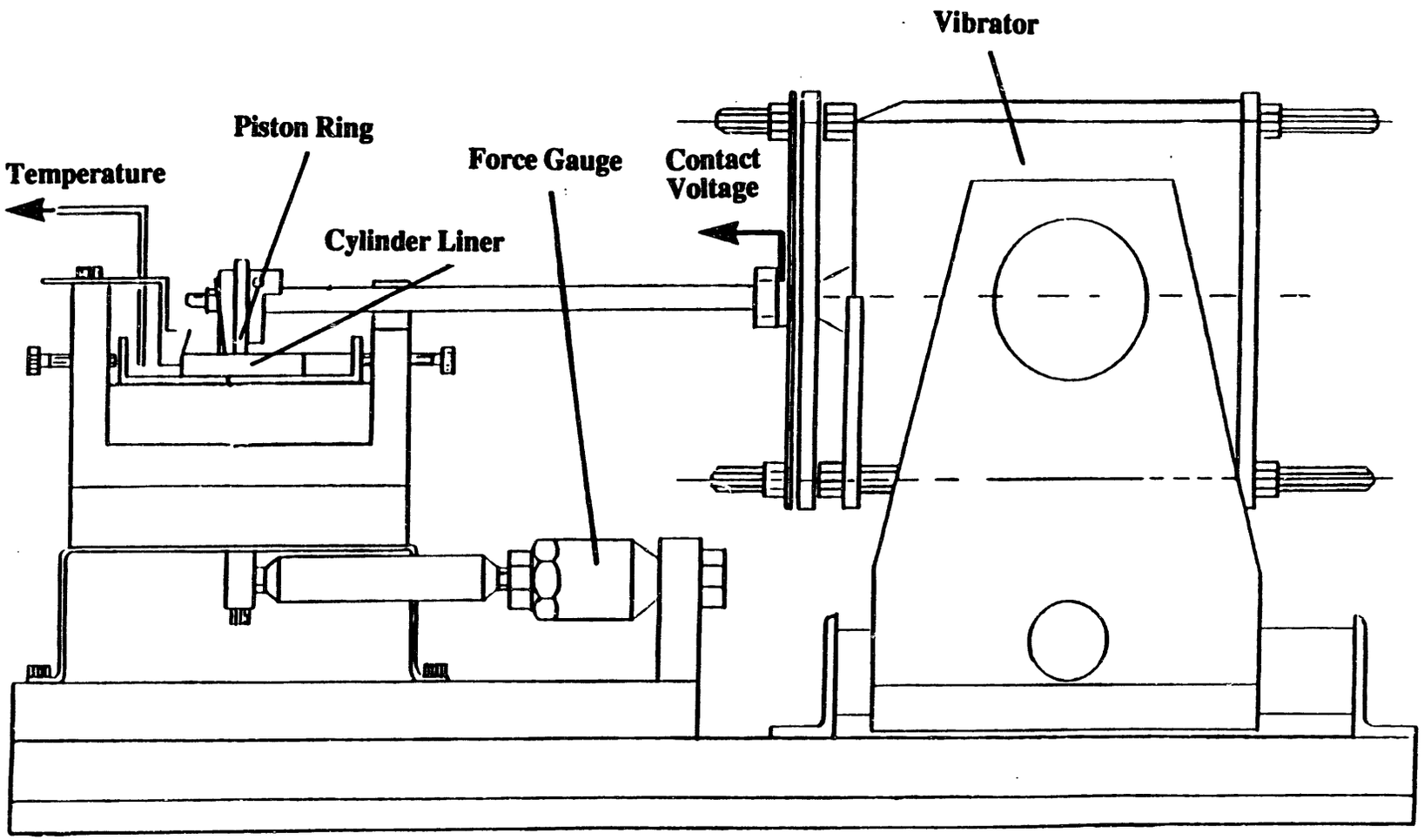

Figure 1. Schematic of the Cameron-Plint Rig

Labeco CLR is a research engine designed for lubricant testing with alloy components representative of those typically used in diesel engines. In this case, a cast iron material was used for the liner. The pieces were machined to dimensions of 55 mm x 25 mm, flattened on the back so that they vary from 3 - 4 mm thick and weighing approximately 37 grams. Ring pieces were cut from 89 mm D x 2 mm thick cast iron rings, and were ground into wedge shaped specimen 1 mm at the face expanding to 3 mm wide at the base and weighing approximately 0.3 grams. The hardness of each piece is listed in Table 2, indicating the ring piece is slightly harder. The wearing surface is 1 mm x 2 mm, which means there is 100 MPa contact pressure between the two pieces if a 200 N force is applied. The contact pressure was at least an order of magnitude higher than the actual force in an engine, but this is commonly accepted practice for accelerated wear tests and is a necessary compromise in order to get measurable wear in a reasonable time period.

Table 1. Cameron-Plint Configuration

Normal Load	200 N
Frequency of Stroke	17 Hz (1020 RPM)
Ring Piece:	
Source	89 mm O.D. cast iron ring
Size	Wedge-shaped piece approximately 3 mm base x 1 mm top x 5 mm wide x 2 mm thick
Approx. Weight	0.3 g
Wear Surf. Area	2 mm^2
Loading	100 MPa
Cylinder Liner Piece:	
Source	96.5 mm I.D. cylinder liner for Labeco CLR engine
Size	55 mm x 25 mm x 3-5 mm thick (thickness varies because of the curvature of the liner).
Approximate Weight	27 g

Table 2. Hardness of Test Specimens	
	Rc
Cylinder Liner Piece	21.3
Ring Piece	22.8
Note: These are the average of three hardness tests at different locations on the specimens. Hardness of the ring piece was measured on the side of the ring, not on its outer surface.	

As described above, the purpose of this study was to investigate the effects of the various contaminants which can get into the lube oil of a coal-fired diesel engine. This was done in an attempt to understand the basic wear-causing mechanism. With that in mind, a test matrix was formulated which involved Cameron-Plint wear tests of four hour duration. The tests were done using a baseline "bright-stock" oil (chosen because it does not contain any additives which may complicate the wear process) into which the following contaminants were added in 5, 10, and 15 percent concentrations.

- Carbon Black
- A Low-Ash Raw Coal
- A High-Ash Raw Coal (Kentucky Splint)
- Kentucky Splint Coal After Most of its Ash Was Removed in a Chemical Cleaning Process
- The Ash Removed From the Kentucky Splint Coal

Details on the baseline oil properties are included in Table 3. The 5 through 15 percent loadings were chosen to represent typical concentrations in the cylinder/ring environment. This is consistent with Mayville (1989) who measured less than 20 percent concentrations just below the ring pack in an operating coal fired diesel. Most of the test conditions listed above were performed a total of five times to obtain a statistically significant sample and to study the repeatability of the process. The remaining test conditions were performed at least twice to verify that a consistent measurement was obtained.

Besides the basic test matrix outlined above, a few extra tests were also performed to study specific questions that were raised during testing. Those extra tests included the following conditions.

- The 15% Kentucky Splint ash condition was repeated at a reduced load of 50 N.
- Two tests were done with a Syloid 63 Silica in 15% concentration. The ring load for those tests was 200 N and 50 N, respectively.
- A set of tests was done using the Kentucky Splint ash ground to a smaller particle size. The test were done using the Table 1 configuration with 5 and 10% concentrations of ash.

Table 3. Properties of Baseline Oil

40°C Viscosity	143.88 cSt
100°C Viscosity	13.99 cSt
V.I.	93
API Gravity	28.6 @ 15.6°C
T.A.N.	0.01
T.B.N.	0.09
Flash Point	293°C
%N	0.012
%Ca	N.D.
%Zn	N.D.
%P	<0.01
%S	0.21

Proximate analyses of the contaminants are contained in Table 4, and particle size analyses are in Table 5. The analyses confirm that the contaminants cover a fairly wide range of ash concentrations. Results of these tests should give a good idea of the relative effects of ash and carbon content in the contaminated oil. Table 5 reveals that the contaminants had reasonably close average particle sizes, indicating that subsequent comparisons of wear rate can be made without considering the complicating effects of particle size. The one exception to this observation is the ash which was slightly larger than the other contaminants, and was then ground to a similar size. The original tests were done with the larger size and most of the comparisons made here are based on that data. There was significant concern, however, about the validity of those comparisons in light of the fact that particle size can have a significant effect on wear. Because of this, some extra tests were run with the smaller size ash to study that particle size

effect. Also listed in Table 5 is a Syloid 63 silica whose particle size is somewhat comparable to the other contaminants. It was used in two extra tests, which were intended to study the effect of ring loading, and to investigate the nature of wear caused by silica vs. wear caused by ash in the coal.

Table 4. Proximate Analysis of Contaminants

Description	Feed Stock	Ash	Vol. Matter	Fixed Carbon
Low-Ash Coal	Unknown	1.00%	34.51%	64.14%
Carbon Black	Mogul-L	0	0	100%
High-Ash Coal	Kentucky Splint	22.9%	30.5%	46.6%
Cleaned Coal	Kentucky Splint	0.38%	37.73%	61.88%
Ash Product	Kentucky Splint	85.3%	10.6%	4.1%

Table 5. Particle Size Averages

	Number Weighted Averages		Volume Weighted Averages	
Contaminant	Arith. Mean	Log Mean	Arith. Mean	Log Mean
Low-Ash Coal	4.8	4.1	13.8	11.5
Carbon Black	3.9	3.1	9.9	9.0
Raw Kentucky Splint Coal	4.1	3.1	15.1	13.2
Cleaned Kentucky Splint Coal	5.5	4.1	18.9	16.7
Ash From Kentucky Splint Coal	13.7	12.5	33.4	27.2
Ash From Kentucky Splint Coal Ground in Fluid Energy Mill	2.8	1.9	9.2	8.3
Syloid 63 Silica	2.4	1.6	10.6	0.6

Further analysis of the contaminants and the ash from the contaminants is presented in Tables 6 and 7. Table 6 lists the Carbon/Hydrogen/Nitrogen analysis results, and indicates a range of carbon contents from 7.41 to 91.99 wt%. (The apparently low carbon content of Carbon Black (91.99%) is partly due to absorbed water. The possiblity of other contaminants is being investigated.) The ash compositions listed in Table 7 were the result of X-ray flouresence

Table 6. C-H-N Analysis

	(Weight %)		
	Carbon	**Hydrogen**	**Nitrogen**
Carbon Black	91.99	0.43	<1
Cleaned K.S. Coal	80.17	5.34	1.57
Low-Ash Coal	82.59	5.32	1.43
Raw K.S. Coal	62.78	4.43	1.19
Ash From K.S. Coal	7.41	1.07	<1

Table 7. Analysis of Contaminant Ash

		(Weight Percent of Ash)			
	Cleaned K.S. Coal	**Low-Ash Coal**	**Raw K.S. Coal**	**Ash From K.S. Coal**	**Syloid 63 Silica**
SiO_2	39.41	41.73	60.85	65.30	98.58
Al_2O_3	14.55	29.20	23.78	22.09	1.18
Fe_2O_3	25.39	14.77	5.34	3.55	0.18
CaO	5.15	8.66	2.06	1.57	0
MgO	1.72	0.92	1.42	1.88	0
NA_2O	0.13	0.07	0	0	0
K_2O	0.78	1.94	4.20	4.78	0.06
Ti_2O	6.17	1.03	0.70	0.82	0
Cr_2O_3	0.37	0.04	0.61	0	0
NiO	3.82	0.19	0.94	0	0
CuO_2	0.72	0.27	0.10	0	0
SO_3	1.77	1.19	0	0	0

analyses (the most stable oxides were assumed) and indicate that silica, alumina and iron compounds are the major constituents. Those results are further summarized in Table 8 which presents the concentrations of major wear-causing species in each of the contaminants. They

indicate that the range of contaminants chosen for these studies represent a range of silica content from 0.15 to 98.58%, alumina from 0.06 to 18.84%, and iron (assumed to be in the form of pyrite) from 0.15 to 4.56%.

Table 8. Concentration of Wear Causing Species in Contaminants (Weight Percent of Contaminant)

	Cleaned K.S. Coal	Low-Ash Coal	Raw K.S. Coal	Ash From K.S. Coal	Syloid 63 Silica
SiO_2	0.15	0.42	13.93	55.70	98.58
Al_2O_3	0.06	0.29	5.45	18.84	1.18
FeS_2	0.15	0.22	1.84	4.56	0.27

Further analysis of the abrasive properties of the contaminants might be accomplished using the Knoop hardness or the Hardgrove grindability tests as suggested by Ryan et. al. (1984). These items are currently being evaluated.

B. Engine Friction and Wear-Rig Tests

1. Apparatus

The engine friction rig used to simulate ring wear on this project was developed as part of another project at SwRI for the Department of Energy. The rig shown schematically in Figure 2 simulates the reciprocating motion of an actual internal combustion engine while simultaneously allowing for the acquisition of ring/liner wear and friction data.

The test rig consists of a stationary piston and reciprocating liner mounted on a single-cylinder Labeco engine crankcase. The Labeco head has been replaced and the engine's crankshaft and connecting rod are used to drive the liner, which oscillates inside an elongated "barrel". Standard Labeco engine parts are employed in the crankcase making the engine's stroke 3.750 inches. The reciprocating liner, piston rings, connecting rod, and wrist pin are standard as well. The rig is driven by a variable speed, electric motor mounted on a common stand. The rig is capable of speeds of up to 2,000 rpm but was limited to approximately 1000 rpm for this experiment.

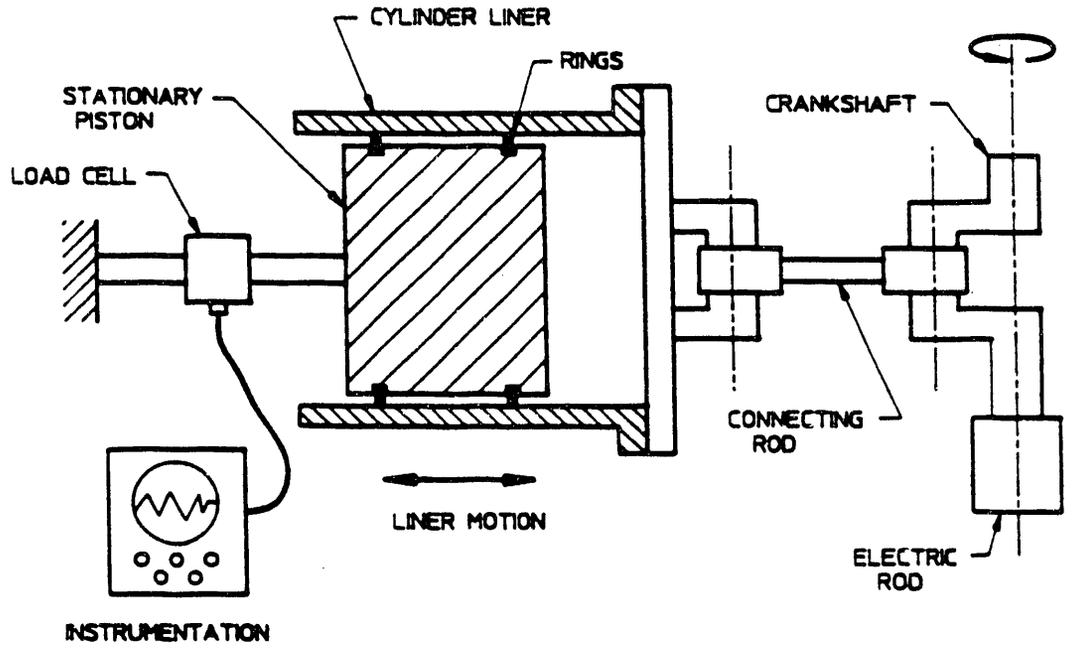

Figure 2. Schematic of Engine Friction and Wear Rig Apparatus

Firing pressures are not attained through normal operation of the rig. Therefore, the rig's original design used compressed gas loads on the piston rings to simulate gas loading from firing pressures. This was accomplished by supplying constant nitrogen pressure through holes machined in the ring grooves. This program however, incorporated an essentially standard piston coupled with a check valve to regulate cylinder pressures. The check valve was installed in the back of the piston (not shown in Figure 1) and connected to a regulated air supply. This was intended to control peak cylinder pressures and hence, gas loading on the rings. The compression ratio was high enough (approximately 15:1) that it was not necessary to regulate additional air into the chamber. In addition, it was also difficult for the check valve to control flow at the higher speeds.

The piston used in this program was a three piece design, incorporating a removable crown for easy access to instrumentation and subsequent assembly. This also provided easy installation and removal of the radioactive top ring while reducing the possibility of breakage. The base of the piston was removable as well and allowed access to the second ring. There was no oil control ring.

The oil control system was developed specifically for this project. Figure 3 is a schematic of the system. Contaminated test oil was pressure fed through open (unthrottled), stainless steel tubing. To ensure that suspended lube oil contaminants did not settle during testing, a stirrer was added to the oil container and run throughout the test. Test oil flow was regulated by controlling supply pressures.

Oil was introduced into the ring/liner interface through two rubber-booted orifices (only one is shown for clarity). Lube oil flow rates were not monitored, except to periodically confirm that the contact patch was flooded. Removal of used, radioactive oil took place through a vacuum pump drawing from the back of the piston. This was found to be an effective way of removing the oil and obtaining a clearer activity signal (due to reduced background radiation). Note from Figure 3 that the gamma-ray detector was mounted close to the engine and was focused on the activated top ring.

A final precaution used in the rig and oiling system was the addition of a scraper ring on the reciprocating liner. The purpose of this ring was to prevent fresh crankcase oil from migrating towards the top of the liner and possibly diluting the contaminated test oil.

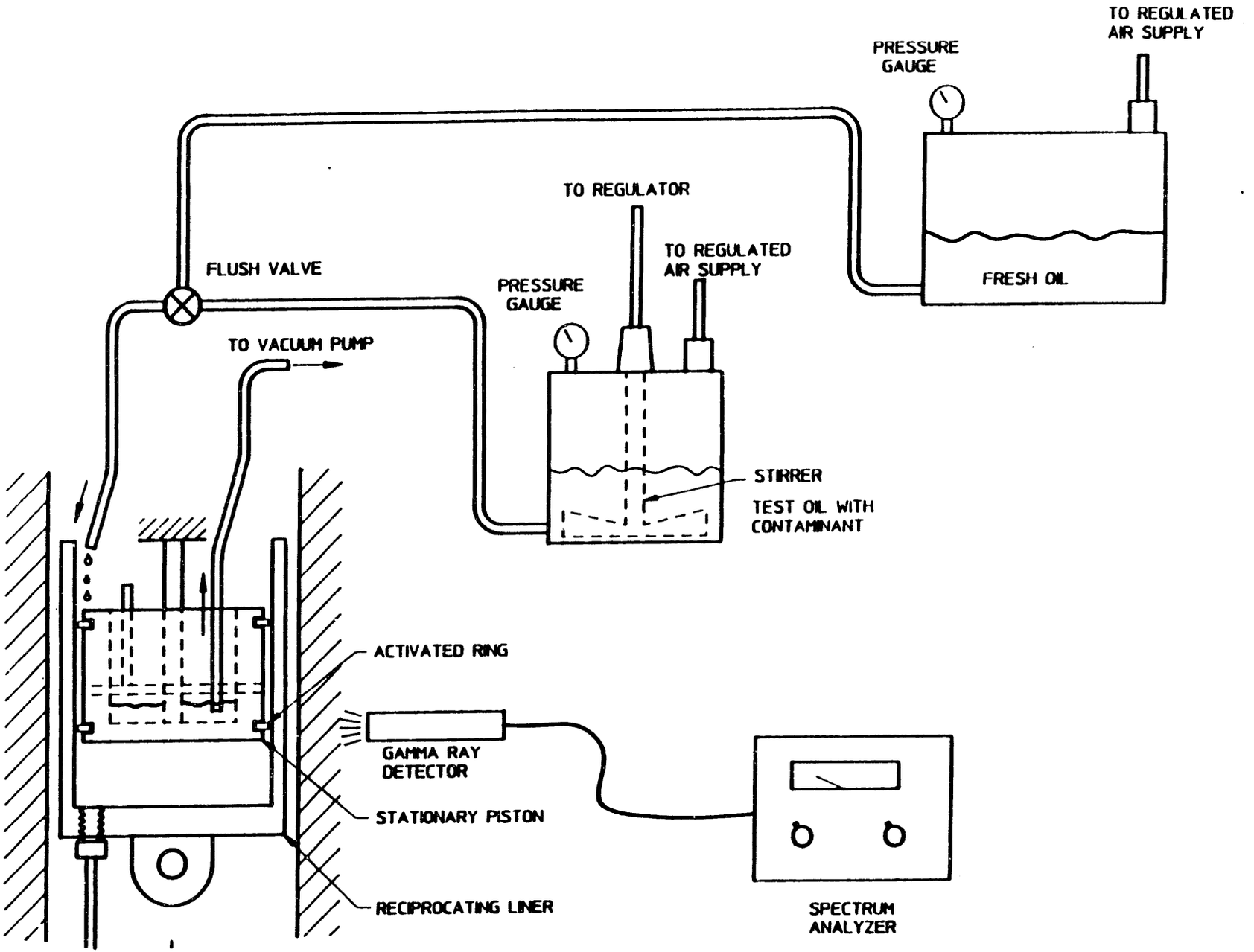

Figure 3. Oil Control System

2. Instrumentation

Instrumentation for the Engine Friction and Wear Rig falls into three categories: standard operating instrumentation, friction measurement equipment, and wear measurement equipment.

a. Standard Operating Instrumentation

To monitor engine and drive motor performance the following parameters were instrumented and monitored:

- Temperatures
  - Top piston ring,
  - Second piston ring,
  - Piston crown,
  - Liner temperature,
  - Oil temperature,
  - Dynomometer water inlet, and
  - Dynomometer water outlet.

- Pressures
  - Water out of dynomometer,
  - Oil pressure, and
  - Cylinder pressure.

The first three thermocouples were epoxied to their respective surfaces. This is an effective means of securing the thermocouple junctions but does introduce an additional source of conduction at the junction. Therefore, ring and crown temperatures were probably slightly higher than indicated.

Liner temperature was obtained by the insertion of a thermocouple into the housing. Oil temperature was obtained in the gallery. It is important to note that the engine's crankcase was sealed and separated from the contaminated oil.

Bourdon pressure gages were used to measure the first two pressures. Cylinder pressure was obtained using a Kistler 6121A2 quartz transducer and corresponding charge amplifier, model no. 5004. The transducer was installed in the back of the piston crown. The signal was displayed on a Norland analog to digital convertor and stored on a computerized data acquisition system.

b. Friction Measurment Equipment

Total friction measurements were acquired for the piston rings using a force transducer installed along the axis of the piston. Referring again to Figure 2, the load cell is shown at the centerline of the piston support system. A Kistler 9031 transducer and AVL 3057 charge amplifier were installed to measure the total force acting on the piston. This transducer measures the force transmitted through the piston's connecting rod via changes in compression of the transducer's quartz crystal. The forces consist of piston ring friction and piston gas loads. Thus, it is necessary to correct the total measured force for the cylinder pressure gas loading. This is accomplished using the cylinder pressure transducer's trace. The pressure is calculated as a resolved force on the piston and then subtracted from the overall force measurement. The balance is attributable to rubbing friction between the two piston rings and the reciprocating cylinder liner. These data were taken, along with cylinder pressure data, every half crank angle.

c. Wear Measurement Equipment

The final instrumentation employed in this program determined the ring wear rates using a technique known as thin film surface layer activation, SLA. This approach is a radioactive marker technique which directly measures the activity decrease from a small activated area on the component of interest as wear occurs (instead of measuring the activity increase in the debris as with tracer techniques).

SLA has been used in numerous applications where quantitative component wear measurements are required and removing the component from service is difficult or disrupts continued testing. Various applications include:

- Evaluating the effects of engine speed and load on piston ring wear in a heavy duty truck engine (Schneider, 1988),

- Measuring valve train wear when developing new passenger car lubricating oils (Shaub, 1987),
- Measuring turbine component wear due to erosion and corrosion (Blatchley, 1986),
- Developing new marine engine lubricating oils (Lane, 1987),
- Continuous wear monitoring of a boiler circulation pump (Blatchley, 1985),
- Engine wear monitoring when developing new lubricating oil filter designs (Milder, 1983),
- Evaluating the effects of fuel sulfur content on cylinder liner wear in a heavy duty diesel engine (Weiss, 1987).

Both Spire Corporation of Bedford, Massachusetts and the Atomic Energy Research Establishment in the U.K. have been developing the SLA technique since the mid-1970's. SLA has four primary advantages over classical tracer techniques:

- The activity of the SLA technique is concentrated on a shallow layer near the surface where very small amounts of wear produce measurable changes in activity.
- The activity is not dispersed in the oil before measurement and the extremely small amounts of concentrated activity are sufficient to insure good precision.
- The distribution of the activity as a function of surface depth can be controlled. Precision of the final measurements is approximately 1 percent of the activation depth into the metal.
- Due to significantly lower radiation levels, SLA is safer than the tracer technique. Activated components can be handled with protective gloves with minimal exposure. The lubricating oil and filter are usually not contaminated to the level where special disposal is required.

The surface layer activation technique shown in Figure 4 involves the following steps in evaluating the average piston ring face wear in the friction test rig:

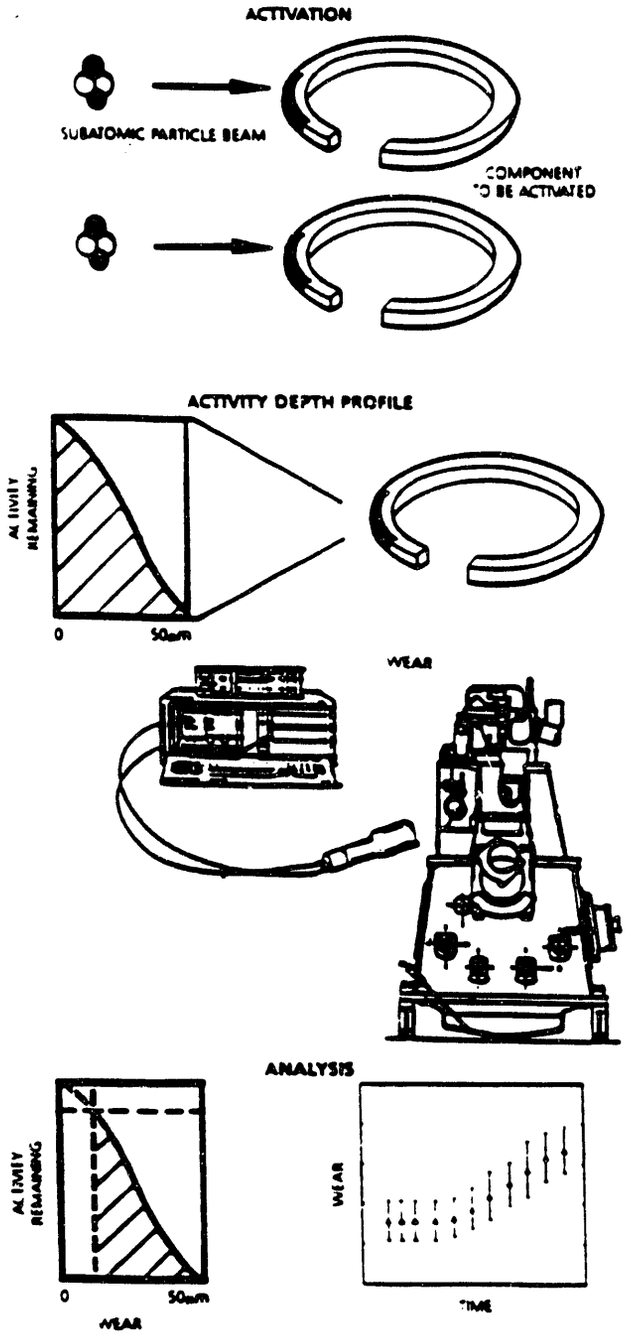

Figure 4. Four Steps in Surface Layer Activation

The first step is the activation of the top piston ring. The activation is produced by high energy particles from a Van de Graaff or cyclotron accelerator. The surface of the ring is exposed to particles of precisely known energy from the accelerator. Some of the particles interact with atomic nuclei in the target spot to produce atoms of a desired radionuclide (approximately 1 atom in 10^9 atoms is converted to the proper radionuclide), i.e., some of the atoms in the bombarded material become radioactive and emit characteristic low level radiation (gamma-rays). The exposure time of the bombardment is short and does not involve an excessive temperature rise. The ion beams are light ion species (protons, alpha particles) which cause minimum radiation damage and the total dose is a factor of 1/100 of that required to cause any mechanical change in the material. The concentration of activity as a function of depth is exactly reproduced whenever the same beam energy and material are used.

Second, an experimental calibration is made to determine the amount of activity left in the irradiated volume as a function of material removed (wear). A duplicate ring (calibration) is activated and then polished under controlled conditions to simulate wear and the activity remaining as a function of material removed (wear depth) is carefully measured. This results in a profile of activity verses metal worn from the surface which is used to calculate the amount of wear from changes in gamma-ray concentration during the actual wear test.

In the third step, the activated piston ring is installed in the engine. A gamma-ray detector is mounted outside of the engine. The gamma-ray intensity is inversely proportional to the square of the distance from the active source. Therefore, the detector is placed as close as possible to produce a strong signal. In addition, intensity falls exponentially on passage through matter, where the more dense the material, the greater the signal attenuation. The detector selects and counts only the radionuclide produced on the activated area of the ring. The radionuclide chosen for a particular application is based on its ease of production, the energy of the resulting photon (which must be in excess of the energy required for the photon to escape and be detected outside of the activated site environment) and by the gamma-ray half-life decay, which must be long enough to allow measurement throughout the effective lifetime of the part or the length of the test. The radionuclide used in this study was ^{56}Co which is the most common isotope used with irradiated iron. The ^{56}Co isotope has a half-life of 77.7 days which

well suited for this type of investigation. The scintillation counter uses a single crystal of NaI (T1) (Sodium Iodide, Thallium activated) which is frequently used in the detection of x-ray and gamma-rays because it has good energy resolution characteristics.

The final step in the SLA technique involves analysis of the system response to determine actual ring wear. This process involves correlating reductions in activity concentration during the wear test with the experimentally determined distribution of activity as a function of depth below the original ring surface calibration profile to determine wear as a function of time or wear rate. This information is stored on computer disk and can be conveniently accessed for analysis.

3. Test Procedure

Prior to executing each test, the SLA equipment was allowed to stabilize by measuring static wear. In other words, a wear slope of zero was established to qualify the operation of the monitoring equipment. Once this was established, the drive motor was allowed to warm up for approximately 10 minutes while operation of remaining instrumentation was checked.

When these tasks were completed, the friction and wear rig was engaged and motored to 500 rpm. No test oil was introduced at this point. Initial operating temperatures and pressures were noted and recorded. After allowing the rig to motor at 500 rpm for approximately 15 minutes, pressure in the oil holding tank was increased to induce flow. Simultaneously, engine speed was increased to 850 rpm and the time was appropriately noted. Within the first 30 minutes of testing, cylinder pressure and friction data were acquired, digitized, and stored for later analysis.

The test was then allowed to proceed until a 5 micron wear limit was reached. In some cases, the wear occurred so quickly that it was not feasible to stop the test before the limit was reached. Operating temperatures and pressures were recorded every 15 minutes. Just prior to shutting down a given test, cylinder pressure and friction data were again acquired. As before, the SLA equipment was allowed to continue monitoring for several hours. This established a new baseline for the next test and provided the cumulative ring wear.

Following the completion of each test, the oil tank was cleaned and the transfer lines were flushed with air and then fresh oil. Radioactive test oil that had been sucked from the back of the piston was removed so that it did not produce extraneous signals for the detector. When this was done, the next lube oil sample was mixed and poured into the oil tank. The transfer lines were then primed and the stirrer was turned on to prevent settling.

This procedure was used to complete a test matrix which included runs with baseline oil, 5% Cleaned Kentucky Splint coal/oil mixture, 5% Raw Kentucky Splint coal/oil mixture and 5% Kentucky Splint ash (air mill ground)/oil mixture as the test lubricants. The contaminants and baseline oil listed above are the same as those used in the Cameron-Plint test matrix described earlier.

III. Experimental Results

A. Cameron-Plint Test Results

The test matrix described above was carried out in its entirety, and results from those tests have been obtained in the following forms, which will be discussed separately in subsequent paragraphs.

- Mass Loss of Cylinder and Ring Pieces
- Electrical Resistance and Friction Load Strip-Chart Data
- Photomicrographic Data
- Profilometric Data

1. Mass Loss of Cylinder and Ring Pieces

Figures 5 and 6 are bar charts indicating the average mass loss at each test condition for ring and cylinder pieces respectively. The groups of five bars at 0, 5, 10 and 15 percent contaminant loadings represent the five different contaminants (arranged in order from lowest ash content to highest ash content) as labeled on the charts. From these figures, the following observations seem readily apparent.

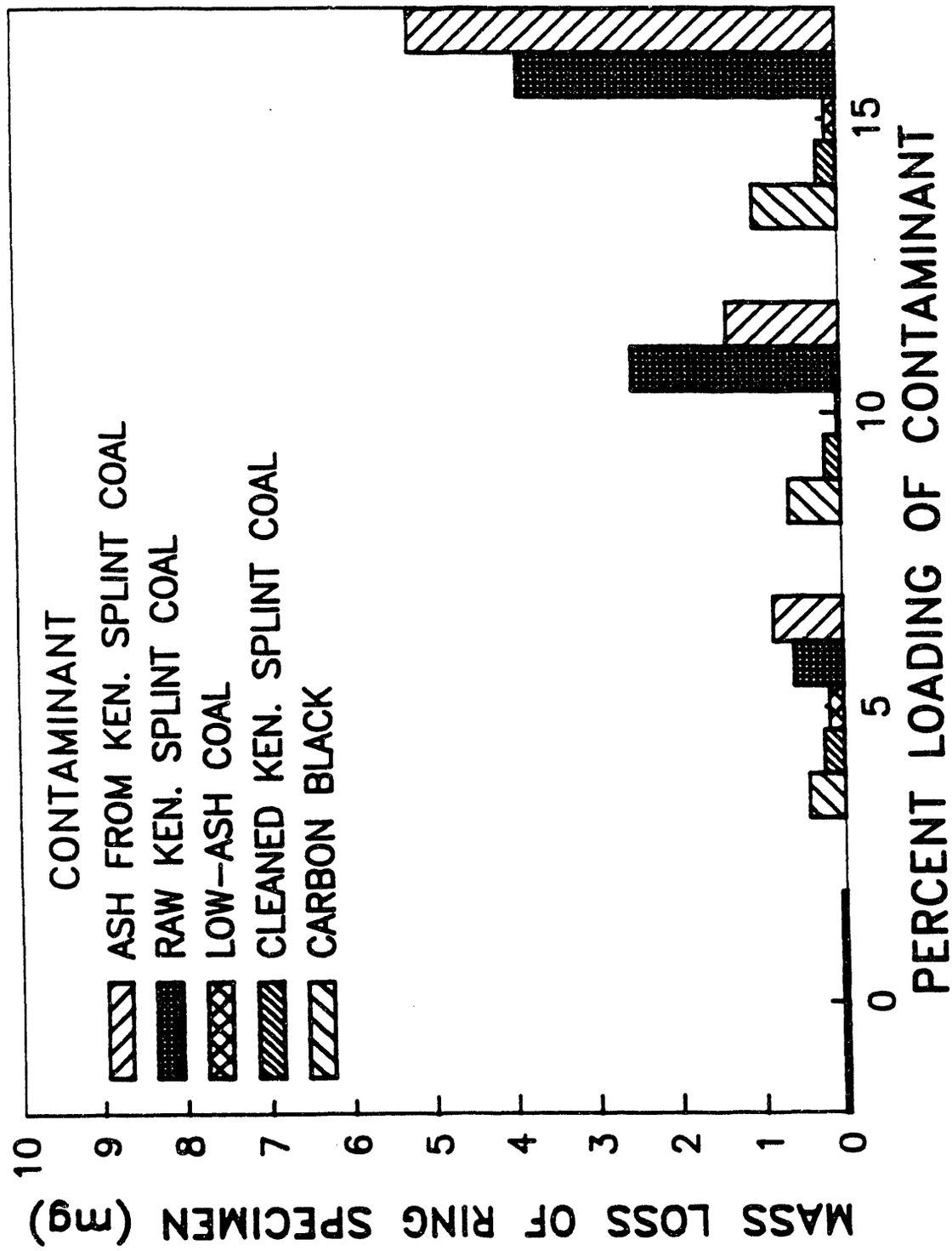

Figure 5. Mass Loss of Ring Specimen

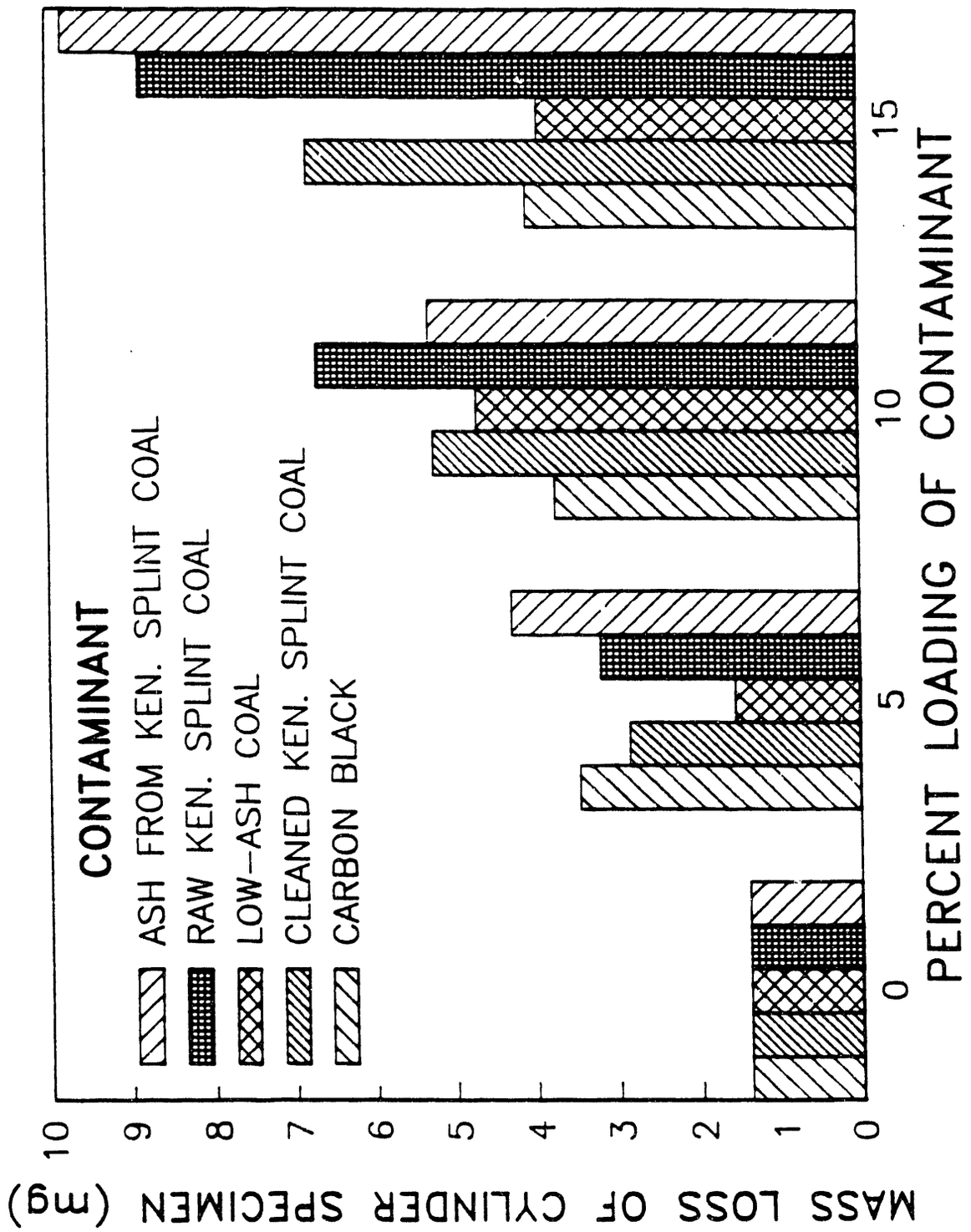

Figure 6. Mass Loss of Cylinder Specimen

- Mass loss of the cylinder specimen was somewhat larger than that of the ring specimen. This is the reverse of what Nydick, et al. (1987) reported, but may be highly dependent on the choice of ring and cylinder materials.
- As contaminant loading and ash content increased, the relative difference between ring mass loss and cylinder mass loss decreased.
- Generally, wear rate increased with percent loading of contaminant. Some of the wear rates seemed to level off at the higher concentrations (carbon black and low-ash coal) while the others seemed to be continuing to increase.
- The low-ash coal wear rates tended to be lower, and were not consistent with the trends established by the other contaminants.
- Overall, the correlation between wear rate and ash content becomes more apparent as loading of contaminant increases.

Perhaps a better idea of the effect of ash content on wear can be obtained by looking at the graphs in Figures 7 and 8. These represent the same data taken from Figures 5 and 6 for mass loss of the ring and cylinder pieces respectively, but they are plotted vs. the ash content of the contaminant. The trend for wear to increase with contaminant loading is reaffirmed in these graphs, but the effect of ash content seems much smaller than one might expect. Figures 9 and 10 show this trend perhaps even more clearly. The graphs represent wear as a function of the total amount of ash in the oil. If one observes the peak point for each contaminant, only a slight increase in wear occurs, even though ash concentration increased by two orders of magnitude. The concentration of contaminant in the oil was a much more important wear determining parameter. Apparently, ash content does have an effect on wear, but there must be other factors which are more significant under these conditions.

All of the above data was taken at a single ring load condition of 200 N. While it was not the intent of this project to do an in-depth study of the effects of load on wear rate, it did seem appropriate to observe the change in wear for a few lower load conditions. Such tests would reveal if there was a significant change in the nature of the wear process at lower loads, and would indicate whether or not the accelerated wear conditions used here were appropriate. With that in mind, a set of tests were done with the 15% concentration of ash and 15% concentration of silica at both the original 200 N ring load and at a reduced ring load of 50 N. The results of those tests seemed to confirm that no significant change in the wear characteristics was occurring. The decrease in wear was reasonably linear as shown

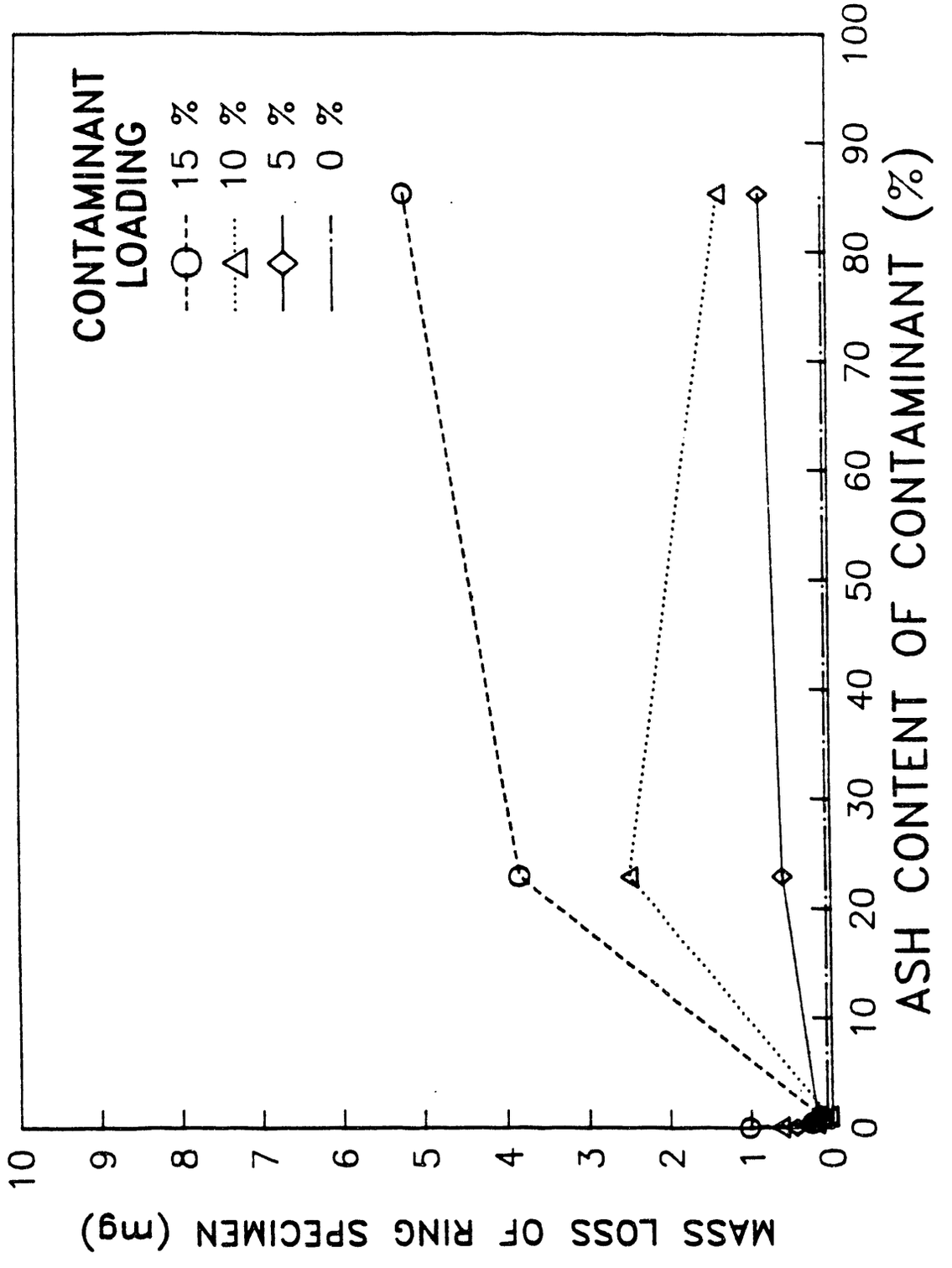

Figure 7. Effect of Ash Content on Wear Rate of Ring Specimen

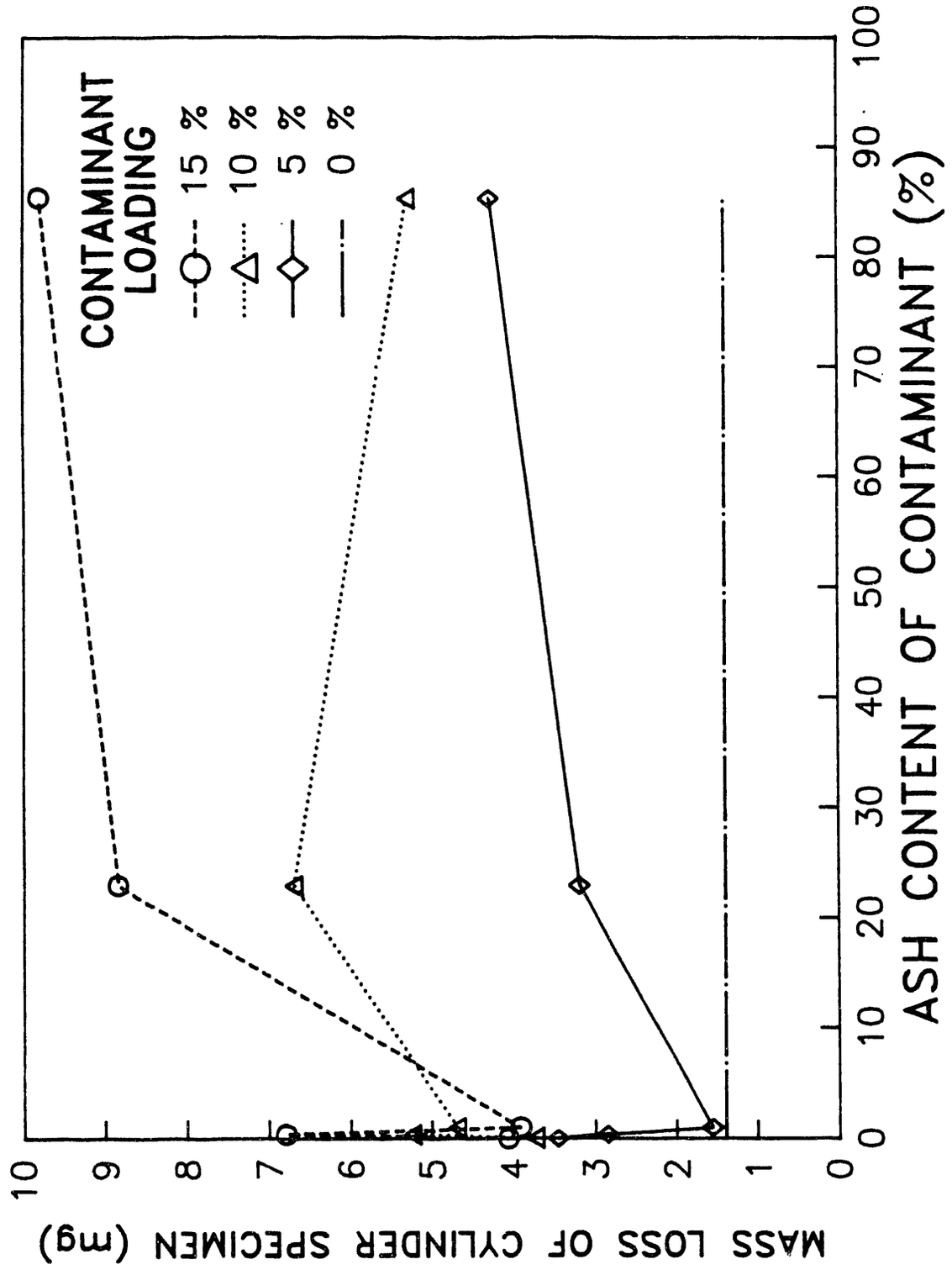

Figure 8. Effect of Ash Content on Wear Rate of Cylinder Specimen

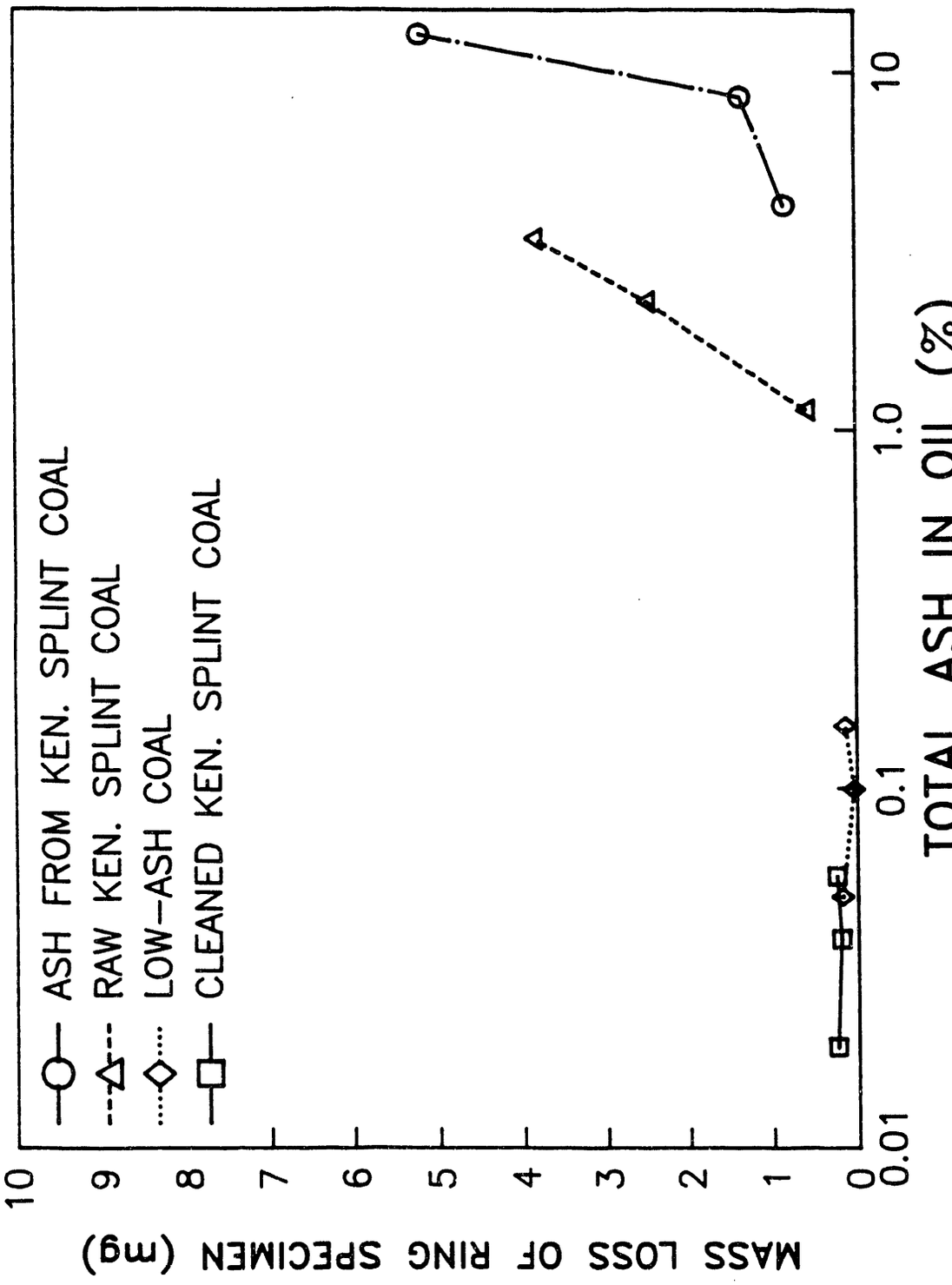

Figure 9. Effect of Total Ash in Oil on Wear Rate of Ring Specimen

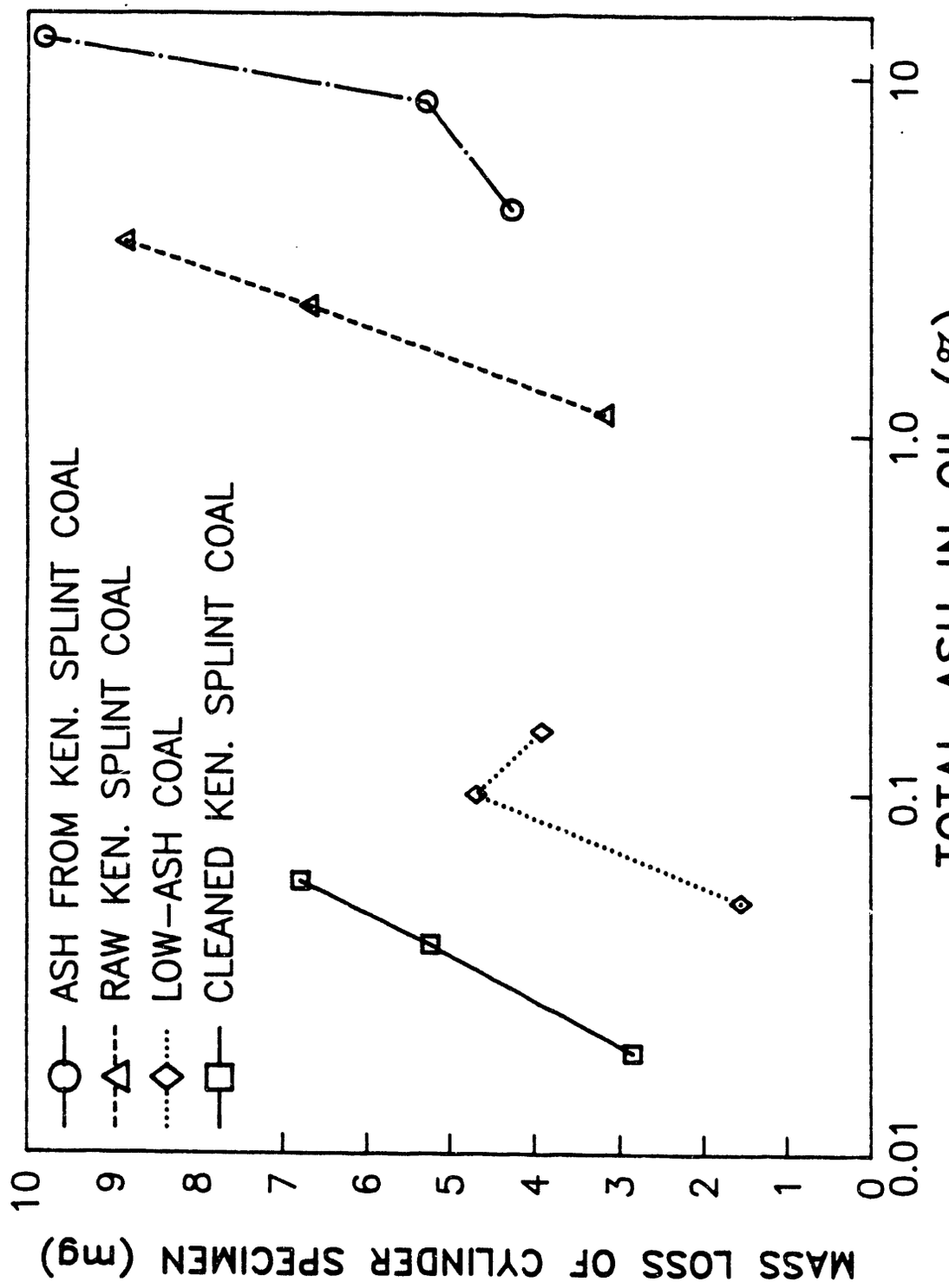

Figure 10. Effect of Total Ash in Oil on Wear Rate of Cylinder Specimen

in Figure 11. Also, the repeatability of the tests was quite similar between the two conditions (the 200 N ash tests had a standard deviation of 4.09 or 41.7% of the mean, while the 50 N tests had a standard deviation of 1.73 or 46.5% of the mean). These results helped build confidence that the accelerated wear conditions used here are representative of the actual wear conditions in an engine.

Another issue that was studied was the effect of particle size on wear. As noted earlier, the original test matrix was performed using a Kentucky Splint ash that had significantly larger particles than the other contaminants. That ash was ground to a smaller size and wear tests were repeated using 5 and 10% concentrations. Those results are presented in Figure 12. As it turned out, wear was significantly higher with the smaller particle size. In fact, the wear at 10% was so high that it caused significant change in the geometry of the ring piece. Under these conditions it was felt that the magnitude of wear was reaching the maximum for which meaningful measurements could be obtained. Also, the friction force was high, causing extreme vibrations of the machine, so it was decided not to continue with a test at 15% concentration. These results do indicate, however, that particle size has an imporant role in the wear process, and they suggest that the relative insensitivity of wear to ash seen in the results of Figures 5 through 10 may be an artifact of the particle size differences. Possibly, particles which are much larger than the hydrodynamic film thickness are simply being swept away by the ring motion and are not entering the wear zone.

One other interesting observation that can be made from the mass loss data concerns the repeatability of the tests and how that is affected by particle size. Table 9 contains a list of the standard deviation of weight loss results for test conditions that were repeated. While the exact reason for this correlation is unknown, there seemed to be an increase in the scatter of data as the particle size of the contaminant was increased, and that trend was noticeable even over the relatively small range of particle sizes used in this study. Possibly, the increase in particle size is causing a change in wear mechanism from typical three-body wear to more of a two-body process in which large particles are following and grinding between the surfaces. The low-ash coal once again proved to be the only exception to this trend.

2. Electrical Resistance and Friction Force Data

Strip-chart recordings of the electrical resistance between ring and cylinder pieces were obtained along with a measurement of the friction force. These recordings provide a qualitative measure of how the wear process changes during of the four-hour test. As it

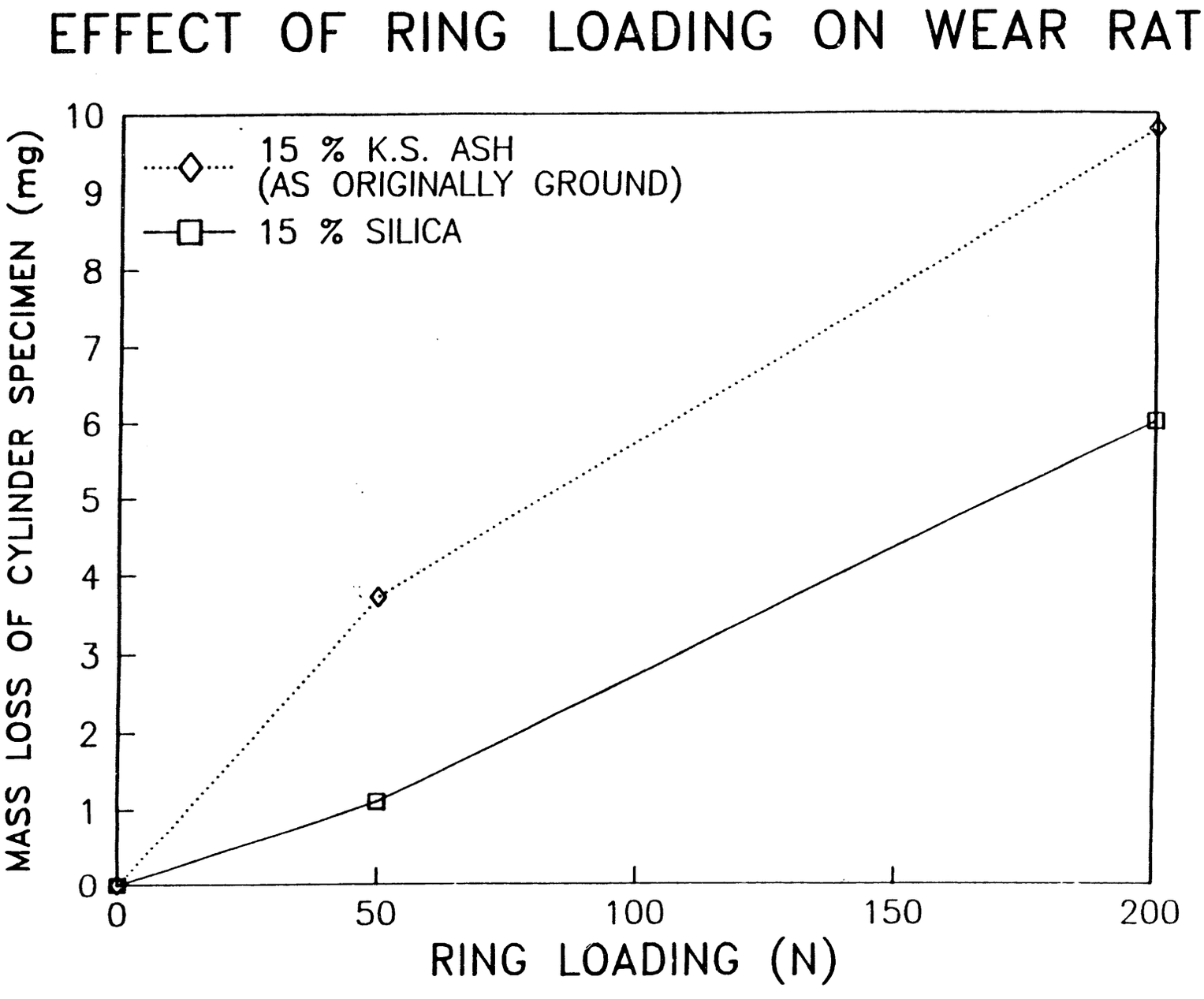

Figure 11. Effect of Ring Loading on Wear Rate

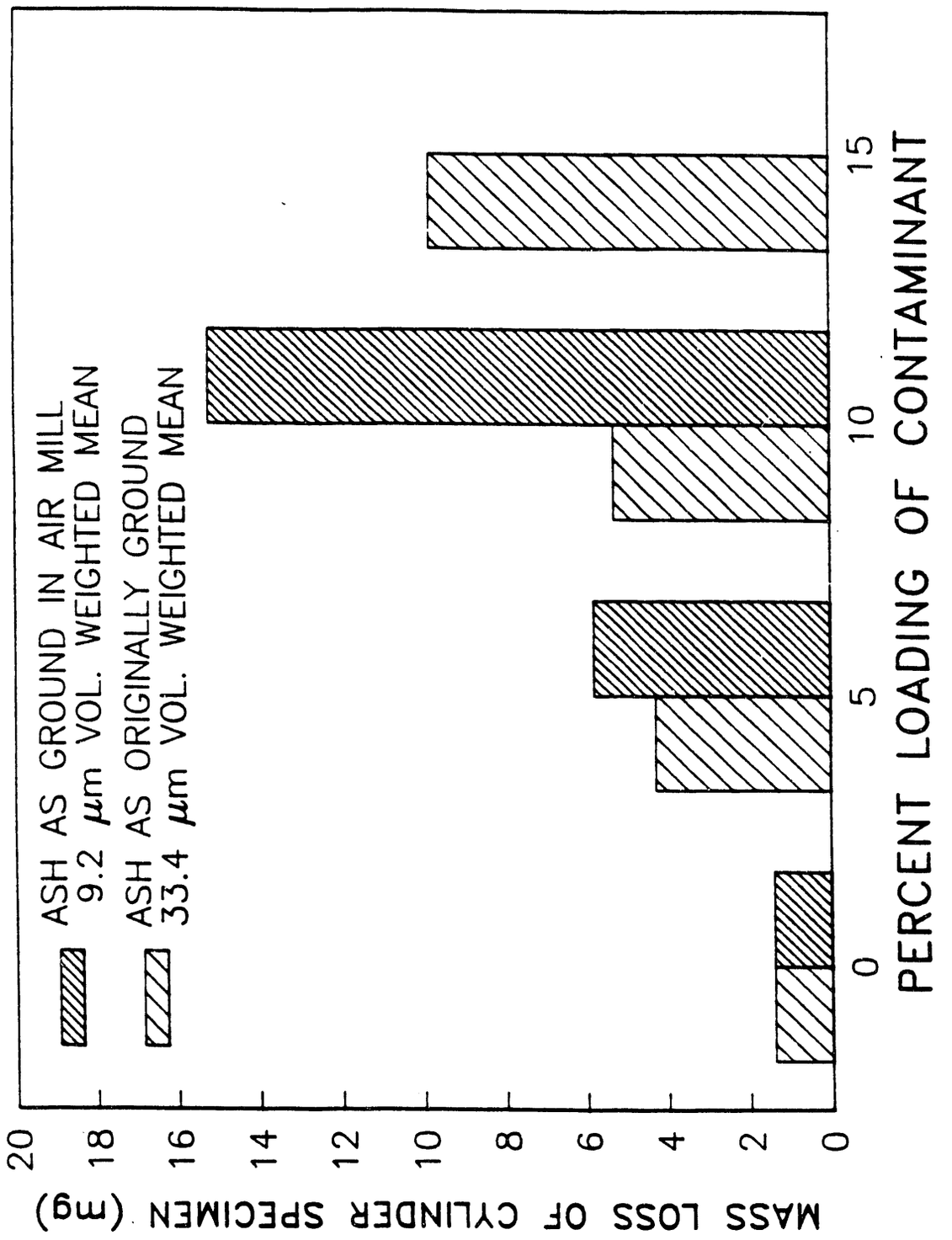

Figure 12. Effect of Particle Size on Wear Rate of Cylinder Specimen

turned out, the electrical resistance in most cases went to zero upon initiation of the test and remand there, indicating physical contact between the two wear pieces. It must be remembered,

Table 9. Statistics on Repeatability of Cylinder Piece Mass Loss

Mean				
	Percent Loading			
Contaminant	**0**	**5**	**10**	**15**
Carbon Black	1.40	3.46	3.74	3.92
Cleaned K.S. Coal	1.40	3.83	5.25	6.80
Low-Ash Coal	1.40	1.56	4.70	3.92
Raw K.S. Coal	1.40	3.20	6.70	8.85
Ash From K.S. Coal	1.40	4.28	5.20	9.80
Standard Deviation				
	Percent Loading			
Contaminant	**0**	**5**	**10**	**15**
Carbon Black	0.86 (61.4)	0.31 (8.96)	0.50 (13.4)	0.54 (13.8)
Cleaned K.S. Coal*	0.86 (61.4	1.70 (44.5)	0.64 (12.1)	0.71 (10.4)
Low-Ash Coal	0.86 (61.4)	0.55 (35.3)	1.10 (23.4)	1.25 (32.1)
Raw K.S. Coal*	0.86 (61.4)	0.00 (0.00)	0.28 (4.20)	1.06 (12.0)
Ash From K.S. Coal	0.86 (61.4)	0.56 (13.1)	0.99 (18.7)	1.73 (41.7)

Numbers in Parentheses are Coeff. of Variation (Std. Dev.))/(Mean) (Expressed in Percent)

*The tests were only repeated once when Raw K.S. Coal and Cleaned K.S. Coal were used.

however, that the signal is time averaged, and would not reflect anything that might happen in small time intervals within a single cycle. A few tests (the 15% ash, 50 N set and the 15% silica, 50 N set) indicated a small finite resistance within the first fifteen minutes before going to zero for the remainder of the test. One might expect an increase in electrical resistance as load is reduced, however, in this case, the reading seemed to only be associated with initial transients.

A qualitative description of the friction force traces for each of the different test conditions is included in Table 10. Almost all of the traces exhibited some sort of initial transient behavior which varied in length and magnitude. Looking beyond that initial break-in period, however, there are two useful conclusions that can be drawn from this data.

Table 10. Qualitative Description of Friction Force Traces

Contaminant	Description
Carbon Black	Overall shape of all traces included a sharp drop in the first half hour which leveled off for the remainder of the test. Traces became rougher (more high frequency oscillations) as particle loading was increased
Low-Ash Coal	Overall shape was fairly flat with some low-frequency waves (approximately half-hour period), and small transients in the first half hour. Traces became rougher as particle loading increased.
Cleaned Kentucky Splint Coal	Overall shape was smooth and flat for all traces, with some small transients in the first half hour.
Raw Kentucky Splint Coal	Overall shape included a large increase in the first hour followed by a flat, slightly increasing trace for the remainder of the test. Traces became rougher as particle loading increased.
Ash From Kentucky Splint Coal	Traces were extremely rough, but overall slightly increasing through the duration of the test. Roughness increased as particle loading increased.

- Increasing ash content and particle loading caused an increase in high-frequency oscillations in the friction force traces, but did not change the overall shape of the curves. The presence of oscillations is evidence that an abrasive process is beginning to occur which involves particles sticking and grinding between the surfaces.
- There were no major changes in any of the friction force traces over the course of the four hour tests. That indicates there were no major changes in the wear mechanism during these tests.

3. Photomicrographic Data

Photomicrographs of the cylinder pieces for each of the contaminants at 15% loading are shown in Figure 13. The pictures were taken at a position approximately 1/4 of the way across the wear scar (in the direction of ring travel), although the characteristics seen in the pictures did not change significantly over the entire length. The second and third photomicrographs from the top show some deep gouges across the finely spaced vertical grooves. These gouges were caused by the original honing process and should not be confused with the vertical grooves caused by the wear process. The honing grooves measured approximately 35 micrometers as compared to the wear grooves which are approximately 14 micrometers (these sizes roughly correlate to the average particle sizes). The microscope was set at 500X and the entire width of each photomicrograph represents approximately 300 micrometers. From these photomicrographs, and general inspections of the ring pieces as well, the following observations were made.

- The grooves in all the wear scars were fairly straight and clean. There was little evidence of sharp breaks or gouges.
- As ash content increased, the wear grooves seemed to become sharper and deeper.
- There was little evidence of particles being embedded in either the ring or cylinder pieces.

The observations listed above seem to indicate a change in wear mechanism as ash content is increased. Carbon black caused fairly smooth grooves with some plastic deformation that seemed characteristic of a soft-abrasive "polishing" type wear. In fact, some of the ring specimens worn with the carbon black contaminant were highly polished to the point where the surface appeared shiny to the naked eye. Under the microscope, even some

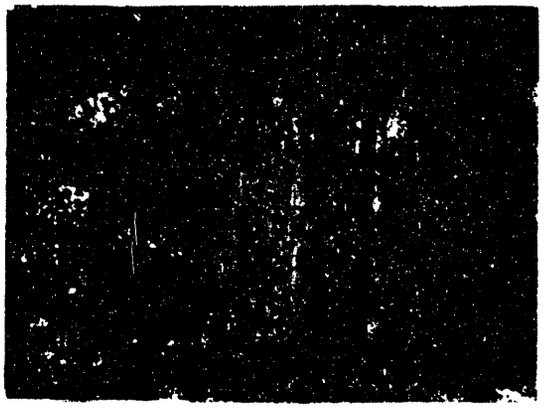

15% Carbon Black

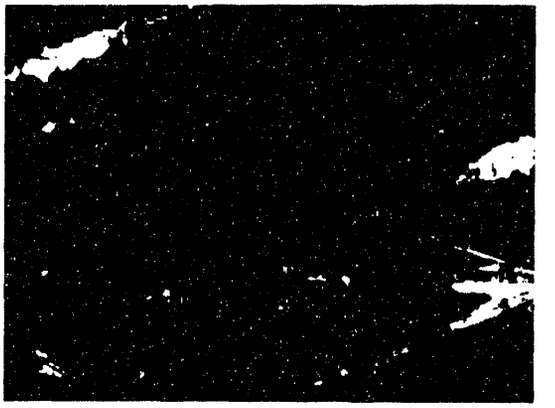

15% Cleaned K.S. Coal

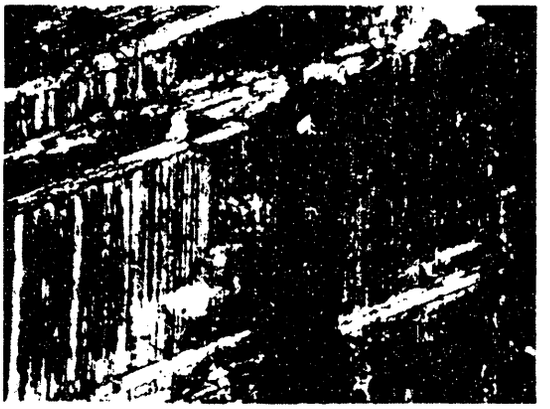

15% Low Ash Coal

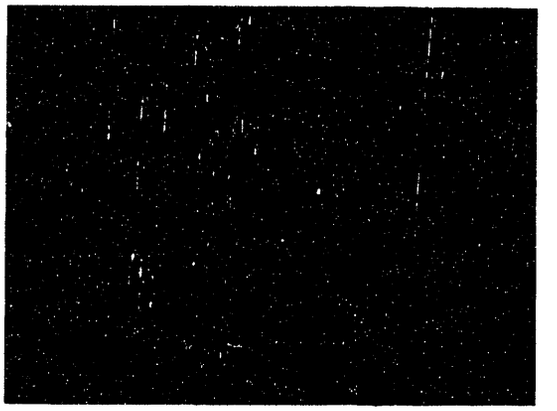

15% Raw K.S. Coal

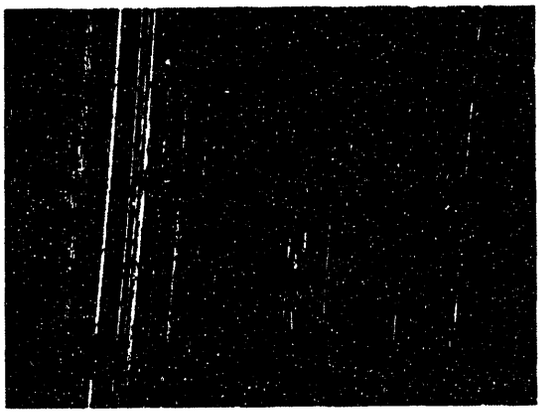

15% Ash From K.S. Coal

Figure 13. Photomicrographs of Cylinder Specimen Wear Scars

of the granular structure of the material was visible. A photomicrograph of one of those ring specimens is presented in Figure 14. As ash content increased, grooves seemed to become deeper and sharper. The polishing process may still have been occurring, but at the same time, a new wearing mechanism was becoming more imporant. The fact that there were few embedded particles or holes where particles might have lodged indicates that mechaism is most likely a three body process involving hard abrasive particles.

Also of note from the microscopic observations of these specimens were the comparative differences between pieces worn with the Kentucky Splint ash contaminant, and those worn with silica. As shown above, the ash worn specimens were characterized by deep, sharp grooves. Silica worn specimens, on the other hand, had fairly smooth, evenly spaced ridges which were quite different in appearance. Weight loss data presented earlier also indicates a much lower wear rate with the silica. This suggests that either the silica contained in the ash is in a different form than the Syloid 63 silica used here, or that the silica is not the predominant wear-causing species in the ash.

4. Profilometric Data:

Profiles of representative cylinder specimen from each of the different test conditions were taken in order to get an idea of the shape of the wear scar and how it varies with ash content. Using a taly-surf profilometer, the profiles were recorded at two positions in the longitudinal direction (the direction of ring travel) and three positions (evenly spaced) in the cross-wise direction. One example of a longitudinal profile is shown in Figure 15. As it turned out these were good enough to get a qualitative description of the shape of most of the wear scars, but it would take quite a few more profiles across the scar to get a good average for quantitative comparisons. The results of qualitative analysis of these profiles can be summarized in the following observations.

- The shape of the longitudinal profile shown in Figure 15 is characteristic of all the wear scars that had a significant amount of wear.
- As ash content and contaminant loading was increased, the wear scars tended to become deeper and relatively flatter (indicating that the effects of hydrodynamic film breakdown are becoming smaller).
- Profiles in the cross-wise direction indicated that grooves in the wear scars tended to become sharper and deeper as ash content was increased.

Figure 14. Photomicrograph of Ring Specimen Wear Scar, Worn With Carbon Black Contaminant

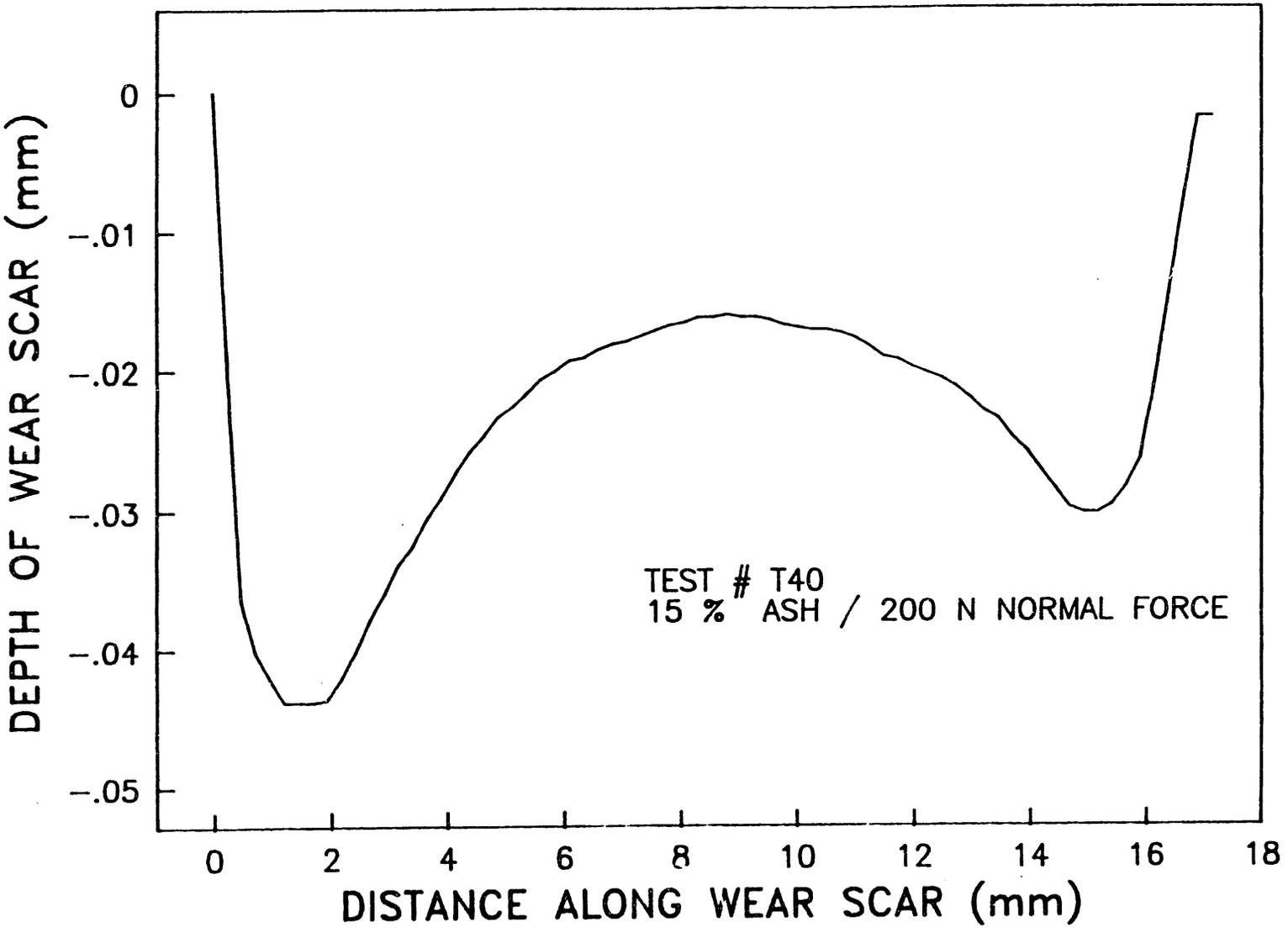

Figure 15. Longitudinal Profile of Wear Scar

The above observations indicate that a wear process is occurring which is dependant on the dynamic motion of the ring piece. Wear of this nature is commonly observed in diesel engines and is believed to be a result of breakdown of the hydrodynamic film at the ring reversal points. The fact that this type of wear was observed builds confidence that even though compromises were made in using high ring loads and a short ring stroke (resulting in lower ring travel velocities), the Cameron-Plint configuration was able to recreate a similar type of wear to that which is observed in operating diesel engines. Evidence that a hydrodynamic film is forming seems to contradict resistance measurements indicating constant metal contact. It must be remembered, however, that the resistance measurements are highly suspect due to the conductive nature of some of the contaminants, and the fact that it is a time averaged signal.

B. Engine Friction and Wear Rig Results

Results of the wear rig testing consisted of in situ wear measurements, friction force traces, and qualitative observation of the rings' wear surfaces. These data are presented in detail in the following sections.

1. Results of Ring Wear Measurements

A total of six tests were run on the engine wear rig to quantify piston ring wear on a transient basis as a function of changes in lube oil. Results are depicted graphically in Figures 16 through 21 and summarized in Table 11. Tests 1 through 4 were done with the same ring using the baseline oil and 5% concentrations of cleaned Kentucky Splint coal, raw Kentucky Splint Coal, and the ash from the Kentucky Splint coal (after it was air-mill ground). Tests 5 and 6 were done with a new ring, and represent repeats of the baseline oil case, and the 5% raw coal case. The repeated cases show excellent agreement, confirming the repeatability of the tests. Baseline oil wear rates were somewhat higher than expected, but this can be attributed to the normally high wear rates associated with break-in of the new rings.

The lowest wear rate was observed with a 5% concentration of raw coal, while the peak ring wear rate was found to occur with a 5% concentration of raw ash. This rate was approximately 26 times that of the oil contaminated with an equal concentration of raw coal.

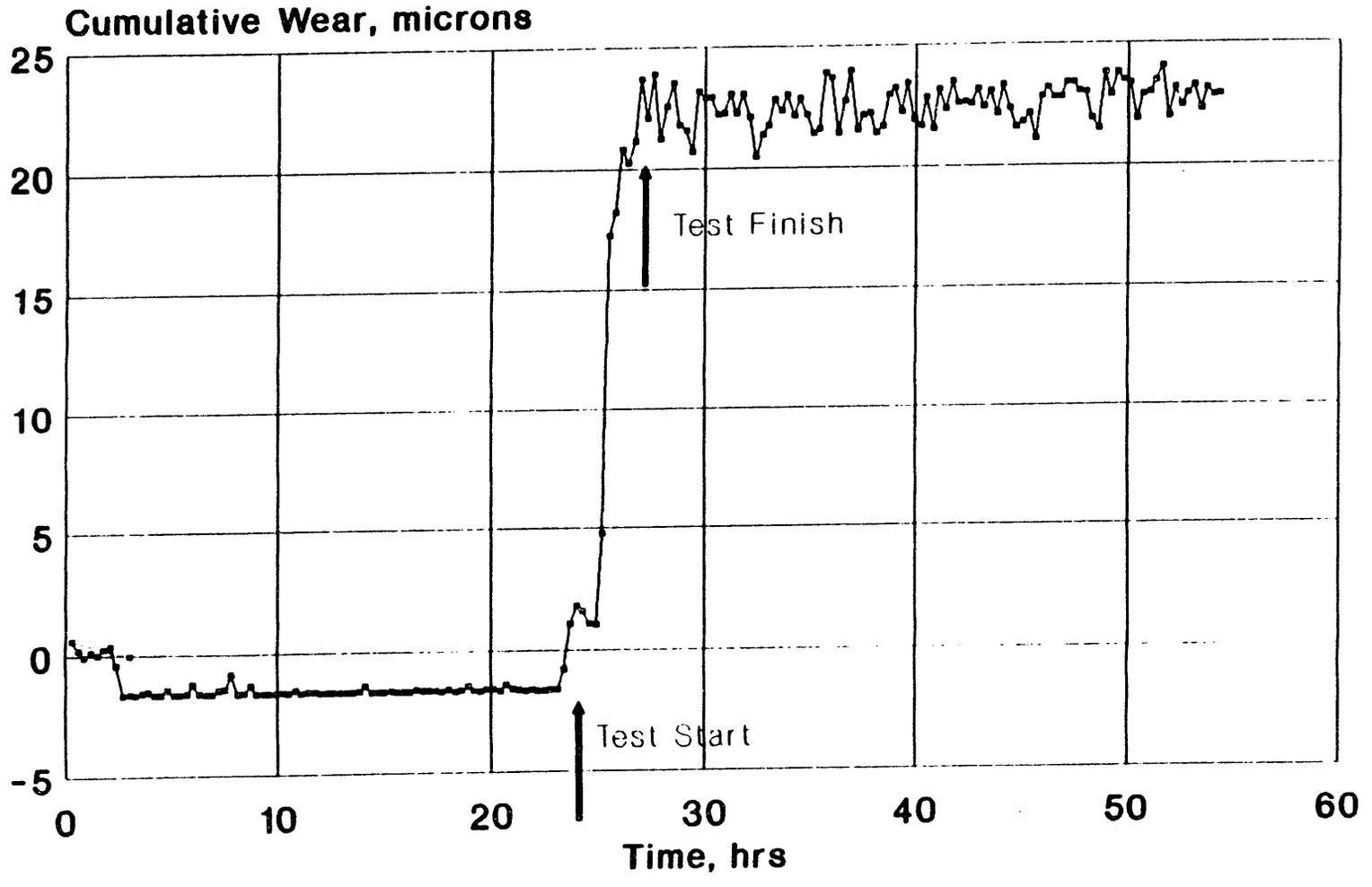

Southwest Research Institute

Figure 16. Lube Oil Effects on Ring Wear Test #1; Baseline Oil; 850 rpm

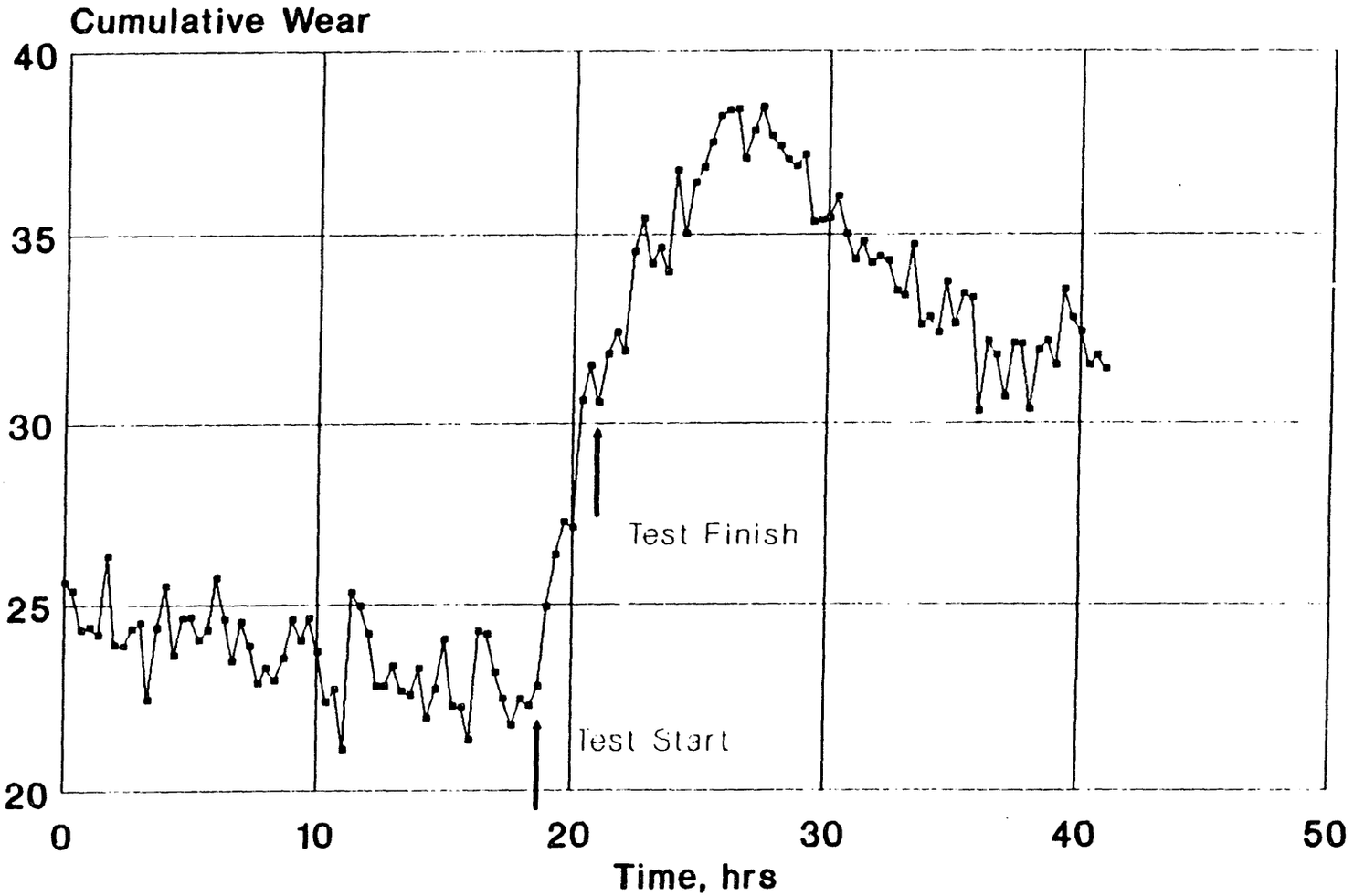

Figure 17. Lube Oil Effects on Ring Wear Test #2; Clean Coal - 5% Concentration

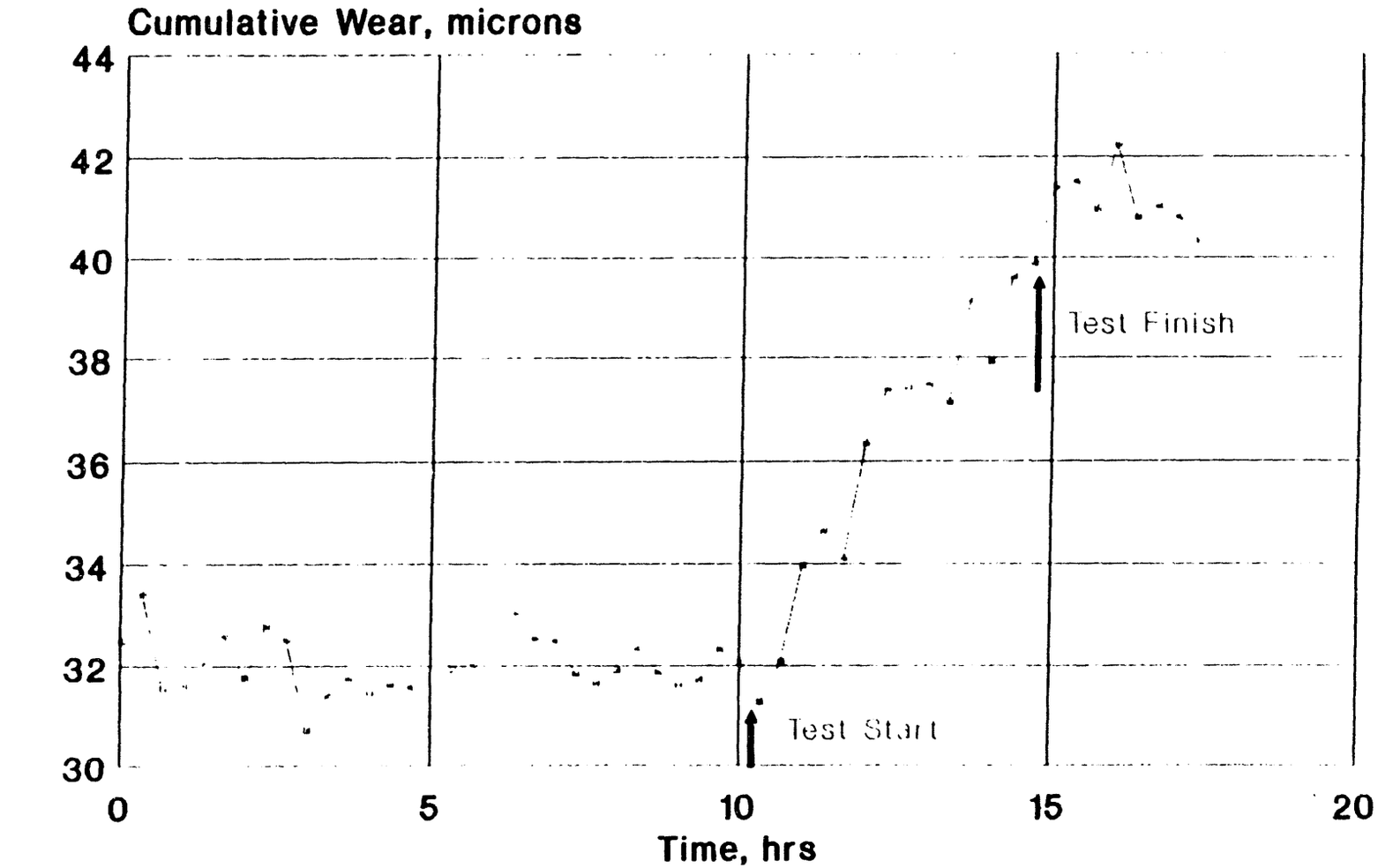

Figure 18. Lube Oil Effects on Ring Wear Test #3; Raw Coal - 5% Concentration

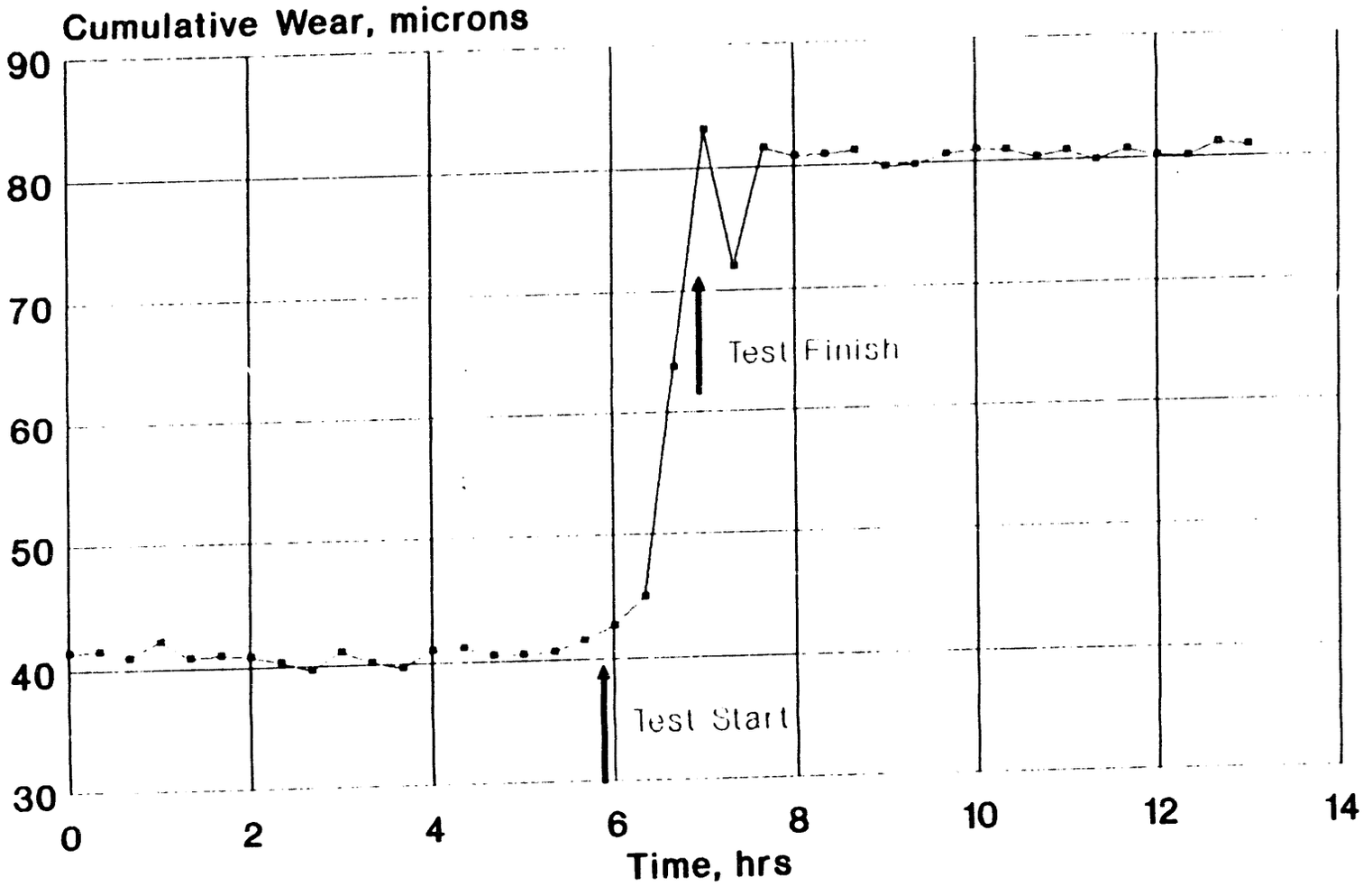

Southwest Research Institute

Figure 19. Lube Oil Effects on Ring Wear Test #4; Raw Ash - 5% Concentration

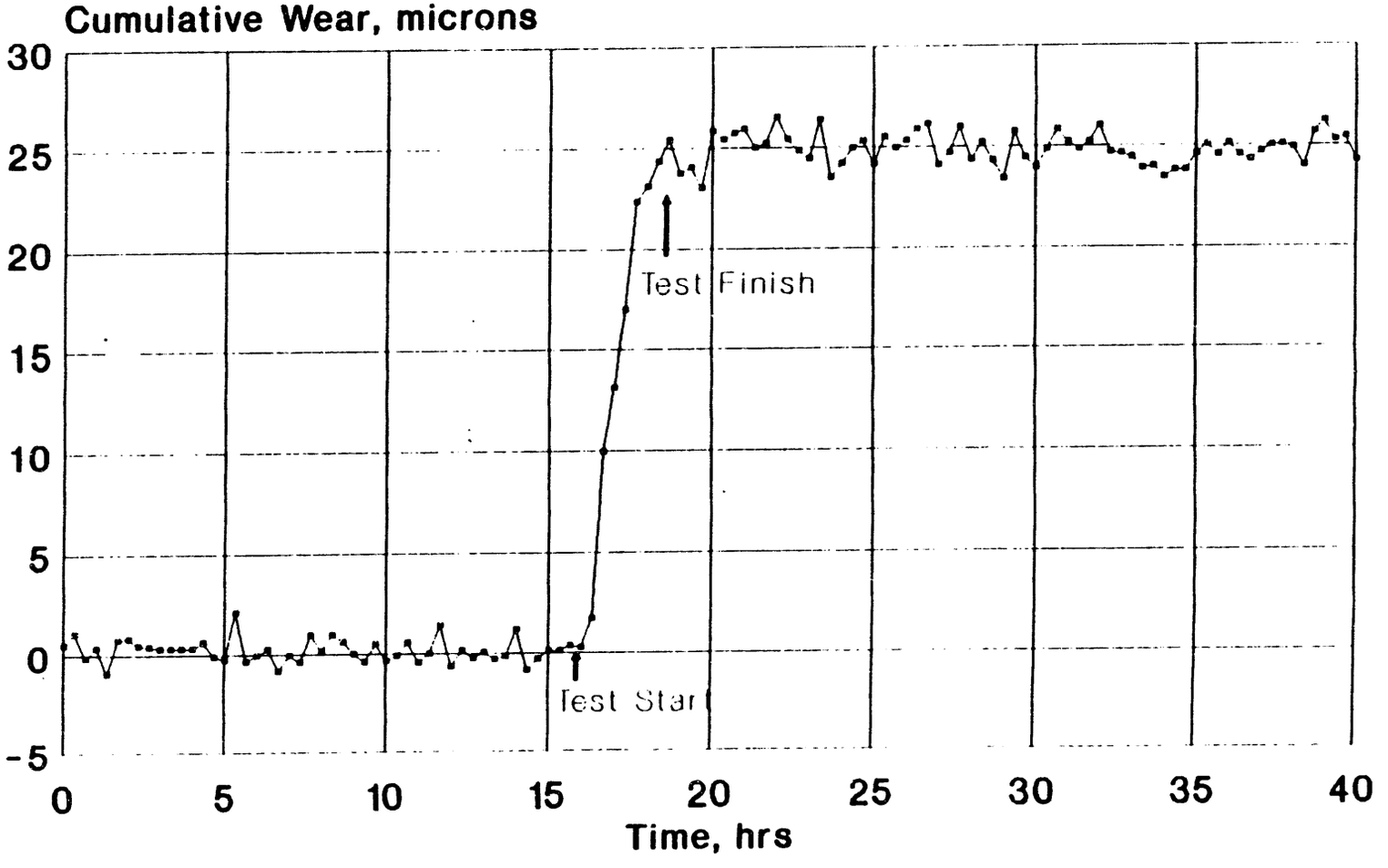

Figure 20. Lube Oil Effects on Ring Wear Test #5; Baseline Oil; 850 rpm Confirmation of Test #1 Results

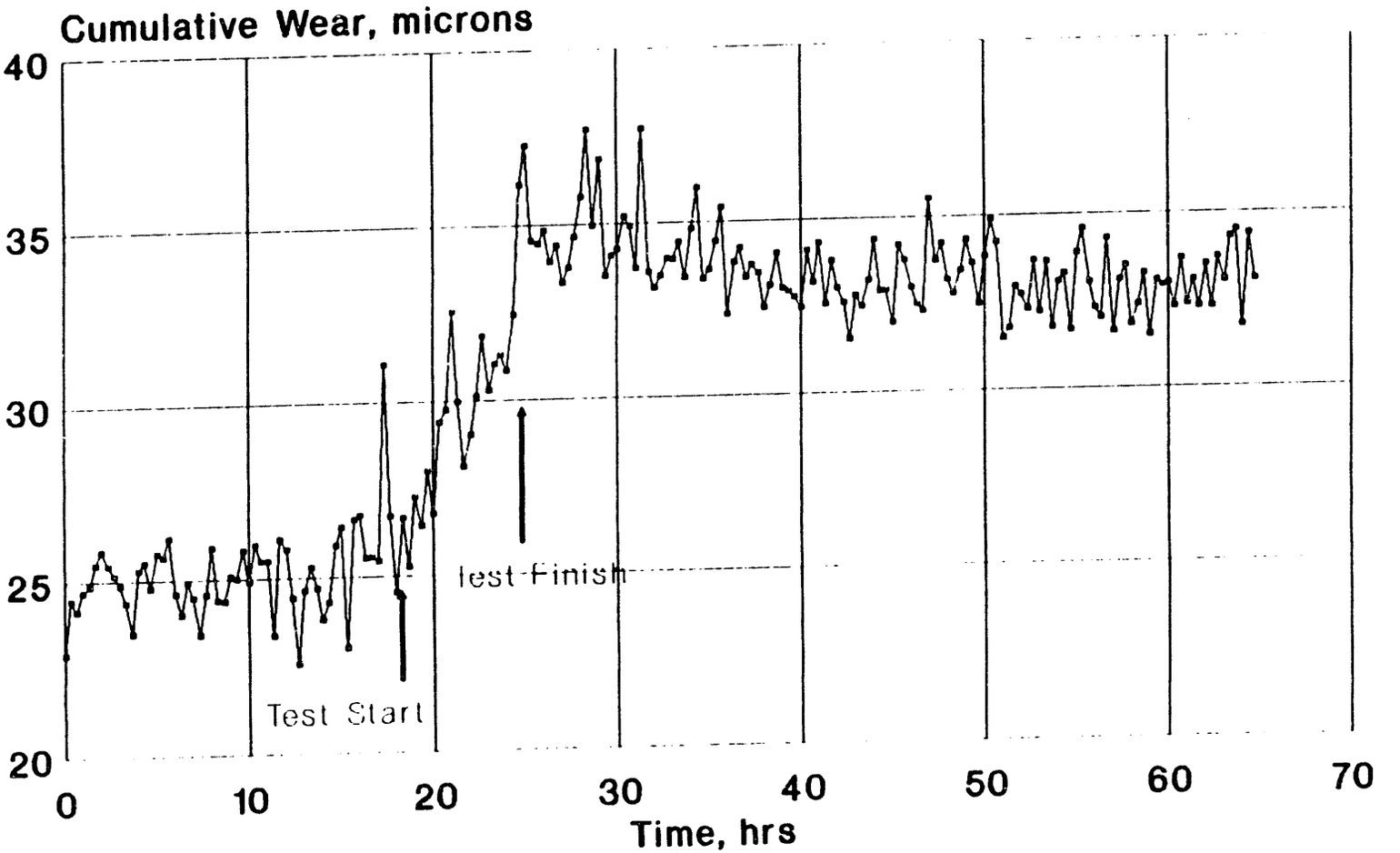

Southwest Research Institute

Figure 21. Lube Oil Effects on Ring Wear Test #6; Raw Coal - 5% Concentration Confirmation of Test #3

Table 11. Engine Friction and Wear Rig Data		
Test No.	Lubricant Type	Wear Rate
1	Baseline Oil	7.5 microns/hr
2	Cleaned K.S. Coal (5% conc.)	2.7 microns/hr
3	Raw K.S. Coal (5% conc.)	1.7 micorns/hr
4	Raw Ash (5% conc.)	39.8 microns/hr
5	Baseline Oil (rerun)	7.8 microns/hr
6	Raw K.S. Coal (rerun)	1.1 microns/hr

The curves in Figures 16 through 21 demonstrate the use of SLA to monitor decreased activity associated with ring wear. The relatively horizontal slopes before and after each test represent static data while the engine was not running.

2. Results of Ring Friction Forces

Friction traces for both piston rings are found in Figures 22 through 30. Curves represent ring friction forces as a function of crank angle for the respective oil formulations. Traces were obtained just after the start of a test and just before the end of a test to assess the difference in ring friction due to ring wear. Skirt friction was negligible as the test piston is configured to reduce these losses.

Though the curves appear somewhat haphazard at first glance, they are repeatable. There was little lubricant to lubricant variation, though the baseline oil trace in Figure 22 was characterized by significantly lower friction. There appears to be little correlation between ring wear and piston ring friction.

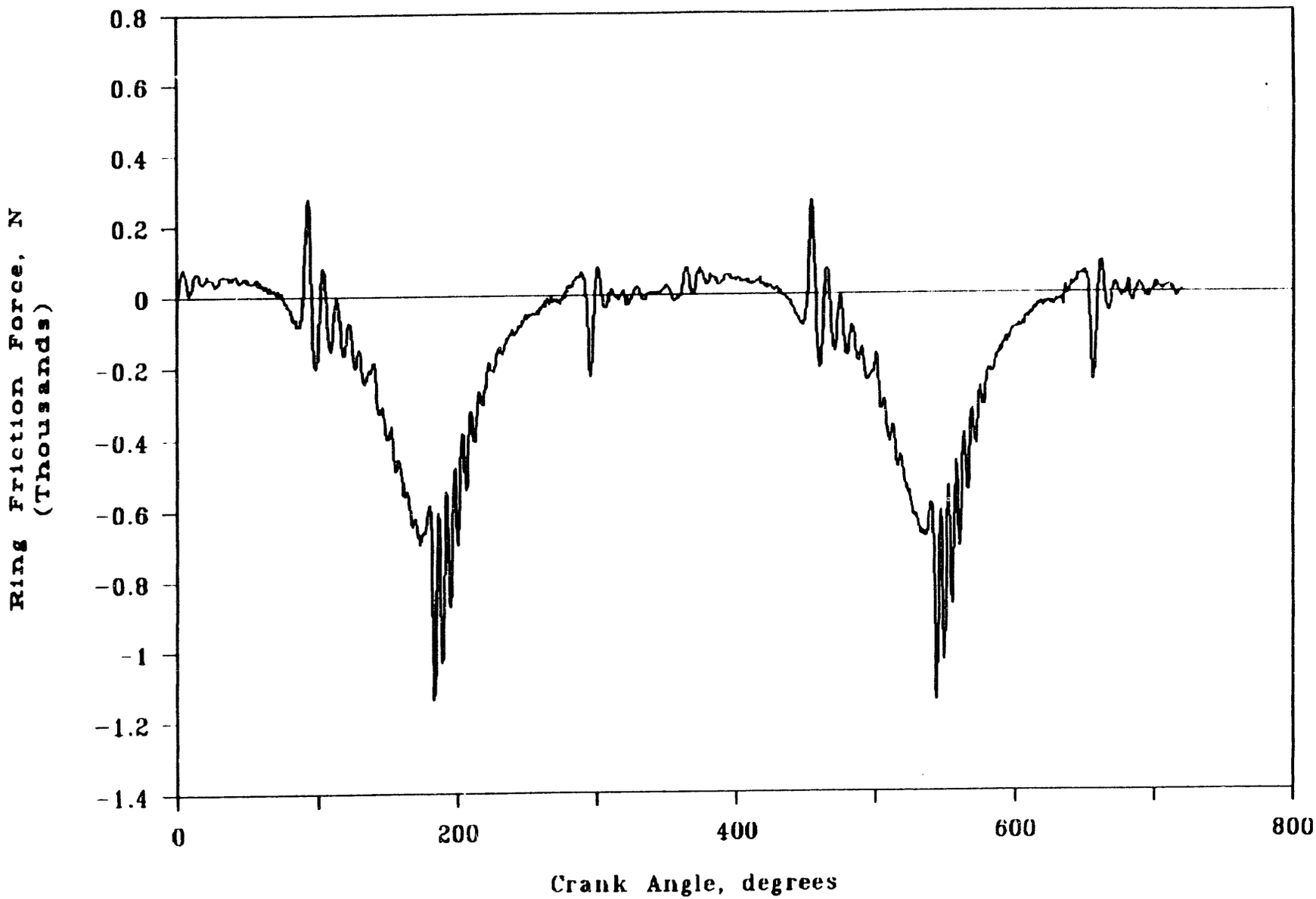

Figure 22. Piston Ring Friction Analysis Typical Ring Friction for Baseline Oil

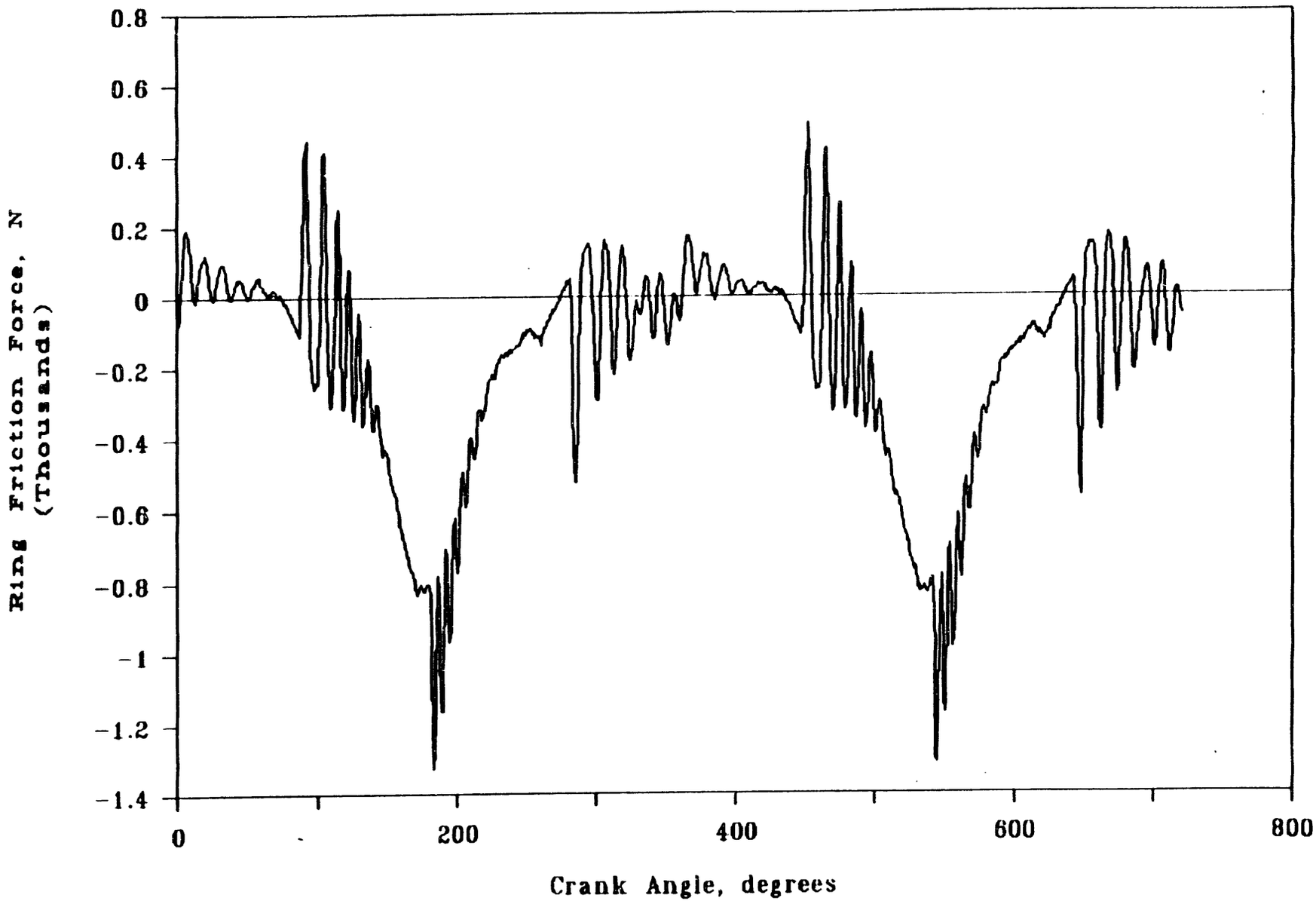

Figure 23. Piston Ring Friction Analysis Test #2; Start of Test Measurements

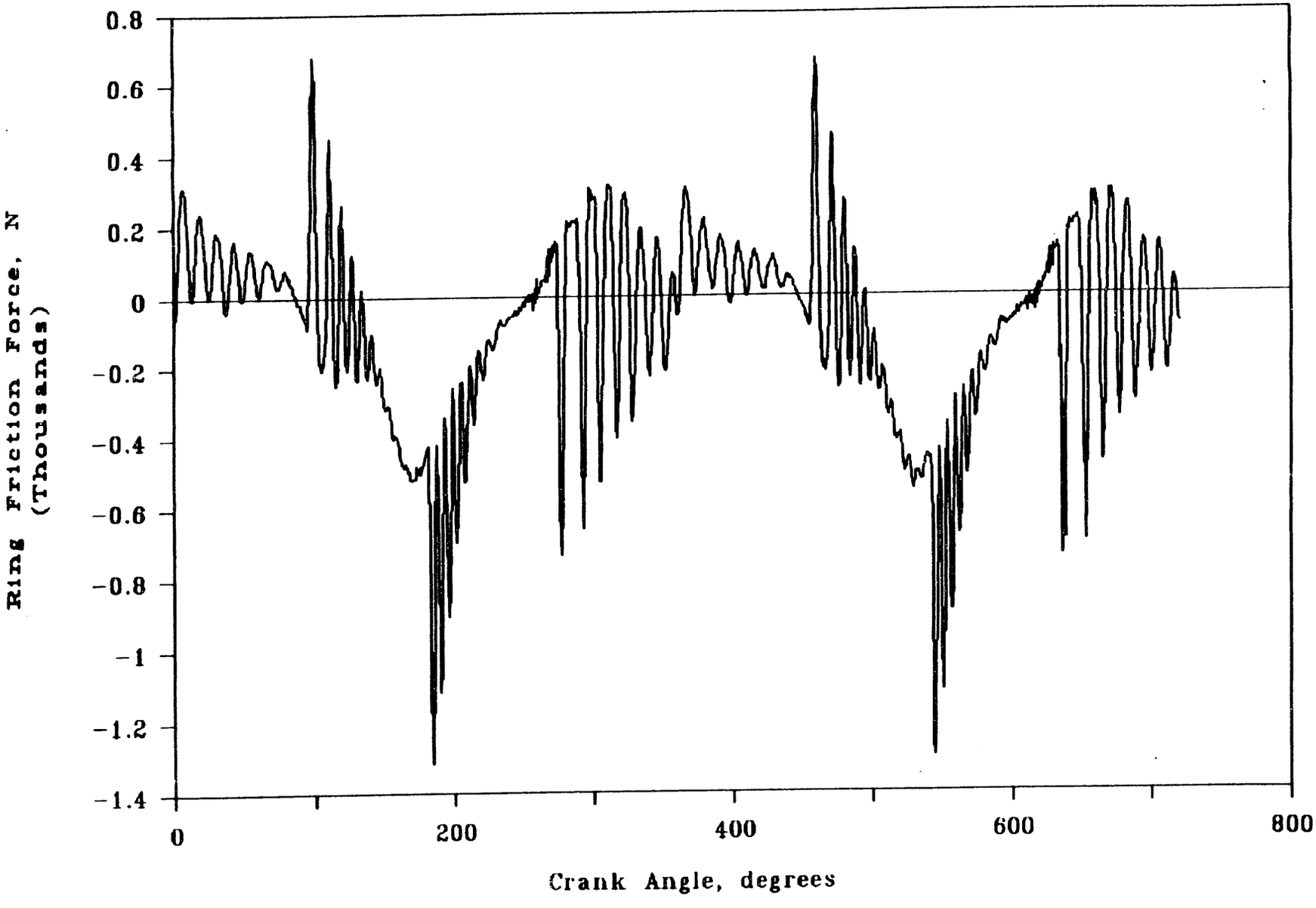

Figure 24. Piston Ring Friction Analysis Test #2; End of Test Measurements

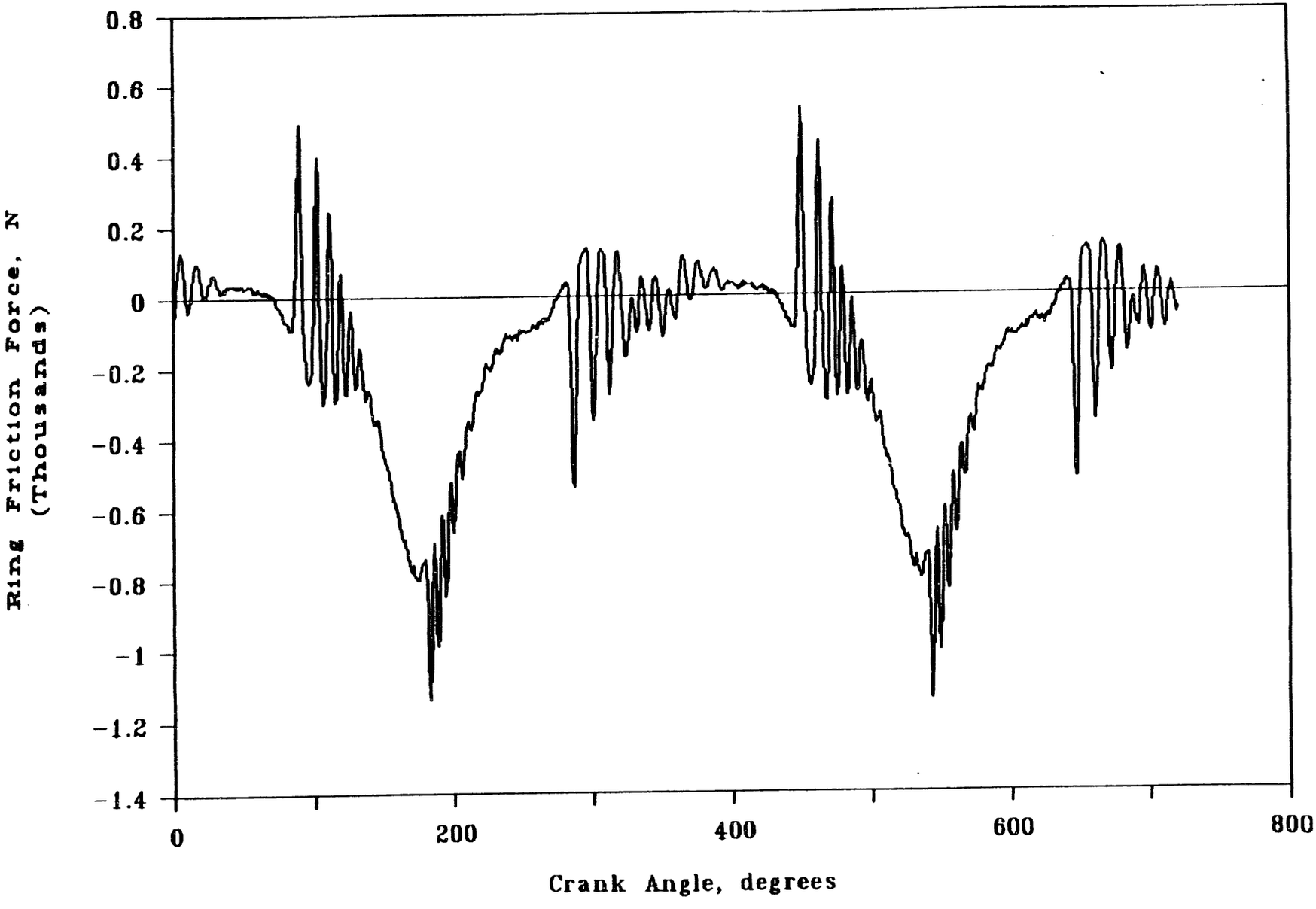

Figure 25. Piston Ring Friction Analysis Test #3; Start of Test Measurements

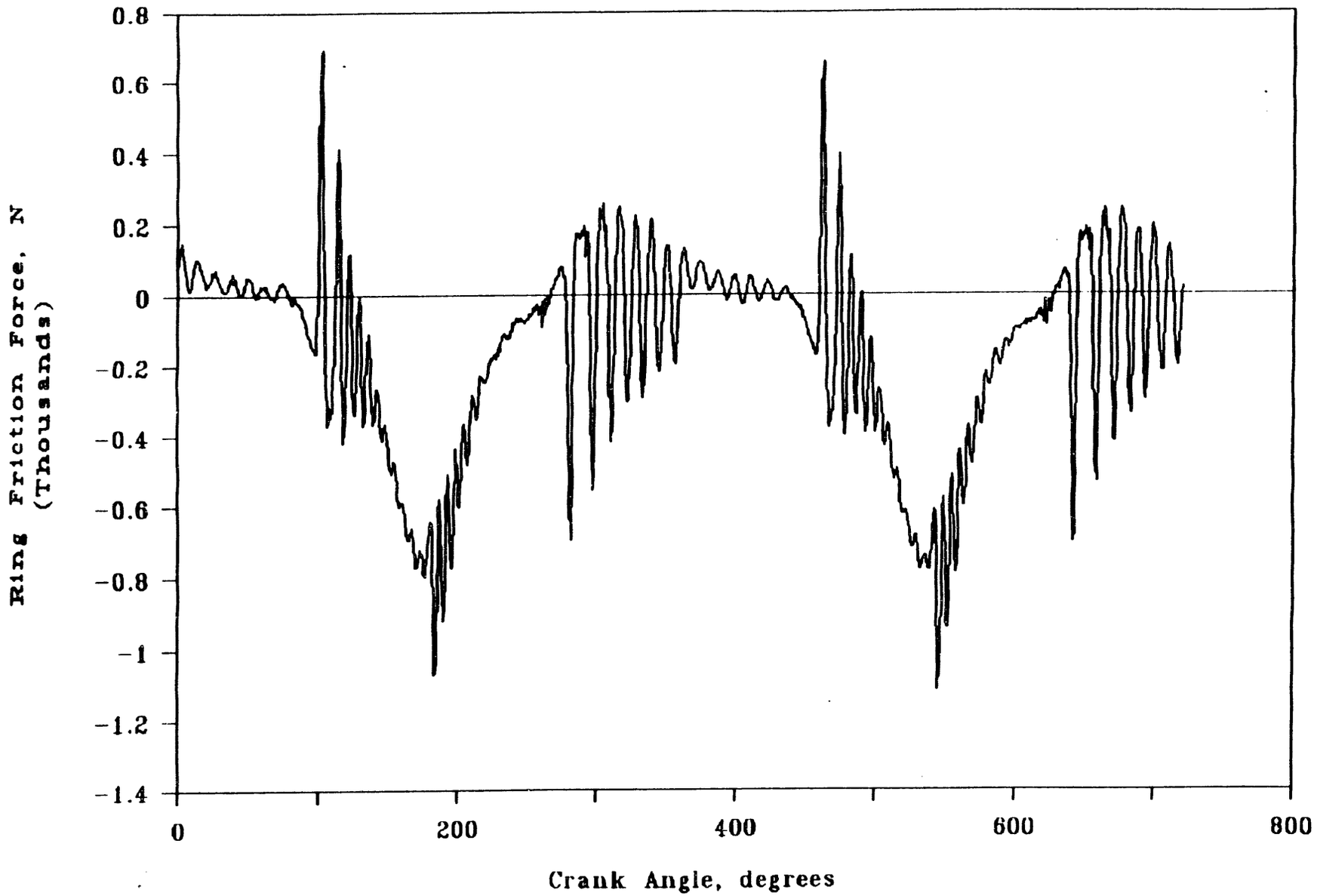

Figure 26. Piston Ring Friction Analysis Test #3; End of Test Measurements

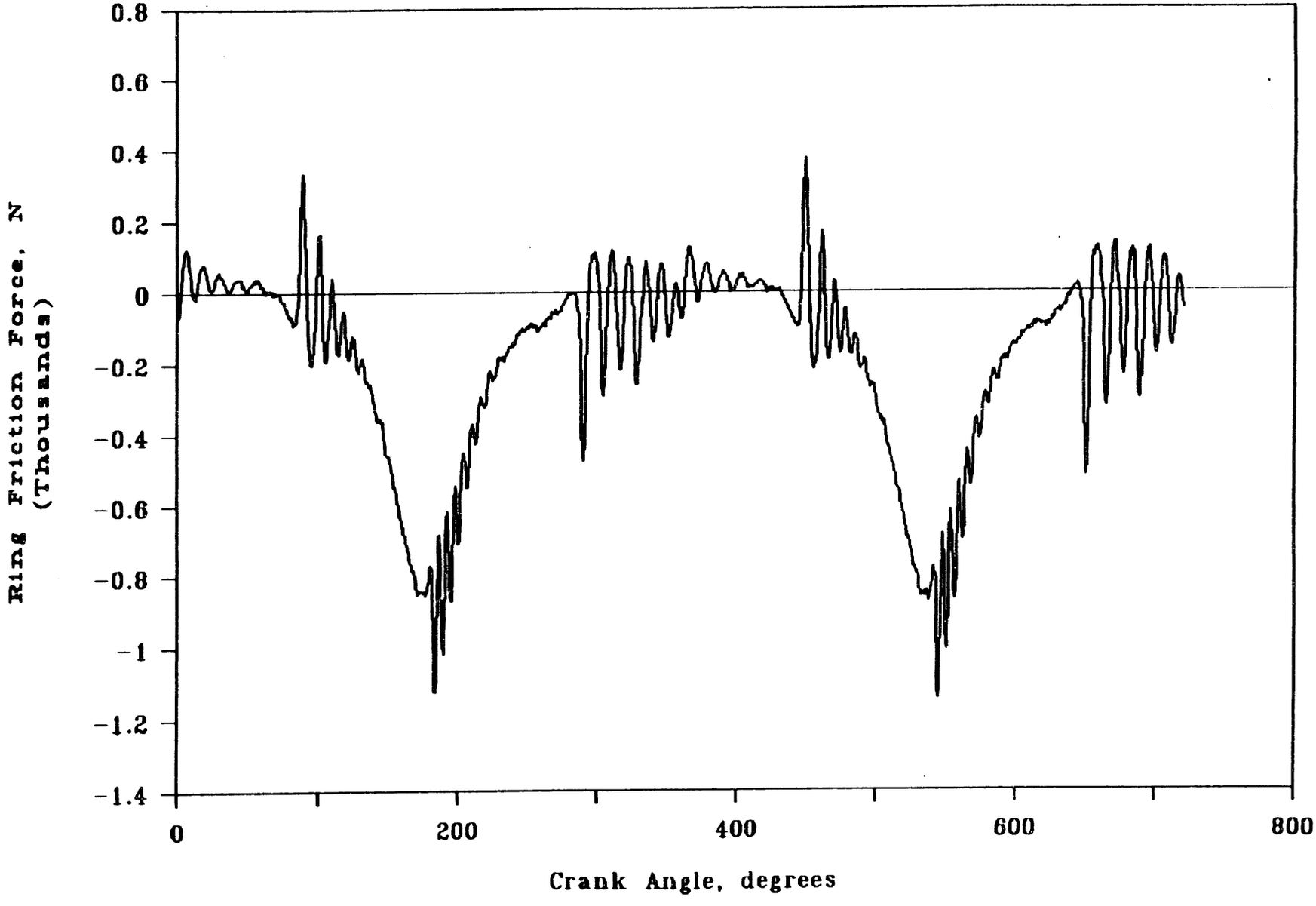

Figure 27. Piston Ring Friction Force Test #4; Start of Test Measurements

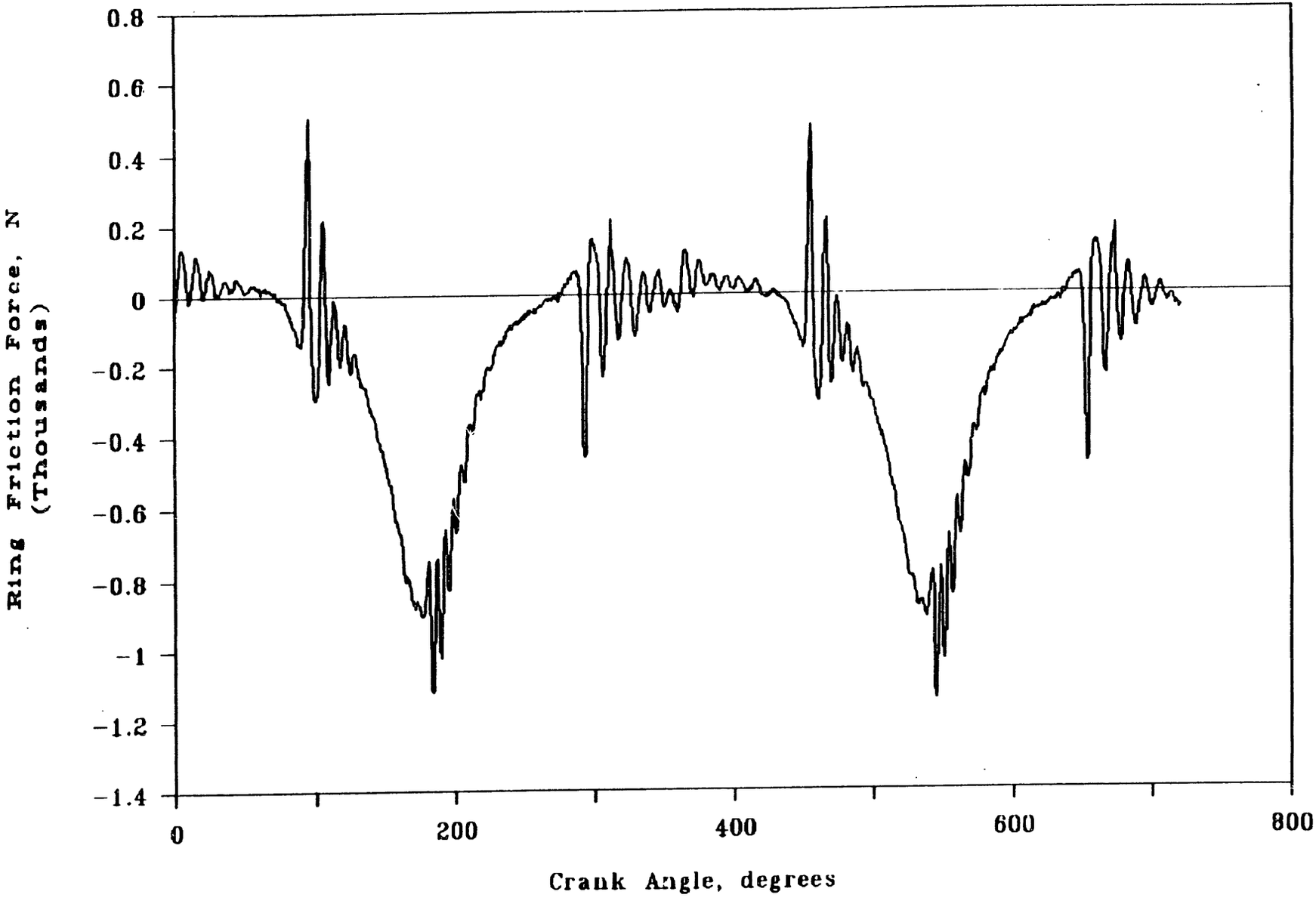

Figure 28. Piston Ring Friction Force Analysis Test #4; End of Test Measurements

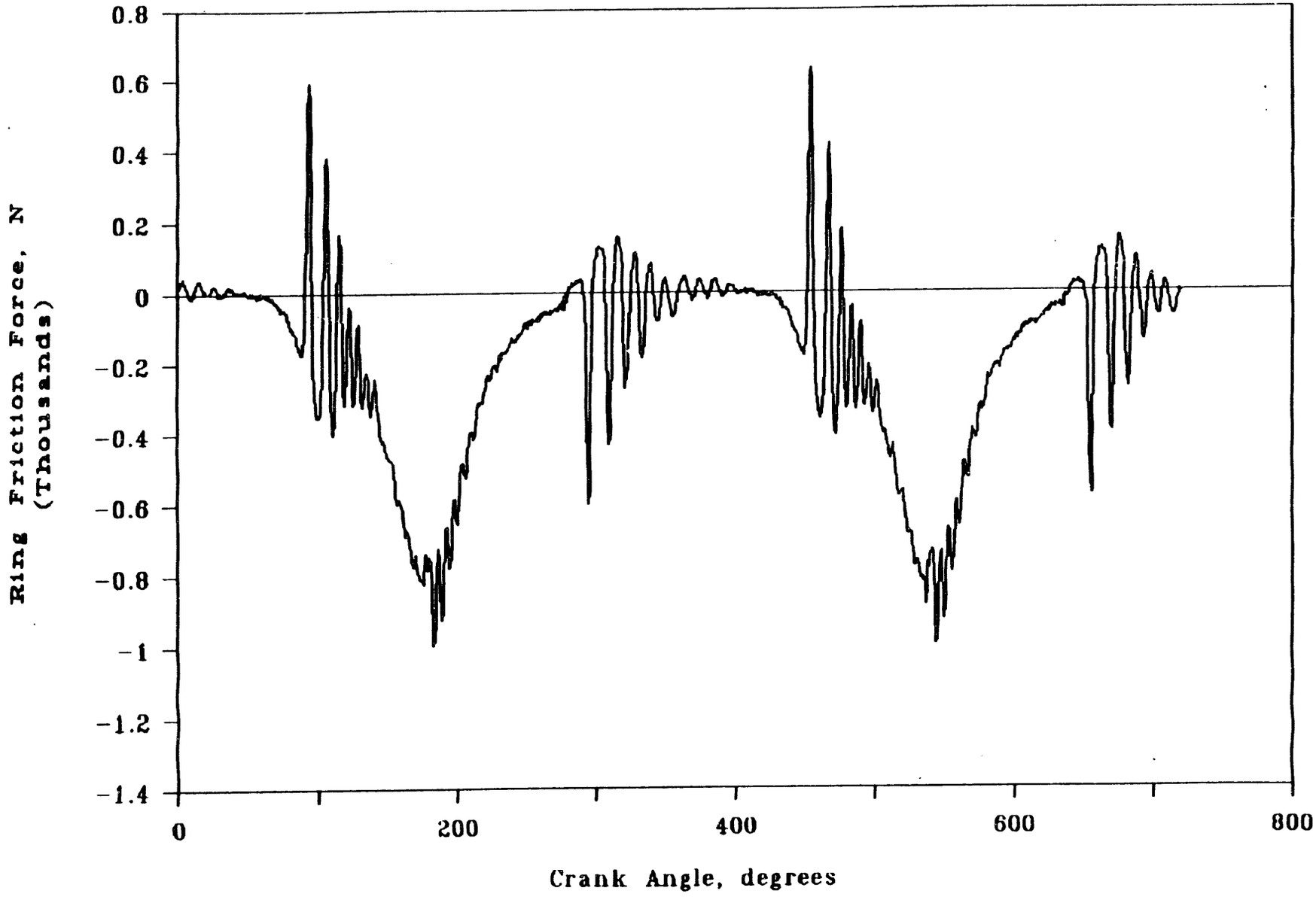

Figure 29. Piston Ring Friction Force Test #6, Start of Test Measurement

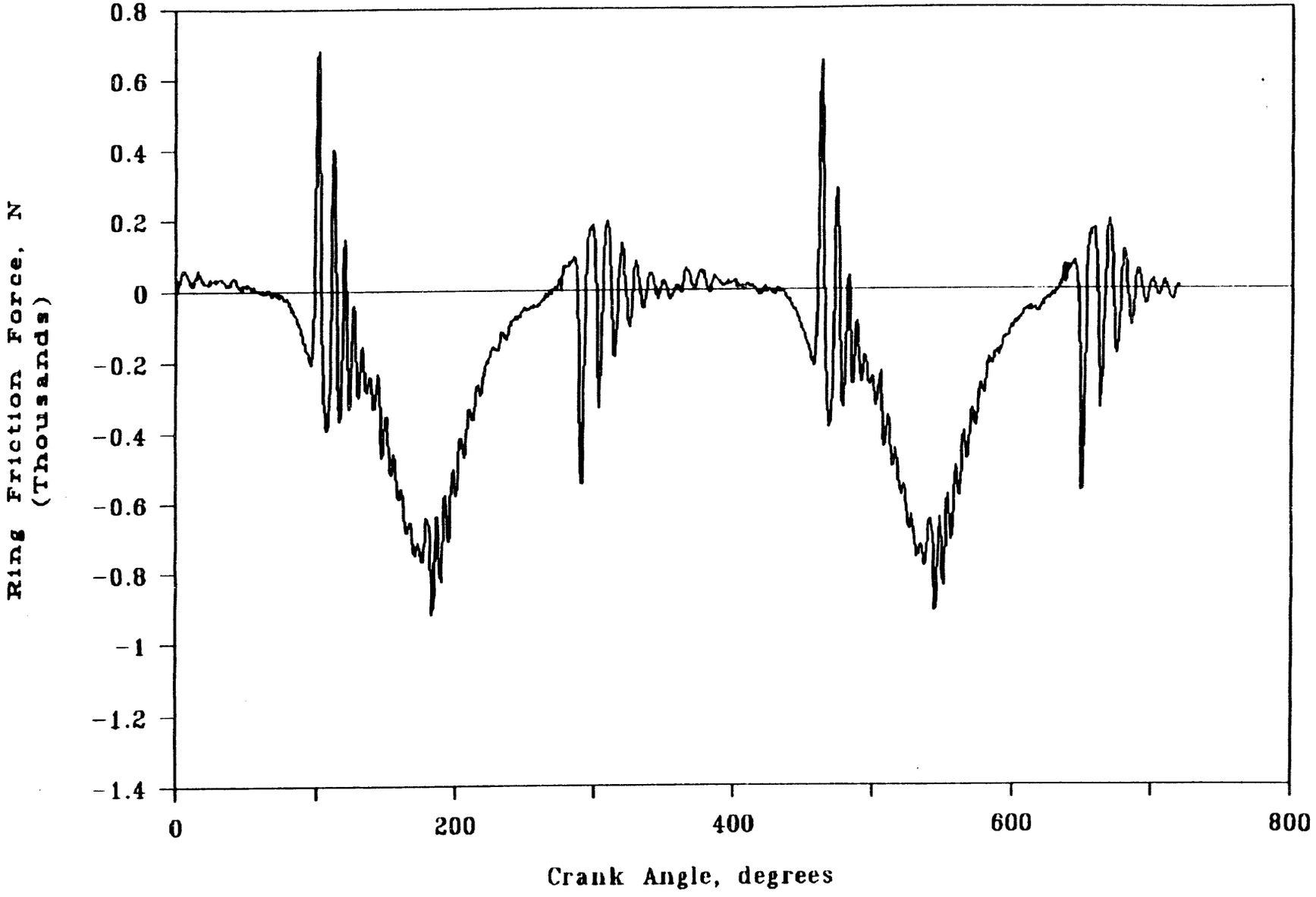

Figure 30. Piston Ring Friction Force Test #6; End of Test Measurement

Top dead center ring reversals are marked by a maximum friction at 180 and 540 crank angle degrees. Bottom dead center ring reversals at 360 and 720 crank angle degrees are characterized by maxima in the friction curve that are much smaller in magnitude. Gas loading of the rings is the cause of this difference in magnitude. (Negative forces simply indicate direction of ring motion and have no bearing on the magnitude of the forces.) Though the experimental set-up attempted to maintain constant compression and expansion pressures, the engine speed of 850 rpm was too fast to compensate for the specified check valve. The actual spikes seen at these points are probably due to the rings movement from one groove land to the other. Sticking or "chucking" of the rings could have caused this.

Comparing start-of-test results with end-of-test results it is apparent that ring friction has increased midway through its stroke. This is true for every test and includes both the compressive and expansion strokes. For example, peak friction in Figure 28 at 90 and 240 crank angle degrees was approximately 445 N and -445 N, respectively. By the end of the test, the friction force at 90 degrees had increased to almost 667 N and -623 N at 240 crank angle degrees. This increase could be due to the increased contaminant concentration at the ring/liner interface, or blow-by of gases past the rings. Also, lubricant temperatures rose somewhat during the course of each test, which may have influenced friction force traces as well.

3. Observation of Wear Surfaces

Two types of observations were made on the worn rings. The first was a measurement of the cumulative change in mass for each ring. The second consisted of visual inspection of the wear surfaces.

The ring used for the first four tests lost a total of 0.5339 grams. The second ring used in the confirmation tests lost a total mass of 0.1627 grams.

Visual analysis of the rings during end of test inspections revealed little information. Wear surfaces were clean and showed no evidence of wear patterns, uneven wear, scoring, scuffing, corrosion, or even excessive wear. In fact, surfaces were unusually bright, indicating that a "polishing" type wear process may have been occurring.

IV. Discussion

A. Observations on the Wear Mechanism

The purpose of this project was to study the mechanism by which contaminants in the lube oil cause accelerated wear in the piston rings and cylinders of coal fired diesel engines. The data presented above indicates that mechanism is fairly complex, and consists of at least two competing processes whose importance depends on the properties and concentration of the contaminants in the lube oil.

The first of those processes seems to be a soft-abrasive "polishing" type wear which involves carbon particles. It is seen most clearly in the test results run with carbon black as a contaminant. Cylinder piece wear scars were fairly flat with a few smooth rounded grooves, while ring pieces were highly polished. The mass loss data indicates higher wear on the cylinder piece, but a tendency for wear to level off as higher concentrations of contaminant are added. All of this is consistent with a process where the original honing marks on the cylinder are being polished off, followed by a much slower wear process on the smooth surfaces. The tendency for wear to slow down as the pieces become more highly polished suggests that this is a self-limiting process.

The second process seemed to become more important as ash content and contaminant concentration increased. Photomicrographs of the wear scars revealed the tendency for grooves to become deeper and sharper, but there was little evidence of embedded particles or holes where particles might have lodged in either the ring or the cylinder piece. Close inspection of the end of the wear track (on one of the cylinder pieces) revealed significant plastic deformation with what appeared to be several layers of deformed metal caused by successive strokes of the piston ring. This evidence suggests a three-body abrasive process is occurring, but the exact mechanism for metal removal is uncertain. Observations of the Kentucky Splint ash/oil mixture following completion of a four hour Cameron-Plint test revealed there were no curled chips, which are generally present if a chip-cutting type process is occurring. Other possibilities include fatigue processes, and adhesion of the metal to particle surfaces, but the most likely process seems to be a groove-forming mechanism. Abrasive particles are dragged through the wear scar, plowing grooves each time the ring passes. After going through several plastic deformations, the ridges on those grooves eventually break off forming wear particles. Material might also be pushed to the end of the wear track, where, once again it could break off due to successive plastic deformations.

Having described the most likely wear mechanisms, it is important to look at them in terms of the physical processes that are occurring in the engine. As discussed earlier, typical diesel engine wear is highest at the ring reversal points, and the Cameron-Plint tests were successful in recreating that phenomena. This is attributed to a breakdown of the hydrodynamic film as the relative velocity of the ring and cylinder approaches zero. Contaminants in the lube oil might have complicating effects on this process. They could change the rheological properties of the lubricant, causing a change in the thickness of the film, or the point at which the film breaks down in the cycle. The fact that higher wear was observed at the ring reversal points even when highly abrasive particles were present indicates that the formation of a hydrodynamic film is still occurring, and it is still beneficial to maintain that film as long as possible through the cycle.

Another important consideration is the ratio of hydrodynamic film thickness to contaminant particle size. Particles larger than the film thickness are likely to be pushed away from the wear zone (this also depends on the shape of the leading edge of the ring) and will not participate in the abrasive wear process. This may explain why reducing the particle size of the ash increased the wear to such an extent. The actual distribution of particles might also be important. Figures 31 and 32 are histograms of the ash particle size before and after grinding (histograms for the other contaminants are included in the appendix). They indicate that there were few particles smaller than approximately 10 microns in the original ash. If the hydrodynamic film thickness was around that same value, fewer of the particles could enter the wear zone. An ash with the same average particle size, but with a broader distribution might have caused significantly more wear.

Particle size may play a different role in the polishing process caused by carbon particles. Since those particles are generally much softer than the ash, they are more easily ground. This means that the larger particles are more likely to break up into smaller particles which can enter the wear zone. By the same token, however, particles in the wear zone will continue to break up until they are too small to cause significant wear. This may be another explanation for why the polishing process appears to be self-limiting. It should be noted, however, that in the actual engine processes, there will probably be a continual supply of new carbon particles to replace those already ground up.

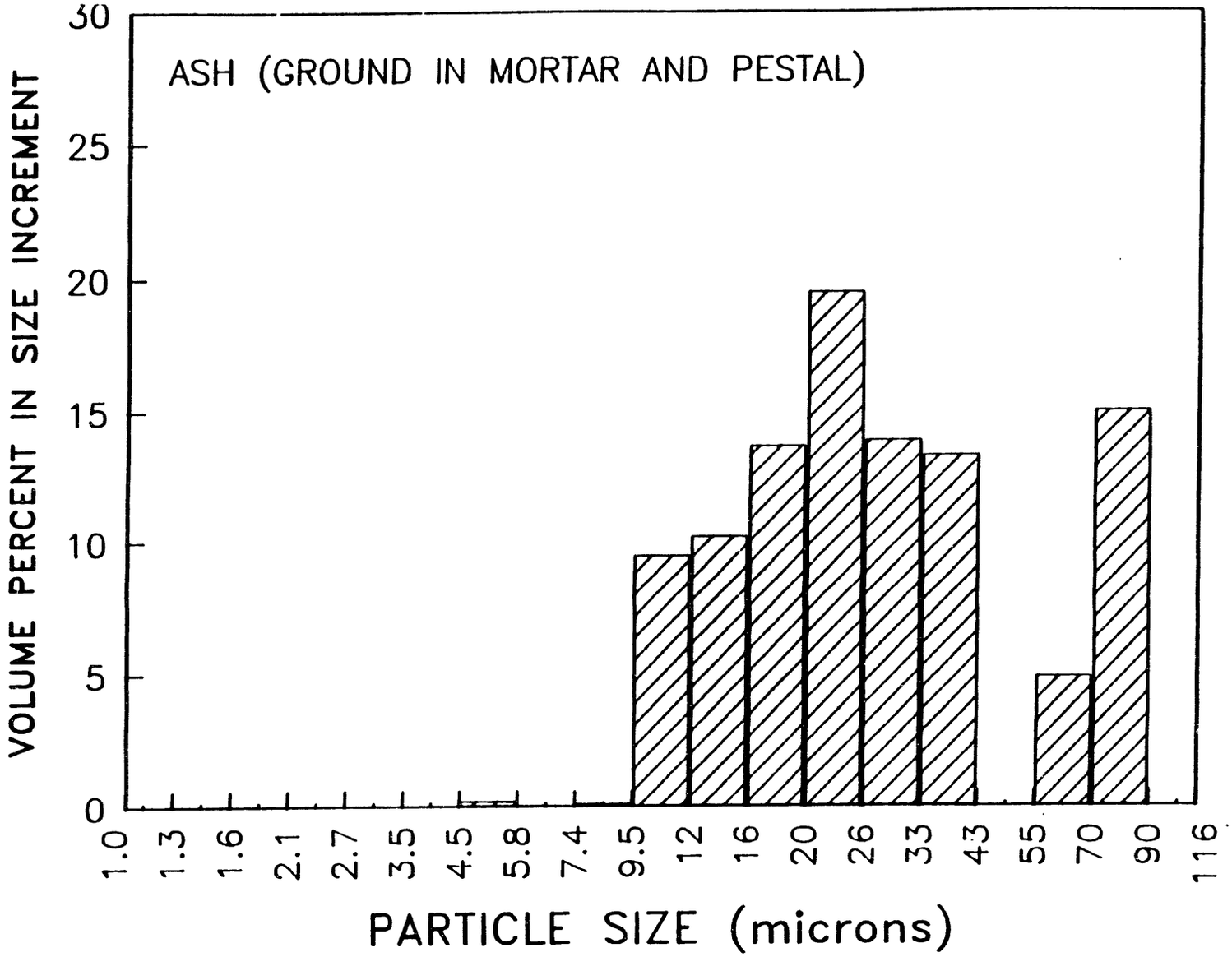

Figure 31. Volume Weighted Particle Size Distribution for K.S. Ash as Originally Ground in Mortar and Pestal

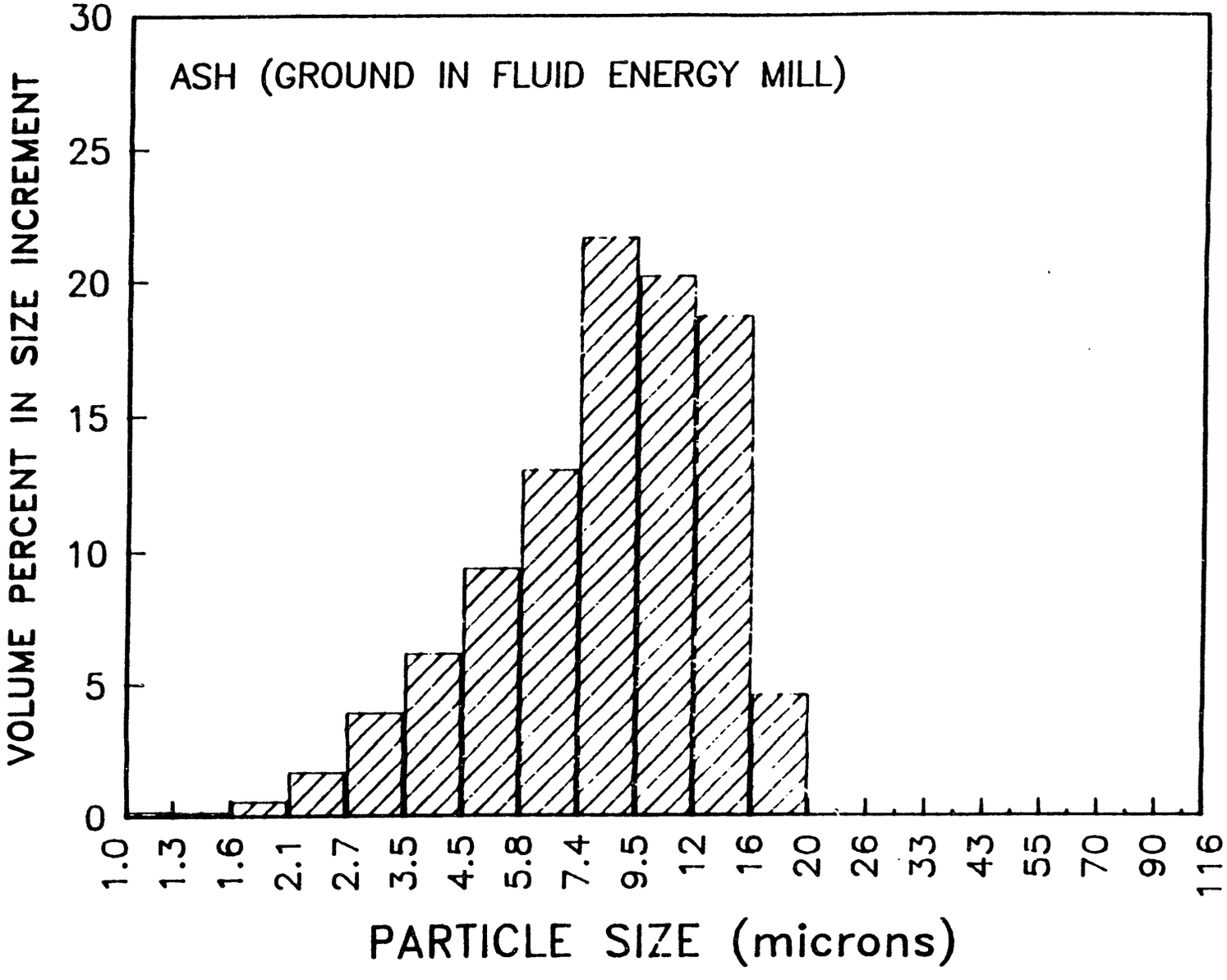

Figure 32. Volume Weighted Particle Size Distribution for Ash as Ground in Fluid Energy (Air) Mill

B. Comparison of Cameron-Plint and Engine Friction and Wear-Rig Results

Part of the basic approach of this program was to conduct wear tests in two separate apparatuses. The Cameron-Plint would provide detailed tests over a broad range of conditions in the test matrix, while tests in the Engine Friction and Wear-Rig would provide a more accurate simulation of the actual engine environment. Comparisons of wear rate results obtained with the two methods are shown in Figure 33 below. It is not surprising that the magnitude of the numbers are different given that they used different loads, were under different temperature conditions, had different means of supplying lubricant to the wear zone, and had different geometries. What is encouraging is the fact that, even with all those differences, the trends appear identical. In both cases, clean coal and raw coal results were fairly close, while wear was highly accelerated with the ash. Apparently, the wear-mode had not changed significantly in going from the Cameron-Plint bench apparatus to a more accurate simulation of the engine in the Engine Friction and Wear Rig.

C. Strategies For Wear Prevention

The above discussions suggest two possible modes of contaminated lube-oil induced wear in a coal-fired diesel engine. The strategy for reducing that wear is highly dependent on which mode is predominant in the engine. If low contaminant levels are causing a breakdown in hydrodynamic film leading to soft-abrasive polishing wear, then it may be possible to introduce chemically active additives which enhance boundary type lubrication and protect the surfaces. Chlorinated esters and tricresyl phosphate are examples of additives which form an organic film on the metal. If, on the other hand, the hard abrasive groove-forming mechanism is occurring the strategy would involve trying to reduce the abrasive interaction. Lubricant additives could be considered which coat the particles or the metal surfaces and allow particles to slide through the wear zone without sticking to the surface and plowing out a groove.

Also worth considering is the engineering of asperities in the metal wear surfaces. Ideally, one would design asperities which are large enough to provide avenues of escape for the medium to small size particles, while still being small enough to exclude the majority of highly abrasive large particles. Even if that can be done, however, the design must also consider the tendency for polishing wear to remove those asperities, and the need for oil retention, no matter what asperity geometry is chosen. It might also be worth investigating different shapes and orien-

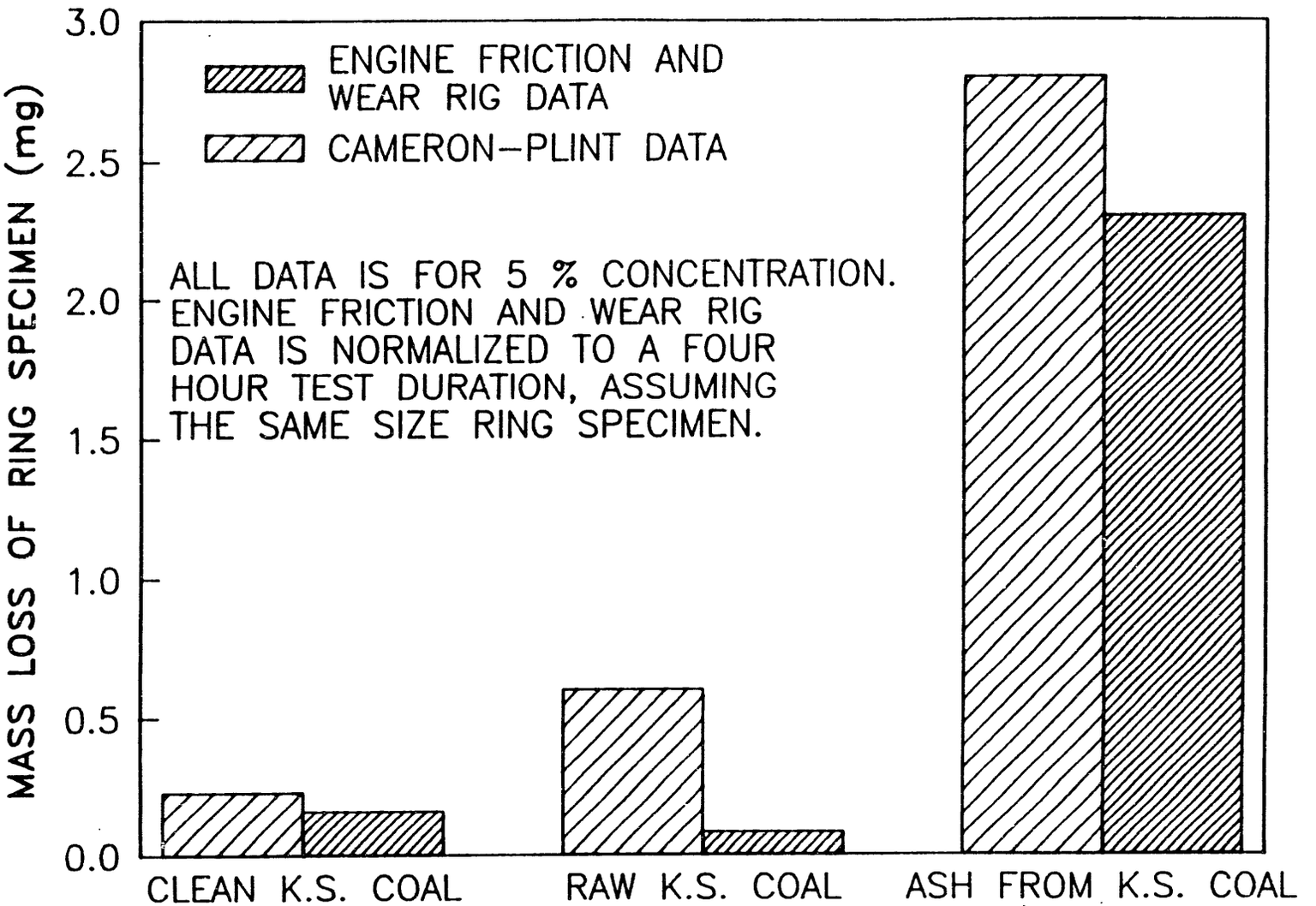

Figure 33. Comparison of Cameron-Plint vs. Engine Friction and Wear Rig Data

tations of asperities. For example, a circumferetial groove in the cylinder liner wall immediately before the point where hydrodynamic film breakdown is expected might allow for the escape of large particles which would otherwise be dragged through the entire stroke of the ring.

Another issue to consider is particle size distribution vs. hydrodynamic film thickness. If higher viscosity base lubricants can be chosen which provide thicker, longer-lasting films, then wear at the ring reversal points should be reduced. As long as most of the particles are significantly smaller than the typical film thickness this statement should hold true. On the other hand, if there are larger particles present, the thicker film may allow them to enter the wear zone and accelerate the wear process. Asperities are also known to have an effect on hydrodynamic film formation and thickness. The effects are somewhat complex, but it may be possible to enhance film formation, while at the same time preventing the inclusion of large particles into the wear zone.

V. Conclusions

The results of this study can be summarized in the following conclusions.

- Two wear mechanisms were observed in this study.
    - Soft abrasive polishing wear caused by carbon particles resulted in removal of honing marks and polishing of the surfaces, but seemed to be a self-limiting process.
    - Hard abrasive three-body wear caused by harder ash particles forming grooves in the wearing surfaces resulted in higher wear rates.
- Wear in all of these cases was dependent on the dynamic motion of the piston ring material indicating a mechanism which was accelerated by breakdown of the hydrodynamic film.
- The two independent means of testing wear used in this program; the Cameron-Plint machine, and the Engine Friction and Wear Rig; created similar wear trends, and are apparently operating in the same wear modes.

- There was significant difference between wear caused by a low-ash coal and wear caused by a cleaned high-ash coal contaminant. Since the ash content was similar, this suggests there may be some complex chemical effects on the boundary lubrication characteristics.

VI. References

Blatchley, C.C., et al., October 1985, "Boiler Circulation Pump Wear Monitoring: A Novel Technique Based on Surface Layer Activation," Joint ASME/IEEE Power Generation Conference, ASME Paper 85-JPGC-PWR-48

Blatchley, C.C. and Soshansi, P., May-June 1986, "Surface Layer Activation Technique for Monitoring and In Situ Wear Measurement of Turbine Components," Jet Propulsion, 3, 3, pp. 248-252.

Buckley, D.H., 1981, Surface Effects in Adhesion, Friction, Wear, and Lubrication, Elsevier Scientific Publishing Co., New York.

Cameron, A. and Pumphrey, G., June 27-29, 1983, "Assessment of Bore Polishing Properties of Lubricating Oils by Bench Tests" Esslingen Conference, W. Germany, Testing and Evaluation of Motor Oils.

Clingenpeel, J.M., Gurney, M.D., and Eccleston, D.B., 1984, "A Combustion and Wear Analysis of a Compression-Ignition Engine Using Coal Slurry Fuels," ASME Paper No. 84-DGP-8.

Dunn-Rankin, D. and Kerstein, A. R., 1988, "Influence of Ash on Particlbe Size Distribution Evolution During Coal Combustion," Combustion and Flame, Vol. 74, pp. 207-218.

Flynn, P.L., Leonard, G.L, and Mehan, R.L., 1989, "Component Wear in Coal Fueled Diesel Engine," ASME Paper 89-ICE-15.

Fusaro, R.L. and Schrubens, D.L., Oct. 5-8, 1987, "Tribological Properties of Coal Slurries," NASA Technical Memorandum 89930.

Gahr, K.H. Zum, 1988 "Modelling of Two-Body Abrasive Wear," Wear, Vol 124, pp. 87-103.

Gaydos, P.A., June 12, 1989, "Characterization of Oil Particulate from the Cooper JSI Engine Operating on Coal/Water Slurry," Topical Report to Arthur D. Little.

Hsu, B.D.., Jan. 1988, "Progress on the Investigation of Coal-Water Slurry Fuel Combustion in a Medium-Speed Diesel Engine: Part 1 and 2, Ignition Studies and Preliminary Full Load Test," ASME Papers 88-ICE-4 ,88-ICE-5.

Janczak, K.J. and Wisniewski, M.R., 1987, "Influence of Surface Roughness Parameters on Elastohydrodyamic Film Thickness," Wear, Vol. 115, p. 75-82.

Kahwani, R.M. and Kamo, R., Jan. 10-13, 1988, "Combustion Characteristics of Dry Coal Powder Fueled Adiabatic Diesel Engine," 1988 ETCE, New Orleans.

Kamo, R. and Valdmanis, E., 1988, "Tribological Properties of Some Selected Materials in a Coal-Fired Environment," Journal of the Society of Tribologists and Lubrication Engineers, Vol. 45, pp. 417-423.

Kanakia, M.D. and Lestz, S.J., May 1989, "Fuel System Component Wear With JP-8," Interim Report BFLRF No. 262, U.S. Army Belvoir Research, Development and Engineering Center , Materials, Fuels and Lubricants Laboratory, Fort Belvoir, VA, Contract No. DAAK70-87-C-0043.

Lane, G., Casale, P.G., and Chadwick, R.E., December 1987, "Development of Marine Lubricants for the Future Low and Medium Speed Engine," Petroleum Review, pp. 43-49.

Leonard, G., Hsu, B., and Flynn, P., March 1989, "Coal-Fueled Diesel Technology Development," Final Report, Work Performed Under Contract No. DE-AC21-85MC22181 for U.S. DOE Office of Fossil Energy by General Electric Co. Research and Development Center, DOE/MC/22181-2694 (DE89000984).

Likos, W. E. and Ryan, III, T. W., Jan. 1988, "Experiments with Coal Fuels in a High Temperature Diesel Engine, " ASME 88-ICE-29.

Mayville, R.A., 1989, "Abrasive Concentration Effects on Wear Under Reciprocating Conditions," Submitted to the International Conference on Wear of Materials, Denver, CO.

Mehan, R.L., 1988, "The Wear of Selected Materials in Mineral Oil Containing a Solid Contaminant," Wear, 124, p. 65-85.

Mecredy, H.E. and Jett B.T., April 21-23, 1987, "A Comparison of the Combustion Characteristics of Three Coal Slurry Fuels," METC Annual Heat Engines and Gas Stream Cleanup Systems CRM.

Milder, F.L., Armini, A.J., and Jones, G.W., February 1983, "The Use of Surface Layer Activation for Filter Design and Evaluation," SAE Paper 810329.

Misra, A. and Finnie, I., 1981, "Correlations Between Two-Body and Three-Body Abrasion and Erosion of Metals," Wear, Vol. 68, pp. 33-39.

Nydick, S.E., Porchet, F., and Steiger, H.A., October 1979, "Continued Development of a Coal/Water Slurry-Fired Slow-Speed Diesel Engine: A Review of Recent Test Results," Journal of Engineering for Gas Turbines and Power, Vol. 109, pp. 465-476.

Nydick, S.E.., Porchet, F., and Steiger, H.A., Feb. 15-18, 1987, "Continued Development of a Coal/Water Slurry-Fired Slow-Speed Diesel Engine - A Review of Recent Test Results," 1987 ETCE, Dallas, TX,.

Odi-Owei, S. and Roylance, B.J., 1986, "The Effect of Solid Contamination on the Wear and Critical Failure Load in a Sliding Lubricated Contact," Wear, Vol. 112, pp. 239-255.

Perrotto, J.A., Riano, R.R., and Murray, S.F., 1979, "Effect of Abrasive Contamination on Ball Bearing Performance," Lubrication Engineering, Vol. 35, No. 12, pp. 698-705.

Prater, J.T. and Courtright, E.L., Jan 1985, "Material and Coating Development Alternative Fuel Applications," Prepared for the U.S. Department of Energy Report #PNL-5259.

Pratt, T.N., Nov. 1982, "The EMD Engine and Blended Fuels - A Progress Report," Electro-Motive Division, General Motors Corporation.

Rao, A.K., Melcher, C.L., Shaub, F.S., Kimberley, J.A., Wilson, R.P. Balles, E.N., Jan. 10-13, 1988, "Operating Results of the Cooper-Bessemer JS-1 Engine on Coal-Water Slurry," 1988 ETC, New Orleans.

Richez, M., Winquist, K. and Storment, J. O., July 1983, "Theoretical and Experimental Study of Ring-Liner Friction," Final Report SwRI Project 05-9300, Prepared for Advisory Committee for Research, Southwest Research Institute.

Ryan, III T.W., Dodge, L.G., May 1984, "Development of Carbon Slurry Fuels for Transportation (Hybrid Fuels - Phase II)," Prepared for National Aeronautics and Space Administration, Lewis Research Center Under Contract DEN3-263 for U.S. Department of Energy Report No. DOE/NASA/0263-1.

Ryan, III T.W., et al., Feb. 10, 1989, "Coal-Fueled Diesel Systems Research" Final Report U.S. DOE Contract DEAC21-85MC22123.

Schneider, E.W., Blossfeld, D.H., and Balnaves, M.A., March 1988, "Effect of Speed and Power Output on Piston Ring Wear in a Diesel Engine," SAE Paper 880672.

Sekar, R.R., Wang, C.S., and Choi, U.S., August 1988, "Viscosity of Coal/Water Slurries at High Shear Rates," work sponsored by U.S. Department of Energy, Report #ANL/CNSV-66.

Shaub, H. and Wong, L.L., 1987, "A Real Time Radioactive Marker Technique for Measuring Valve Train Wear," SAE Paper 872156.

Torrance, A.A. and d'Art, J.M., 1986, "A Study of Lubricated Abrasive Wear," Wear, Vol. 110, pp. 49-59.

Urban, C.M., Mecredy, H.E., Ryan, III, T.W., Ingalls, M.N., and Jett, B.T., Jan. 1988, "Coal-Water Slurry Operation in an EMD Diesel Engine," ASME Paper 88-ICE-28.

Appendix

Histograms of Volume Weighted Size Distribution for Each Contaminant

VOLUME WEIGHTED SIZE DISTRIBUTION

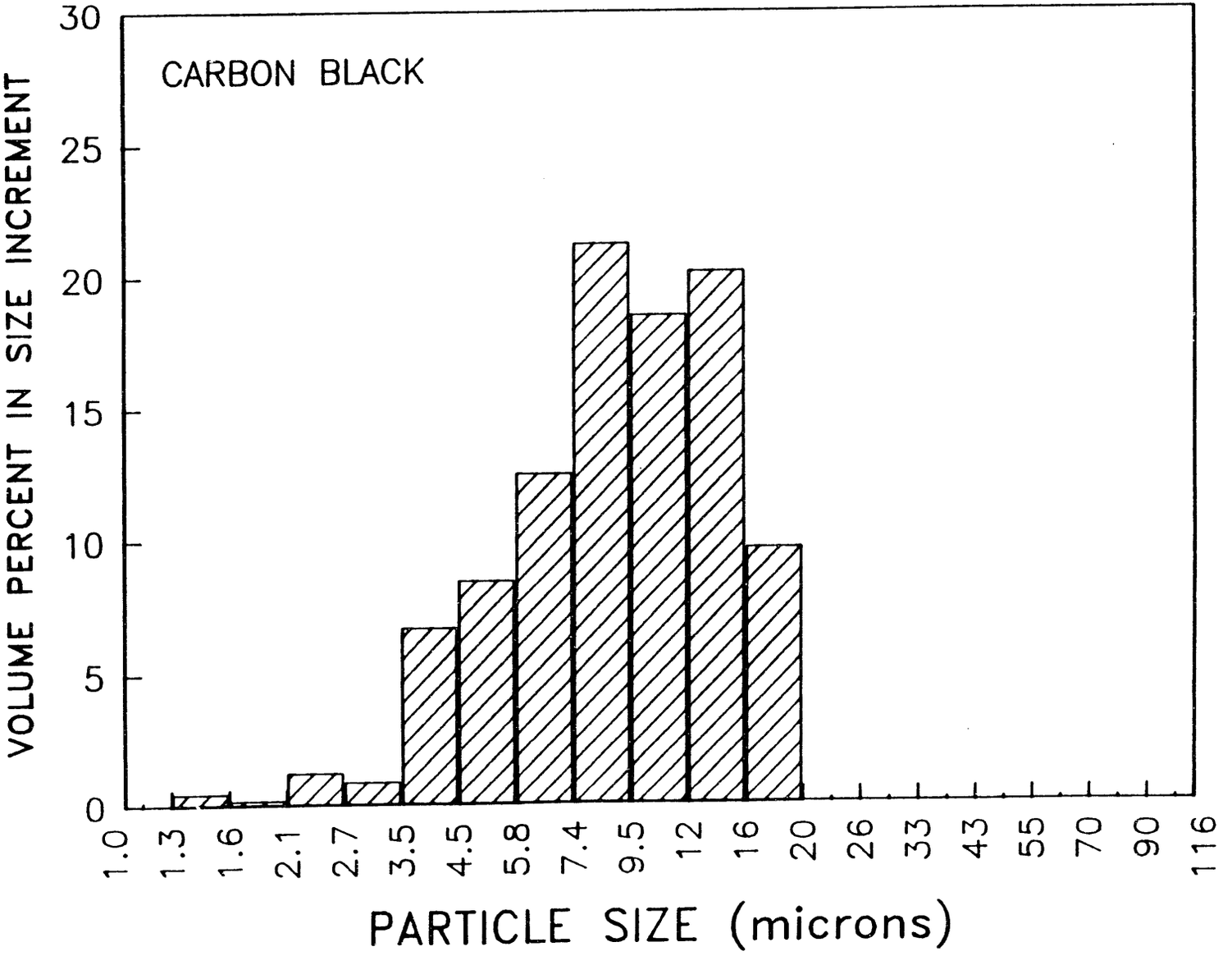

VOLUME WEIGHTED SIZE DISTRIBUTION

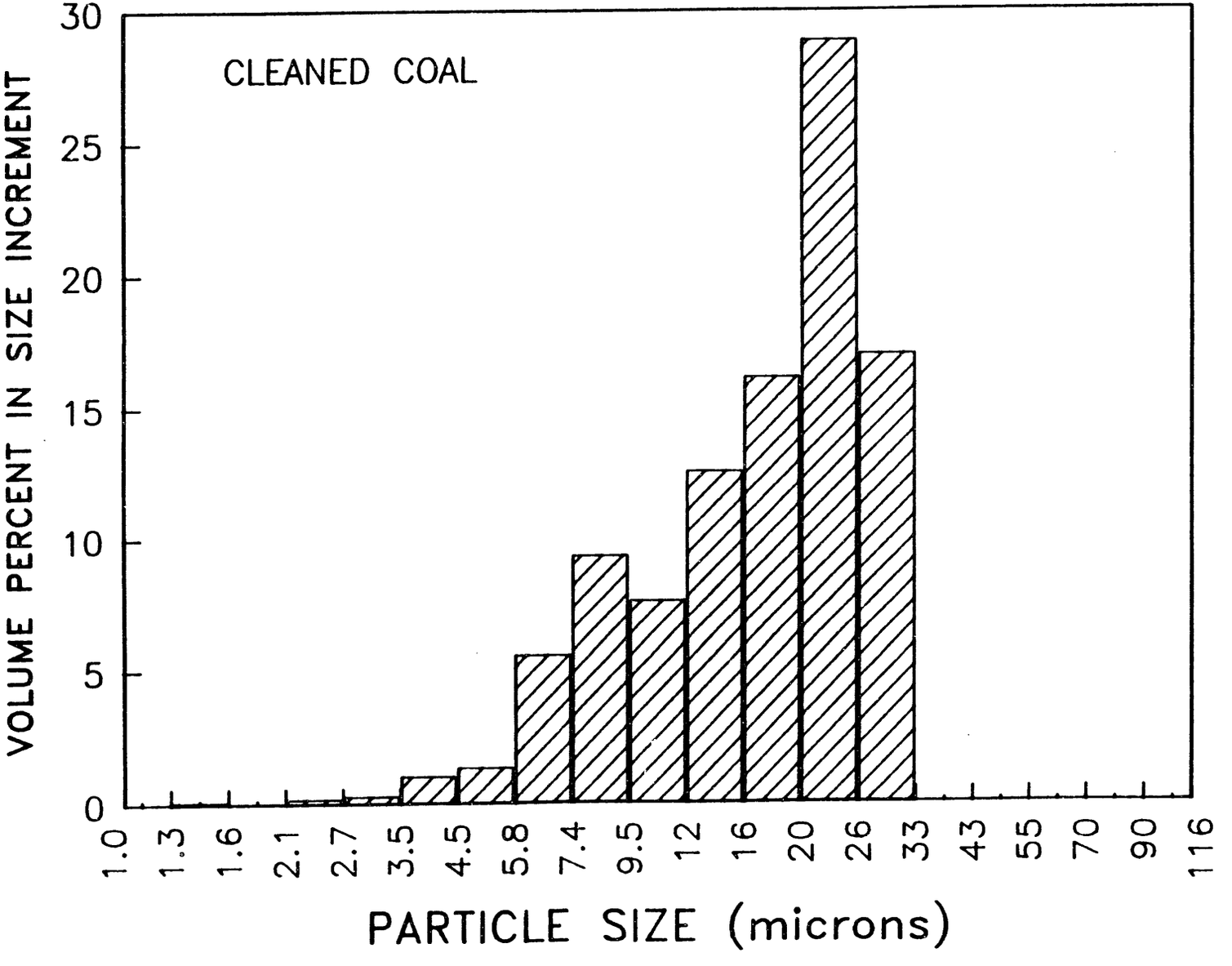

VOLUME WEIGHTED SIZE DISTRIBUTION

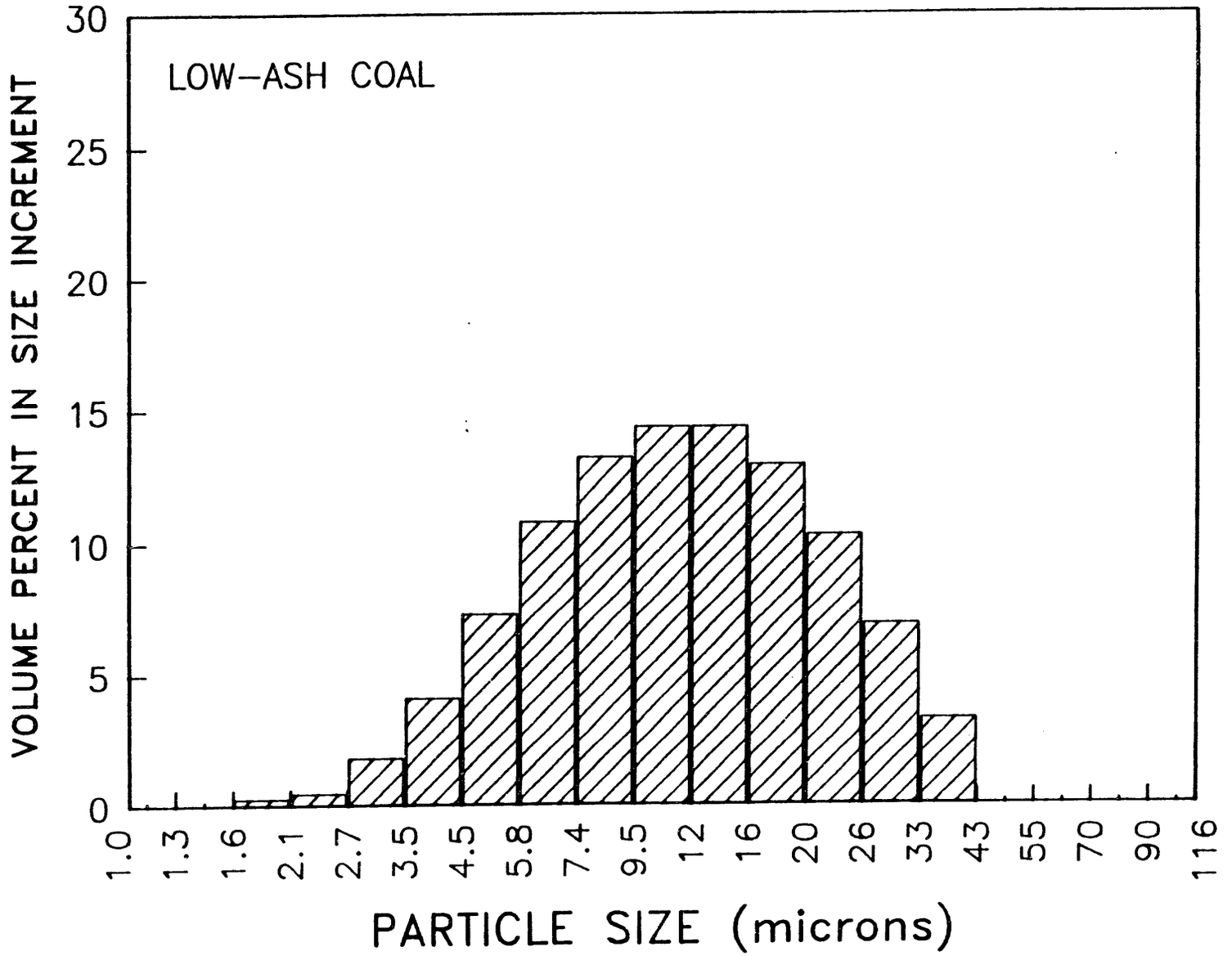

VOLUME WEIGHTED SIZE DISTRIBUTION

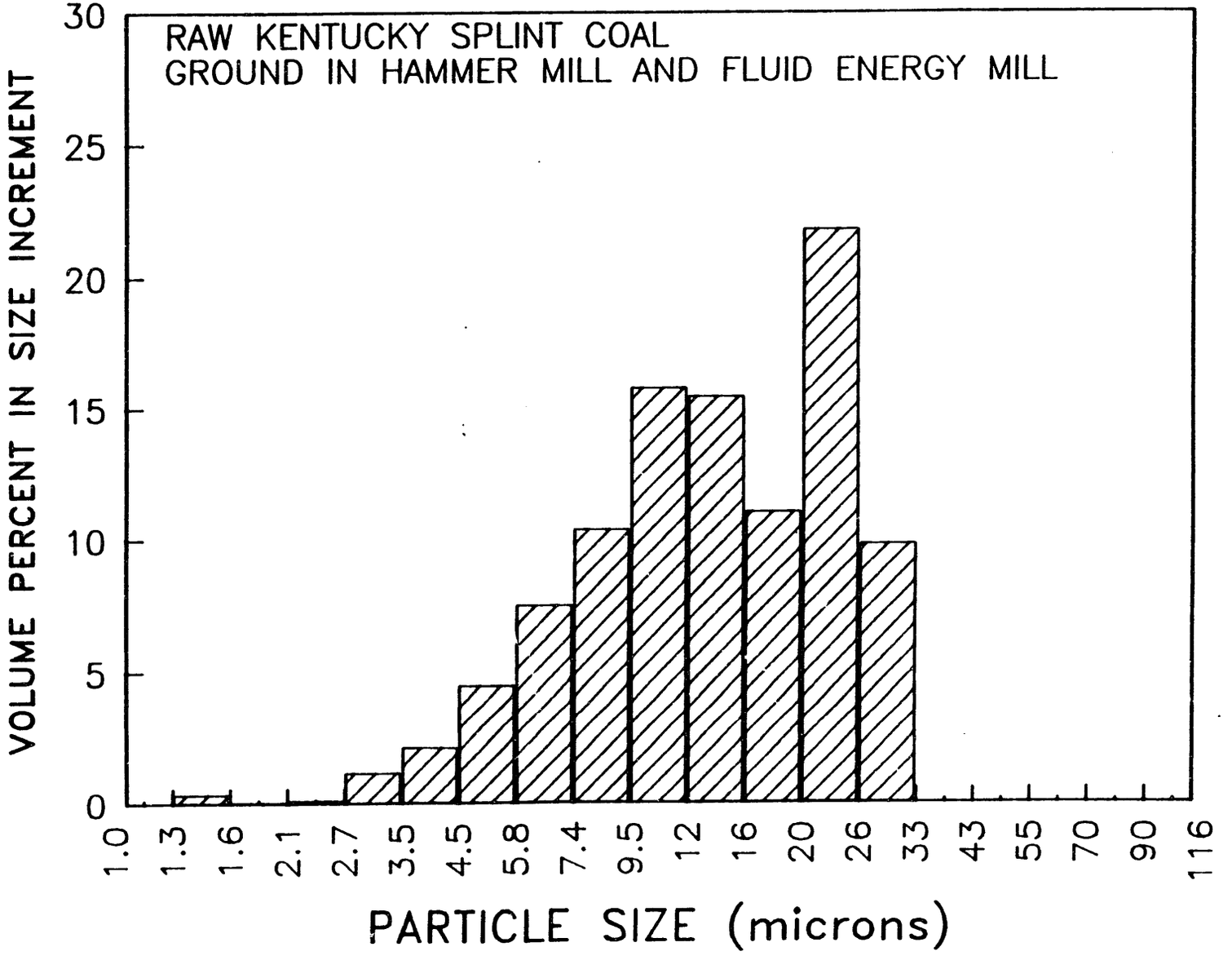

VOLUME WEIGHTED SIZE DISTRIBUTION

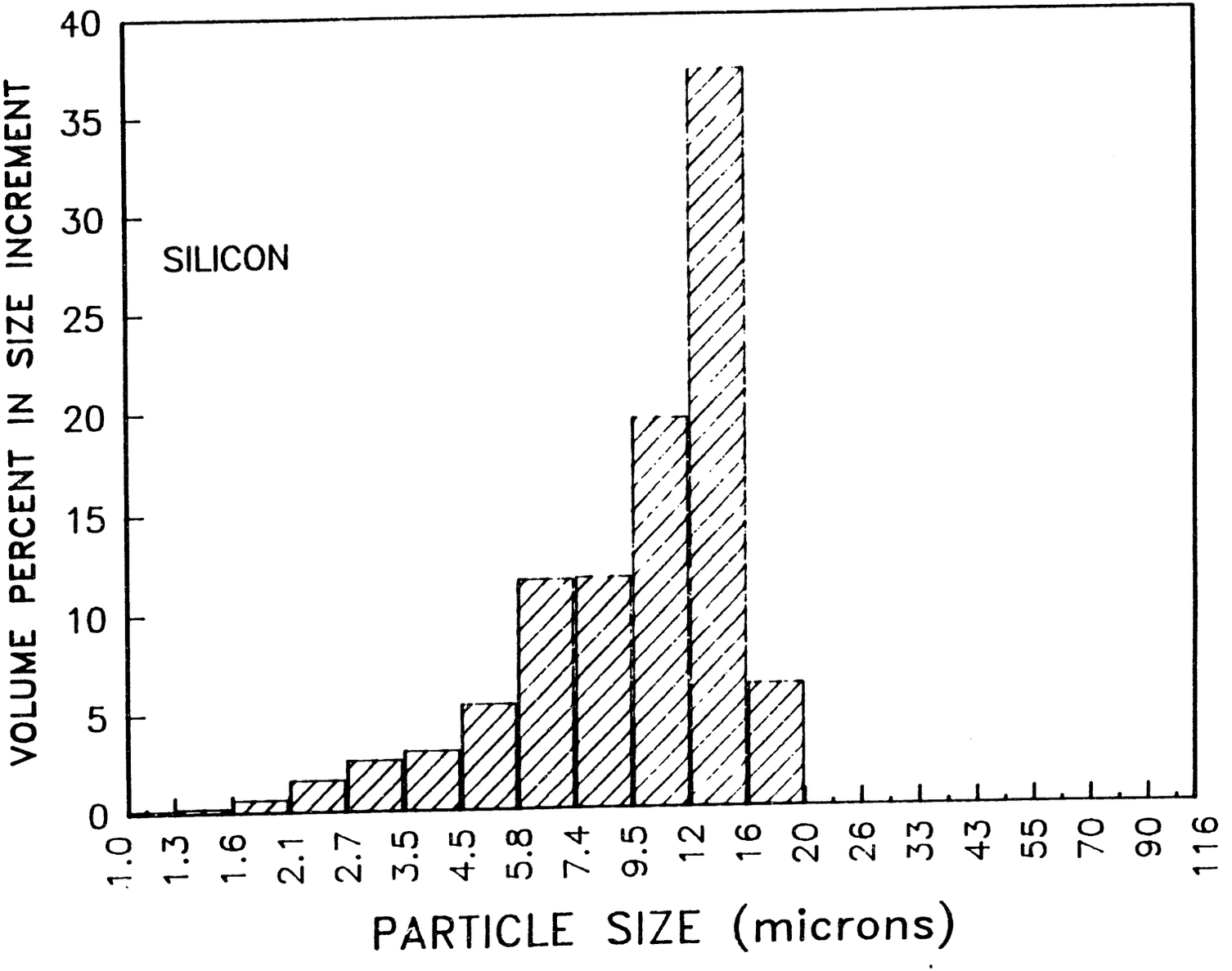

APPENDIX B

Task III - Traditional Approaches to Wear Prevention

WEAR MECHANISM AND WEAR PREVENTION IN COAL-FUELED DIESEL ENGINES

TASK III: TRADITIONAL APPROACHES TO WEAR PREVENTION

U.S. DOE Contract DE-AC21-88MC26044
Southwest Research Institute Project No. 03-3851

Prepared for:

U.S. Department of Energy
Morgantown Energy Technology Center
P.O. Box 880
Morgantown, WV 26507-0880

Prepared by:

James Schwalb, Research Engineer

Approved:

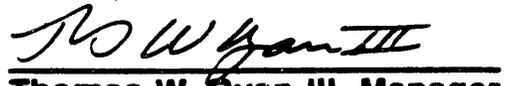

Thomas W. Ryan III, Manager
Combustion Technology
Department of Engine Research

TABLE OF CONTENTS

TABLE OF CONTENTS (Continued)

LIST OF TABLES

LIST OF ILLUSTRATIONS

LIST OF ILLUSTRATIONS (Continued)

ABSTRACT

Contamination of the lube-oil with hard abrasive particles leads to a three-body abrasive wear mechanism that highly accelerates piston ring/cylinder liner wear in coal-fueled diesel engines. One approach to reducing that wear is to modify the size and orientation of surface asperities on the cylinder to enhance the formation of a hydrodynamic film, and to provide avenues of escape for particles that would otherwise be trapped in the wear zone. Another approach is to introduce additives into the contaminated lube-oil that further enhance hydrodynamic film formation, form chemical films on the wearing surfaces, or form films on the contaminant particles. This work focuses on defining the effects of cylinder liner surface finish, various configurations of slots in the cylinder liner surface, and various additives in the contaminated lube-oil on the wear process. Wear tests were initiated in a bench apparatus using coal-ash contaminated lube-oil to test the various wear configurations.

The results of these tests indicate that the formation of a hydrodynamic film between the ring and cylinder specimens is enhanced by increasing surface roughness, and by orienting the surface asperities normal to the direction of ring travel, but modifications to the cylinder liner surface did not greatly reduce the wear rate. Additives to the lubricant seemed to have a much more significant effect on wear, with a dispersant additive highly accelerating the wear, while a detergent additive was able to reduce the wear almost to the rate achieved when there was no contaminant.

I. INTRODUCTION

This report covers Task 3 of a seven-task program entitled "Wear Mechanisms and Wear Prevention in Coal-Fueled Diesel Engines." The program is a study of piston ring and cylinder liner wear, in support of the DOE line programs at General Electric and A.D. Little/Cooper Bessemer to develop commercially viable coal/water slurry fueled locomotive and stationary diesel engines. Overall, the line programs have concentrated their efforts on developing harder liner and ring materials or coatings. This program, on the other hand, looks at alternative strategies for wear prevention. It was outlined to provide a more fundamental understanding of the wear processes (already completed in Task 1), to investigate novel design approaches to wear prevention (Task 2), to investigate traditional approaches to wear prevention (reported here in Task 3), and to refine and present the most promising wear prevention strategy (Tasks 4 - 6). Task 7 was recently added as a parallel study of wear in a locomotive engine fueled with a coal-derived liquid fuel.

Task 3, entitled "Traditional Approaches to Wear Prevention," focussed on determining the effects of the following three parameters on wear in the abrasive coal/water slurry fueled engine environment.

- Cylinder Surface Finish Conditions
- Various Configurations of Slots in the Cylinder Surface
- Various Additives to the Lube-Oil

After presenting some background information on the nature of the wear problem, this report will describe the experiments performed to study each of the above items.

II. BACKGROUND

Interest continues in the development of coal/water slurry fueled diesel engines that could utilize the large U.S. coal reserves and reduce dependence on foreign oil. Among the obstacles to development is accelerated wear of piston rings and cylinder liners, reported to be as high as 150 times that of engines running on conventional diesel fuel (Kamo and Valdmanis, 1988; Clingenpeel, et al., 1984; Prater and Courtright, 1985; Nydick, et al., 1987; Hsu, 1988; Leonard, et al., 1989; Rao, et al., 1988; Kakwani and Kamo, 1988; Pratt, 1982). This project is an effort to define the mechanisms causing accelerated wear, and to find commercially acceptable means of reducing or preventing it. A previous paper (Schwalb, et al., 1990) analyzed the literature in this subject, and concluded that, although a significant amount of work had been done and a general understanding of the effects of contaminated lube-oil has been obtained, there was still a need for a detailed understanding of the wear mechanism. An in-depth investigation was outlined involving bench scale wear tests with various coal-related contaminants introduced into the lube-oil. The results revealed a complex wear mechanism involving soft abrasive "polishing" type wear caused by carbon particles, and hard abrasive three-

body wear caused by hard minerals in the coal. The carbon wear process was significant, but seemed to be self-limiting, while the hard abrasive process continued to increase with concentration of abrasive. This seems consistent with the literature that indicates that carbon can be of concern (Yahagi (1987) and Berbezier, et al. (1986) are examples of studies concerned with accelerated wear caused by soot) but that the harder minerals found in the ash are the primary focus of most of the engine test research. Flynn, et al. (1989) present an example of the type of wear observed in engine tests where a nitrided cylinder surface appeared polished after wearing. Aghan and Samuels (1970) suggest that this is an abrasive wear mechanism, identical to the mechanism caused by larger particles which result in much rougher surfaces. It should be noted that adhesive wear also remains a possibility. Rabinowicz and Mutis (1965) and Sudarshan and Bhaduri (1983) reiterate the fact that adhesive wear commonly occurs at TDC in engines operating on diesel fuel, and may be occurring in conjunction with abrasive wear in the coal-fueled engines.

Having established some understanding of the wear mechanisms, the question remains of how to reduce or eliminate the accelerated wear process in a way that is economically acceptable. Typically, researchers (Kamo and Valdmanis, 1988; Prater and Courtright, 1985; Mehan, 1988; Flynn, et al., 1989) have concentrated on hardening the liners and rings, making them more resistant to the wear process. Hardening has reduced wear, but serious questions remain about the economic feasibility of the various hardening processes. The approach of this study was to look at more conventional approaches which depend on the unique interactions of particle size, hydrodynamic film thickness, surface finish, surface geometry, and lubricant formulation.

For example, it is known that particles much larger than the hydrodynamic film thicknesses do not participate in the wear process because they simply cannot get into the wear zone (Fitzsimmons and Clevenger (1975), Ives, et al. (1988) and Mehan (1988) observed this phenomenon). One might conclude that it is advantageous to have a thin hydrodynamic film and somehow eliminate smaller particles from the contaminant. On the other end of the spectrum, it is known that particles much smaller than the hydrodynamic film thicknesses do not cause significant wear either. If this is the case, then it may be advantageous to maximize hydrodynamic film thickness while minimizing the particle size.

Wear will also be influenced by changing surface finish. Traditionally, surface finish practices have been determined by trial and error experience over the years (Hesling, 1963). Plateau hones in the range of R_a = 0.5 to 0.75 micron and cross-hatch angles from 22° - 32° were the generally accepted specifications, chosen because it was felt they accomplished the following goals.

- As suggested by Sreenath and Raman (1976), they provide a fairly rough initial surface that promotes quick conformance ("seating") of the ring to the cylinder geometry.

- The large grooves store oil to prevent scuffing at start-up and at times of overloading.

- There is a hydrodynamic effect caused by thermal expansion of oil in the grooves.

- It was speculated that the grooves act as a repository for wear particles (Barber, et al., 1987).

How can surface finish be used to reduce wear? For one thing, the items listed above suggest that large grooves might provide repositories, or avenues of escape for abrasive particles that might otherwise enter the wear zone. Also, Janczak and Wisniewski (1987) and Richez, et al. (1983) suggest that increased surface asperity height can increase the hydrodynamic film thickness. On the other hand, rougher surface finish increases the risk of adhesive wear, and could allow more and larger abrasive particles into the wear zone.

The above discussions illustrate some of the tradeoffs that exist between particle size, hydrodynamic film thickness, and surface finish. The approach of this study was to investigate those interactions in a bench scale simulation of the engine wear environment. Tests were completed under varying conditions of contaminant particle size, cylinder liner surface roughness, orientation of asperities on the surface, cylinder surface slot configurations, and lubricant formulations. Comparisons were made based on detailed analysis of the wear specimens.

III. EXPERIMENTAL APPARATUS AND PROCEDURES

A. The Cameron-Plint High-Frequency Friction Machine

The apparatus chosen for these tests is the Cameron-Plint high frequency friction machine. The commercially available machine, shown schematically in Figure 1, provides a reciprocating motion through a scotch yoke drive mechanism that simulates the relative motion of the piston ring and cylinder liner in a diesel engine. A specimen of piston ring material is mounted to the bottom of a reciprocating arm where it can rub against a rigidly mounted cylinder liner specimen. Both the ring and cylinder specimens are immersed in a bath containing the contaminated lubricant being tested. Above the reciprocating arm is a spring tensioned bar that applies a force normal to the direction of travel. The arm is also instrumented to measure friction force (force in the direction of ring travel) and electrical resistance between the ring and cylinder specimens (an indication of the thickness of the hydrodynamic film). Friction force and electrical resistance measurements were monitored for some cases on an oscilloscope where cycle resolved information was obtained, and for all cases on a strip-chart recorder where a time-averaged signal was recorded. Details of how the Cameron-Plint machine was configured for all the tests reported here are contained in Table 1.

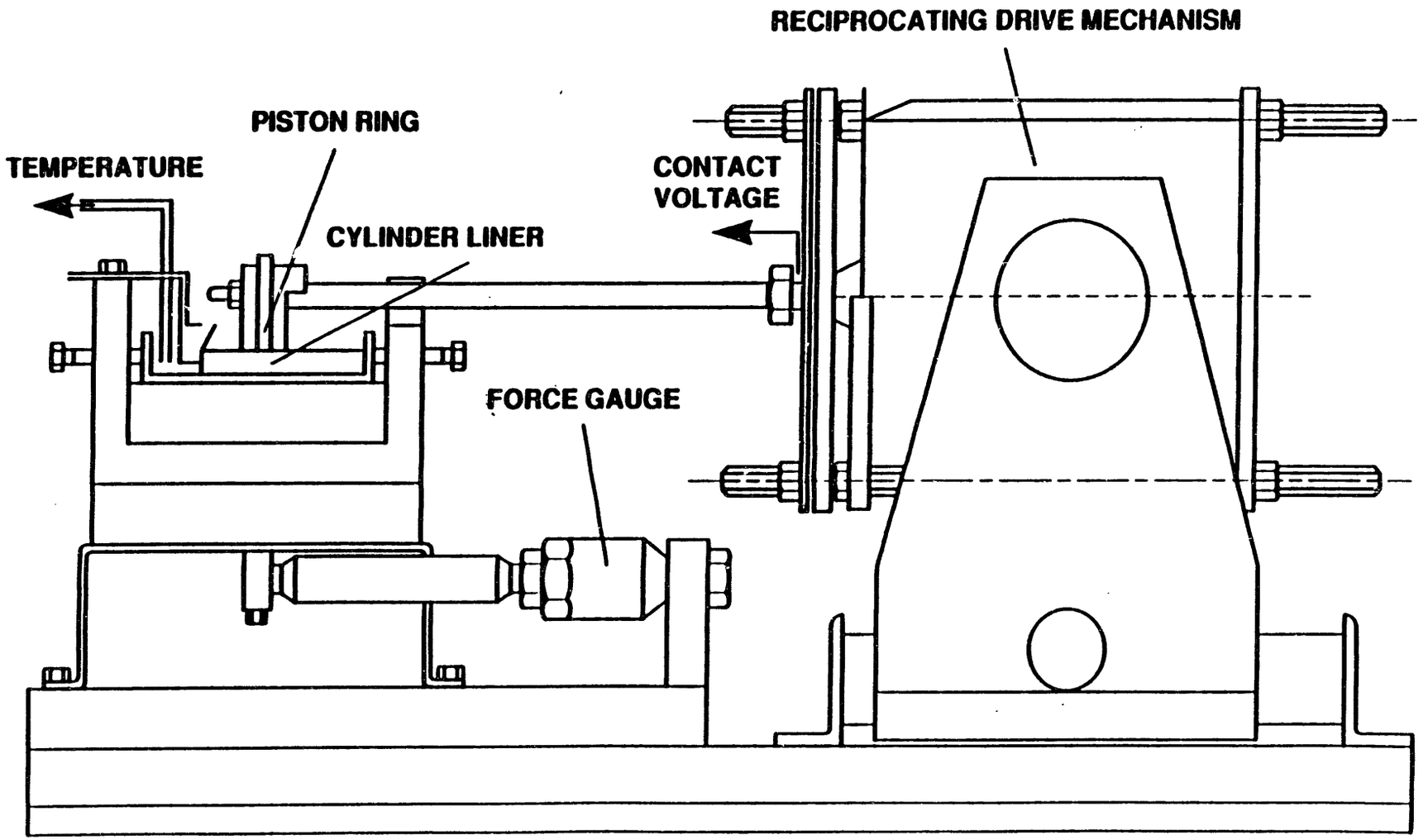

Figure 1. Cameron-Plint High Frequency Friction Machine

Table 1. Cameron-Plint Configuration	
Normal Load	200 N
Frequency of Stroke	17 Hz (1020 RPM)
Ring Piece:	
Source	89 mm O.D. cast iron ring
Size	Wedge-shaped piece approximately 3 mm base x 1 mm top x 5 mm wide x 2 mm thick
Approx. Weight	0.3 g
Wear Surf. Area	2 mm^2
Loading	100 MPa
Cylinder Liner Piece:	
Source	96.5 mm I.D. cylinder liner for Labeco CLR engine
Size	55 mm x 25 mm x 3-5 mm thick (thickness varies because of the curvature of the liner).
Approximate Weight	37 g

Test specimens were chosen to represent typical cast-iron materials used in diesel engines. Cylinder pieces were cut from the 96.5 mm I.D. cylinder liners of a Labeco CLR engine. Each piece was machined to dimensions of 55 mm x 25 mm, flattened on the back so that it varies from 3 - 4 mm thick and weighing approximately 37 grams. Ring specimens were cut from 89 mm D x 2 mm thick cast iron rings and were ground into a wedge shape, 1 mm at the face expanding to 3 mm wide at the base, and weighing approximately 0.3 grams. The wearing surface of 1 mm x 2 mm is exposed to a normal force of 200 N, resulting in 100 MPa contact pressure (approximately an order of magnitude higher than the maximum pressure seen in actual diesel engines). With a stroke of 17 mm, the maximum velocity of the ring specimen is approximately 0.9 m/s. This information, along with information on the geometry of the wear specimens was input into a hydrodynamic flow model to calculate Hertzian stress and hydrodynamic film thickness assuming an elliptical contact region (Harris, 1984, Dawson and Higginson, 1977, Chittenden, et al., 1985, and Johnson 1985 provide detailed descriptions of the model).

The result of those calculations was a maximum film thickness about 0.34 micrometers. Surface roughness for the tests in this program varied from 0.12 to 2.1 micrometers, so it seems apparent that at almost all times, the wear specimens are in the boundary lubrication regime (indicating there is probably some contact of asperities always) as opposed to hydrodynamic lubrication. This does not preclude the possibility of hydrodynamic effects in which wear is reduced because part of the load is being born by a thin hydrodynamic film.

Details of the baseline lube-oil properties are contained in Table 2. The oil was chosen as representative of typical diesel lube-oil properties, but without any additives.

Table 2. Properties of Baseline Oil

40°C Viscosity	143.88 cSt
100°C Viscosity	13.99 cSt
V.I.	93
API Gravity	28.6 @ 15.6°C
T.A.N.	0.01
T.B.N.	0.09
Flash Point	293°C
%N	0.012
%Ca	N.D.
%Zn	N.D.
%P	<0.01
%S	0.21

B. Analysis of Ash Contaminant

Proximate analyses of the contaminants used in this program are included in Table 3, and particle size analyses in Table 4. The contaminants were originally chosen to represent a range of carbon versus ash content. Since the intent for this Task of the program was to study particle size and surface finish effects, only the Kentucky Splint ash (after fluid-energy mill grinding) was used. Table 5 contains the results of X-ray fluorescence analysis on that ash which confirms that silicon, aluminum, iron and calcium

Table 3. Proximate Analysis of Contaminants

Description	Feed Stock	Ash	Vol. Matter	Fixed Carbon
Low-Ash Coal	Unknown	1.00%	34.51%	64.14%
Carbon Black	Mogul-L	0	0	100%
High-Ash Coal	Kentucky Splint	22.9%	30.5%	46.6%
Cleaned Coal	Kentucky Splint	0.38%	37.73%	61.88%
Ash Product	Kentucky Splint	85.3%	10.6%	4.1%

Table 4. Particle Size Averages

Contaminant	Number Weight Averages		Volume Weighted Averages	
	Arith. Mean	Log Mean	Arith. Mean	Log Mean
Low-Ash Coal	4.8	4.1	13.8	11.5
Carbon Black	3.9	3.1	9.9	9.0
Raw Kentucky Splint Coal	4.1	3.1	15.1	13.2
Cleaned Kentucky	5.5	4.1	18.9	16.7
Ash From Kentucky Splint Coal	13.7	12.5	33.4	27.2
Ash From Kentucky Splint Coal Ground in Fluid Energy Mill	2.8	1.9	9.2	8.3
Syloid 63 Silica	2.4	1.6	10.6	0.6

seem to be the major elements present, although the form of those elements is not so certain. A brief review of the literature on coal ash mineralogy (Mitchell and Gluskoter, 1976; Tsai, 1982; Jones, et al., 1985; Wilson, et al., 1986; Unsworth, et al., 1987; Unsworth, et al., 1988) indicates that silicon is most likely present in quartz. Aluminum might be present as alumina, but is more likely to be found with silicon in aluminosilicate compounds. Iron is predominantly in some form of pyrite, and calcium can be present as calcite, bassanite, or dolomite. The heat of combustion will, of course alter those compounds, primarily in the dehydration of various silicate materials, the release of CO_2 from carbonates, and the oxidation of pyrites to iron oxides. For wear processes, the hard minerals, quartz, alumina, and pyrite primarily are of the most concern.

Table 5. Analysis of Contaminant Ash

	(Weight Percent of Ash)				
	Cleaned K.S. Coal	**Low-Ash Coal**	**Raw K.S. Coal**	**Ash From K.S. Coal**	**Syloid 63 Silica**
SiO_2	39.42	41.72	60.85	65.31	98.58
$A1_2O_3$	14.55	29.20	23.78	22.09	1.18
Fe_2O_3	25.40	14.77	5.34	3.55	0.18
CaO	5.15	8.66	2.06	1.57	0
MgO	1.72	0.92	1.42	1.88	0
NA_2O	0.13	0.07	0	0	0
K_2O	0.78	1.94	4.20	4.78	0.06
Ti_2O	6.17	1.03	0.70	0.82	0
Cr_2O_3	0.37	0.04	0.61	0	0
NiO	3.82	0.19	0.94	0	0
CuO_2	0.72	0.27	0.10	0	0
SO_3	1.77	1.19	0	0	0

C. Test Matrices

1. Surface Finish Tests

Machining of the cylinder specimen faces was done using honing, lapping and milling processes as outlined in Table 6 so that a range of different surface roughness and cross-hatch orientations could be obtained. Some of the processes were done on individual specimens while others were done on whole cylinders before they were cut into pieces, but it is felt that they all represent fairly common machining practices which could be easily adapted for large scale processes. As is conventionally done, the roughness values are presented as "R_a", an arithmetic average of the magnitude of peaks and valleys in the roughness profile. Caution should be used, however, in interpreting these values since R_a says nothing about the spacing, symmetry, or distribution of grooves in the surface. Lapped surfaces, for example, appear quite different from honed or milled surfaces under the microscope (they tend to have short, overlapping scratches rather than continuous grooves) even though they may have similar R_a values. The other concern is the fact that specimens with 90° cross-hatch angles (axially oriented machining marks) could not be measured with the existing profilometer equipment because the orientation of the grind marks (referred to as the "lay" of the surface finish) is parallel to the direction of travel of the profilometer stylus.

Table 6. Surface Finish Conditions

R_a (microns)	Cross-Hatch Angle
0.65	0
1.80	0
2.10	0
0.18	20
0.43	20
1.62	20
0.42	25
1.80	25
0.62	90
0.80	90

2. Tests With Various Slot Configurations

Table 7 lists the different slot configurations machined into the surface of the cylinder specimens. The basic idea behind using slots in cylinder liners was that they might enhance the formation of a hydrodynamic film, while providing avenues of escape for wear particles that would otherwise be dragged over or along the entire stroke of the ring piece. Slots were provided both longitudinally (in line with the direction of ring travel) and circumferentially (normal to the direction of ring travel). The spacings were chosen to provide comparisons of various slot widths with equivalent surface area as well as various surface areas at equivalent slot width. Because of the Cameron-Plint configuration it was not possible to measure the ring sealing, although it is recognized that blow-by could be a serious concern, especially with the longitudinal slots.

Table 7. Cylinder Specimen Slot Configuration

Number of Slots	Slot Width (mm)	Spacing Between Slots (mm)	Slot Orientation (Circumferential or Longitudinal)
90	0.15	0.30	C
12	0.15	0.30	L
60	0.15	0.50	C
8	0.15	0.50	L
60	0.25	0.50	C
8	0.25	0.50	L
60	0.35	0.50	C
8	0.35	0.50	L
2	0.25	10.00	C

3. Lubricant Formulation Investigations

For coal-fueled diesel engine applications, it may be possible to reduce wear by tailoring the lubricant formulation to handle abrasive contaminants. It was beyond the scope of this project to do a thorough study of the many available lubricant additives and the many combinations of additives that are possible. Instead, a few additives were chosen from the general classifications and were tested individually, when mixed in an additive-free baseline

lubricant. The results could not be used to optimize lubricant formulation, but they would indicate the magnitude of the effect of lubricant formulation, and give at least a qualitative feel for how different classes of additives affect the wear process. Wear tests were performed with clean additive/oil mixture, and with a 5 percent concentration of coal ash contaminant in the mixture. Descriptions of the additive/oil mixtures are included in Table 8.

Table 8. Lube-Oil Additives

Additive	Concentration (% by mass)
Highly Basic Calcium Sulfonate Detergent	19
Ashless Dispersant	5.2
Alkyl Zinc Dithiophosphate	0.630 (approx. 0.1 % Zn)
Aryl Zinc Dithiophosphate	0.466 (approx. 0.1 % Zn)
Non-Dispersant Olefin Co-polymer (VI Improver)	10
Olefin Thickener	10

Further analysis of the additive/oil mixtures has been performed, and the results are outlined in Table 9.

IV. EXPERIMENTAL RESULTS

A. Surface Finish Tests

The following data was compiled for the test matrix described above.

- Mass Loss of Cylinder and Ring Specimens
- Electrical Resistance Between Ring and Cylinder Specimens as a Function of Time During Each Test

- Friction Force as a Function of Time During Each Test
- Photomicroscopic Observations of the Cylinder and Ring Specimens
- Observations of Wear Particles Using a Ferrographic Technique
- Profilometric Data

Table 9. Analysis of Additive/Base Oil Mixtures

	Baseline Oil	19% Calcium Sulfonate Detergent	5.2% Ashless Dispersant	0.47% Aryl Zinc Dithio-phosphate	0.63% Alkyl Zinc Dithio-phosphate	10% Non-Dispersant Olefin Co-polymer	10% Olefin Thickener
Kinematic Viscosity at 40° C (cSt)	143.9	163.1	160.9	144.9	143.5	260.3	184.8
Kinematic Viscosity at 100° C (cSt)	13.99	14.98	15.69	13.97	13.88	24.89	17.53
Viscosity Index	93	90	99	92	93	122	99
API Gravity (at 15.6° C)	28.6	20.1	27.8	28.2	28.2	28.6	28.9
TAN	0.01	1.18	0.12	0.28	0.90	0.04	0.06
TBN	0.09	79.61	0.30	0.27	0.45	0.24	0.15
Flash Point (° C)	293	260	266	254	268	257	274
% N	0.012	0.009	0.026	0.012	0.012	0.010	0.010
% Ca	N.D.	0.897	0.008	0.007	0.007	0.006	0.007
% Zn	N.D.	0.0002	0.3 ppm	0.019	0.074	0.002	0.002
% P	<0.01	0.007	0.012	0.012	0.021	0.010	0.014
% S	0.21	0.487	0.279	0.329	0.431	0.312	0.269

1. Mass Loss of Cylinder and Ring Specimens

Figures 2 and 3 present mass loss of ring and cylinder specimens as a function of average surface roughness for cross-hatch angles of 0°, 20°, 25°, and 90° (it should be noted that the 0° case represents all circumferential grind marks while the 90° case represents all axially oriented marks). Data is presented for tests run with baseline oil alone (labeled on the graph as the "0 % Ash" case) and for those run with a 5 percent mixture of ground Kentucky Splint ash. The following observations can be made about these graphs.

- The variation of surface roughness and cross-hatch orientation did not significantly degrade the wear performance under clean oil conditions.
- There was an effect of cross-hatch angle on wear. Although there is not a clear trend, the smaller angles (0° and 20°) cause slightly less wear.
- The general trend is for wear to increase with surface roughness, although that trend is not so obvious for the 0° case.
- There is a notable increase in wear for the smoothest finish in both the clean oil and 5 percent ash tests.

As surface finish becomes smoother and smoother, one might expect that the effect of groove orientation would disappear, and that all the 5 percent ash curves in Figures 2 and 3 should converge to a single value at zero roughness. Assuming this is true, the trend established by the smoothest data points (plotted in Figures 2 and 3 on the 20° cross-hatch angle curves) suggests that wear starts out at a high value, reaches a minimum somewhere in the 0.4 - 0.8 micron range, and then increases again. Again, the 0° curves are somewhat of an exception to this trend since they seem to be leveling off at higher surface roughness. At any rate, an important point to make is that there appears to be no advantage in going to extremely smooth cylinder surfaces.

2. Electrical Resistance Data

Electrical resistance between the ring and cylinder specimens was recorded for the four hour duration of each of the tests described above. For most of these tests, resistance was zero on both the oscilloscope trace and the strip-chart recording for the entire duration. In those cases where ash contaminant was added to the lube-oil, the readings may be in question because of the conductive properties of the contaminant, but for the clean oil tests there must be some degree of metal to metal contact at all times.

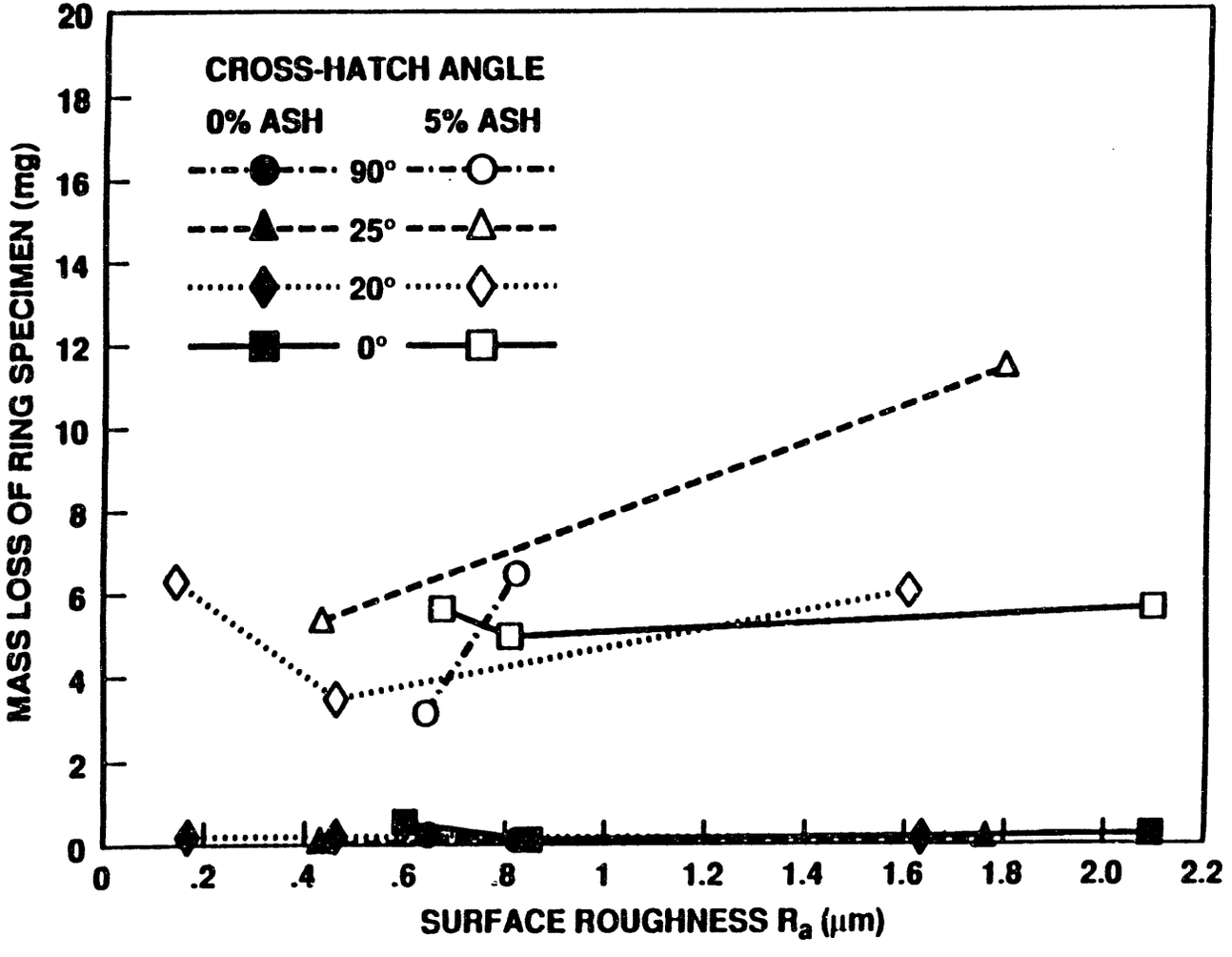

Figure 2. Mass Loss of Ring Specimens as a Function of Surface Roughness

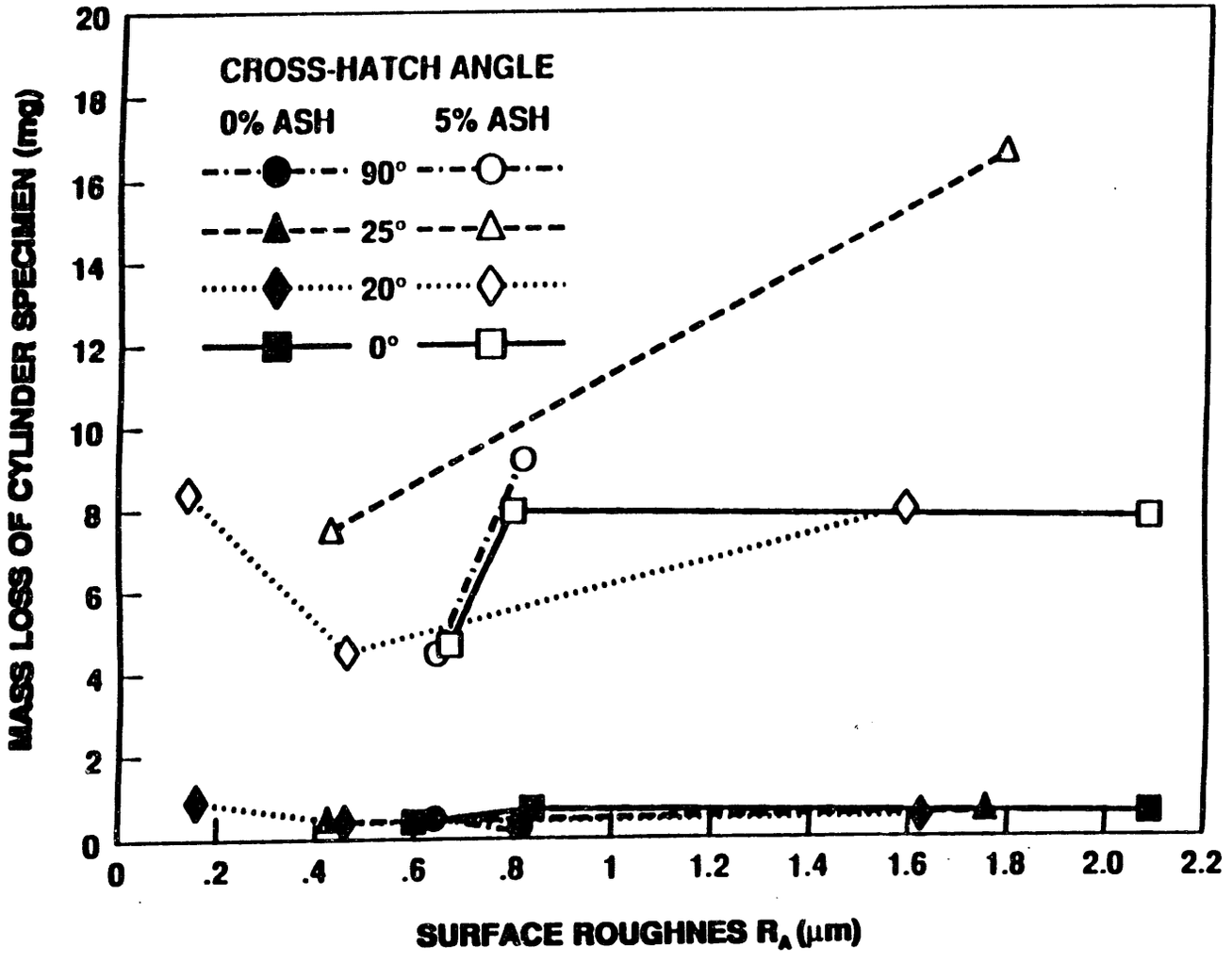

Figure 3. Mass Loss of Cylinder Specimens as a Function of Surface Roughness

The interesting aspect about this data, however, is those few cases where a finite resistance was measured, confirming the formation of a complete film. The only case that consistently registered finite resistance measures was with the 0° cross-hatch and 2.1 micron R_a. This seems to confirm that rougher surfaces can, in fact, enhance the formation of the hydrodynamic film as proposed by Janczak and Wisniewski, and Richez, et al. The film formation process, however, is also dependent on the orientation of the surface grooves relative to the ring motion. Other cases where films were seen include the 0°, 0.4 micron case and the 90°, 0.4 micron case, but these did not form consistently in all test repeats. In all cases where a film formed, the resistance measurement started at zero and fluctuated, but steadily increased over the four hour test.

3. Friction Force Data

Friction force was also recorded over the four hour duration of each of the tests performed. In some cases, the friction force signal was monitored on an oscilloscope as well. Figure 4 is a photograph of a typical oscilloscope trace. This trace happens to be for a test with clean baseline oil, and using a 20° cross-hatch, 0.4 micron roughness cylinder specimen, but the shape of all the friction force traces did not vary significantly from this basic outline. The shape of the trace indicates an initial spike as the ring specimen breaks away from the static position at the ring reversal point. The force then drops to a fairly constant value with a few oscillations for the remainder of the stroke. The next ring reversal is characterized by a change in sign, and a similar shaped curve is traced on the negative side. The fact that the trace is symmetrical, and that the force is constant for most of the stroke gives confidence that the normal force is being applied uniformly over the duration of the cycle.

The strip-chart recordings of cycle-averaged friction force have been analyzed as well. A few conclusions can be drawn from that analysis.

- All tests exhibited some initial transient behavior (a kind of "break-in" period), but settled to an established trend within the first half hour of testing.
- Tests performed with clean lube-oil had a fairly constant friction force for the entire duration.
- Tests performed with ash contaminant had constant, or slowly increasing friction force throughout the test duration.
- Tests with ash contaminant exhibited high frequency oscillations in the friction force trace that make it appear much rougher than the corresponding clean-oil traces.

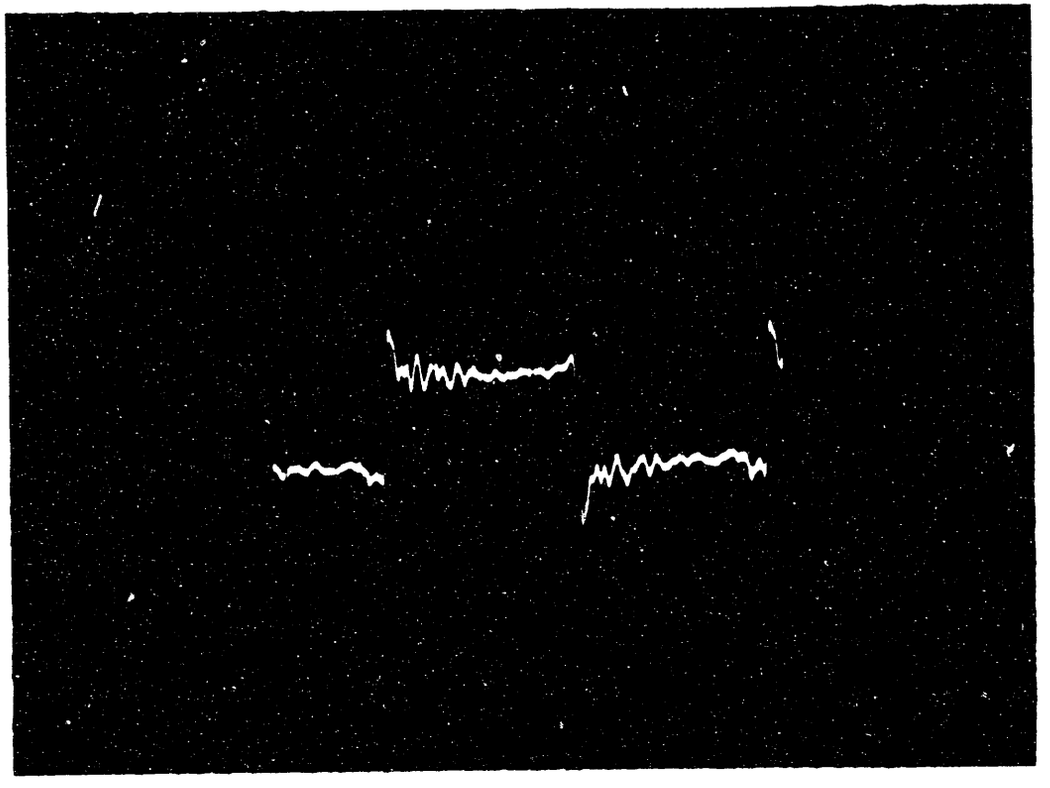

Figure 4. Oscilloscope Trace of Friction Force; 20° Cross-Hatch Angle, 0.4-mm Roughness Average, and Clean Oil Case

- Magnitude of friction force was 1.5 - 2.0 times higher for the ash contaminated oil than for the clean oil.

4. Photomicroscopic Observations

Ring and cylinder specimen wear scars were observed using light microscopy for several of the test conditions. Figures 5 and 6 are photomicrographs of ring and cylinder specimens (0° cross-hatch, 2.1 micron surface roughness cases run with the clean oil, and with the ash-contaminated oil). Comparing clean oil to contaminated oil cases reveals the difference in wear mechanisms. Clean oil resulted in smoothing over of the surface, gradually removing the original surface finish. Figure 6 shows some of the original finish is still present in the form of large vertical gouges, but the spaces in between have been smoothed by the wear process. Contaminated oil, as in the previous study (Schwalb, et al., 1990) resulted in deep, sharp grooves in both the cylinder and ring pieces. In all cases with contaminated oil, the original finish was completely removed by the end of the test.

The wear scars presented in Figures 5 and 6 were typical for all the original surface finish conditions tested. This indicates that the finish has not significantly affected the wear mechanism in the clean oil cases. The contaminated oil cases are more difficult to interpret. Since the wear in all cases was enough to remove the entire original surface finish, it is not surprising that there is little difference in the appearance of wear scars. On the other hand, since the wear magnitude was significantly affected by original surface finish, the finish must have had an effect, at least in the initial stages of the wear process.

5. Observations of Wear Particles

Wear particles were deposited onto a microscope slide for several cases using the ferrography technique described by Anderson (1982). The technique involves taking a sample of the lubricant/contaminant combination used in the wear test, and allowing it to flow slowly over a slightly inclined microscope slide that is located in a magnetic field. Ferrous particles will be attracted by the magnet, and will deposit on the slide while non-ferrous particles are more likely to remain suspended in the oil, or will deposit at a location farther downstream. The ferrous particles can also be identified because of their tendency to line up in straight lines along the magnetic field lines.

As it turned out, the technique was not effective for the cases where ground Kentucky Splint ash was used. There were simply too many non-ferrous ash particles in the sample that deposited uniformly over the whole slide and made it impossible to pick out the wear particles. The technique was effective, however, for the unground Kentucky Splint ash, and photomicrographs of two types of wear particles are presented in Figure 7. The platelets shown in Figure 7 were the predominant type of particle seen. They are definitely ferrous as evidenced by the way they line up, and appear similar to wear particles seen in normal rubbing wear which has been accelerated by a three-body abrasive mechanism. A few large flakes were also seen, although it cannot be confirmed

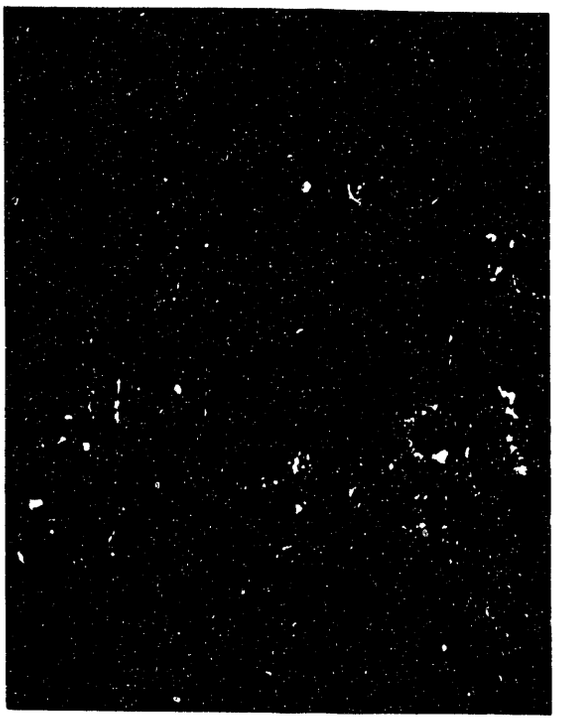

(a) Clean Oil

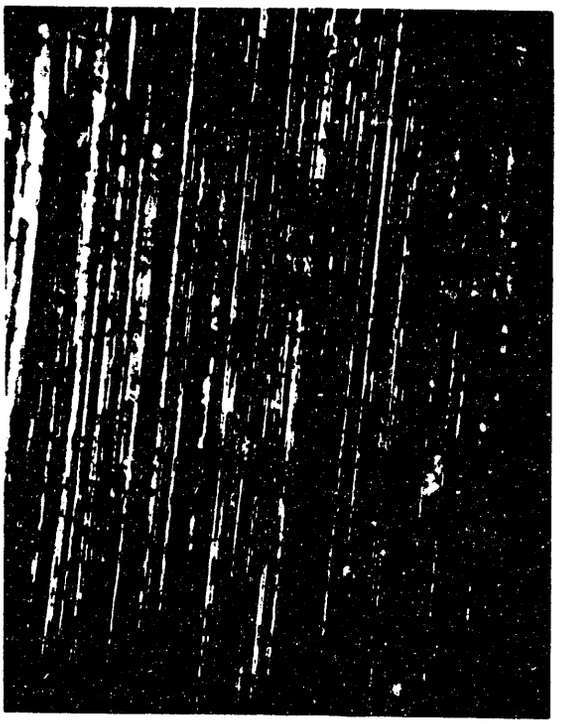

(b) 5% Kentucky Splint Ash

Figure 5. Photomicrographs of Ring Specimens for 0° Cross-Hatch, 2.1 μm Surface Roughness Cases

program was to stu
(after fluid-energy mill grinding) was
fluorescence analysis on that ash which

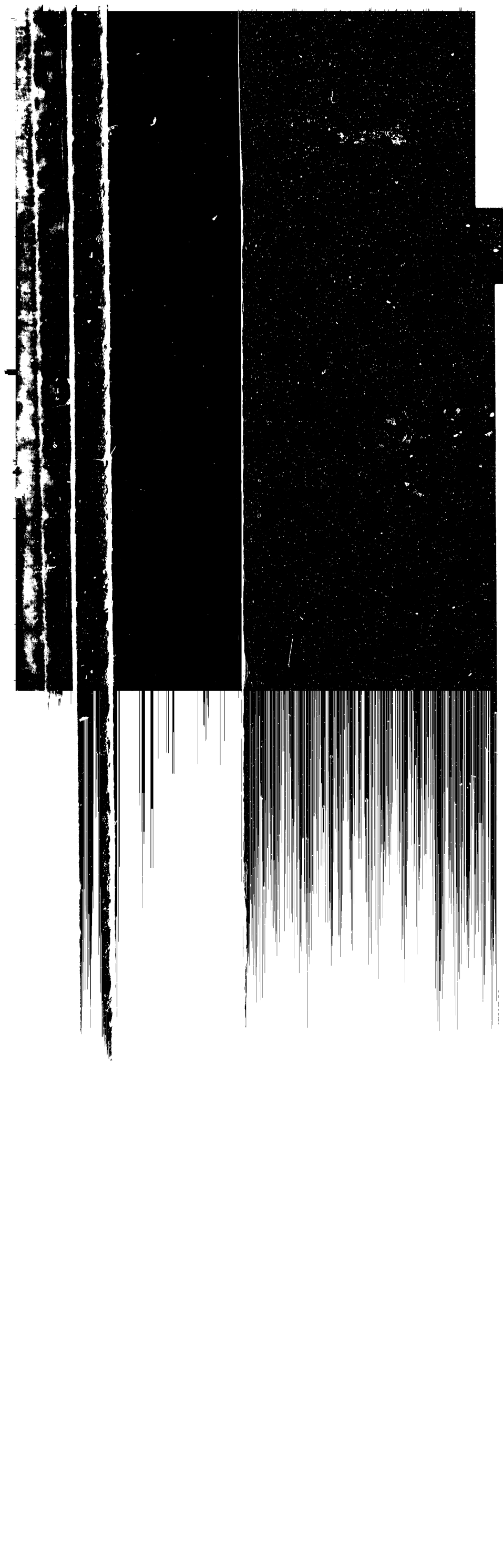

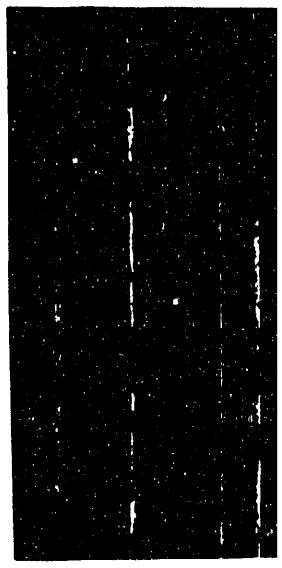

(b) 5%

Figure 6. Photomicrographs
Angle, 2.

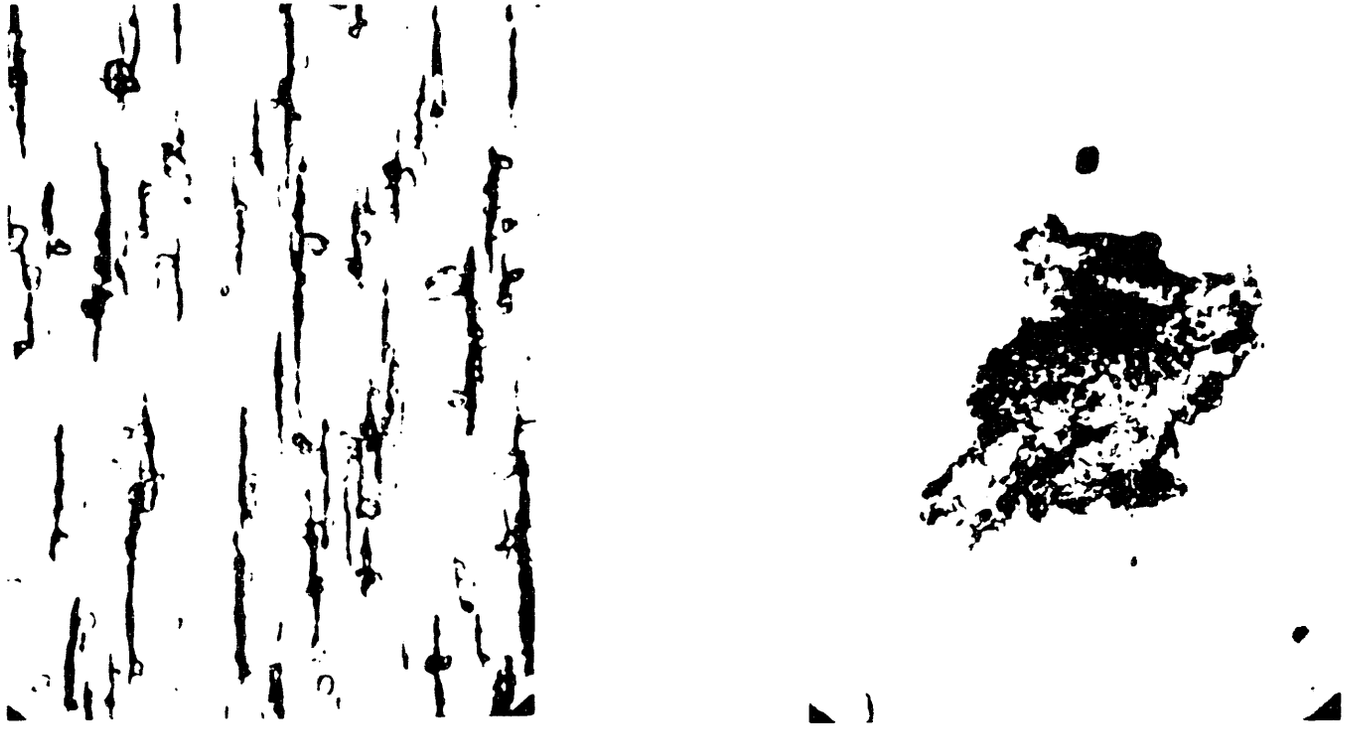

Small Platelets

Large Flake

Figure 7. Wear Particles Generated by Ash Contaminant (Photomicrographs at 1000 X Magnification)

that they are ferrous wear particles. This type of particle is more typically seen in rolling wear applications where fatigue is a problem, so it is unclear why it would be present in these cases.

The technique was also used for a clean oil case, the results of which are shown in Figure 8. Again, the predominant wear particles were small platelets typical of normal rubbing wear, while a few large, thin flakes also appeared. It is interesting to compare these particles with those produced when a more carbonaceous contaminant was introduced into the oil. Figure 9 shows photomicrographs of wear particles obtained when carbon black and low-ash coal were used as contaminants (these tests were run during the previous study (Task 1) and data for them is presented in Schwalb, et al. (1990), and in the topical report for Task 1). The carbon black photomicrograph shows a scattered range of particles, some of which appear spherical, but they are not lined up enough to determine whether they are ferrous wear particles. The low-ash coal photomicrograph reveals some particles that are definitely ferrous, and are spherical. The spherical type particles are also typical of a rolling fatigue type wear, so it is interesting that they appear in what should be exclusively sliding wear.

6. Profilometric Data

Profiles of the cylinder specimen wear scar surfaces have been obtained for each test using a Talysurf 10 profilometer. The profiles were recorded at two positions in the longitudinal direction (the direction of ring travel) and three positions (evenly spaced) in the crosswise direction. Examples of longitudinal profiles for a few cases are shown in Figure 10. The profiles, show the original surface finish, and how it is smoothed by clean oil wear. They also show how the entire surface finish is removed during the ash-contaminated oil test, confirming what was seen in the photomicrographic data. Also of note is the characteristic shape of the scars that reach their deepest points at the ring reversal locations. This characteristic shape was noted for all the tests presented here which had a significant amount of wear, and is consistent with what was seen in the previous study (Schwalb, et al., 1990). It indicates that the wear is definitely dependent on the dynamic motion of the ring, and suggests that there is a hydrodynamic effect at the center of travel of the ring that breaks down at its reversal points.

B. Slot Configuration Tests

1. Mass-Loss of Cylinder and Ring Specimens

Table 7 lists the different slot configurations that were machined into the surface of cylinder specimens for testing on the Cameron-Plint Machine. Each of the configurations listed in Table 7 was tested twice with clean baseline oil and twice with 5 percent ground Kentucky Splint ash contaminant in the oil. The mass-loss wear results (averaged over the two test repeats at each condition) are presented in the bar chart in Figure 11. A few general conclusions can be made about these results.

Figure 8. Wear Particles Generated With Clean Baseline Oil (Photomicrograph at 1000 X Magnification)

Figure 9. Spherical-Shaped Wear Particles (Photomicrographs at 500 X Magnification)

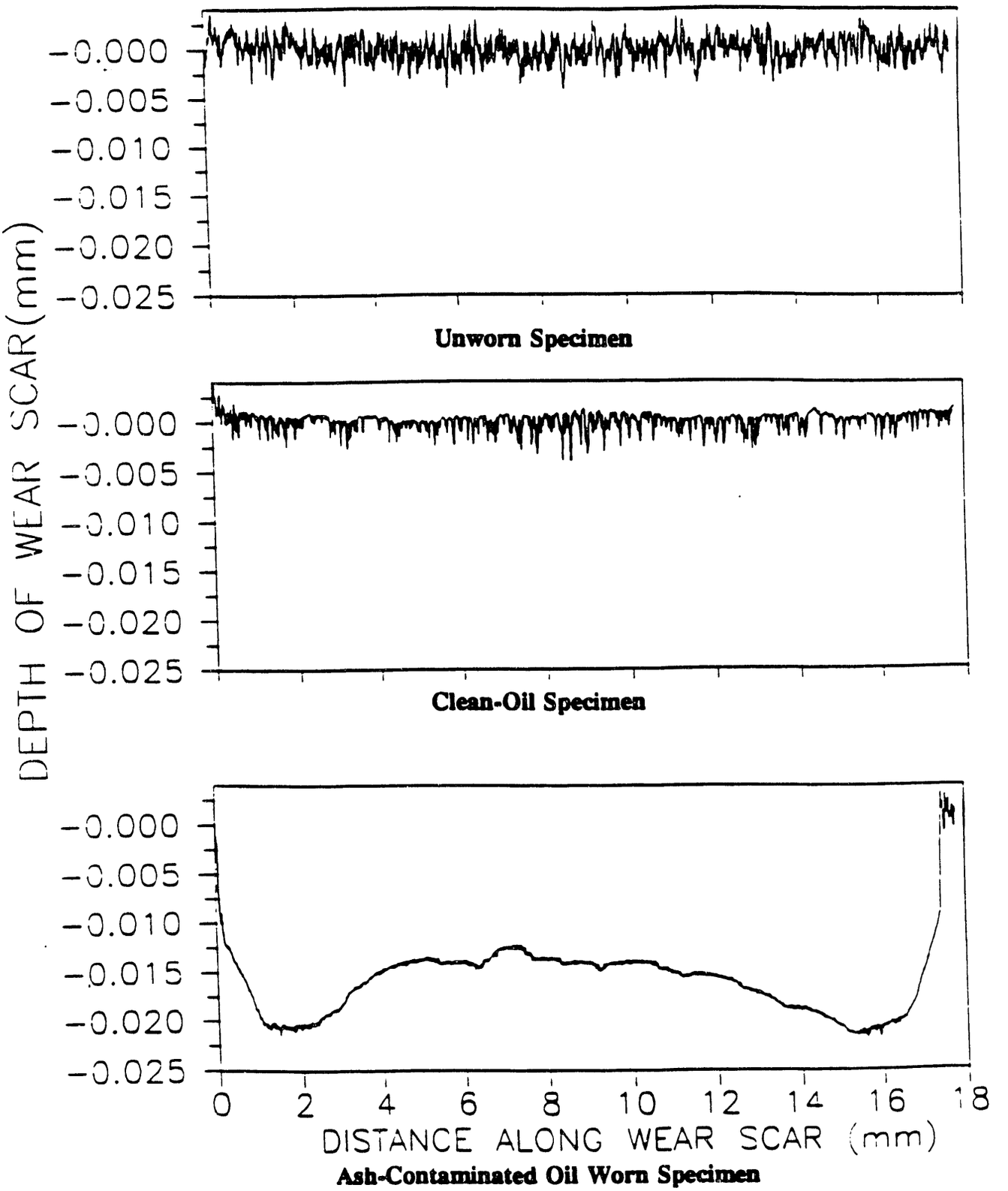

Figure 10. Longitudinal Wear Scars, 0° Cross-Hatch Angle, 2.1 μm Ra

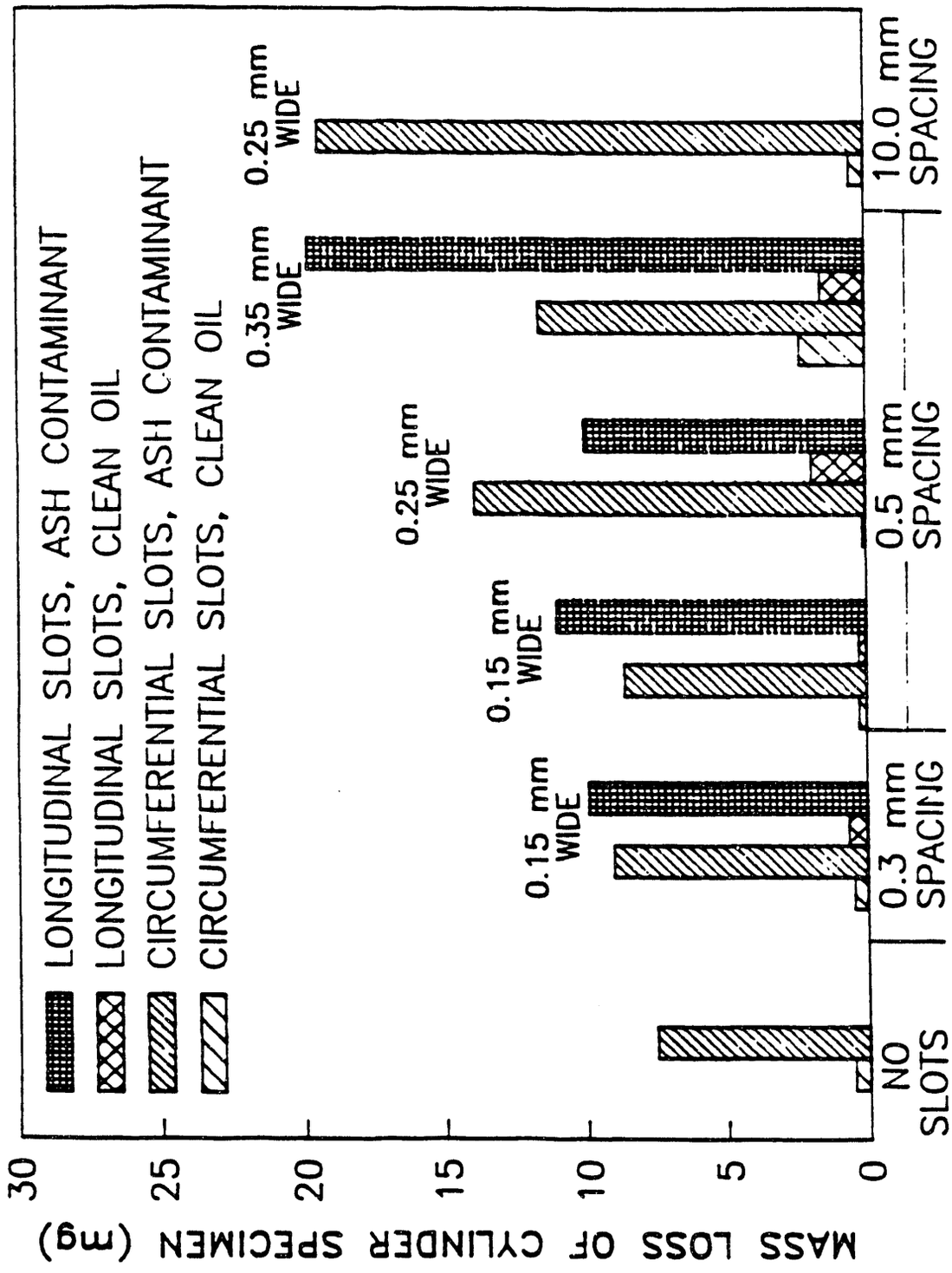

Figure 11. Mass Loss of Cylinder Specimen (mg)

- All the configurations displayed at least as much, if not more wear than the un-slotted specimens.

- With one exception, longitudinal slots had slightly more wear than circumferential slots of the same width and spacing.

- Generally, wear increased with slot width

- There was not a clear correlation of slot spacing (or number of slots in the ring travel area) with wear. In fact, a configuration with only two circumferential slots (the 0.25 mm wide, 10.0 mm spacing configuration) had even more wear than a configuration with 34 circumferential slots in the ring travel area (the 0.25 mm wide, 0.5 mm spacing configuration).

2. Photomicroscopic Data

Under a photomicroscope, the slotted specimens revealed the same wear patterns as were seen in the un-slotted specimens; long straight grooves that became sharper and deeper when an ash contaminant was mixed with the lube-oil. Figures 12 and 13 are sample photomicrographs of cylinder specimens worn without and with ash contaminant, respectively. The large gray area running horizontally through the middle of each photomicrograph is a circumferential slot, while the vertical light and dark lines are wear grooves parallel to the direction of ring travel. It is apparent from the figures that wear grooves that begin on one side of the slot continue on the other, indicating (as expected) that there must be some degree of conformity between the wear groove pattern on the ring and the pattern on the cylinder. Figures 14 and 15 are photomicrographs of the ring/cylinder specimens used when longitudinal slots were cut into the cylinder specimen. This time, the large dark bands running parallel to the wear scar marks are the slots. Conformity is even more apparent in Figure 14. The photomicrograph of the ring specimen shows alternating bands of worn versus unworn material directly corresponding to the slot spacing.

It seems apparent from this data that the introduction of slots, either longitudinally or circumferentially has not reduced the magnitude of the wear, nor has it changed the appearance of the worn areas. The fact that wear grooves continue from one side of a slot to another gives testament to the statistical nature of the wear process, and the natural tendency for wearing pieces to conform to one another. Apparently, the actual abrasive wear occurs on a smaller scale than the easily visible grooves in the wear scar, and occurs with enough frequency that a fairly smooth, continuous wear scar is produced.

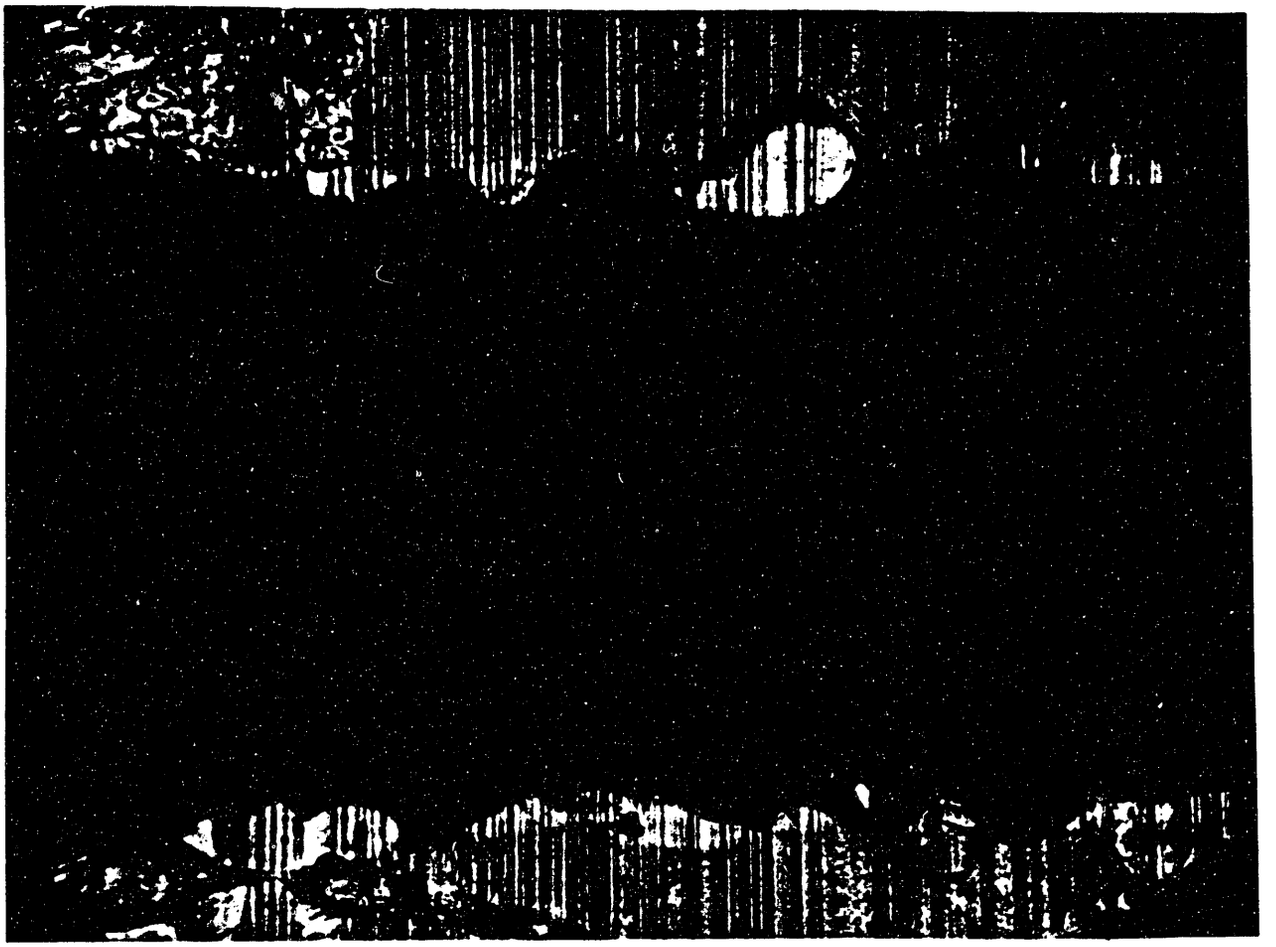

Figure 12. Photomicrograph of Cylinder Specimen With 0.15 mm Wide Circumferentially Oriented Slot - Specimen Worn in Clean Lubricant (500 X Magnification)

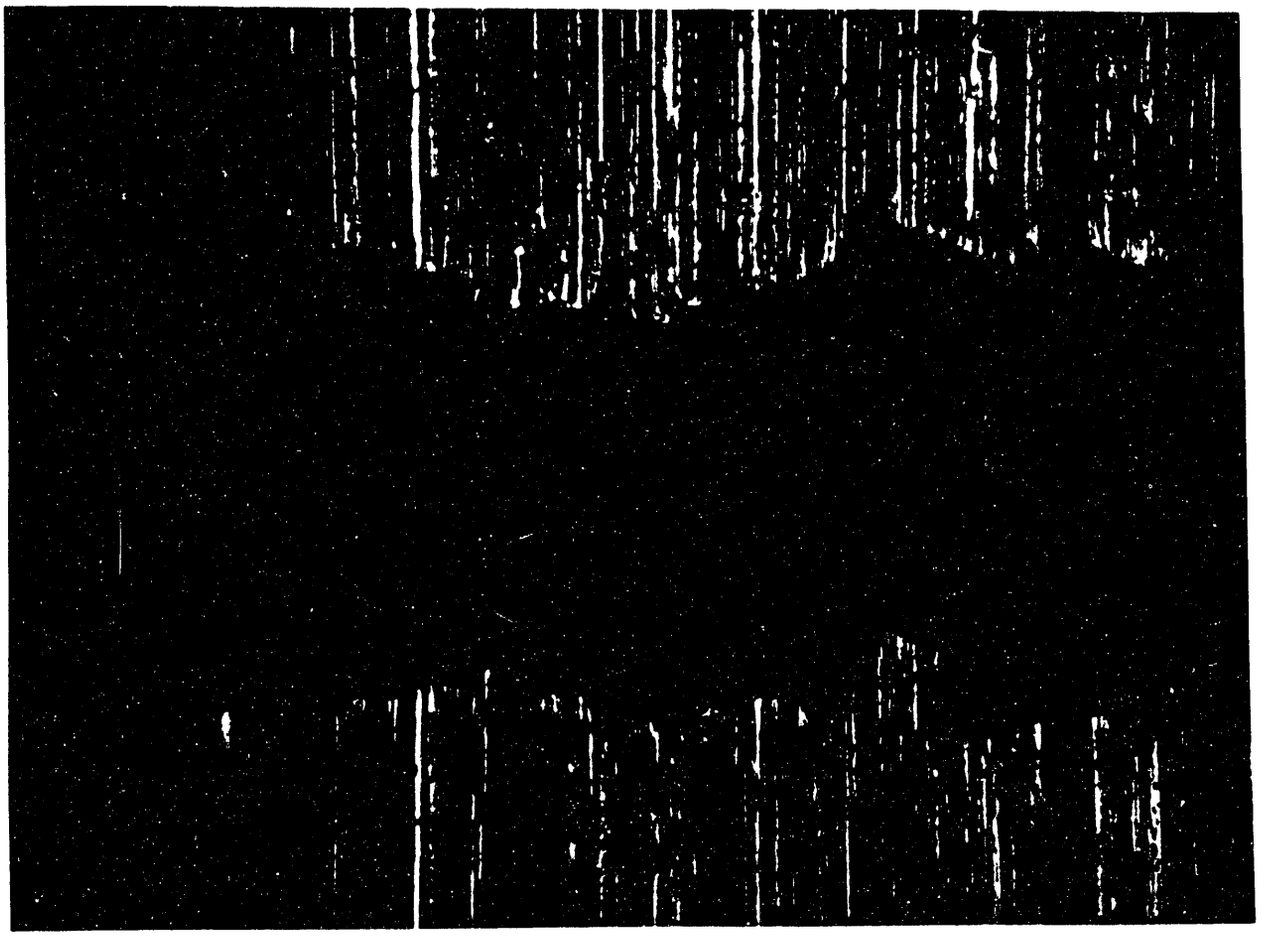

Figure 13. Photomicrograph of Cylinder Specimen With 0.15-mm Wide Circumferentially Oriented Slot - Specimen Worn in Lubricant/5% Ash Contaminant Mixture (The slot width shown above is considerably smaller than the original slot width because the wear scar has almost reached the bottom of the slot.) (500 X Magnification)

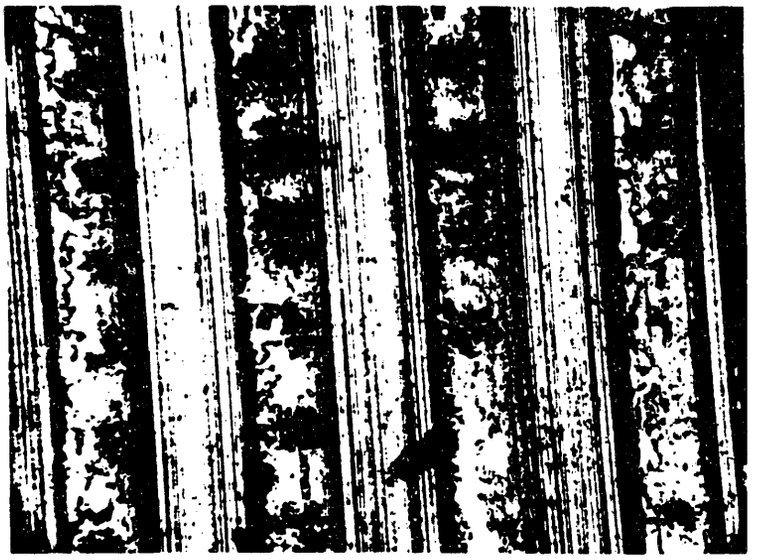

Figure 14. Photomicrograph of Ring Specimen Worn With 0.15-mm Wide, Longitudinal Slots in the Cylinder Specimen (Specimen Worn in Clean Lubricant) - 100 X Magnification

Figure 15. Photomicrograph of Cylinder Specimen Corresponding to the Ring Specimen in Figure 14 Above, (0.15-mm Longitudinal Slots) - 100 X Magnification

It is significant, however, that in comparing Figures 12 and 13, the piece worn with the ash contaminant appears rougher and fuzzier between the wear grooves. That roughness may be the accumulation of many individual gouges caused by small abrasive particles.

While the introduction of slots does not significantly change the wear mechanism, it might still reduce the magnitude of the wear rate by channeling abrasive particles away and/or diluting the concentration of particles in the wear zone. The current Cameron-Plint test is not a fair indicator of this process since the entire wear zone is immersed in a bath of constant concentration particles. If there were any channeling or dilution effect, the removed particles would simply be replaced by new particles of the same concentration. In the engine, on the other hand, the ring/cylinder zone is constantly supplied from one side by relatively clean oil. Future studies may look at modifications to the current Cameron-Plint configuration to allow for the introduction of clean oil to one side of the wear zone.

3. Electrical Resistance Data

As in all the Cameron-Plint tests performed for this study, the electrical resistance between ring and cylinder specimens was monitored continuously throughout each wear test. The presence of a resistance is significant since the measurement of a non-zero resistance indicates the developed hydrodynamic film or a chemical film. In most of the cases tested in this study, the resistance went to zero and stayed there for the entire duration of the test, but with the slotted specimens, there were a few cases where a finite resistance was measured. Table 10 outlines the conditions where a finite resistance occurred. All of them were cases in which no contaminating additive was present.

Table 10. Non-Zero Electrical Resistance Traces

Test Number	Slot Width/Spacing (mm/-mm)	Slot Orientation
T121	0.15/0.30	Circumferential
T131	0.25/0.50	Circumferential
T143	0.35/0.50	Circumferential

Generally the traces started at zero and gradually developed a finite resistance as the test went on. The trace was generally rough with high frequency oscillations that sometimes dropped the trace back into a zero resistance mode. Also of note is the fact that all the cases listed in Table 10 had circumferential slots. Evidence was presented in the previous section that orienting grind marks (comprising the surface finish) normal to the direction of ring travel enhanced the formation of a hydrodynamic film. It seems likely that orienting the much larger slots normal to the direction of ring travel has the same effect. In either

case, however, the effect was not enough to significantly reduce the wear.

4. Friction Force Data

A time averaged friction force was also recorded over the duration of each test. In general, following some transient behavior in the first 30 minutes of the test, the traces leveled off to a fairly constant value. Traces for tests with ash contaminant were overall rougher than their corresponding clean-oil cases, and sometimes exhibited a general trend to increase or decrease slightly over the duration of the test. Figure 16 shows the approximate friction coefficient data for all the slotted specimen tests. The magnitude of the coefficient data indicates that adhesive wear is, at least, a possibility. Also, most of the data indicates a marginal increase in friction force with the ash contaminant.

C. Lube-Oil Additive Tests

1. Mass-Loss of Cylinder and Ring Specimens

Figure 17 presents the averaged cylinder specimen mass-loss data that was obtained when testing various additive packages. The matrix, of course, was not meant to be an all-inclusive study of available additives, but it did allow for testing of at least one additive from several of the major categories. The results presented in Figure 17 show a dramatic reduction of wear with the calcium sulfonate detergent, a dramatic increase of wear with the ashless dispersant, and a less significant increase of wear with the remaining additives (although that increase is probably within the variability of the data).

2. Photomicroscopic Data

For most of the cases, observations of the wear scars revealed the same predominant wear patterns as were observed in the "no-additive" cases; long, straight grooves which became much sharper and deeper when ash contaminant was added to the mixture. The detergent/contaminant case was an exception in that it did not show obvious differences between clean lubricant and contaminated lubricant cases. Another slight exception to this trend was the dispersant/no contaminant case shown in Figure 18 that had a highly polished surface, similar to the surfaces seen in the previous study where lubricant was contaminated with carbon black. Whatever the difference was, however, it did not seem to affect the wear process when ash contaminant was present. The ash contaminated case is shown also in Figure 18 that confirms the long straight groove wear pattern. As in all cases observed in this program, there was little evidence of particles sticking in either wear specimens, again confirming that this is probably not a two-body mechanism. The size of grooves in the photomicrographs is approximately 10 micron and smaller, indicating that the grooves roughly correlate with the size of the particles.

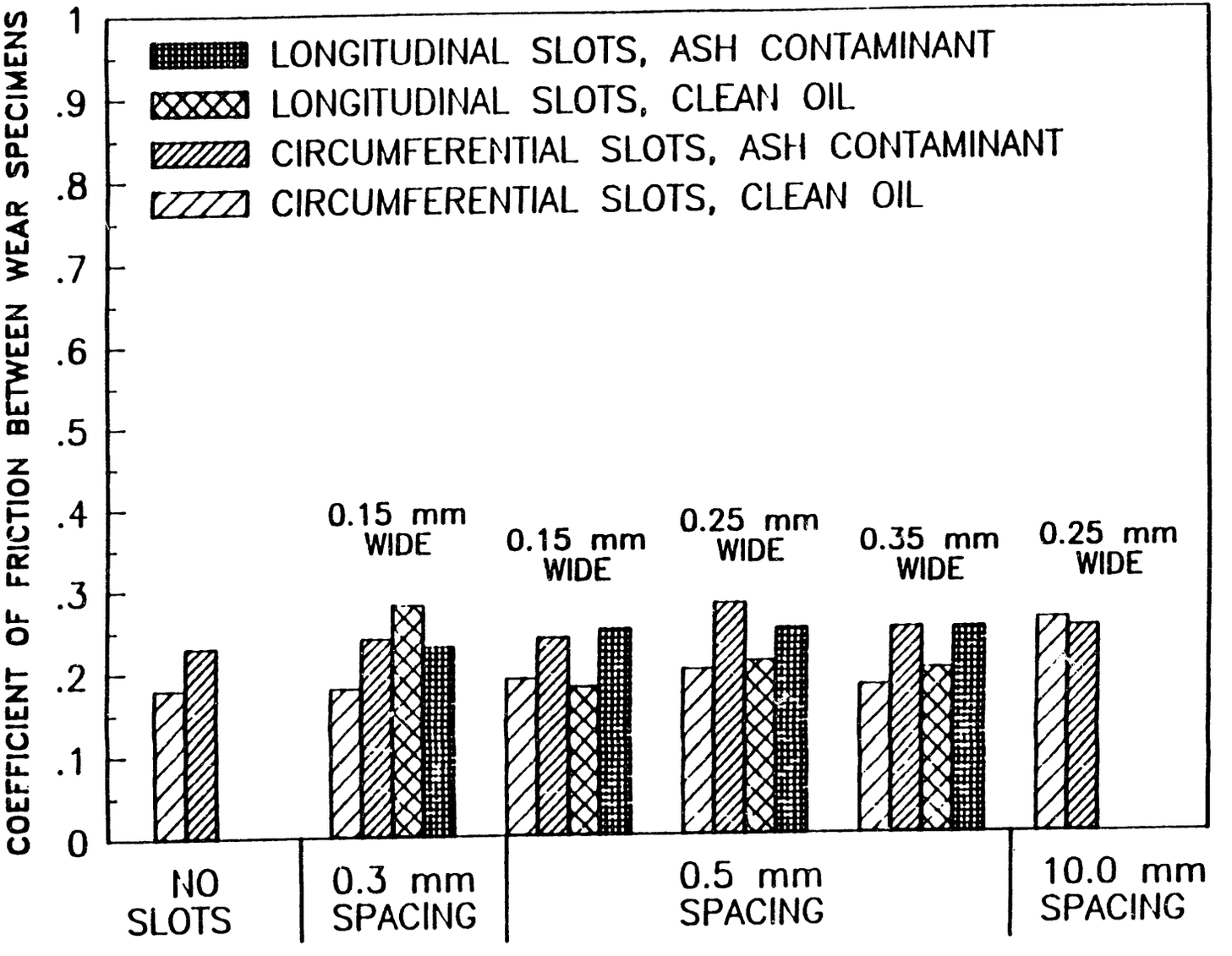

Figure 16. Average Friction Coefficient For Slotted Specimen Tests

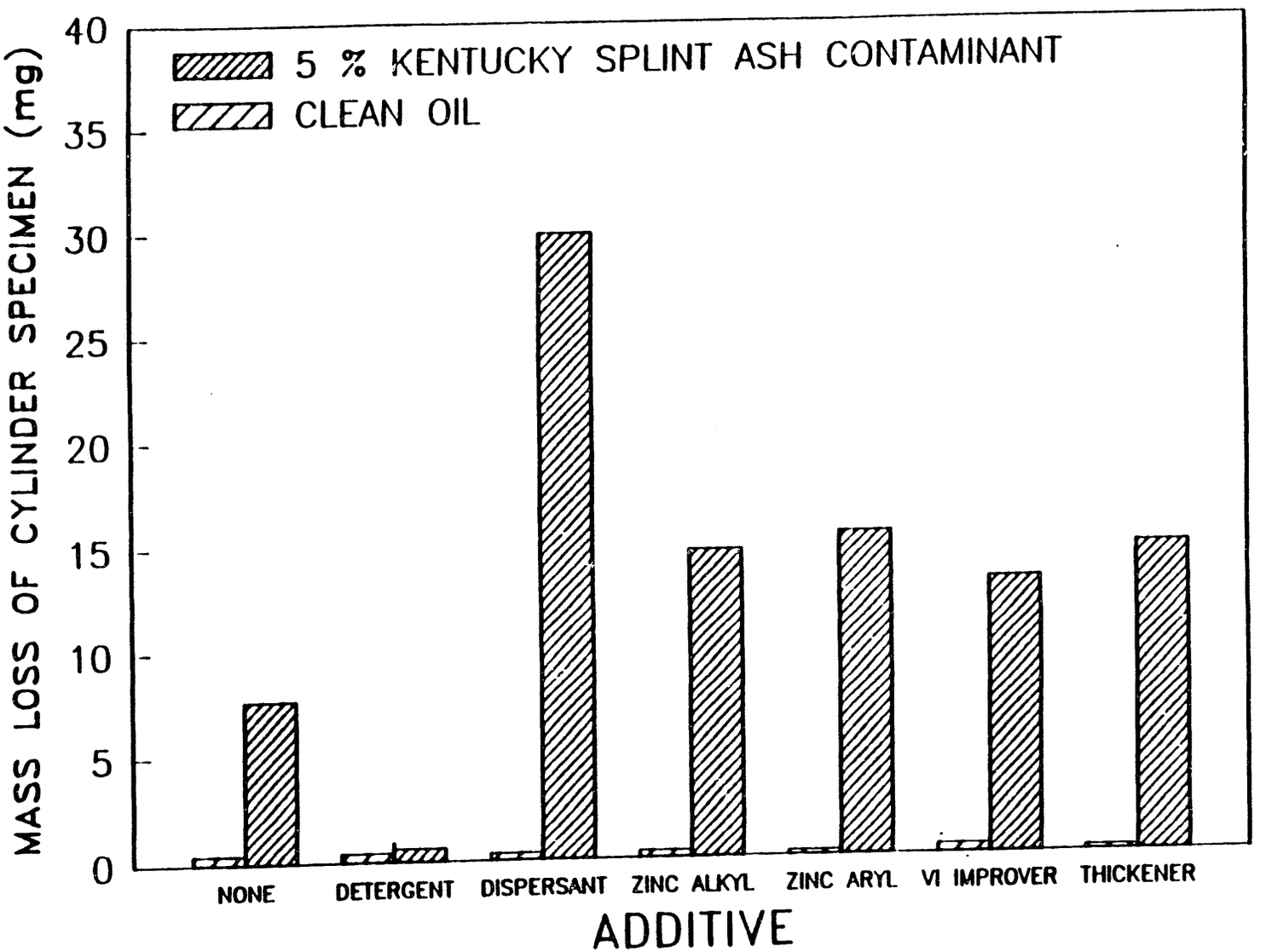

Figure 17. Lube-Oil Additive Effects on Wear

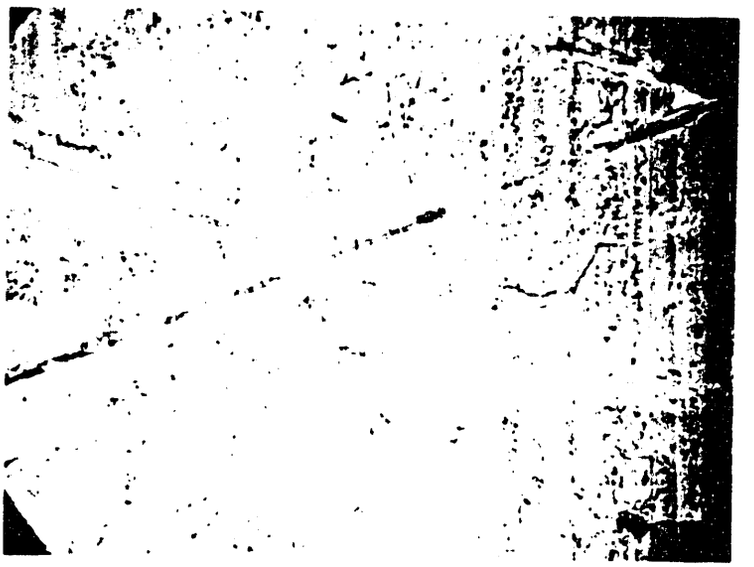

Clean Lubricant-Worn Specimen
(500 X Magnification)

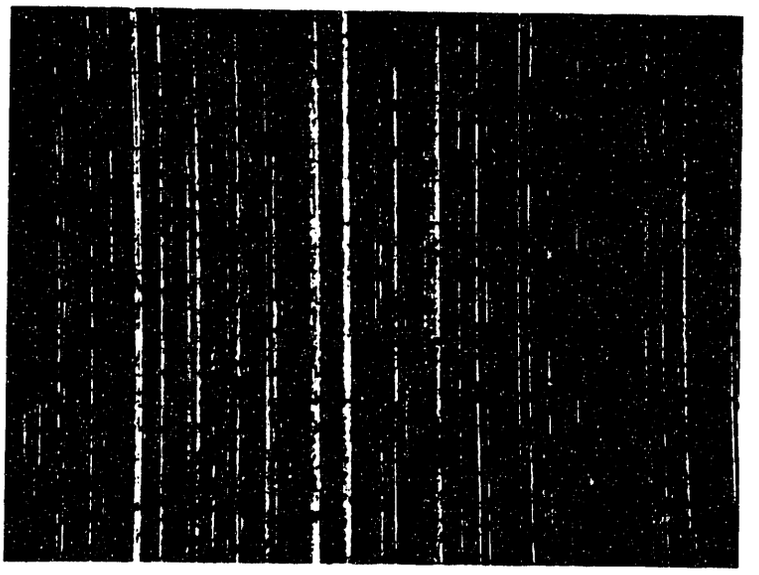

Lubricant + 5% Ash Worn Specimen
(500 X Magnification)

Figure 18. Photomicrographs of Cylinder Specimens Used in Tests With Baseline Lubricant/Dispersant Additive Mixtures

3. Electrical Resistance Data

Except for the Syton 100 thickener runs, all the clean lubricant tests exhibited a measurable resistance between the wear specimens. This is not particularly surprising since most of the additives are designed to have some surface reactivity. Once ash contaminant was added to the lubricant mixture, however, that measurable resistance quickly went to zero for all cases except the calcium sulfonate detergent runs. They exhibited a widely fluctuating, but finite electrical resistance measurement even when ash contaminant was present in the mixture. This is quite significant because of all the tests done in this study, including variations of additives, surface slot configurations, surface finish parameters, and contaminant composition it was the only condition that resulted in a non-zero resistance in an ash-contaminated test. Clearly this indicates the existence of a much thicker hydrodynamic film, or a much more durable surface coating, which may explain the significant wear reduction.

4. Friction Force Data

Friction coefficient for tests with the additives was 0.15 - 0.18 for the clean lubricant tests and rising to 0.25 - 0.28 for tests with ash contaminant in the lubricant. (Tests with the clean baseline oil without any additives were in the 0.15-0.18 friction coefficient range also.) The one exception to this trend was the detergent additive, for which the friction coefficient stayed at approximately 0.18 even though an ash contaminant was present.

5. Ferromagnetic Data

The ferromagnetic technique for separating wear particles was also employed on lubricant samples following tests with the calcium sulfonate detergent and the ashless dispersant. Once again the ferrograms revealed small rounded platelets that are typical of both normal rubbing wear and three-body abrasion. No cutting wear particles were observed.

6. Profilometric Data

Profiles of the cylinder specimen wear scars are shown in Figure 19 for the longitudinal direction and Figure 20 for the circumferential direction. The two profiles shown in each figure represent cases where the detergent additive was used with and without ash contaminant in the lube-oil. The traces are shown as examples of the type of data that was obtained, but also illustrate the fact that, even though the magnitude of wear was similar between the two cases, there were slight differences in the wear scar produced. Traces for the other additives were not significantly different from the "no-additive" case.

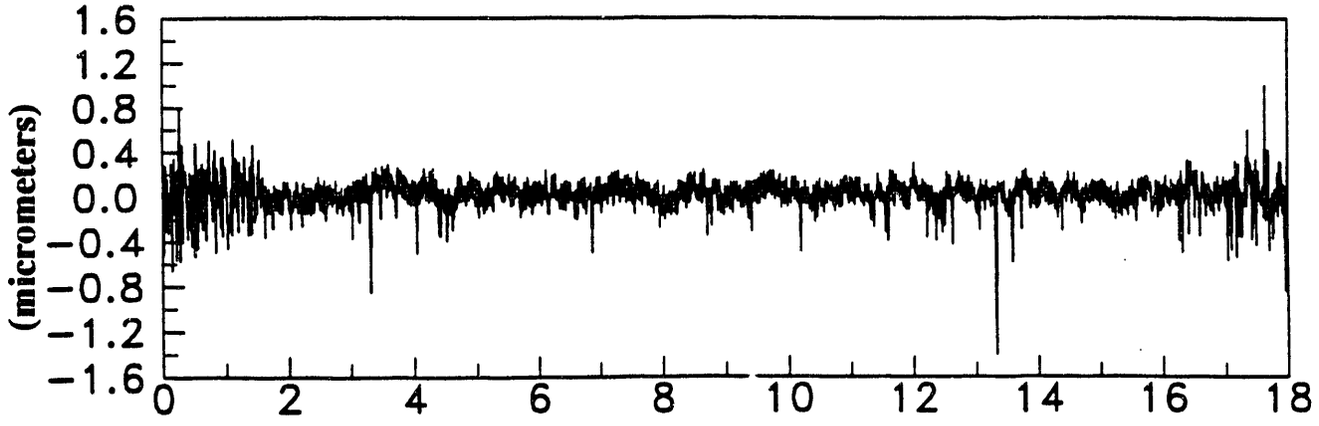

a. Clean Oil/Detergent Mixture

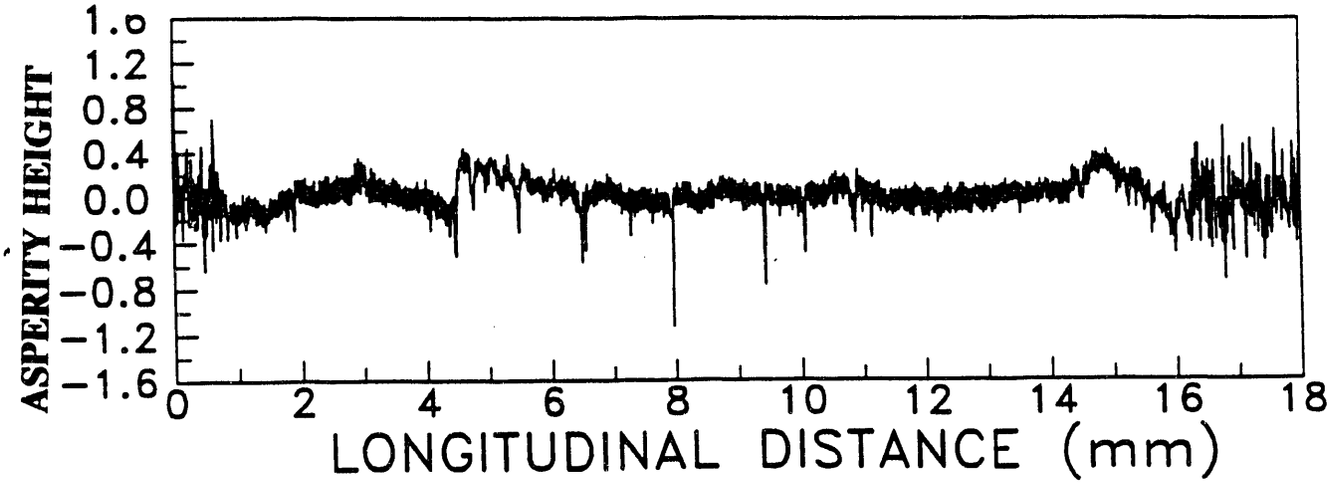

b. Ash Contaminated Oil/Detergent Mixture

Figure 19. Cylinder Specimen Longitudinal Wear Scar Profiles

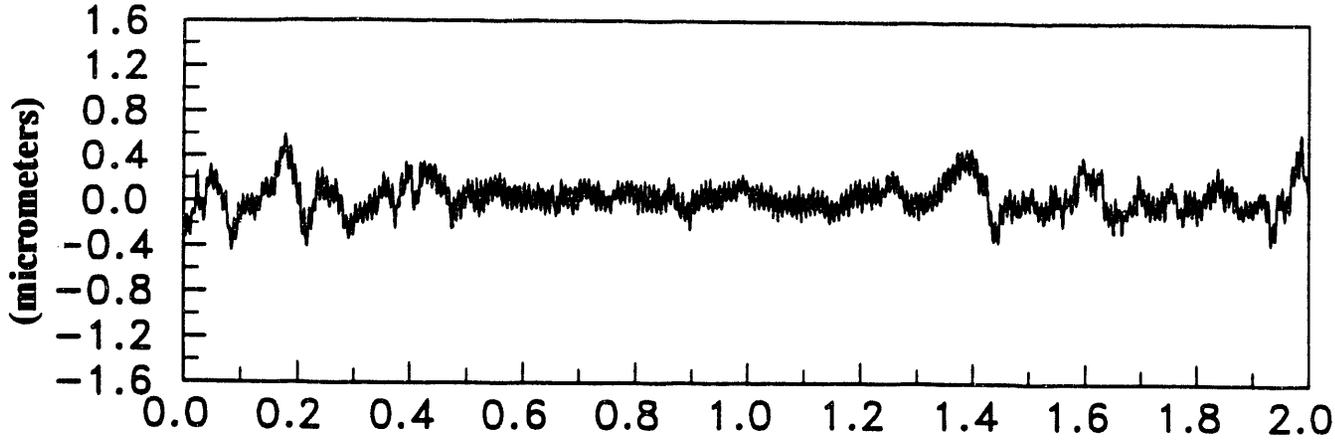

a. Clean Oil/Detergent Mixture

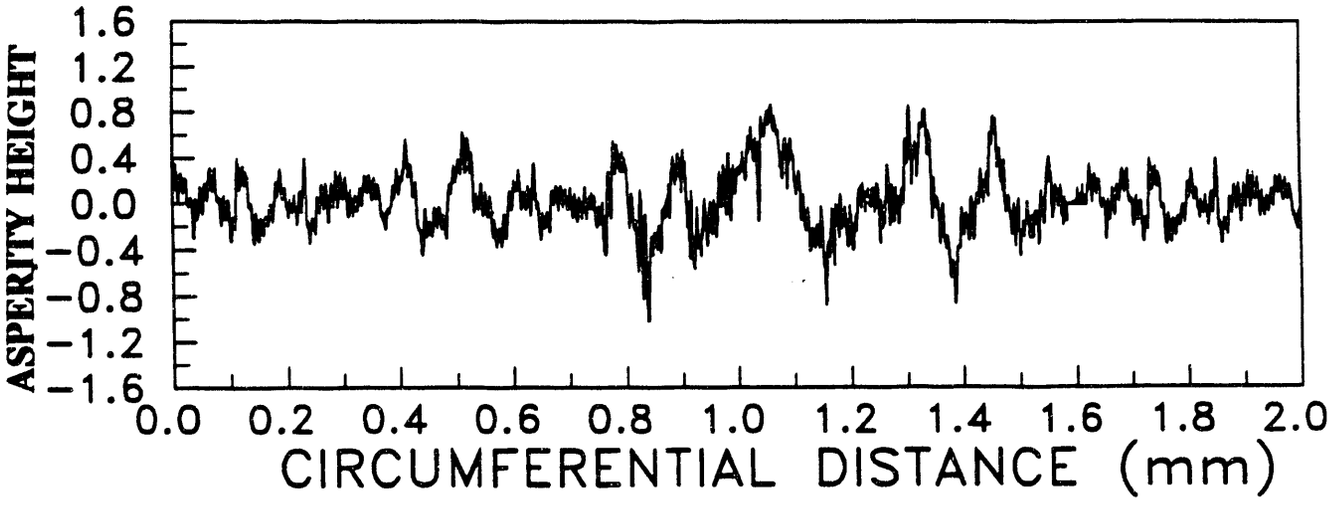

B. Ash Contaminated Oil/Detergent Mixture

Figure 20. Cylinder Specimen Circumferential Wear Scar Profiles

V. DISCUSSION

A. Surface Finish Investigations

The study reveals some useful information about how surface finish can be used to enhance the formation of a hydrodynamic film, and thus reduce, or at least minimize the rate of increase of wear rate. It was shown that film formation depends, not only on asperity height, but also on the orientation of surface grooves relative to the direction of ring travel. While it would take more data to prove it absolutely, the existing data does suggest that film formation is enhanced by having the surface finish grooves oriented normal to the direction of ring travel. Sadeghi and Sui (1989) present a numerical solution of compressible elastohydrodynamic lubrication that agrees with these results. It was also shown that the ability to form that film under clean-oil conditions increases the resistance to wear under contaminated oil conditions.

B. Slotted Specimen Data

The basic idea behind using slots in cylinder liners was that they might enhance the formation of a hydrodynamic film, while providing avenues of escape for wear particles that would otherwise be dragged the entire stroke of the ring piece. There is some evidence that slots do, in fact, enhance hydrodynamic film formation. In several of these a finite resistance was measured between the ring and cylinder-liner wear specimens. Since that resistance was zero for the unslotted specimen, there must be a thicker film formed with the slotted specimens. That film seems to be enhanced by orienting slots normal to the ring travel direction (as observed with the surface finish grind marks). Perhaps this also explains why a specimen with only two slots had more wear than a specimen with 34 slots in the same space (assuming the 34-slot specimen was able to sustain a hydrodynamic film while the 2-slot specimen was not). Typically film thickness can only be increased by increasing viscosity or the relative speed between the ring and liner, but in this case, the presence of slots change the flow dynamics between the two wearing specimens such that the film thickness is enhanced.

There was little evidence, however that the slots were effective in allowing particles caught in the wear zone to escape. Photomicrographs indicated that wear grooves starting on one side of the slot simply continue on the other. This suggests that the visible grooves are really a conforming of the mating wear specimens. The real wear process occurs on a smaller scale that involves thousands of repeated wear events. Apparently, there are a statistically large number of particles available so that as soon as one particle is released, another is there to take its place. Individual particles would play a role only in the immediate area they are located. If this is the case, then the presence of a circumferential slot would serve to interrupt the wear process only for as long as the ring surface is above the slot itself. Once the ring reaches the opposite side of the slot, the wear process would pick up where it left off.

It also seems evident, however, that the existing Cameron-Plint configuration is not adequate to test the channeling or dilution effect of the slots. In the engine, the wear zone is supplied from one side by relatively clean oil, and on the other by the contaminated oil. Slots might enhance the dilution of the contaminant particles by clean oil and aid in channeling the particles out of the wear zone. A test configuration that supplies clean oil to one side of the rings, and contaminated oil to the other would be a more accurate simulation of the real engine environment.

C. Lube-Oil Additive Investigations

The most promising wear reduction obtained in this program so far was the result of mixing 19 % calcium sulfonate detergent in the lube oil. The additive resulted in a thick hydrodynamic or chemical film (as evidenced by the measurement of resistance between the wear specimens), a reduction in friction force, and most importantly a reduction in wear almost to the clean lubricant level. It is, of course, recognized that actual engine lubricants must contain a mix of many additives (including several of the additives tested here) whose interactions cannot be predicted. Finding a workable lubricant formulation must involve testing with the fully formulated product rather than individual additive components as was done here. Still, the results of this investigation do say some important things about the sensitivity of the wear process to additive formulation. In all the surface finish and slotted specimen tests, there was not one configuration that decreased wear as much as the detergent did, or increased wear as much as the dispersant did.

VI. CONCLUSIONS

The following conclusions can be drawn from the results of this study.

- Varying surface roughness and cross-hatch orientation over a wide range did not significantly change the wear rate under clean-oil conditions.

- There is evidence that using rougher surfaces with grooves oriented normal to the direction of ring travel can enhance the formation of a hydrodynamic film.

- The ability to form a hydrodynamic film under clean-oil conditions increases the wear resistance under contaminated oil conditions as well.

- Orienting cylinder surface slots normal to the direction of ring travel enhances hydrodynamic film formation.

- Wear was highly sensitive to additive formulation.

- A 19 percent mixture of calcium sulfonate detergent reduced the contaminated lubricant wear to almost the clean lubricant wear level.

It seems apparent from the results so far that lube-oil additives had the most significant effect on wear. Surface finish and slots in the cylinder surface affected the hydrodynamic film formation process, but there was not an obvious affect on wear as seen in the mass-loss wear results. It should also be said, however, that the test conditions chosen for the previous tasks were, out of necessity, fairly severe. They were effective in screening a large number of contaminant variations, specimen surface variations, and lubricant mixtures, but they may not have been sensitive to subtle effects such as the effect of cylinder surface condition on hydrodynamic films. Examples of the possible insensitivity of the tests can be seen most clearly in some of the cases where the entire surface finish had been completely removed. In addition, the use of a somewhat high ring loading (approximately an order of magnitude higher than the maximum loading in the engine) may have introduced a larger proportion of adhesive wear, and changed the dynamics by which lube-oil additives affect wear. A separate issue concerns the way lubricant is supplied to the wear zone, especially as it pertains to slotted specimen tests. Since part of the purpose of slots was to allow for highly contaminated oil to be diluted and/or flushed out of the wear zone, it is not fair to test those configurations in a constant concentration lubricant bath. A configuration where fresh oil is supplied on one side and contaminated oil on the other side of the ring would provide a more accurate test.

VII. RECOMMENDATIONS

The purpose of future work in Task 4, will be to further investigate questions raised in Task 3 to allow for more specific recommendations as to the appropriate wear prevention strategies. The task will involve wear tests at lower load conditions (those approaching actual engine loads) in which only minimal damage is done to the surface finish on the wear specimens. Wear evaluations will be made based on profilometric and microscopic observations rather than weight-loss measurements. The intent of these tests will be to identify any differences in wear processes between these and the high load cases so that appropriate adjustments can be made to the interpretation of high-load data. One special area of focus will be cases run with a detergent/baseline oil/contaminant mixture. These will be tested at several different load conditions to determine whether detergent plays the same role in preventing wear at low loads as it did in the high-load cases. Similar tests will also be done with various surface finishes to see if correlations exist which the high-load tests were not sensitive to. Finally, some tests will be performed with slotted specimens in which clean baseline oil is steadily dripped on one side of the ring, while contaminated oil is dripped on the other side. Once again the intent will be to stop testing before significant damage has been done to either wear specimen, and evaluations will be made based on profilometric and microscopic observations.

One other issue that Task 4 will investigate concerns the correlation of particle size with the size of grooves in the wear specimens. Photomicroscopic observations of wear

specimens (Figure 18 for example) indicate wear grooves of the order of 10 microns wide and smaller, but profilometric traces such as Figure 20 indicate that those grooves can be superimposed on larger grooves of the order of 100 microns. The larger grooves are apparent in both the clean oil and the contaminated oil cases, indicating they may have more to do with an adhesive or normal rubbing wear process than the abrasive process. These issues will be explored in more detail in Task 4.

VIII. REFERENCES

Aghan, R.L., and Samuels, L.E., 1970, "Mechanisms of Abrasive Polishing," Wear, Vol. 16, pp. 293-301.

Anderson, Daniel P., 1982, "Wear Particle Atlas (Revised)," Prepared for: Advanced Technology Office Support Equipment Engineering Department, Naval Air Engineering Center, Lakehurst, New Jersey, Report NAEC-92-163.

Barber, G.C., Lee, J.C., and Ludema, K.C., 1987, "Materials and Surface Finish Effects in the Breaking-in Process of Engines," Transactions of the ASME, Vol. 109, pp. 380-387.

Berbezier, I., Martin, J.M., and Kapsa, Ph., 1986, "The role of carbon in lubricated mild wear," Tribology International, Vol. 19, No.3, pp. 115-122.

Cameron, A., and Pumphrey, G., 1983, "Assessment of Bore Polishing Properties of Lubricating Oils by Bench Tests," Esslingen Conference, W. German, Testing and Evaluation of Motor Oils.

Chittenden, R.J., Dowson, D., Dunn, J.A., and Taylor, C.M., 1985, "A Theorectical Analysis of Isothermal EHL Concentrated Contracts - Parts I and II," Proc. R. Soc. Lond. A387, pp. 245-269 and pp. 271-294.

Clingenpeel, J.M., Gurney, M.D., and Eccleston, D.B., 1984, "A Combustion and Wear Analysis of a Compression-Ignition Engine Using Coal Slurry Fuels," ASME Paper No. 84-DGP-8.

Czichos, Horst, and Habig, Karl-Heinz, 1986, "Wear of Medium Carbon Steel: A Systematic Study of the Influences of Materials and Operating Parameters, Wear, 110, pp. 389-400.

Danyluk, S., and Reaves, R., 1982, "Influence of Fluids on the Abrasion of Silicon by Diamond," Wear, Vol. 77, pp. 81-87.

Dowson, D., and Higginson, G.R., 1977, Elastohydrodynamic Lubrication, Pergamon Oxford.

Fitzsimmons, B., and Clevenger, H.D., 1975, "Contaminated Lubricants and Tapered Roller Bearing Wear," ASLE Transactions, Vol. 20, 2, pp. 97-107.

Flynn, P.L., Leonard, G.L., and Mihan, R.L., 1989, "Component Wear in Coal-Fueled Diesel Engines," Journal of Engineering for Gas Turbines and Power, Vol. 111, pp. 521-529.

VIII. REFERENCES (Continued)

Harris, T.A., 1984, Rolling Bearing Analysis, 2nd Ed., John Wiley & Sons.

Hesling, D.M., 1963, "A Study of Typical Bore Finishes and Their Effects on Engine Performance," 1963 Annual Meeting, ASLE, New York.

Hsu, B.D., 1988, "Progress on the Investigation of Coal-Water Slurry Fuel Combustion in a medium-Speed Diesel Engine: Part 1 and 2, Ignition Studies and Preliminary Fuel Load Tests," ASME Papers 88-ICE-4, 88-ICE-5.

Imai, Masaya, Teramoto, Hitoshi, Shimauchi, Yoshinori, and Tonegawa, Etsuo, 1986, "Effect of Oil Supply on Fretting Wear," Wear, 110, pp. 217-225.

Ives, L.K., Peterson, M.B., and Whitenton, E.P., 1988, "NIST-3-Mechanisms of Galling and Abrasive Wear," Semi-annual Progress Report for the U.S. DOE Fossil Energy Advanced Research and Technology Development Fossil Energy Materials Program.

Janczak, K.J., and Wisniewski, M.R., 1987, "Influence of Surface Roughness Parameters on Elastohydrodynamic Film Thickness," Wear, Vol 115, pp. 75-82.

Johnson, K.L., 1985, Contact Mechanics, Cambridge University Press, Cambridge.

Jones, R.B., McCouet, C.B., Morley C., and King, K, 1985, "Maceral and rank influences on the morphology of coal char," Fuel, Vol. 64, pp. 1406-1467.

Kakwani, R.M., and Kamo, R., 1988 ,"Combustion Characteristics of Dry Coal Powder Fueled Adiabatic Diesel Engine," 1988 ETCE, New Orleans.

Kamo, Roy, and Valdmanis, Edgers, 1988, "Tribological Properties of Some Selected materials in a Coal-Fired Environment," Journal of the Society of Tribologists and Lubrication Engineers, Vol. 45, No. 7, pp. 417-423.

Kayaba, T., Hokkirigawa, K., and Kato, K., 1986, "Analysis of the Abrasive Wear mechanism by Successive Observations of Wear Processes in a Scanning Electron Microscope," Wear, 110, pp. 419-430.

Leonard, G., Hsu, B., and Flynn, P., 1989, "Coal-Fueled Diesel Technology Development," Final Report, Work Performed Under Contract No. DE-AC21-85-MC22181 for U.S. DOE Office of Fossil Energy by General Electric Company, Research and Development Center, DOE/MC/22181-2694 (DE89000984).

Likos, W.E., and Ryan, III, T.W., 1988, "Experiments with Coal Fuels in a High Temperature Diesel Engine," ASME 88-ICE-29.

Lustgarten, G.A., and Aeberli, K., 1988, "Improved Liner and Ring Wear Properties of Two-Stroke Diesels," Diesel and Gas Turbine Worldwide, Vol. 20, No. 3, pp. 45-48.

VIII. REFERENCES (Continued)

Mayville, R.A., 1989, "Abrasive Concentration Effects on Wear Under Reciprocating Conditions," Submitted to the International Conference on Wear of Materials, Denver, CO.

Mehan, Richard L., 1988, "The Wear of Selected Materials in Mineral Oil Containing a Solid Contaminant," Wear, 124, pp. 65-85.

Mitchell, Richard S., and Gluskoter, Harold J., 1976, "Mineralogy of ash of some American coals: variations with temperature and source," Fuel, Vol. 55, pp. 90-96.

Nydick, S.E., Porchet, F., and Steiger, H.A., 1987, "Continued Development of a Coal/Water Slurry-Fired Slow-Speed Diesel Engine: A Review of Recent Test Results," Journal of Engineering for Gas Turbines and Power, Vol. 109, pp. 465-476.

Prater, J.T., and Courtright, E.L., 1985, "Material and Coating Development Alternative Fuel Applications," Prepared for the U.S. DOE Report No. PNL-5259.

Pratt, T.N., 1982, "The EMD Engine and Blended Fuels--A Progress Report," Electro-Motive Division, General Motors Corporation.

Rabinowiez, E., and Mutis, A., 1965, "Effect of Abrasive Particle Size on Wear," Wear, Vol. 8, pp. 381-390.

Rao, A.K., Melcher, C.L., Shaub, F.S., Kimberley, J.A., Wilson, R.P., Balles, E.N., 1988, "Operating Results of the Cooper-Bessemer JS-1 Engine on Coal-Water Slurry," 1988 ETC, New Orleans, LA.

Rao, A.K., Wilson, R.P., Balles, E.N., Mayville, R.A., McMillian, M.H., and Kimberley, J.A., 1989, "Cooper Bessemer Coal-Fueled Engine System--Progress Report," Journal of Engineering for Gas Turbines and Power, Vol. 111, pp. 498-506.

Richez, Martin, Winquist, Knut, and Storment, John O., 1983, "Theoretical and Experimental Study of Ring-Liner Friction," Final Report SwRI Project 05-9300, Prepared for Advisory Committee for Research, Southwest Research Institute.

Sadeghi, F., and Sui, P.C.,"Compressible Elastohydrodynamic Lubrication of Rough Surfaces," Transactions of the ASME, Vol. 111, January 1989, pp. 56-62.

Schwalb, J.A., Ryan, III, T.W., and Smith, W.C., 1990, "Lube Oil Contamination Induced Wear in Coal-Fueled Diesel Engine," ASME Paper, ICE-Vol. 12, Coal-Fueled Diesel Engines, Book No. 600507.

Sreenath, A.V., and Raman, N., 1976, "Running-In Wear of a Compression Ignition Engine: Factors Influencing the Conformance Between Cylinder Liner and Piston Rings," Wear, Vol. 38, pp. 271-289.

VIII. REFERENCES (Continued)

Sudarshan, T.S., and Bhaduri, S.B., 1983, "Wear in Cylinder Liners, Wear, Vol. 91, pp. 269-279.

Tsai, S.C., 1982, Fundamentals of Coal Beneficiation and Utilization, Elsevier Scientific Publishing Company, New York.

Unsworth, John F., Barratt, David J., Park, David, and Titchener, Keith J., 1988, "Ash formation during pulverized coal combustion; 2. The Significance of crystalline anorthite in boiler deposits," Fuel, Vol. 67, pp. 632-641.

Unsworth, John F., Cunliffe, Frank, Graham, Stephen, C., and Morgan, Paul A., 1987, "Ash formation during pulverized coal combustion 1: Aerodynamic influences," Fuel, Vol. 66, pp. 1672-1679.

Wilson, Michael A., Heng, Sammy, Fredericks, Peter M., Collin, Philip J., and Vassallo, Anthony M., 1986, "The Chemical and Physical Structure of Hydrogenation Residues of Maceral Concentrates," Fuel Processing Technology, 13, Elsevier Science Publishers B.V., pp. 243-260.

Yahagi, Y., 1987, "Corrosive wear of diesel engine cylinder bore," Tribology International, Vol. 20, No. 6, pp. 365-373.

APPENDIX C

Task IV - Refinement of the Most Promising Approach to Wear Prevention

WEAR MECHANISM AND WEAR PREVENTION IN COAL-FUELED DIESEL ENGINES

TASK IV: REFINEMENT OF THE MOST PROMISING APPROACH TO WEAR PREVENTION

U.S. DOE Contract DE-AC21-88MC26044
Southwest Research Institute Project No. 03-2681

Prepared for:

U.S. Department of Energy
Morgantown Energy Technology Center
P.O. Box 880
Morgantown, WV 26507-0880

Prepared by:

James Schwalb, Research Engineer

Approved:

Thomas W. Ryan III, Manager
Combustion Technology
Department of Engine Research

ABSTRACT

Piston ring/cylinder liner wear in coal/water slurry fueled engines remains a major obstacle to the development of a practical engine design. Previous phases of this program have looked at the wear mechanisms causing accelerated ring/liner wear, and traditional approaches to wear prevention. This task of the program looked at some of the issues left unanswered in the previous phases, including the effects of short test duration (or "break-in" wear effects), the effects of low-load conditions, and the effects of using separate oil supplies to simulate the separation of clean and contaminated oil seen in the engine. Each of these items was investigated in bench-scale wear tests, and analysis was made on the resulting wear specimens. In addition, using the results of these tests, a simple wear model was formulated based on the assumption that abrasive wear is proportional to the concentration of particles that are small enough to enter the wear zone, but large enough to contact the two wearing surfaces.

The results from these tests observed a finite, but small amount of accelerated "break-in" wear to occur in the first 15 minutes of each wear test. Ring loading was found to have a significant affect on the wear characteristics. Wear became much more sensitive to surface finish at lower load conditions (10 MPa and less). To explain these characteristics, the wear model was utilized, and conditions were extrapolated to surface finishes and particle sizes not specifically tested in the program. Through the wear model analyses, it became apparent that the predominant parameters affecting the abrasive wear process are the particle size of contaminant relative to surface roughness and hydrodynamic film thickness. In fact, the most highly accelerated wear occurs when the mean contaminant particle is equal to the surface finish + hydrodynamic film thickness.

Tests with the separated/dripped oil supplies were mainly performed using cylinder specimens in which various sizes, spacings and orientations of slots were cut into the surface. The idea of slots was to enhance hydrodynamic film thickness, help dilute the concentration of contaminant on the contaminated oil side of the ring, and to help channel abrasive particles away from the wear zone. None of the slot configurations tested in this program were able to decelerate the wear beyond that seen in an un-slotted specimen. Further, profilometer traces indicated the wear scar profiles were highly asymmetric (scars became deeper on the contaminated oil side of the ring), indicating that the slots are not significantly enhancing the mixing of the clean and contaminated oils. Out of the configurations tested in this program a relatively narrow (0.15 mm wide) slot, longitudinally oriented, with a relatively wide spacing (0.5 mm) caused the least amount of wear.

TABLE OF CONTENTS

LIST OF TABLES

LIST OF ILLUSTRATIONS

LIST OF ILLUSTRATIONS (Continued)

I. INTRODUCTION

Previous work in this program investigated the wear mechanism and traditional approaches to wear prevention, but there were some unanswered questions, which were investigated in Task 4. The major issues dealt with in Task 4 were as follows.

- All of the Cameron-Plint wear tests evaluated in previous Tasks were for test durations of four hours. Questions remained as to whether the entire wear process proceeded at a constant rate over those four hours, or whether there were accelerated wear periods.

- The Cameron-Plint tests in previous tasks were completed using a 100 MPa contact pressure between the wearing specimens. While this loading is low relative to loads typically used in the pin-on-disk or four-ball wear tests, it is still an order of magnitude higher than the typical load at Top Dead Center in the engine. Questions remained as to whether the same wear modes applied at the higher load conditions.

- The conclusions in Task 3 above indicated that the use of a constant concentration bath lubricant supply was not a fair means of evaluating the effectiveness of slotted specimens. Dripped oil supplies that supply clean oil to one side of the ring and contaminated oil to the other would be a more accurate simulation of the actual engine situation.

In response to these issues, three test matrices were formulated involving continued Cameron-Plint testing with various test durations, under lower load conditions than were used in previous tests, and using the double dripped oil supply configuration described above. Once again wear evaluations were made based on weight loss, photomicroscopic observations, and profilometric measurements. Micrometer measurements of the depth of the ring specimen wear scar were also added in an attempt to obtain a more accurate measurement at the lower wear conditions expected.

Also, after completing the low-load wear test matrix, it became apparent that a simple wear calculation might be a useful tool in explaining the trends observed. A model was developed, based on the supposition that abrasive wear is proportional to the concentration of particles that are in the right size range to enter the wear zone. Various coefficients were adjusted to fit the calculation to the data obtained. Calculations were then extrapolated to predict the effects of surface finishes, hydrodynamic film thicknesses, and contaminant particle sizes not specifically tested in the program.

II. APPARATUS AND TEST PROCEDURE

A. The Cameron-Plint High-Frequency Friction Machine

The apparatus chosen for these tests is the Cameron-Plint high frequency friction machine. The commercially available machine, shown schematically in Figure 1, provides a reciprocating motion through a scotch yoke drive mechanism that simulates the relative motion of the piston ring and cylinder liner in a diesel engine. A specimen of piston ring material is mounted to the bottom of a reciprocating arm where it can rub against a rigidly mounted cylinder liner specimen. Both the ring and cylinder specimens are immersed in a bath containing the contaminated lubricant being tested. Above the reciprocating arm is a spring tensioned bar that applies a force normal to the direction of travel. The arm is also instrumented to measure friction force (force in the direction of ring travel) and electrical resistance between the ring and cylinder specimens (an indication of the thickness of the hydrodynamic film). Friction force and electrical resistance measurements were monitored on a strip-chart recorder where a time-averaged signal was recorded. Details of how the Cameron-Plint machine was configured for all the tests reported here are contained in Table 1.

Test specimens were chosen to represent typical cast-iron materials used in diesel engines. Cylinder pieces were cut from the 96.5 mm I.D. cylinder liners of a Labeco CLR engine. Each piece was machined to dimensions of 55 mm x 25 mm, flattened on the back so that it varies from 3 - 4 mm thick and weighing approximately 37 grams. Ring specimens were cut from 89 mm D x 2 mm thick cast iron rings and were ground into a wedge shape, 1 mm at the face expanding to 3 mm wide at the base, and weighing approximately 0.3 grams. The wearing surface of 1 mm x 2 mm is exposed to a normal force of up to 200 N, resulting in 100 MPa contact pressure (approximately an order of magnitude higher than the maximum pressure seen in actual diesel engines). With a stroke of 17 mm, the maximum velocity of the ring specimen is approximately 0.9 m/s. This information, along with information on the geometry of the wear specimens was input into a hydrodynamic flow model to calculate Hertzian stress and hydrodynamic film thickness assuming an elliptical contact region (Harris, 1984, Dawson and Higginson, 1977, Chittenden, et al., 1985, and Johnson 1985 provide detailed descriptions of the model). The result of those calculations was a maximum film thickness approximately 0.34 micrometers. Surface roughness for the tests in this program varied from 0.15 to 1.76 micrometers, so it seems apparent that at the higher loads, the wear specimens are in the boundary lubrication regime (indicating there is probably some contact of asperities always) as opposed to hydrodynamic lubrication. This does not preclude the possibility of hydrodynamic effects in which wear is reduced because part of the load is being born by a thin hydrodynamic film.

EXPERIMENTAL APPARATUS

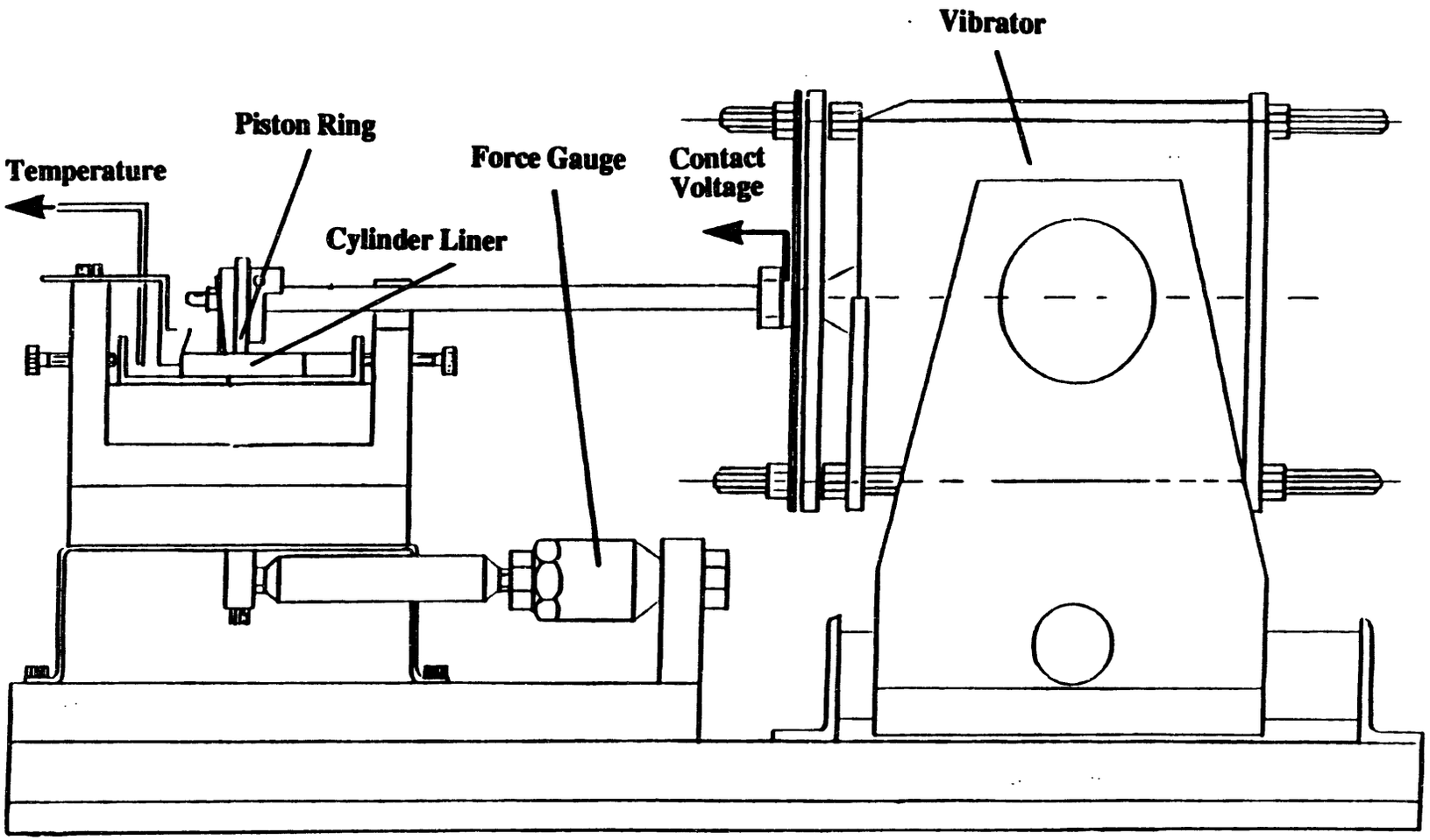

Figure 1. Schematic of the Cameron-Plint Rig

Table 1. Cameron-Plint Configuration	
Normal Load	10 - 200 N
Frequency of Stroke	17 Hz (1020 RPM)
Ring Piece:	
Source	89 mm O.D. cast iron ring
Size	Wedge-shaped piece approximately 3 mm base x 4 mm top x 5 mm wide x 2 mm thick
Approx. Weight	0.3 g
Wear Surf. Area	2 mm^2
Loading	5 - 100 MPa
Cylinder Liner Piece:	
Source	96.5 mm I.D. cylinder liner for Labeco CLR engine
Size	55 mm x 25 mm x 3-5 mm thick (thickness varies because of the curvature of the liner).
Approximate Weight	37 g

Details of the baseline lube-oil properties are contained in Table 2. The oil was chosen as representative of typical diesel lube-oil properties, but without any additives.

B. Analysis of Ash Contaminant

Proximate analyses of the contaminants used in this program are included in Table 3, and particle size analyses in Table 4. The contaminants were originally chosen to represent a range of carbon versus ash content. Since the intent for this Task of the program was to study low load conditions, shorter time durations, and a different oil supply configuration, only the Kentucky Splint ash (after fluid-energy mill grinding) was used. Table 5 contains the results of X-ray fluorescence analysis on that ash which confirms that silicon, aluminum, iron and calcium seem to be the major elements present,

Wilson, et al., 1986; Unsworth, et al., 1987; Unsworth, et al., 1988) indicates that silicon is most likely present in quartz. Aluminum might be present as alumina, but is more likely to be found with silicon in aluminosilicate compounds. Iron is predominantly in some form of pyrite, and calcium can be present as calcite, bassanite, or dolomite. The heat of combustion will, of course alter those compounds, primarily in the dehydration of various silicate materials, the release of CO_2 from carbonates, and the oxidation of pyrites to iron oxides. For wear processes, the hard minerals, quartz, alumina, and pyrite primarily are of the most concern.

Table 2. Properties of Baseline Oil

40°C Viscosity	143.88 cSt
100°C Viscosity	13.99 cSt
V.I.	93
API Gravity	28.6 @ 15.6°C
T.A.N.	0.01
T.B.N.	0.09
Flash Point	293°C
%N	0.012
%Ca	N.D.
%Zn	N.D.
%P	<0.01
%S	0.21

Table 3. Proximate Analysis of Contaminants

Description	Feed Stock	Ash	Vol. Matter	Fixed Carbon
Low-Ash Coal	Unknown	1.00%	34.51%	64.14%
Carbon Black	Mogul-L	0	0	100%
High-Ash Coal	Kentucky Splint	22.9%	30.5%	46.6%
Cleaned Coal	Kentucky Splint	0.38%	37.73%	61.88%
Ash Product	Kentucky Splint	85.3%	10.6%	4.1%

Table 4. Particle Size Averages

Contaminant	Number Weight Averages		Volume Weighted Averages	
	Arith. Mean	Log Mean	Arith. Mean	Log Mean
Low-Ash Coal	4.8	4.1	13.8	11.5
Carbon Black	3.9	3.1	9.9	9.0
Raw Kentucky Splint Coal	4.1	3.1	15.1	13.2
Cleaned Kentucky	5.5	4.1	18.9	16.7
Ash From Kentucky Splint Coal	13.7	12.5	33.4	27.2
Ash From Kentucky Splint Coal Ground in Fluid Energy Mill	2.8	1.9	9.2	8.2
Syloid 63 Silica	2.4	1.6	10.6	0.6

Table 5. Analysis of Contaminant Ash

	(Weight Percent of Ash)				
	Cleaned K.S. Coal	Low-Ash Coal	Raw K.S. Coal	Ash From K.S. Coal	Syloid 63 Silica
SiO_2	39.41	41.73	60.85	65.30	98.58
$A1_2O_3$	14.55	29.20	23.78	22.09	1.18
Fe_2O_3	25.39	14.77	5.34	3.55	0.18
CaO	5.15	8.66	2.06	1.57	0
MgO	1.72	0.92	1.42	1.88	0
NA_2O	0.13	0.07	0	0	0
K_2O	0.78	1.94	4.20	4.78	0.06
Ti_2O	6.17	1.03	0.70	0.82	0
Cr_2O_3	0.37	0.04	0.61	0	0
NiO	3.82	0.19	0.94	0	0
CuO_2	0.72	0.27	0.10	0	0
SO_3	1.77	1.19	0	0	0

C. Wear Evaluation Techniques

Evaluation of wear was accomplished using photomicroscopic, profilometric, and mass-loss techniques as described in previous papers concerning this project (Schwalb, et al., 1990, and Schwalb and Ryan, 1991). Of those techniques, the mass-loss of the wear specimens was the only one used for a real quantitative measurement. This was of some concern, because with mass-loss measurements, a relatively large magnitude of wear isrequired to get measurable differences in mass. Since this program involved conditions in which less wear would occur, it was felt that a new means of quantitative wear measurement should be initiated. Micrometer measurements of the ring-piece thickness before and after the wear tests were found to give a consistant indication of the depth of the ring-specimen wear scar. Further, it was found that even under the minimum wear

conditions, the change in ring-thickness was still within the measurable range of the micrometer instrument. These micrometer measurements were recorded for all of the wear tests conducted in this phase of the program.

As before, individual wear specimens were qualitatively evaluated by observations under a photomicroscope. Profiles of cylinder specimen wear scars were obtained in digital form using a Talysurf 10 Profilometer instrument. The cross-wise profiles of cylinder specimen wear scars were used to correlate the distribution of wear groove dimensions with the contaminant particle size distribution.

D. Test Matrices

The purpose of these tests was to investigate the effects of test duration, load, and oil supply configuration on the wear mechanism so that a more proper interpretation of previous results could be made. A test matrix was formulated for each of the items listed above. The matrices are described below.

1. Test Duration Matrix

Previous wear tests in this program were conducted for a full four hour period, after which a single evaluation of wear magnitude was made. Friction force was monitored for all of these tests as a means of determining whether any significant changes in wear rate were occurring throughout the four hour period. Generally, those friction force traces indicated minor anomalies within the first half hour associated with a "break-in" period, but there were no major changes for the remainder of the test. This was taken as an indication that no major changes in wear mechanism or wear rate were occurring. As a further check of the consistency of the wear process, Cameron-Plint tests of various duration were initiated to determine if the wear was occurring at a constant rate. The test matrix developed is described in Table 6 below.

Table 6. Test Duration Matrix

Description of Cylinder Test Specimen	Applied Normal Load (N)	Test Durations (hours)
Surface Roughness (R_a) = 0.46 μm, 20° Cross-Hatch Angle	200	2, 1, 0.5, 0.25
Same as Above	10	2, 0.5, 0.25

Each of the above tests was initiated with a new/unworn set of cylinder liner and ring specimens, and each condition was repeated once to get an idea of the spread of the data. The four hour/200 N tests in the above matrix were actually completed in a previous phase of the project and the data was added to this matrix. The set of tests at 10 N normal load was initiated to confirm if the wear process was constant at lower load conditions as well.

2. Low-Load Conditions Matrix

Most of the wear tests from previous phases of this program were performed with a 200 N load on a 2 mm^2 surface translating into 100 MPa of pressure on the wear specimens. That pressure is approximately an order of magnitude higher than is typically seen at TDC in a diesel engine. The use of higher load conditions is common in bench-scale wear tests in which researchers are trying to create a measurable amount of wear in a reasonable time period. In fact, the 100 MPa pressure used in this program is low compared to pressures typically used in other bench-scale apparatuses (the pin-on-disk and four-ball apparatuses for example). Still, it is recognized that increased load can alter the wear mechanism so that parameters such as surface finish and lube-oil additives might not have the same effects. To investigate the effects of load more completely, the test matrix described in Table 7 below was formulated.

Table 7. Low-Load Conditions Matrix

Cylinder Specimen Surface Conditions	Applied Normal Loads (N)	Lubricant Formulation	Duration of Test (hours)
0.15 μm R_a, 20° Cross-Hatch Angle	200, 50, 25, 10	Baseline Oil + 5 % Ash Contaminant	2
0.46 μm R_a, 20° Cross-Hatch Angle	200, 50, 25, 10	Baseline Oil + 5 % Ash Contaminant	2
1.76 μm R_a, 20° Cross-Hatch Angle	200, 50, 25, 10	Baseline Oil + 5 % Ash Contaminant	2
0.46 μm R_a, 20° Cross-Hatch Angle	200, 50, 25, 10	(Baseline Oil/19% Calcium Sulfonate Detergent Mixture) + 5 % Ash Contaminant	2

The matrix involves a range of surface finish conditions as well as a single set of tests with a 19% calcium sulfonate detergent additive in the mixture (the detergent

additive was chosen because it had the most significant effect on wear in previous tests). A test duration of 2 hours was chosen instead of the 4 hours used in previous tests. The change was initiated in part because it was found in some previous tests that too much wear was occurring. Wear scars were much deeper than the original surface finish groove marks and the geometry of the ring specimens were significantly changing over the course of the test. It was found that in most cases 2 hour tests created enough wear to be measurable without significantly changing the geometries of the wear specimens. The other obvious advantage of 2 hour tests was that more tests could be performed and thus more conditions evaluated with the remaining funds.

3. Dripped Oil Supply Test Matrix

Tests with the dripped oil supplies were initiated because it was argued that engine conditions involved a steady supply of relatively clean oil on one side of the ring, and contaminated oil on the other. Wear mitigation strategies that depend on the flow of oil from the contaminated side to the clean oil side (such as the machining of slots in the cylinder liner surface) could not be properly evaluated in a constant concentration bath. To accomplish the dripped oil supplies configuration, the Cameron-Plint rig was set up with two oil containers, one containing clean baseline oil and the other containing a 5 percent mixture of Kentucky Splint ash in the baseline oil. Each oil was fed by gravity through a small stainless steel tube whose outlet touched the cylinder specimen surface just above the ring reversal location. A schematic of the configuration is shown in Figure 2 below. The entire rig was then tilted (towards the bottom of the schematic in Figure 2) so that each oil would flow slowly over the respective ring reversal points and then drip off the bottom of the specimen. The specimens were also cut axially just below the ring travel path area so that oil would not build up in the curvature of the specimen. The idea was to keep the two oil supplies separated, except for the mixing initiated by the ring itself. Visual observations indicated there was not any large scale mixing of the two oil supplies.

As suggested above, the primary focus of these tests was on evaluation of slotted specimens, whose wear mitigation strategy depends on the stratification of clean and contaminated oil. Table 8 below outlines the different configurations of slot width and spacing that were evaluated. The intention of this matrix was to investigate the effect of slot width at equivalent spacing, and vice versa. Each configuration listed in the table was tested on a single set of wear specimens for two hour duration. Oil supply flowrates were controlled through pinch valves to allow 1 ml/min. flow.

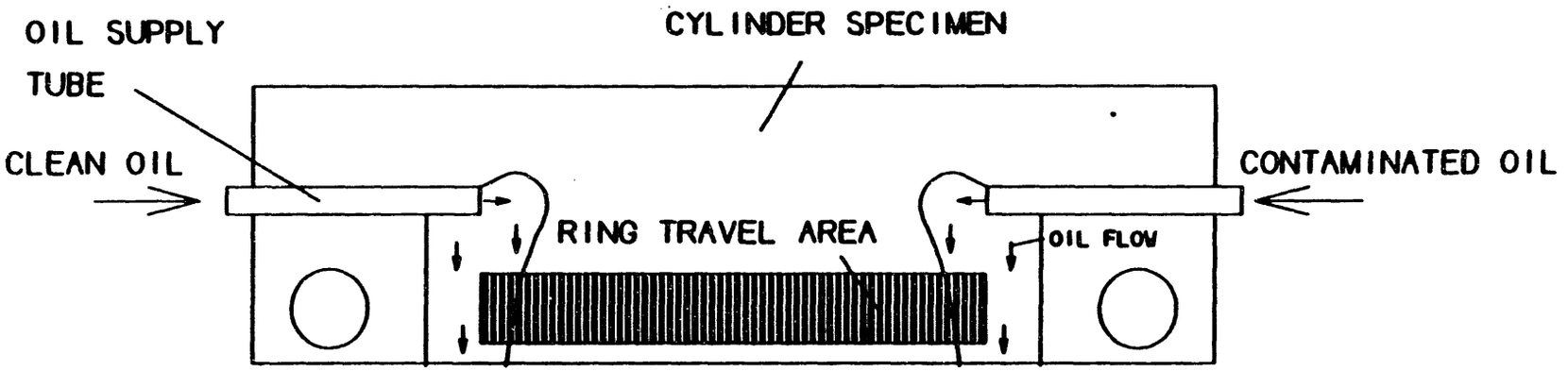

Figure 2. Dripped Oil Supplies Configuration

Table 8. Cylinder Specimen Slot Configuration			
Number of Slots	**Slot Width (mm)**	**Spacing Between Slots (mm)**	**Slot Orientation (Circumferential or Longitudinal)**
90	0.15	0.30	C
12	0.15	0.30	L
60	0.15	0.50	C
8	0.15	0.50	L
60	0.25	0.50	C
8	0.25	0.50	L
60	0.35	0.50	C
8	0.35	0.50	L
2	0.25	10.00	C

III. RESULTS

A. Tests With Varying Duration

Figures 3 - 5 detail the data obtained in Cameron-Plint tests of differing duration. Figures 3 and 4 represent the mass loss of ring and cylinder specimens respectively and Figure 5 represents the depth of the ring wear scar. All the wear data is plotted against test duration. As stated above, the purpose of these tests was to determine the rate of wear as a function of test duration. The figures indicate a fairly constant increase in wear with time at high load conditions with a tendency to slightly flatten out as the test duration approaches zero. The low-load wear curve seemed to flatten out also, but over longer test durations. All three figures reflect the same shape curves, indicating that all three wear measurements are consistently determining the wear trends. The curves also indicate that the magnitude of the ring wear is slightly smaller than the cylinder liner wear. The accelerated wear in the initial stages of each test is probably associated with a "break-in" period and corresponds with the anomalies seen in friction force traces. The magnitude of this break-in wear, however, is not large compared to the total wear for two or four hour duration tests.

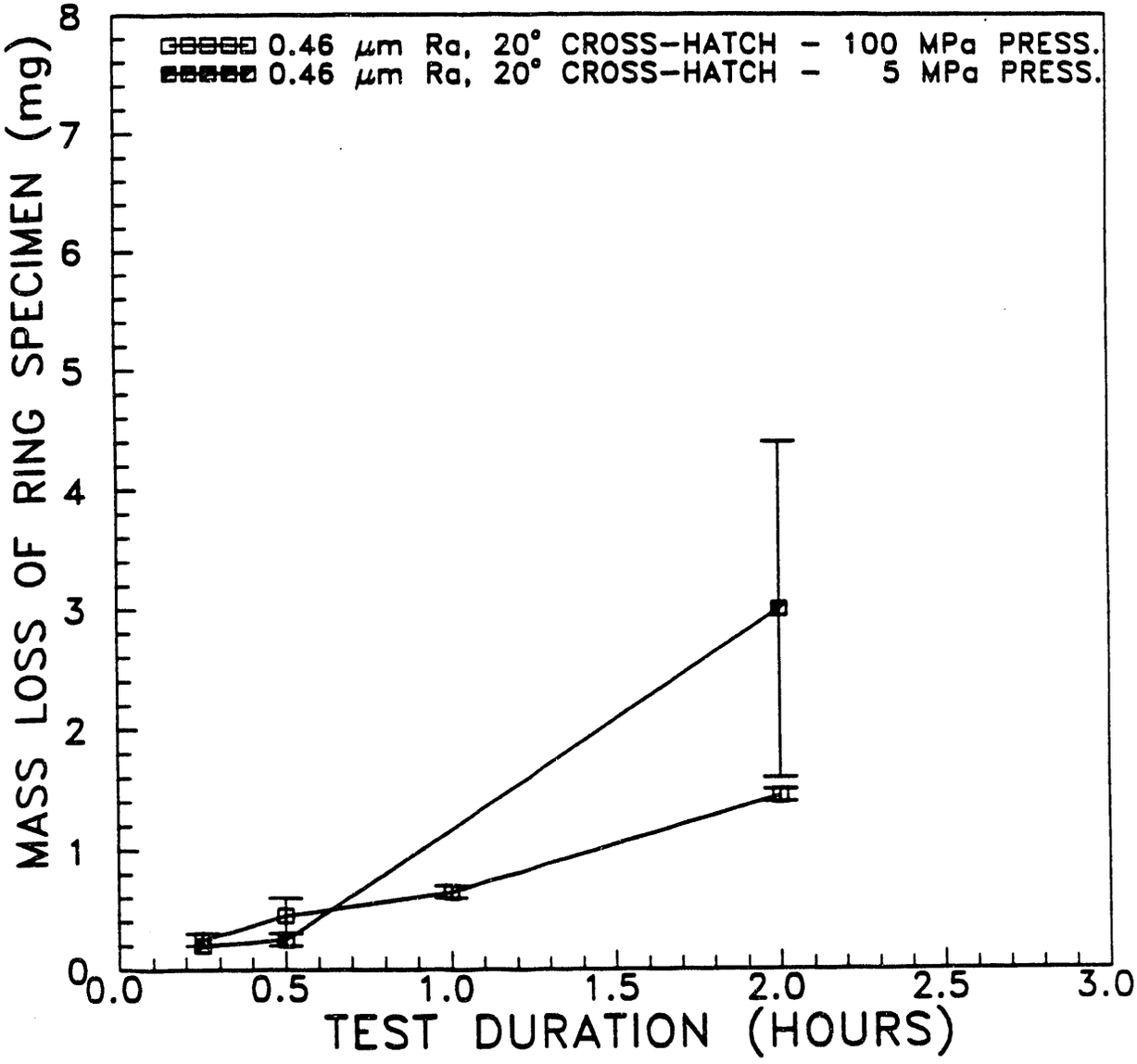

Figure 3. Effect of Test Duration on Ring Specimen Mass Loss

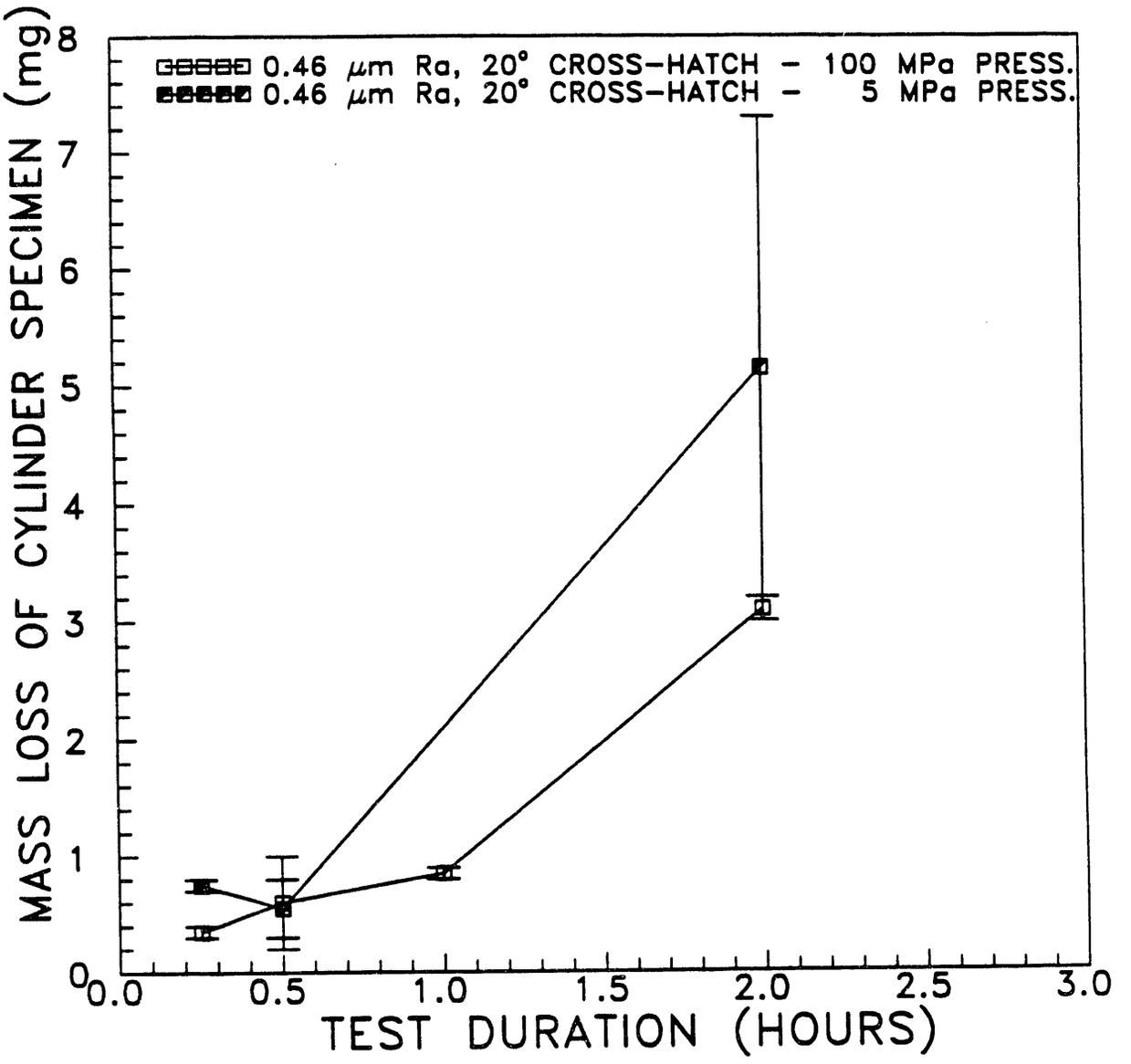

Figure 4. Effect of Test Duration on Cylinder Specimen Mass Loss

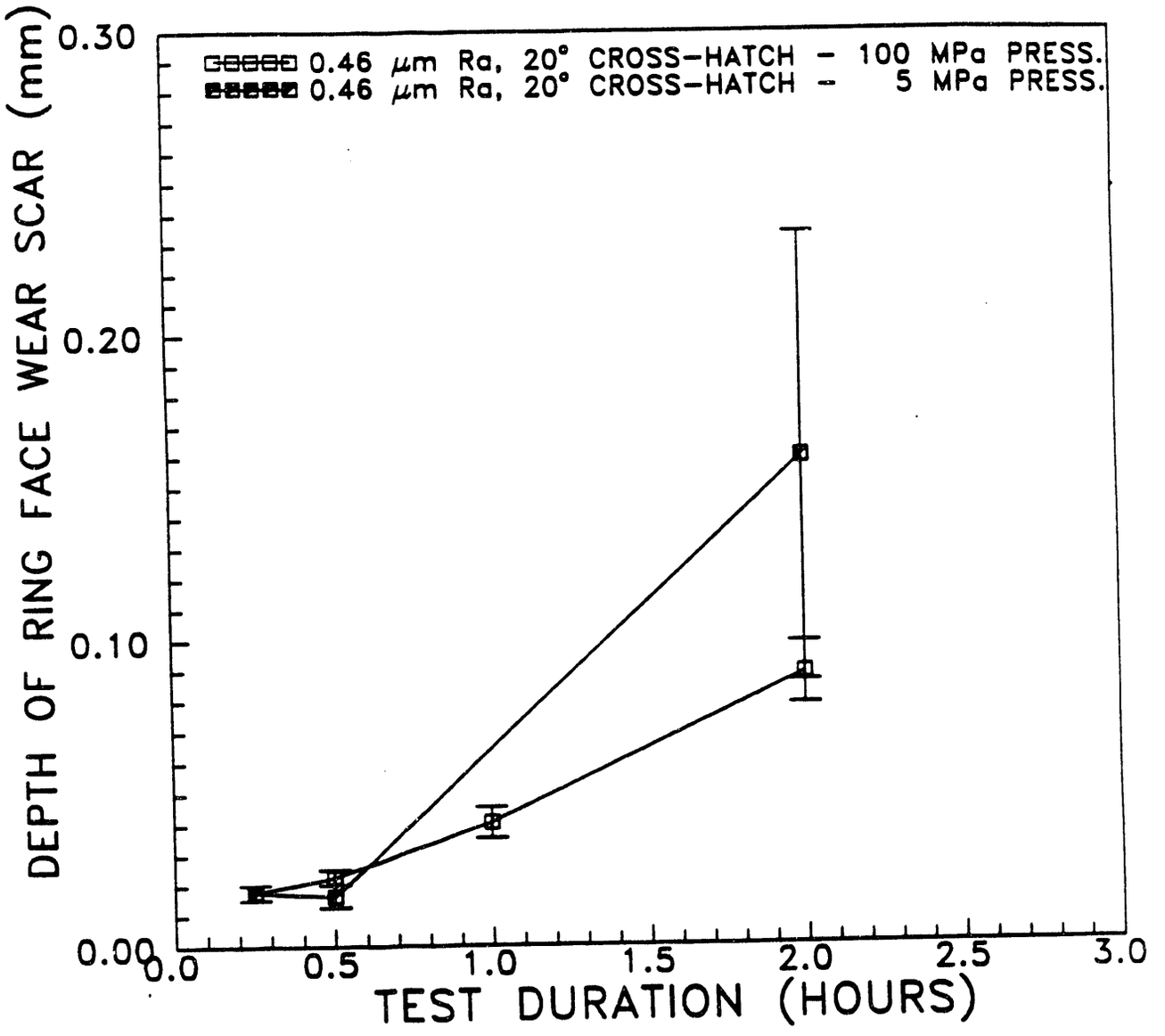

Figure 5. Effect of Test Duration on Depth of Ring Face Wear Scar

B. Tests at Low-Load Conditions

The initiation of tests at lower load conditions than were used in previous tests lead to some interesting results which explain much about the actual wear mechanisms occurring. Figures 6 - 8 are graphs of the low-load data plotted as ring specimen mass loss, cylinder specimen mass-loss, and depth of the ring specimen wear scar vs. the corresponding applied normal load.

The most surprising result of this data is the consistant trend for wear to increase as the load is reduced. That trend goes against the existing theories for both adhesive and abrasive wear, although abrasive wear is generally less sensitive to load. It is believed the explanation for this behavior lies in the fact that, as the normal load is reduced, conditions allow for larger and higher concentrations of abrasive particles to enter the wear zone. There are two main reasons why lower-load conditions favor larger particles in the wear zone.

- Hydrodynamic film thickness increases as the load is reduced, increasing the distance between the wear specimens.

- At higher load conditions, there is a significant degree of elastic and plastic deformation of asperities making up the surface roughness.

Another significant observation is that the reduction of surface roughness significantly reduced wear at the lower load conditions. This is a reversal of an earlier conclusion that there was not an obvious advantage of reducing surface roughness. It is consistent, however, with the theory that the wear level is determined by the maximum particle size that can get into the wear zone. Obviously, a rougher surface will allow more and larger particles into the wear zone because of the large cracks and crevices present. It is also known to increase hydrodynamic film thickness (Sadeghi and Sui, 1989). The insensitivity of wear to surface finish at higher loads might be explained as a result of increased proportion of adhesive wear (adhesive wear is a result of plastic deformations which quickly wipe off the original surface finish).

A final observation that can be made concerns the data obtained when a Calcium Sulfonate Detergent was added to the lubricant. Original tests at high load conditions generated some excitement because they showed significant wear reductions. The data in Figures 6 - 8 indicate that, when the additive is present, wear is fairly constant with load. At the high loads, this behavior might be a consequence of the increased proportion of adhesive wear (which is highly sensitive to surface reactive additives). It is difficult to explain why the additive also held wear constant under low-load conditions where abrasive wear is more predominant. The detergent additive, with its surface reactivity might be expected to reduce adhesive wear more than it did abrasive wear. At any rate, it appears there is still an advantage to using the detergent additive, but the magnitude of that

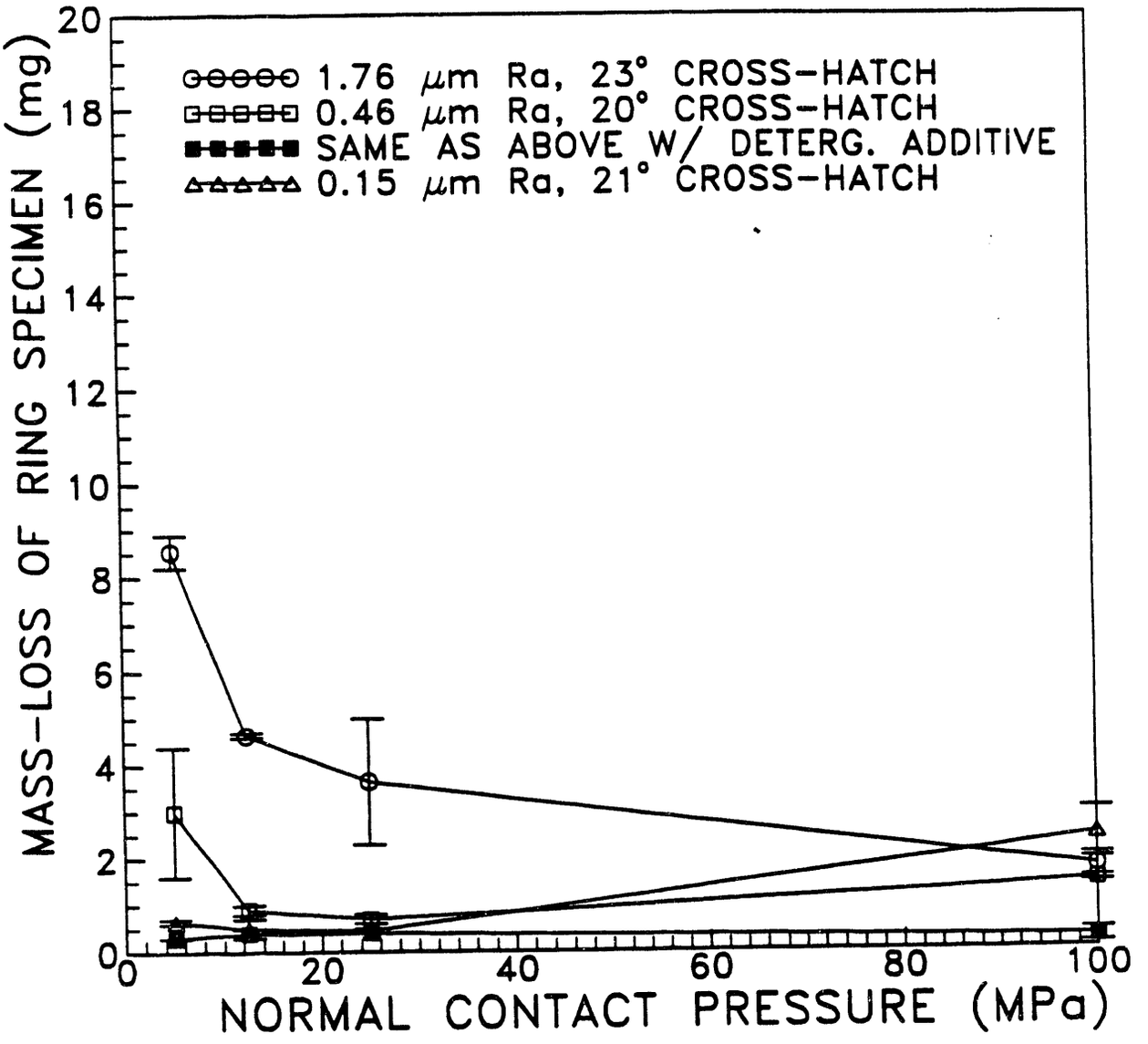

Figure 6. Effect of Contact Pressure on Ring Specimen Mass Loss

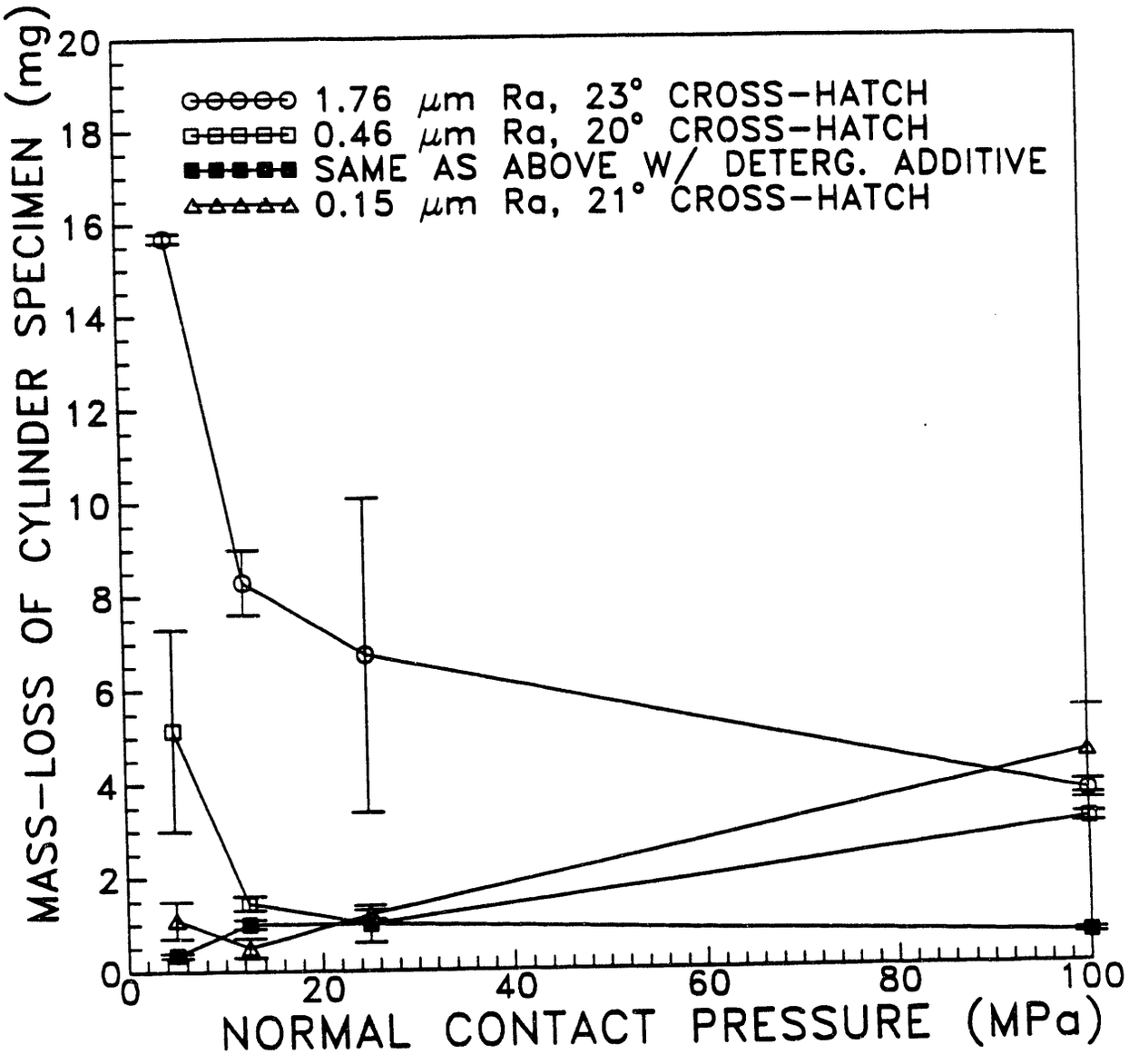

Figure 7. Effect of Contact Pressure on Cylinder Specimen Mass Loss

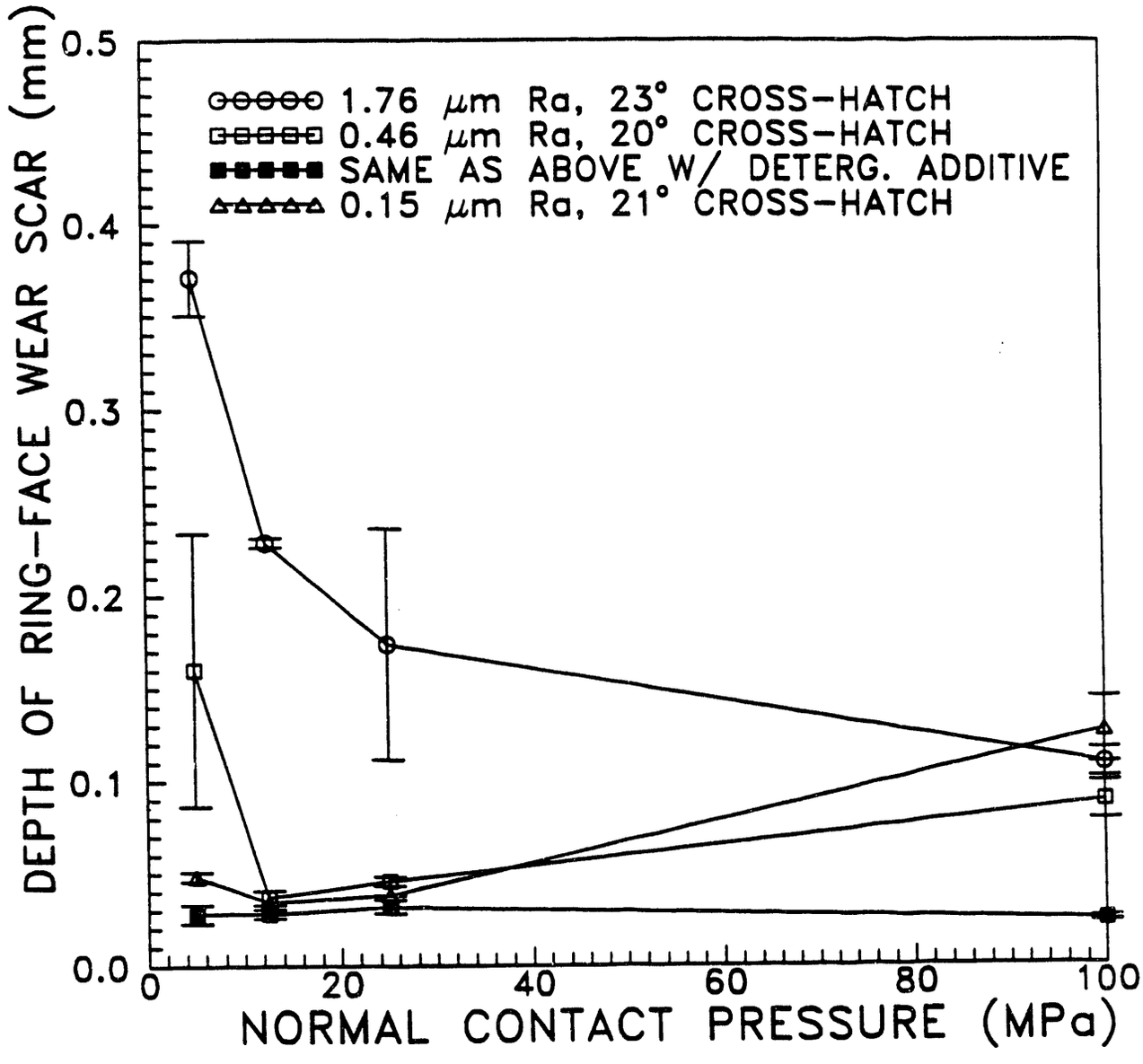

Figure 8. Effect of Contact Pressure on Depth of Ring Face Wear Scar

advantage is dependent on where the conditions fit on the wear vs. load curve. For the range of data tested here, if the load was extremely high, or extremely low, the detergent significantly reduced wear. Somewhere in the middle, the effect of detergent was not so significant.

C. Wear Curve Calculation

As a tool to help understand the subtle aspects of the wear vs. load data, a simple model was developed based on the supposition that abrasive wear is proportional to the concentration of particles that can enter the wear zone. The assumptions are further illustrated in Figure 9, a schematic of the lubricated abrasive wear zone. Shown in the figure are two particles, one of diameter XMAX and the other with a diameter equivalent to the hydrodynamic film thickness. Those two particles represent the range of particle sizes which are assumed to cause wear. In addition, a linear weight factor is introduced which weights the XMAX size particles as causing the highest wear and the Y_H sized particles as causing zero wear.

The value of XMAX is determined by adding the hydrodynamic film thickness to a term which represents the surface roughness minus the elastic/plastic deformation of the asperities. A simplified calculation of hydrodynamic film thickness is employed (shown below in Equation 1) which assumes the thickness proportional to the square-root of velocity divided by contact pressure. In general, this relation is true for pure hydrodynamic films, but for elastohydrodynamic films the exponent on the contact pressure term approaches a smaller value of 0.073 is typically used (these relations are presented in the Mechanical Engineers' Handbook, (1986)). Of course this simple calculation does not take into account any changes in geometry or contact area due to deformations. The calculation also does not take into account surface roughness effects.

Equation 1.) $$Y_H = K_H (V/P)^{1/2}$$

where:
K_H = constant film thickness coefficient
V = relative velocity of ring
P = contact pressure
Y_H = hydrodynamic film thickness

The surface roughness - deformation term is assumed to be an exponential of the form $R_a \exp(-K_e P)$, where P is the contact pressure, R_a is the surface roughness, and K_e is a constant which is dependent on the elasticity and plasticity of the cylinder specimen material. (The term is equal to R_a at $P = 0$, and approaches 0 as P approaches infinity.)

Having determined the size range of particles which cause wear, the abrasive concentration is found by integrating the particle size distribution curve shown in Figure 10 over the critical size range (the weight factor is included in this integration process). To facilitate the integration process, it was assumed the particles follow a log-normal distribution (for the ash shown in Figure 10 the log-normal mean was calculated to be 8.2

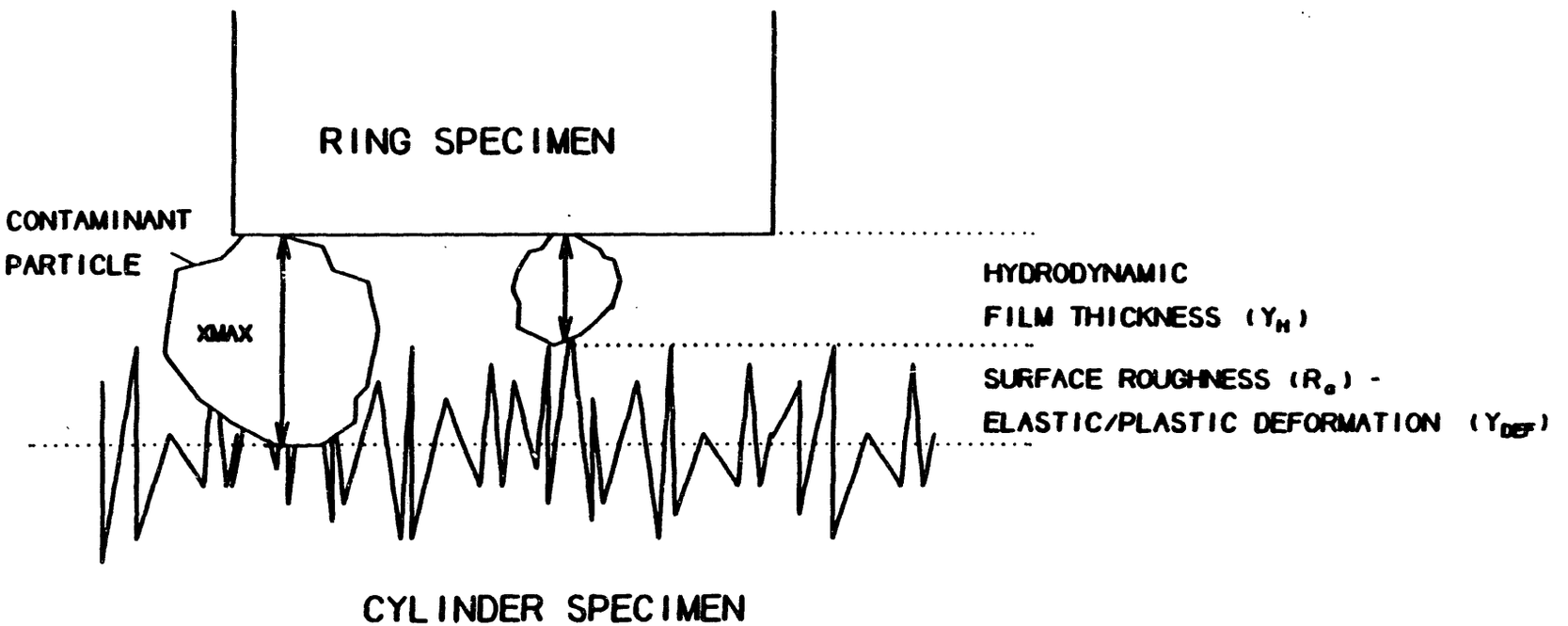

Figure 9. Schematic of the Lubricated Abrasive Wear Zone

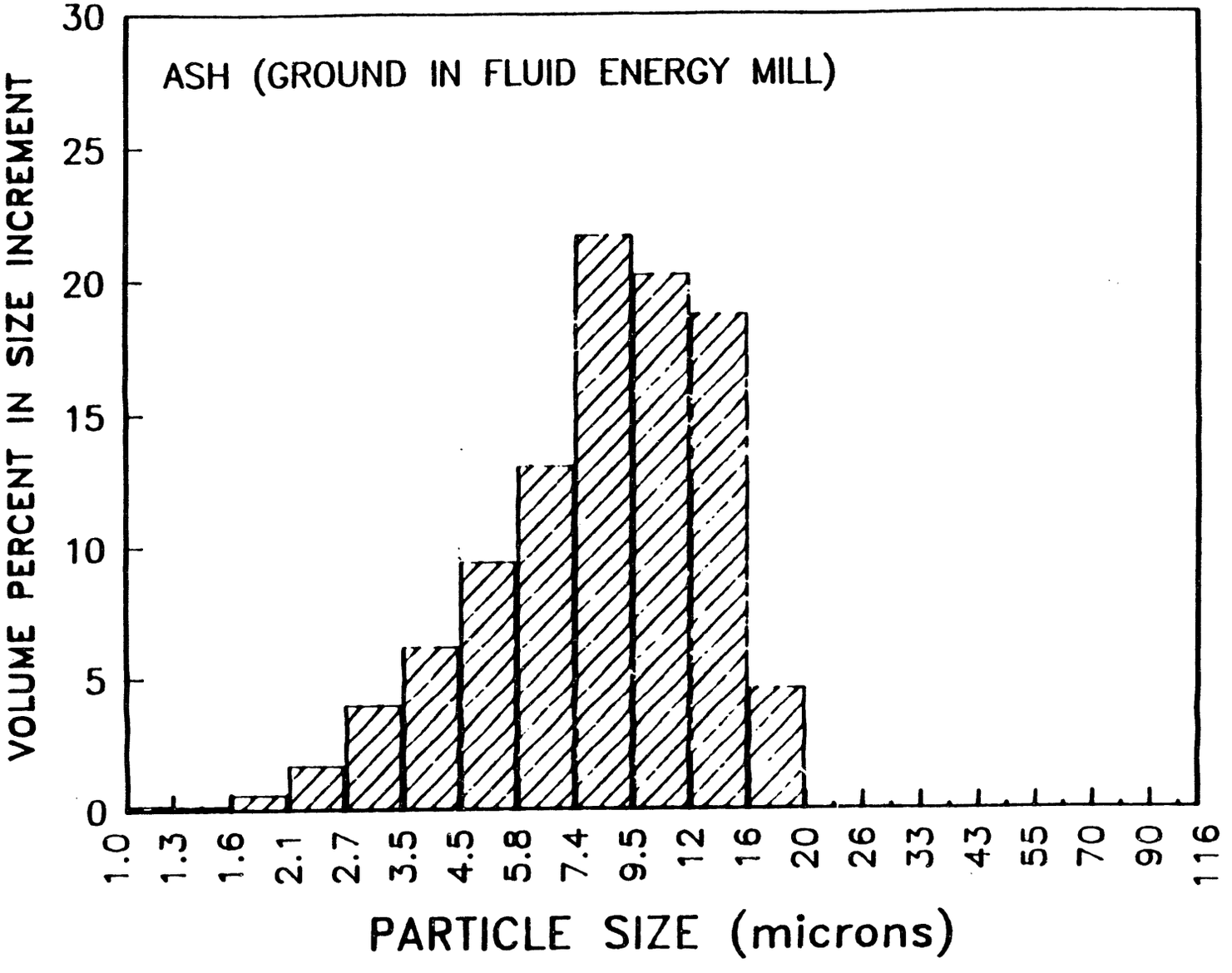

Figure 10. Volume Weighted Particle Size Distribution for Air-Mill Ground Ash

μm and the standard deviation 0.49). The integrated concentration is then plugged into the equation below to calculate the total abrasive wear (a modified version of the abrasive wear relation presented by Rabinowicz (1965)).

Equation 2. $\quad$ Abrasive Wear = K_{ab} P G / H

where:
- P = contact pressure
- G = integrated particle concentration
- H = hardness of the wearing specimens
- K_{ab} = abrasive wear coefficient

The total wear is then calculated as the sum of the abrasive wear, and two other wear components. One is a constant "break-in" wear which seems to occur quickly and requires little contact pressure, but is generally small in magnitude. The other component is adhesive wear, which is assumed to follow the Archard equation listed in Equation 3 below (Archard, 1953, 1980).

Equation 3. Adhesive Wear = K_{ad} P / H

The characteristic shape of the wear vs. load curve using this calculation procedure is illustrated in Figure 11. At low loads, the hydrodynamic film is much thicker than the particle size, resulting in low wear rates. As load is increased, film thickness decreases and a larger proportion of particles enter the critical size range. Eventually, the point is reached where the maximum particle size that can enter the wear zone is equal to the mean particle size, and the maximum concentration of particles is in the critical range. Increased load beyond that point further decreases the critical size range and begins excluding the larger particles. Eventually the abrasive wear component becomes less significant and the adhesive component takes over resulting in a linear increase in wear with load in the high-load range. Because of the exponential term used in the calculation of abrasive wear, the abrasive component approaches zero as the load becomes large. The result is that, at higher loads there is a dimishing effect of surface finish.

The calculation procedure described above contains five factors which could be adjusted to fit the data. The five factors are as follows.

- Break-In - constant break-in wear
- K_H - a constant to scale the hydrodynamic film thickness
- K_e - constant determining the degree of asperity deformation due to load
- K_{ab} - abrasive wear coefficient
- K_{ad} - adhesive wear coefficient

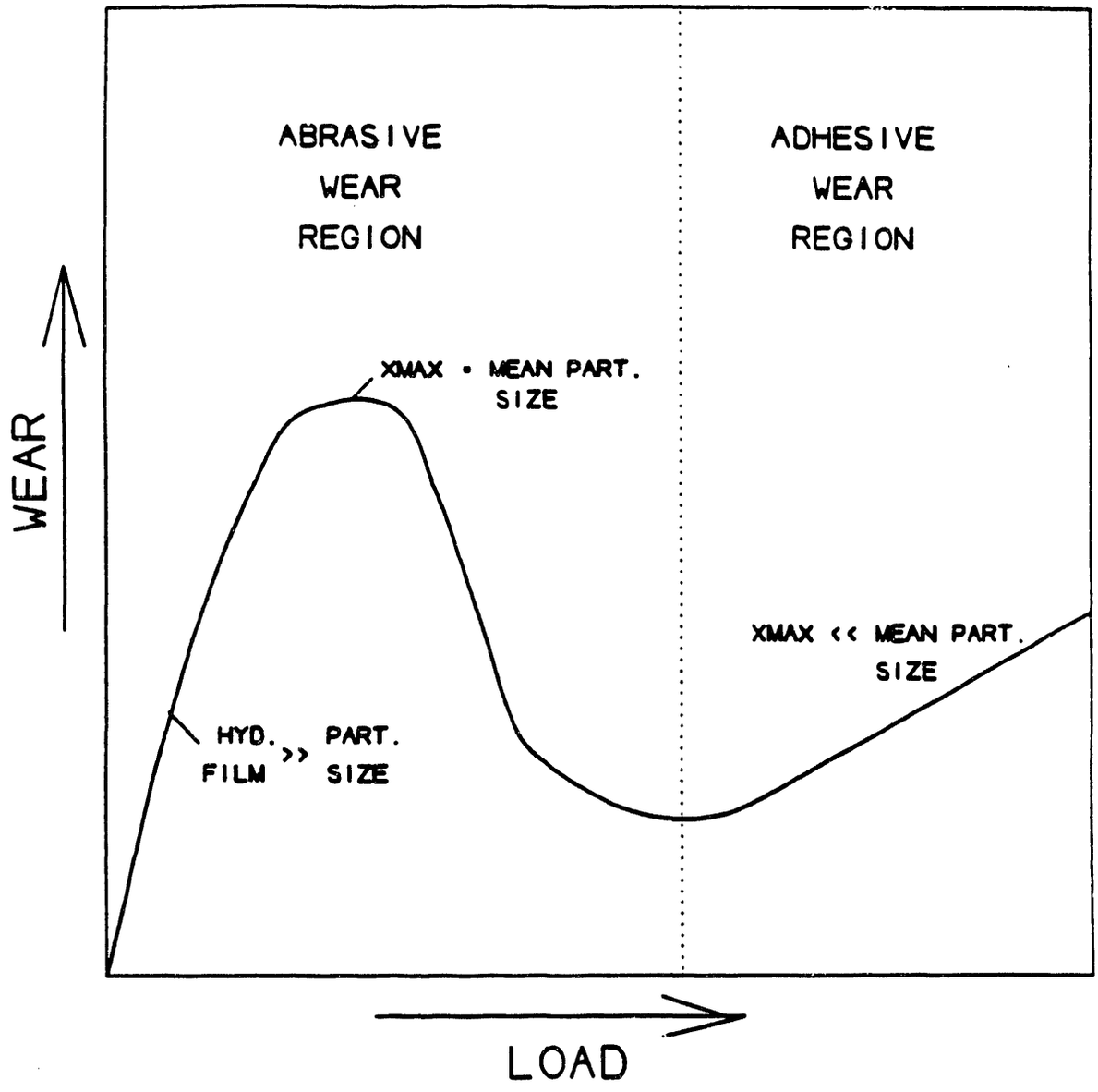

Figure 11. Characteristic Shape of Wear Curves

Using a trial and error procedure, these factors were adjusted to best fit the data presented in the previous section. The calculation results are plotted in Figure 12 along with the data previously presented (the wear data has been converted to a wear volume per unit sliding distance). The factors used for these calculations are as follows.

- Break-In = 10^{-8} mm^3/mm
- $K_H = 8.433\ (mg/s)^{1/2}$
- $K_e = 0.015\ (MPa^{-1})$
- $K_{ab} = 5.6 \times 10^{-4}\ (mm^3/mm)/(Br*MPa)$
- $K_{ad} = 8 \times 10^{-8}\ (mm^3/mm)/(Br*MPa)$

The calculations successfully simulate the shape of the wear curves, the relative effects of surface finish, and the fact that surface finish effects diminish as load is increased.

Using the same fitting factors, comparisons were also made for data taken in previous phases of this project. Those comparisons are shown in Figures 13 and 14. In Figure 13, the data shown is for the same ash used in this program, but at both 5 and 10 percent concentrations. As expected, the 5 percent data point is reasonably predicted, but the model predicts that wear caused by the 10 percent concentration will be approximately the same. This was not observed in the data. Apparently, there is an effect of ash concentration on wear, even at the higher loads. Figure 14 shows data taken with a significantly larger particle size. Once again, there appear to be effects of concentration and particle size at high loads that are not predicted by the model. If the model is correct in assuming that adhesive wear takes over at the higher loads, then it must be said that the particle size distribution and concentration of contaminant have an effect on the adhesive wear coefficient. It is also possible that abrasive wear is still a significant factor at the higher loads, because even though the wear specimens are tightly fit, some particles can still enter the wear zone. At any rate, the data presented in Figures 13 and 14 illustrate that the model cannot be used to extrapolate to conditions at extremely high loads and with extremely large particle size distributions. Conditions in the engine, however, are at lower loads and with probably much smaller particle distributions than were used in the Figure 12 data. It seems reasonable that the model would be more accurate under the lower load conditions, and could at least be used as a tool to investigate the wear trends as particle size, surface roughness, hydrodynamic film thickness, and other parameters are varied.

As a further exercise, wear curves were re-calculated assuming a 3 μm log-mean particle size and 0.5 standard deviation (these numbers are closer to what Gaydos (1989) measured in an actual engine). Those results for several different surface finishes are presented in Figure 15. The calculations illustrate that reducing the size of surface

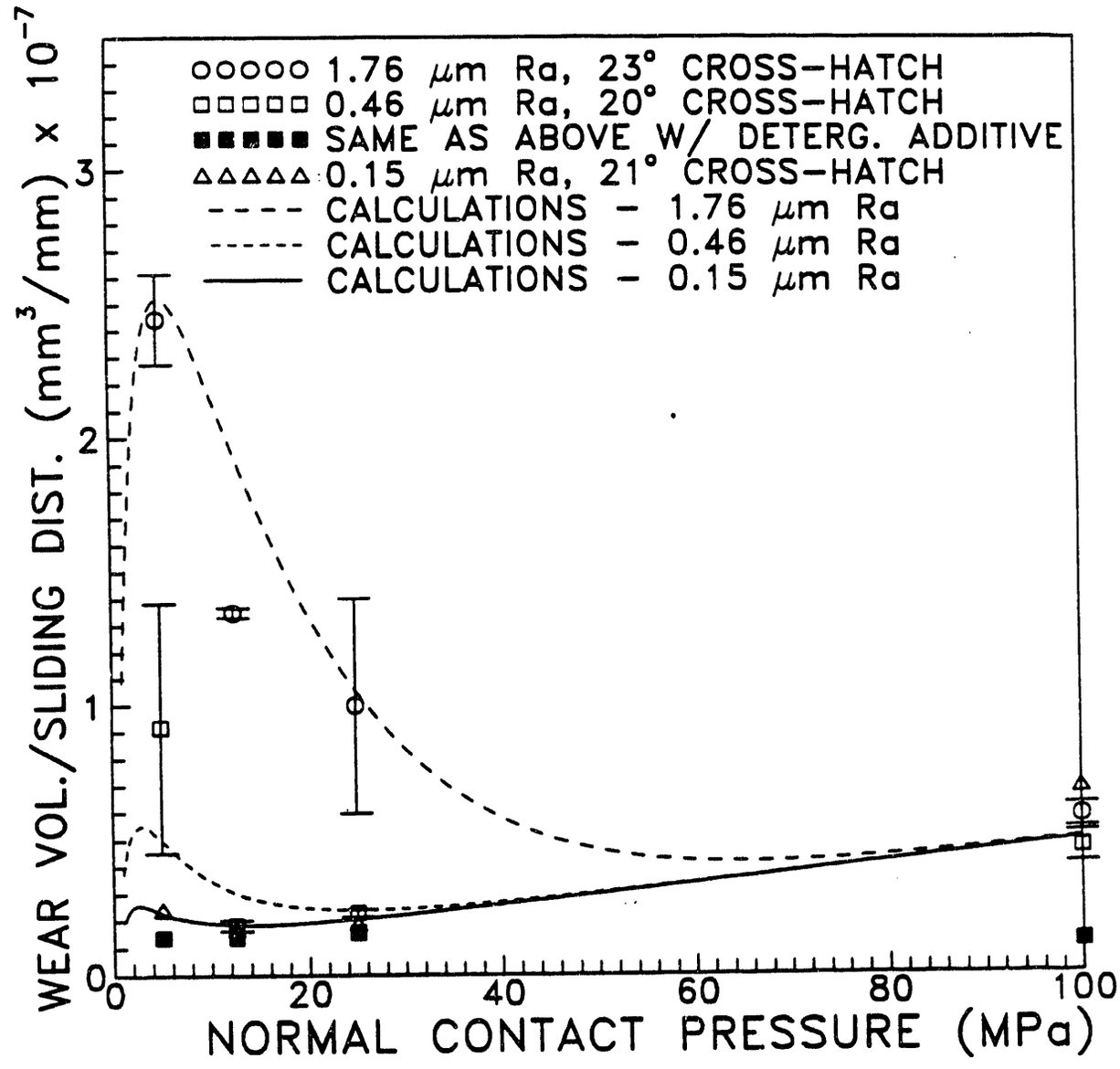

Figure 12. Comparison of Wear Model and Ring Wear Data

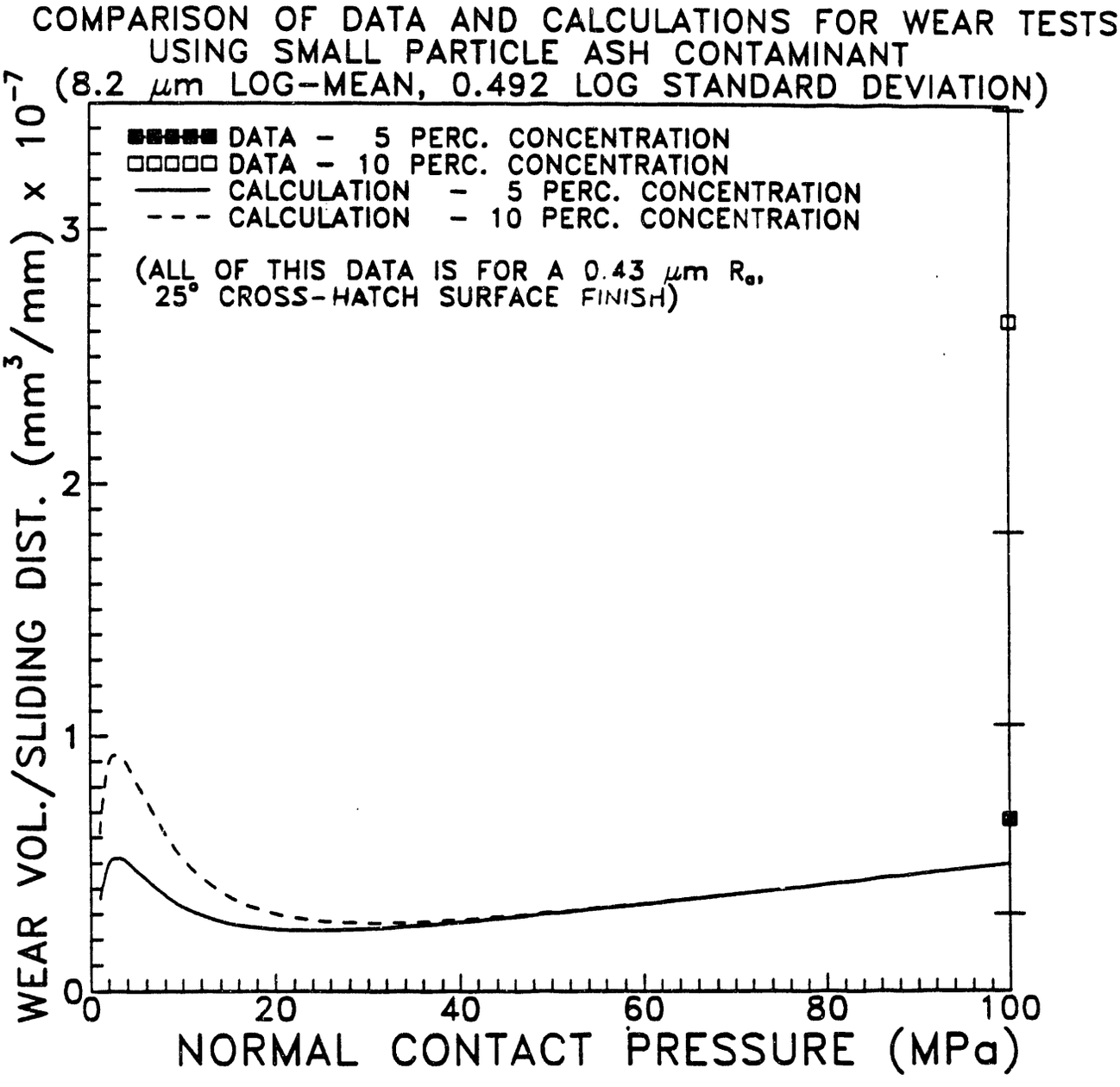

Figure 13. Comparison of Wear Model With Data Taken in Previous Work - Small Particle Distribution

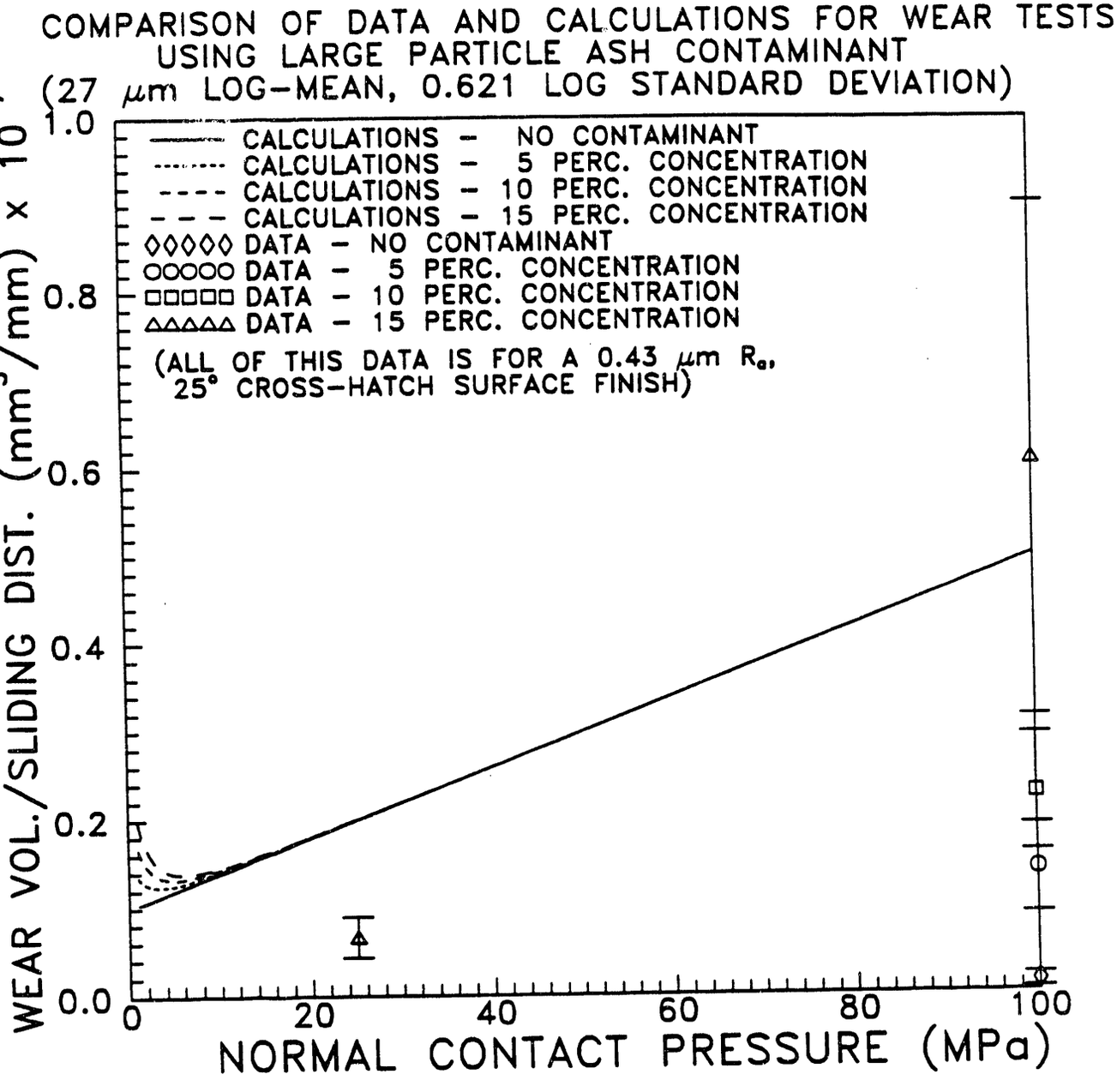

Figure 14. Comparison of Wear Model With Data Taken in Previous Work - Large Particle Distribution

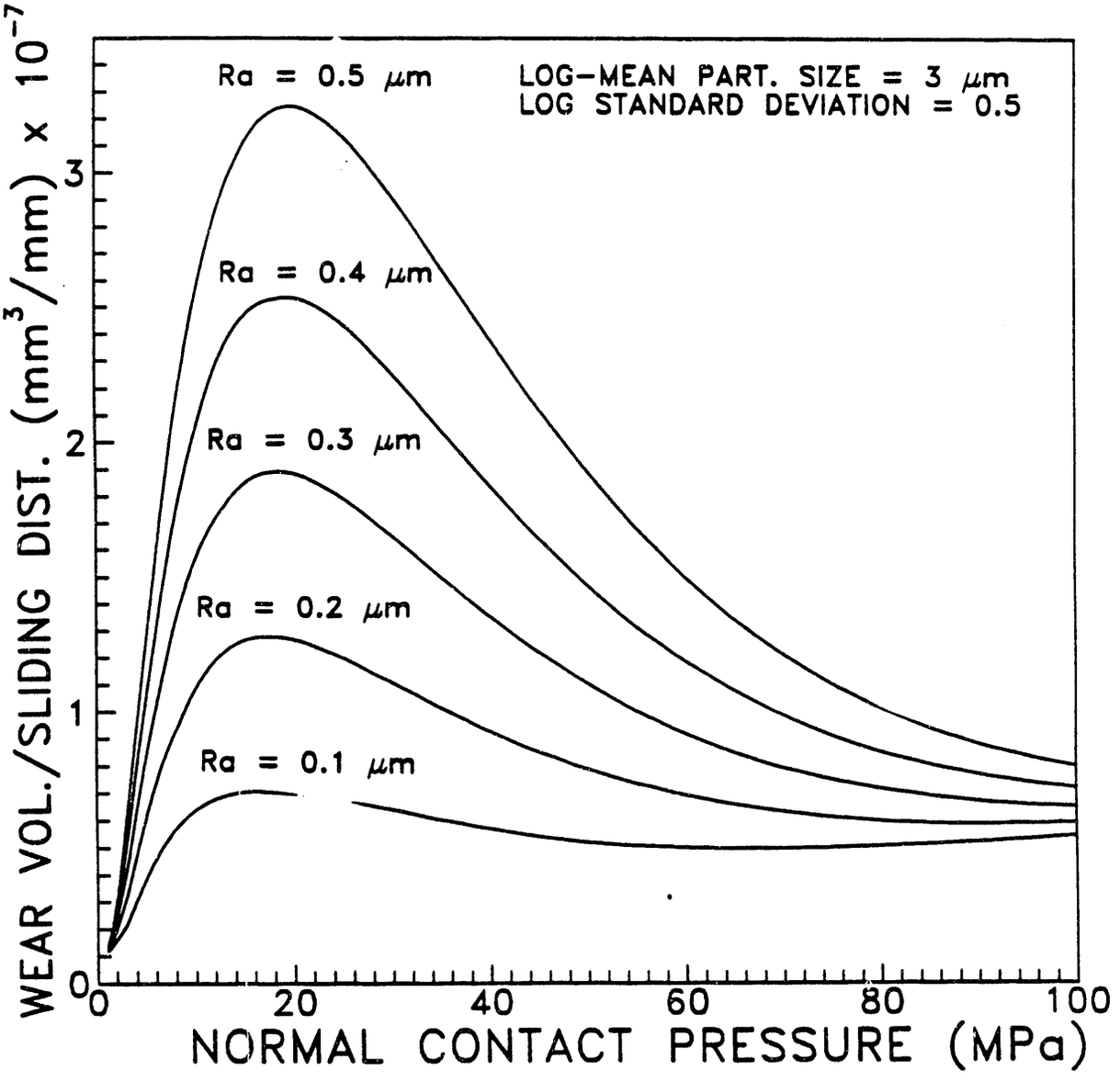

Figure 15. Calculation of Wear Curves for a Range of Surface Roughnesses

asperities will almost always reduce wear. Reducing particle size, however, has a more complicated effect. Figure 16 illustrates the model predictions of wear for particle sizes ranging from 8 to 0.5 μm. The model predicts increased wear as particle size decreases, but the hump in the wear vs. load curve also begins moving to the right. Assuming an engine operates in the 10 MPa and lower load range, then the calculations indicate that the 0.5 μm particles can cause less wear than the larger particles.

The size of particles relative to the hydrodynamic film thickness and surface roughness are the parameters determining the behavior of these wear curves. If particle size is much larger than the typical film thickness and surface roughness, then the surface finish curves tend to converge much faster, and abrasive wear is only significant at the low loads. If particle size is smaller than surface finish, the hump in the wear curve is broadened and moved to the right, and abrasive wear has an effect over a much wider range of loads.

In summary, the wear calculations developed here indicate some subtle observations about the parameters affecting ring/cylinder liner wear. It appears it is always to the advantage to reduce surface finish asperity height, but the effects of contaminant particle size and hydrodynamic film thickness must be considered in terms of their magnitudes relative to the surface roughness.

D. Tests with the Dripped Oil Supplies

As discussed above, tests were initiated with separated oil supplies, flowing contaminated oil on one side, and clean oil on the other side of the reciprocating ring specimen. The results of tests with various slot configurations are illustrated in Figures 17 - 19 below. There still appears to be little advantage to be gained in using any of the slot configurations over the un-slotted specimen. In general longitudinal slots caused less wear than circumferential slots of the same width and spacing. The configuration with the smallest width and largest spacing slot gave the lowest wear results. It seems apparent that, in the configurations tested in this program, if there were any effect of channeling and diluting of contaminant, it is overshadowed by the negative effects of putting slots in the cylinder surface (increased relative load on remaining surfaces). To reduce these effects, a configuration which involves slots over only a small portion of the ring contact area would be more appropriate.

The effects of slot configurations on channeling and flow of lubricant in the wear zone might also be deduced from information on the shape of the wear profile on cylinder wear specimens. Figures 20, 21 and 22 are wear scar profiles taken on specimens without slots, with circumferential slots and with longitudinal slots respectively. The characteristic shape of the wear scars is to have deep depressions at each end corresponding to the location of ring reversal points. This was characteristic of tests with the contaminant/lubricant bath as well, but the asymmetry of the wear scars is a unique characteristic of tests with the two dripped supplies (it should be noted in Figures 20 - 22 that the

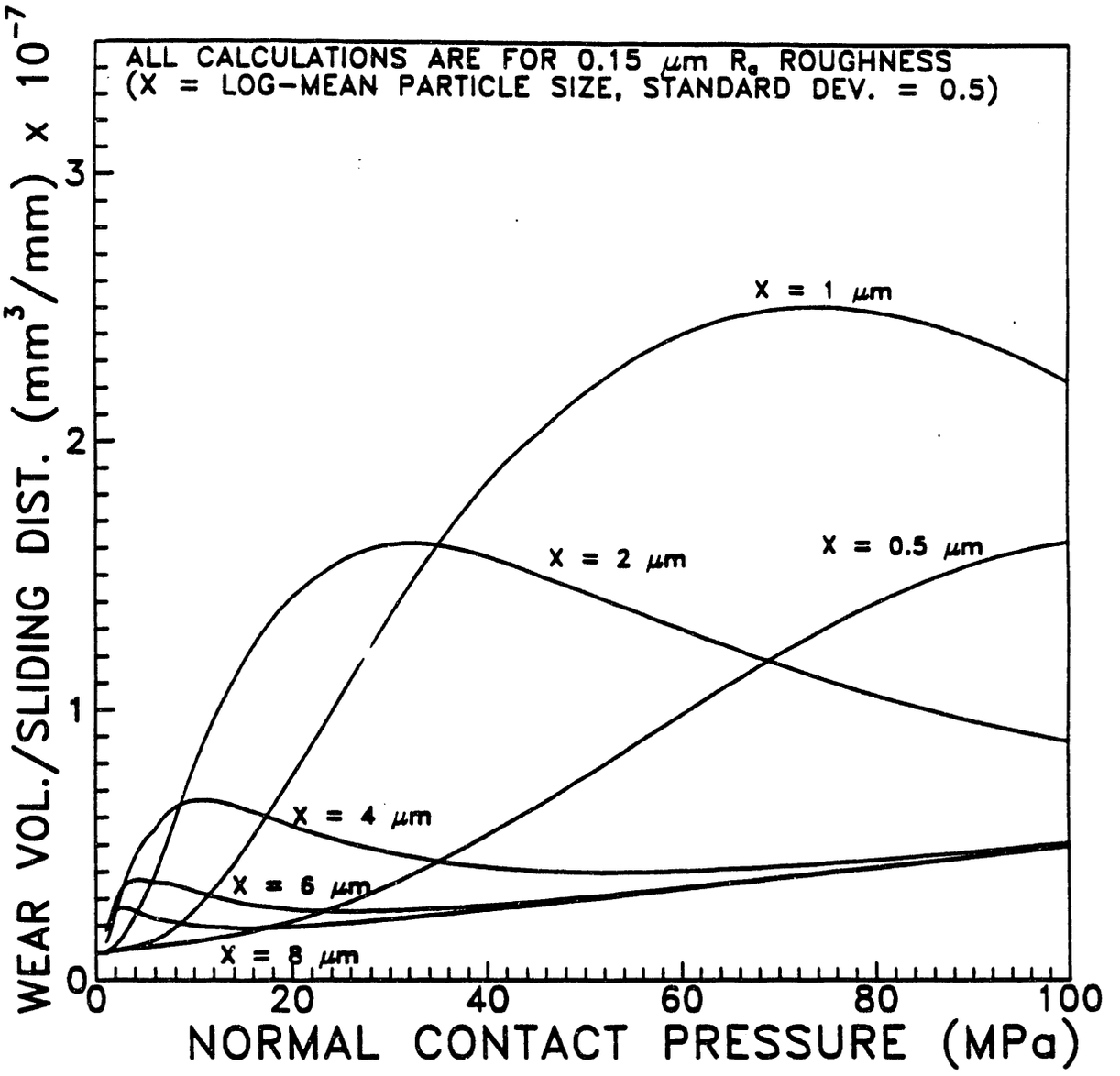

Figure 16. Calculation of Wear Curves for a Range of Contaminant Particle Sizes

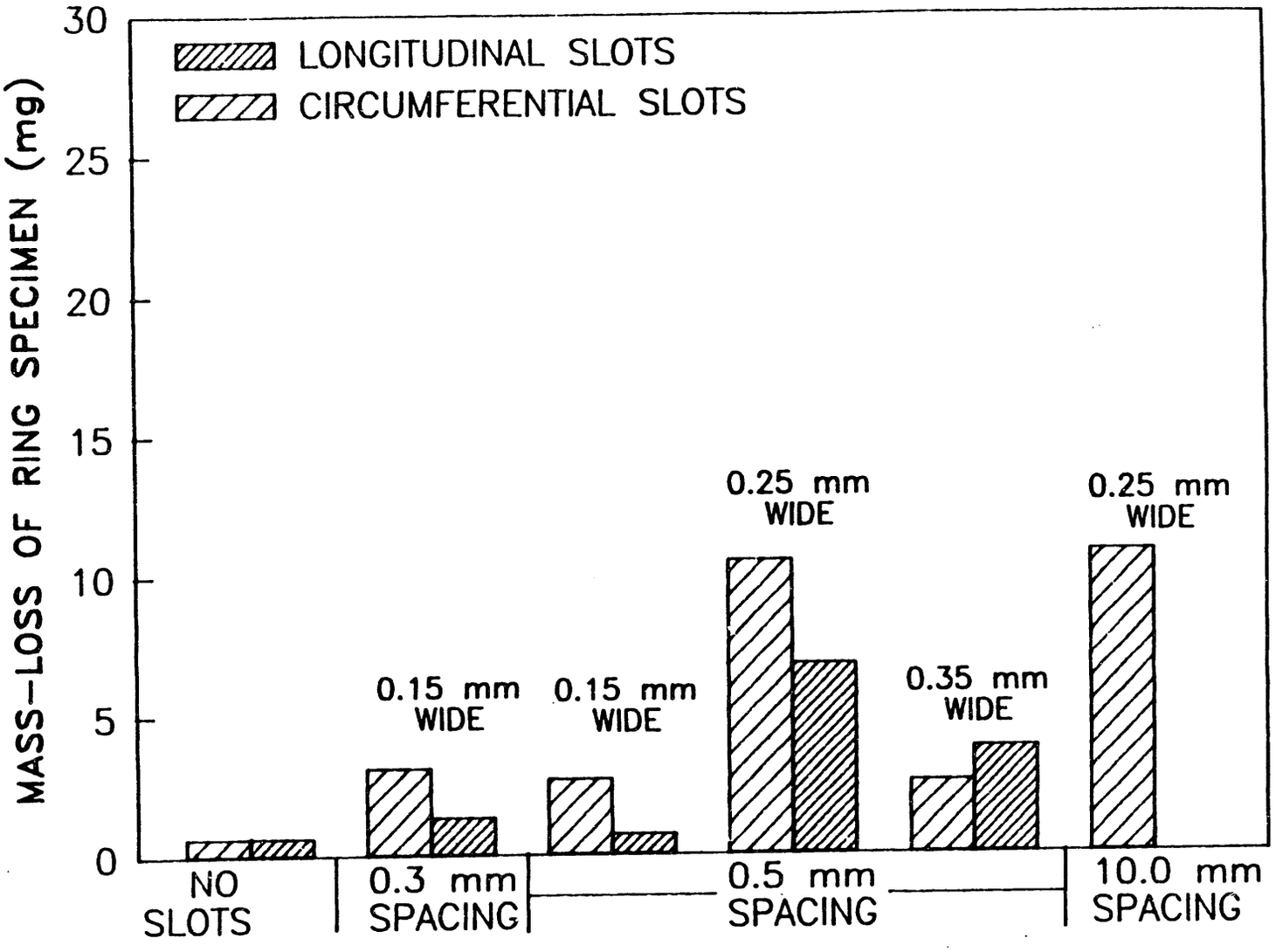

Figure 17. Effect of Slot Configuration on Ring Specimen Mass Loss

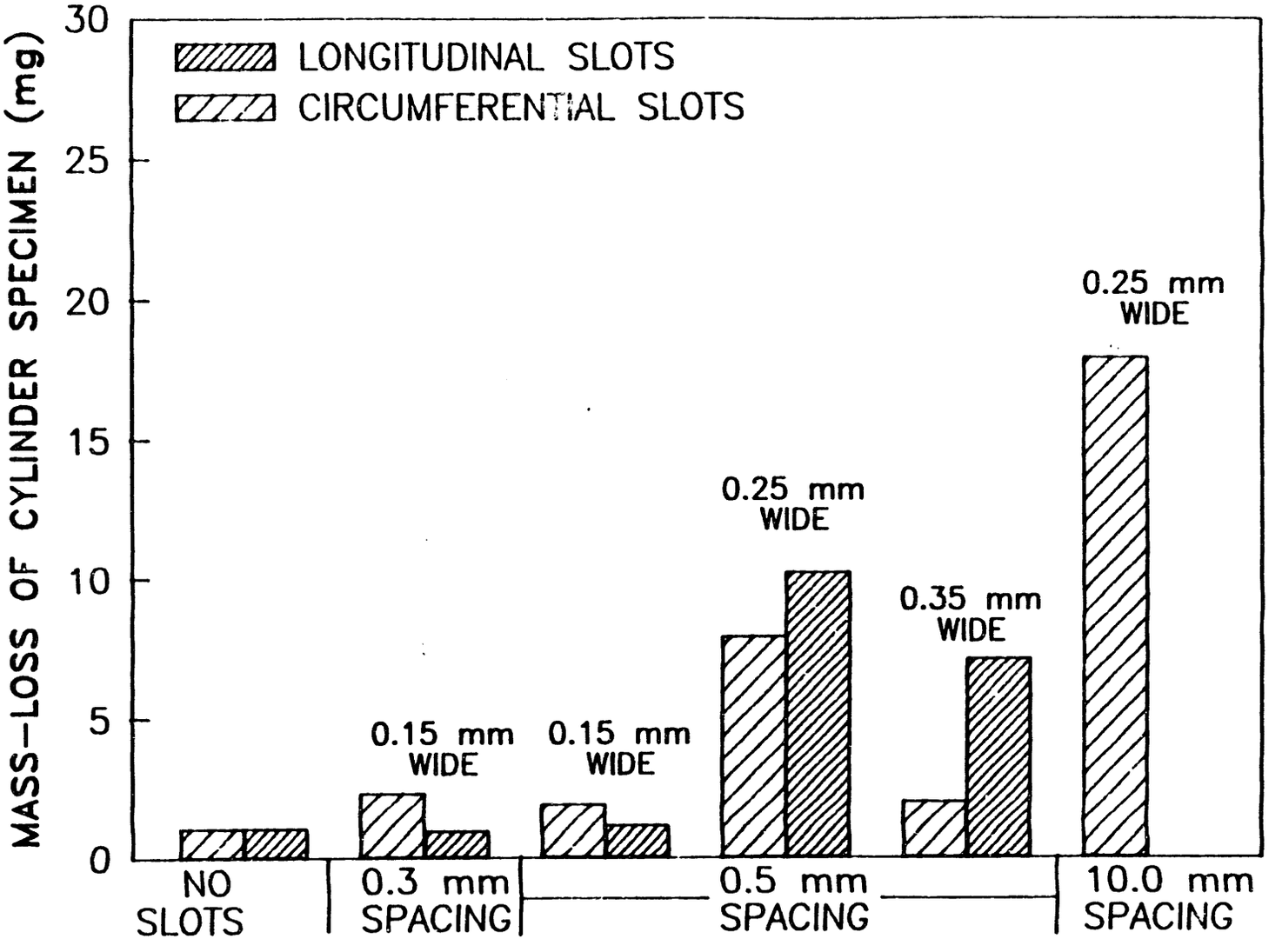

Figure 18. Effect of Slot Configuration on Cylinder Specimen Mass Loss

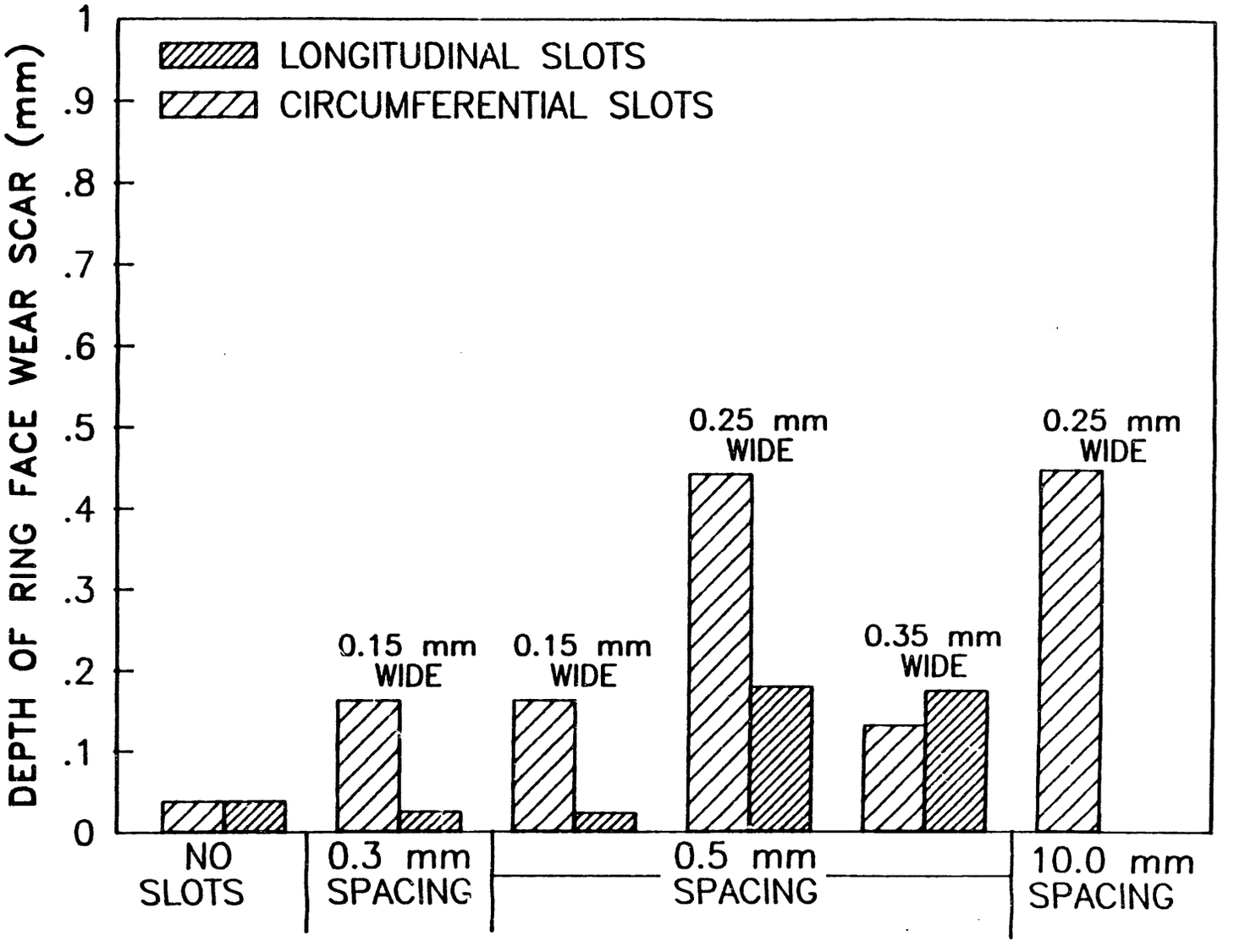

Figure 19. Effect of slot Configuration on Depth of Ring Face Wear Scar

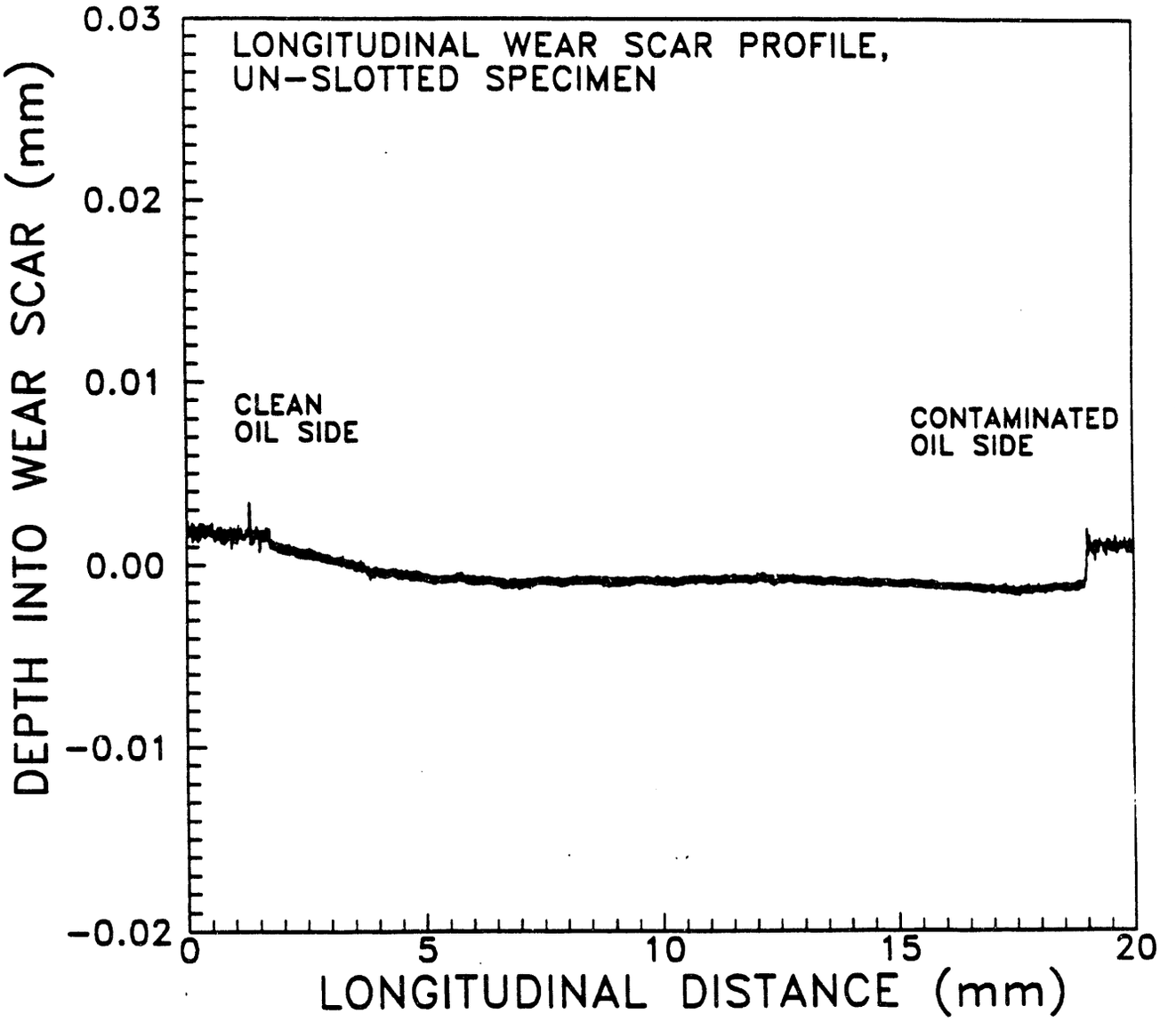

Figure 20. Longitudinal Wear Scar Profile for Un-Slotted Specimen

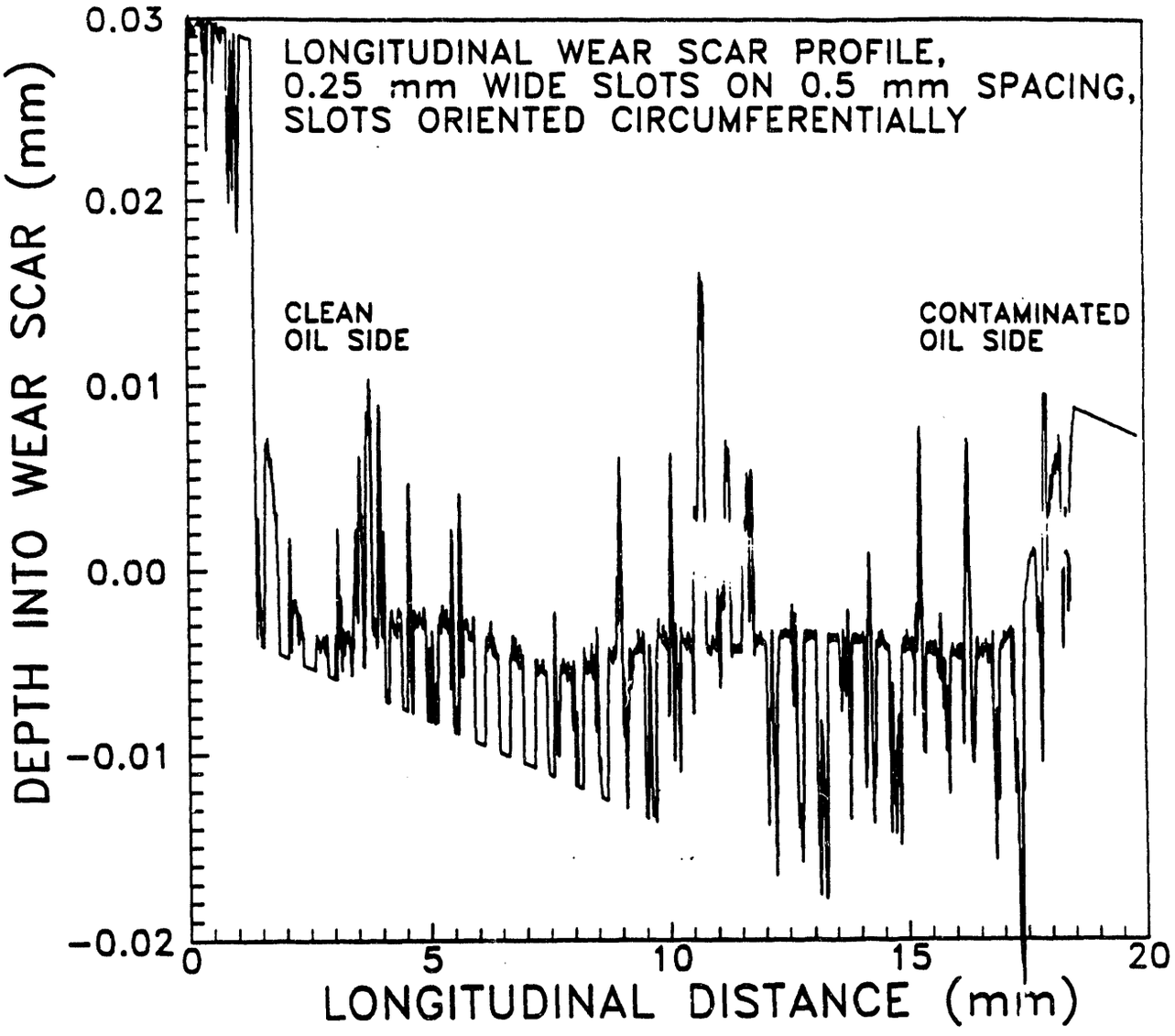

Figure 21. Longitudinal Wear Scar Profile for Specimen With Circumferential Slots

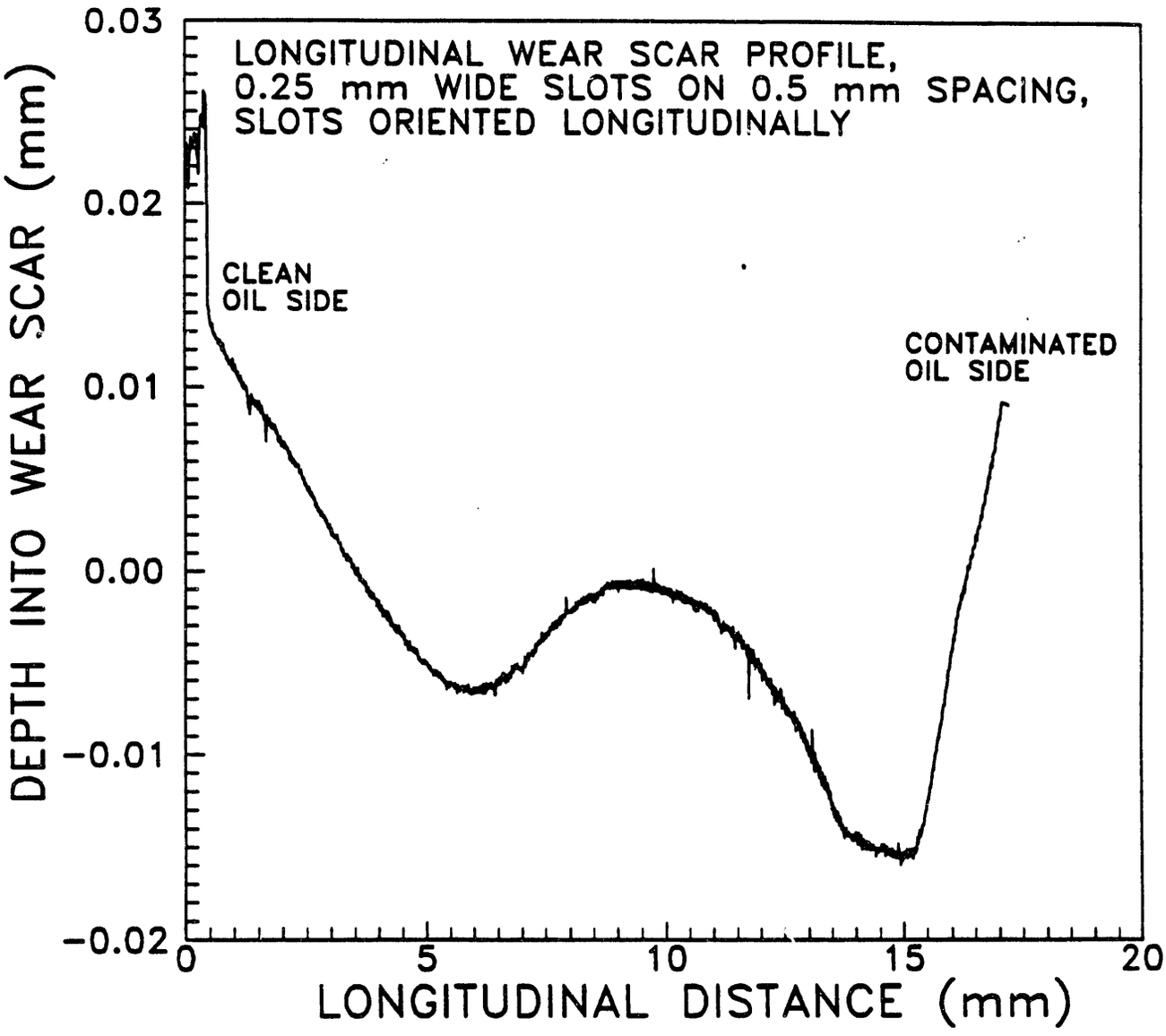

Figure 22. Longitudinal Wear Scar Profile for Specimen With Longitudinal Slots

contaminated oil was dripped on the right side of the wear path and the clean oil on the left). As expected, in all cases wear was higher on the contaminated oil side. The effect of circumferential slots was to magnify the wear to the point where any hump in the center or asymmetry was completely wiped out. In order to take the profile with the circumferentially slotted specimen, it was necessary to fill the slots with a compound. The areas where it appears there are large spikes in the surface are probably simply areas where the compound spilled out of the slots. Other than that roughness, and obviously the appearance of the slots themselves in the profile, the curve appears fairly smooth. The longitudinal slots profile showed the characteristic hump in the center and significant asymmetry, indicating that they do not promote as much mixing and dilution of the contaminated oil as might be expected.

E. Analysis of Wear Groove Spacing in Circumferential Profiles of Wear Scars

As a separate issue, it has been noted that for most of the tests performed in this program, the wear scars consisted of long, straight wear grooves oriented parallel to the direction of ring travel. The width and spacing of these grooves might be an important parameter, especially if they can be correlated with a characteristic particle size of the contaminant. With that in mind, an analysis was done using the taly-surf profilometer to record profiles taken across the wear scars in the circumferential direction. Analyses were done on two cylinder wear specimens, one of which was worn with an 8.2 micrometer log-mean particle size, and the other which was worn with a 27.2 micrometer log-mean particle size. The two circumferential profiles are shown in Figures 23 and 24. The data from Figures 23 and 24 was then input into a computer routine to calculate the magnitude of the real and imaginary parts of the Fourier transform coefficients. Those results are shown in Figures 25 and 26. In general, the Fourier transform represents the relative significance of various frequencies present in the wear trace. The x-axis in Figures 25 and 26 can be thought of as starting at zero frequency and increasing as one moves to the right. Conversely, the characteristic size starts at its maximum (in this case 1.8 mm) at the x-axis zero and decreases as one moves to the right. It is obvious from the two traces that the predominant groove sizes are on the large end of the spectrum, on the order of the width of the wear scar itself. This is at least two orders of magnitude larger than the mean particle sizes. It is also significant that, even though there was a factor of three difference in the log-mean particle sizes between the two cases, there was little difference in the location of the predominant spikes in the frequency spectrum. These factors suggest that there is probably little correlation between the characteristic size of grooves in the wear scars and the particle size.

IV. DISCUSSION

The data presented above and the wear model calculations suggest a wear mechanism that is dominated by abrasive wear at load conditions typical of the diesel engine. Further, the magnitude of wear is determined by the concentration of particles that are in a critical size range, small enough to enter the wear zone, but large enough to

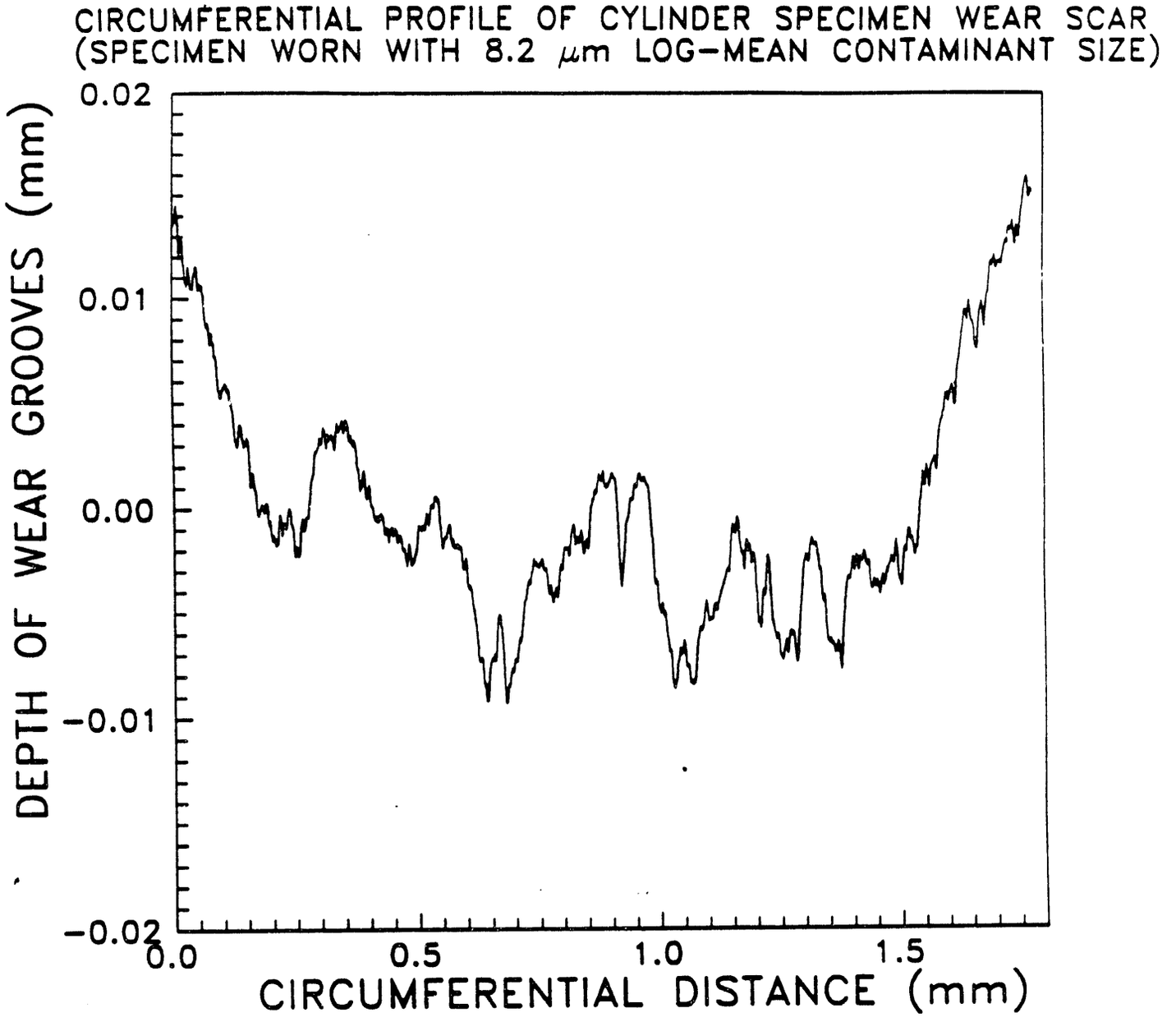

Figure 23. Circumferential Wear Scar Profile for Specimen Worn With the Small Particle Distribution

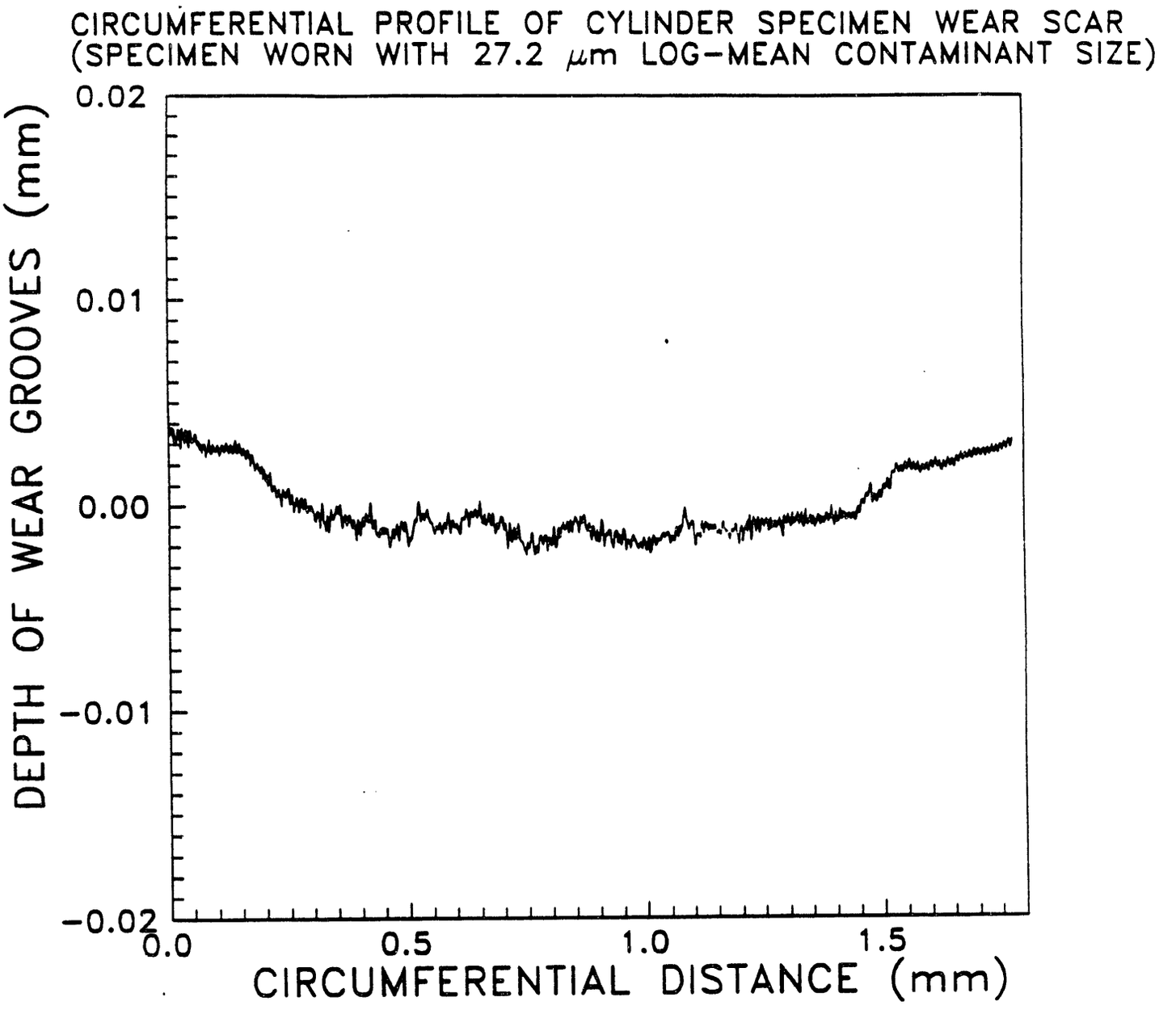

Figure 24. Circumferential Wear Scar Profile for Specimen Worn With the Large Particle Distribution

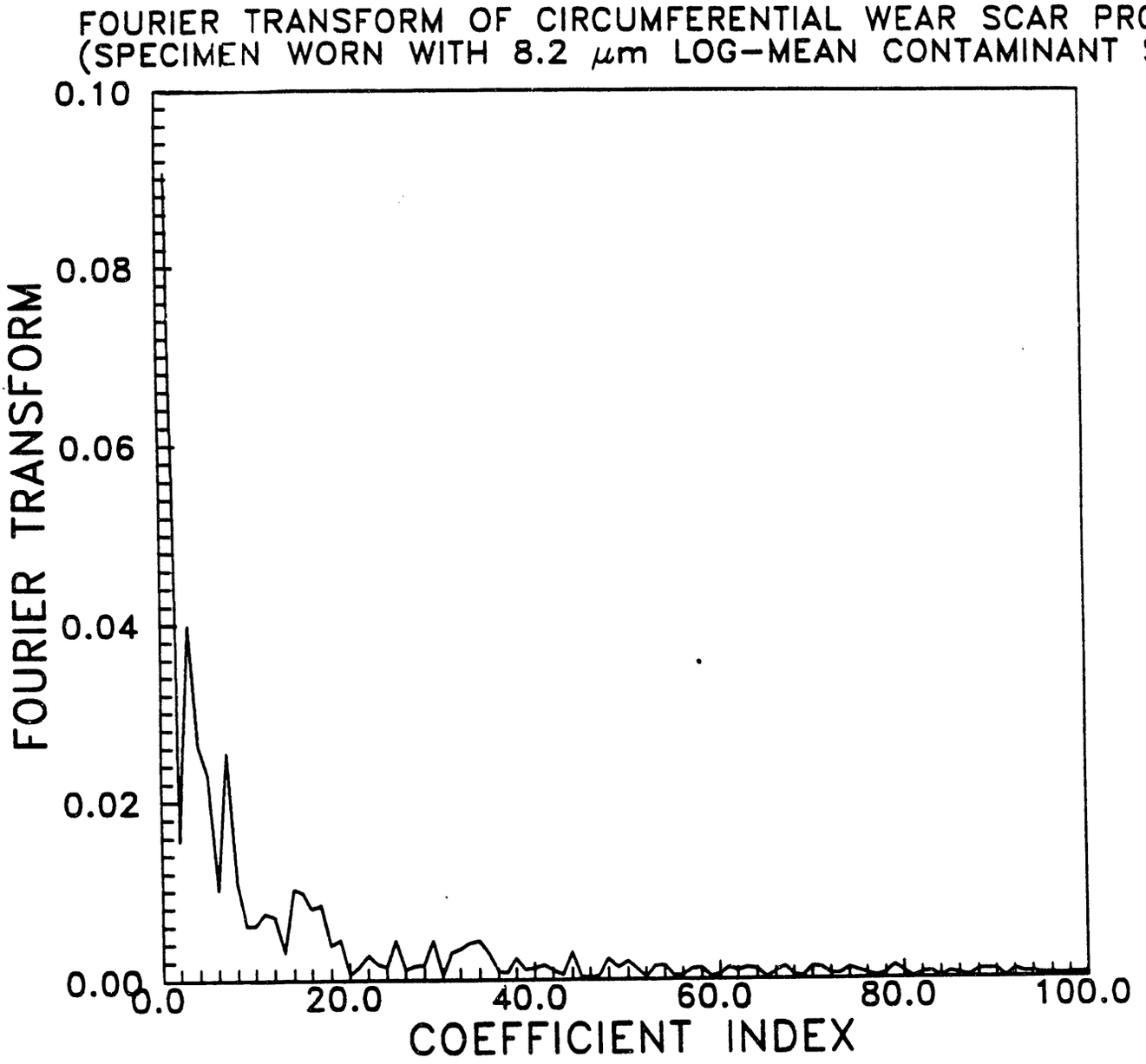

Figure 25. Fourier Transform of Circumferential Wear Scar Profile for Specimen Worn With the Small Particle Distribution

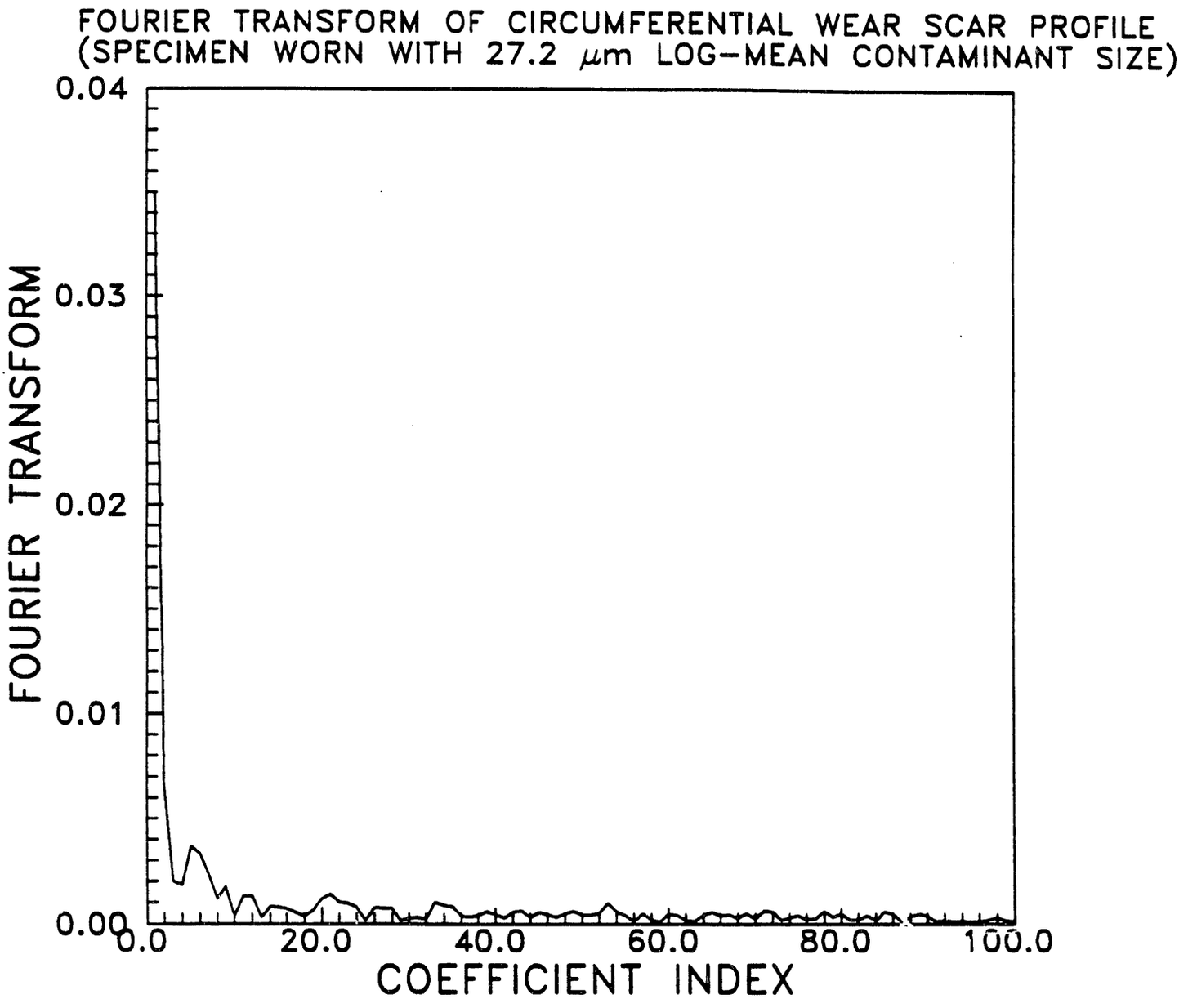

Figure 26. Fourier Transform of Circumferential Wear Scar Profile for Specimen Worn With the Large Particle Distribution

contact the two wearing surfaces. In such a scenario, the main parameters determining the behavior of the wear curve are the mean particle size relative to the surface roughness and hydrodynamic film thickness. This identifies the worst possible wear situation as the point at which the mean particle size is equal to the surface roughness + hydrodynamic film thickness term described in the model above (the model corrects the surface roughness term for elastic and plastic deformation, but at the low loads in a typical diesel engine this correction term is probably not significant). Wear mitigation strategies in this situation are to adjust parameters so that the particle size is either much larger or much smaller than the surface finish + hydrodynamic thickness term. Common sense dictates that extremely rough surfaces are going to lead to accelerated adhesive wear, and extremely large particles are going to cause problems in other parts of the engine, so the most practical options are to: 1.) try to maintain a moderately large particle size (at least 3 micrometers or so seems practical) while minimizing surface roughness, or 2.) try to maintain an extremely small particle size (calculations indicate it would have to be 0.5 micrometers or smaller) while maximizing hydrodynamic film thickness. In either case it is to the advantage to have as smooth a surface finish as possible (it should be remembered that the critical particle size range in the model above is determined by the surface roughness, i.e. the smoother the surface, the narrower the range of abrasive particle sizes).

In reference to the strategy of machining slots into the cylinder surface, the data presented here do not show much advantage to any of the configurations tested. The idea behind that strategy was that, hopefully, slots might enhance hydrodynamic film formation, promote dilution of the contaminated lubricant and channel wear particles out of the wear zone. There is evidence that slots do, in fact, enhance hydrodynamic film formation, although, as shown by the wear model presented above, it is not obvious whether a slightly thicker film will increase or decrease the wear. There was little evidence that the slots helped in mixing clean lubricant with contaminated lubricant, however, this might be a consequence of the fact that the configurations tested here probably did not leave enough un-machined area to handle the loads. If future work is to be done with slotted cylinders, they should probably use configurations with slot widths approximately 0.15 mm and spacings of at least 0.5 mm.

In reference to the strategy of tailoring lube-oil formulation to the coal/water slurry fueled engine situation, it appears that significant reductions in wear rate might be possible. While it is difficult to explain on a fundamental basis, the test results presented here indicate that even the abrasive wear process at lower loads seems to be sensitive to lubricant formulation. Future tests should probably use a fully formulated oil and the exact engine materials currently being utilized to obtain a more accurate determination of that sensitivity.

V. CONCLUSIONS

The conclusions from Task 4 work can be summarized as follows.

- There appears to be a short region of accelerated wear at the beginning of the Cameron-Plint tests (within the first 15 minutes) which is associated with a "break-in" period. The "break-in" wear, however, is much smaller in magnitude than the total wear for two or four hour duration tests.

- There is a significant effect of load on the wear magnitude and on the trends observed in Task 3. In particular, it was found that wear is much more sensitive to surface finish at the lower load conditions than it was at the higher load conditions used in Task 3.

- The wear model, which assumed the abrasive wear was proportional to the number of contaminant particles that could enter the wear zone, was successful in fitting the Cameron-Plint data obtained at low-load conditions.

- Based on the wear model assumptions, the parameters determining abrasive wear characteristics are the mean contaminant particle size relative to the size of surface finish asperities, and the hydrodynamic film thickness.

- Profilometer traces indicated that the cylinder specimens with longitudinal slots were not overly effective in promoting mixing of clean and contaminated oil supplies separated by the ring. There was not, any significant wear reduction with the longitudinal slots.

- Data with the slotted specimens indicates that longitudinal slots with relatively wide spacing and relatively narrow width (although the slot width should still be much larger than the contaminant particle size) resulted in the lowest wear.

- Wear tests with a detergent additive indicate that the additive is still effective in reducing wear, even at low-load conditions where abrasive wear is predominant.

REFERENCES

Archard, J.F., 1953, "Contact and Rubbing of Flat Surfaces," J. Appl. Phys., Vol. 24, pp. 981-988.

Archard, J.F., 1980, "Wear Theory and Mechanisms," in Wear Control Handbook (M.B. Peterson and W.O. Winer, eds.) pp. 35-80, ASME, New York.

Chittenden, R.J., Dowson, D., Dunn, J.A., and Taylor, C.M., 1985, "A Theorectical Analysis of Isothermal EHL Concentrated Contracts - Parts I and II," Proc. R. Soc. Lond. A387, pp. 245-269 and pp. 271-294.

Dowson, D., and Higginson, G.R., 1977, Elastohydrodynamic Lubrication, Pergamon Oxford.

Gaydos, P.A., June 12, 1989, "Characterization of Oil Particulate from the Cooper JS1 Engine Operating on Coal/Water Slurry," Topical Report to Arthur D. Little.

Harris, T.A., 1984, Rolling Bearing Analysis, 2nd Ed., John Wiley & Sons.

Johnson, K.L., 1985, Contact Mechanics, Cambridge University Press, Cambridge.

Jones, R.B., McCouet, C.B., Morley C., and King, K, 1985, "Maceral and rank influences on the morphology of coal char," Fuel, Vol. 64, pp. 1406-1467.

Mechanical Engineers' Handbook, 1986, (Myer Kutz, ed.) John Wiley and Sons Inc., New York.

Mitchell, Richard S., and Gluskoter, Harold J., 1976, "Mineralogy of ash of some American coals: variations with temperature and source," Fuel, Vol. 55, pp. 90-96.

Rabinowicz, E., 1965, Friction and Wear of Materials, Wiley, New York.

Sadeghi, F., and Sui, P.C.,"Compressible Elastohydrodynamic Lubrication of Rough Surfaces," Transactions of the ASME, Vol. 111, January 1989, pp. 56-62.

Schwalb, J.A., Ryan, III, T.W., 1991, "Surface Finish and Particle Size Effects on Wear in Coal-Fueled Diesel Engines," ASME Paper, ICE-Vol. 14, Coal-Fueled Diesel Engines, Book No. G00591.

Schwalb, J.A., Ryan, III, T.W., and Smith, W.C., 1990, "Lube Oil Contamination Induced Wear in Coal-Fueled Diesel Engine," ASME Paper, ICE-Vol. 12, Coal-Fueled Diesel Engines, Book No. G00507.

Tsai, S.C., 1982, Fundamentals of Coal Beneficiation and Utilization, Elsevier Scientific Publishing Company, New York.

Unsworth, John F., Barratt, David J., Park, David, and Titchener, Keith J., 1988, "Ash formation during pulverized coal combustion; 2. The Significance of crystalline anorthite in boiler deposits," Fuel, Vol. 67, pp. 632-641.

Unsworth, John F., Cunliffe, Frank, Graham, Stephen, C., and Morgan, Paul A., 1987, "Ash formation during pulverized coal combustion 1: Aerodynamic influences," Fuel, Vol. 66, pp. 1672-1679.

Wilson, Michael A., Heng, Sammy, Fredericks, Peter M., Collin, Philip J., and Vassallo, Anthony M., 1986, "The Chemical and Physical Structure of Hydrogenation Residues of Maceral Concentrates," Fuel Processing Technology, 13, Elsevier Science Publishers B.V., pp. 243-260.

APPENDIX D

Task V - Presentation of the Most promising Approach to Wear Prevention

WEAR MECHANISM AND WEAR PREVENTION IN COAL-FUELED DIESEL ENGINES

TASK V: PRESENTATION OF THE MOST PROMISING APPROACH TO WEAR PREVENTION

U.S. DOE Contract DE-AC21-88MC26044
Southwest Research Institute Project No. 03-2681

Prepared for:

U.S. Department of Energy
Morgantown Energy Technology Center
P.O. Box 880
Morgantown, WV 26507-0880

Prepared by:

James Schwalb, Research Engineer

Approved:

Thomas W. Ryan III, Manager
Combustion Technology
Department of Engine Research

TABLE OF CONTENTS

I. INTRODUCTION

The intent of this report is to discuss and present the results of this program in a format that could be easily used by engine manufacturers looking for specific recommendations on wear reduction strategies. The following sections discuss contaminant particle size, cylinder surface finish, and hydrodynamic film thickness as separate issues. Specific recommendations are made on the ideal values of each of these parameters, and the tradeoffs that result if those ideal values cannot be attained. The report also discusses the effects of lube-oil additives and cylinder surface slots. Although the results of this program are not conclusive enough to make specific recommendations in these areas, general recommendations are presented, as well as suggestions for future investigations.

II. DISCUSSION

A. Recommendations on Contaminant Particle Size, Surface Finish, and Hydrodynamic Film Thickness

Previous reports in this program outlined bench wear tests and wear modelling results, leading to the conclusion that abrasive wear in the piston ring/cylinder liner area is dependent on the concentration of contaminant particles that are in a critical size range, small enough to enter the wear zone, but large enough to contact both wearing surfaces. The maximum wear condition in this scenario occurs when the mean particle size of contaminant is equal to the sum of surface roughness and hydrodynamic film thickness. Minimizing wear then becomes a problem of making sure the contaminant particle size is either much larger or much smaller than the sum of surface roughness and hydrodynamic film thickness. For example, if the mean particle size is around 3 μm, it should be possible to hone the cylinder liner so that asperities are at least an order of magnitude smaller (0.3 μm Ra is well within the capabilities of current honing techniques). That order of magnitude decrease represents two standard deviations from the mean in a distribution with a 0.5 log standard deviation. The same logic would dictate that the hydrodynamic film thickness should be minimized as well. It should be remembered, however, that the real engine probably depends on hydrodynamic lubrication at the midstroke of the ring, and at other places where highly contaminated oil and high ring loadings will not be encountered. If the mean particle size is much smaller, for example 0.5 μm, then it may not be possible to hone the surface asperities significantly smaller than the particles. In that situation, the only practical approach is to attempt to maximize hydrodynamic film thickness to the point where the film thickness is much larger than the particles. Film thickness can be increased by increasing lubricant viscosity, orienting surface finish grooves normal to the ring travel direction, or introducing slots in the surface (to be discussed in the section below) although each of these modifications should be carefully considered in terms of their effects on ring friction, machining costs, blowby, and other issues. In either case, it is still to the advantage to have the wearing surfaces as smooth as possible because the surface roughness determines the range of sizes that are causing wear. The specific recommendations that can be made are summarized as follows:

- Under all circumstances it is advantageous to have as smooth a surface finish as is economically feasible. Standard honing practices can reduce surface roughness to around 0.15 μm, which is sufficient if the contaminant particles are 3 μm or larger.

- If the particles are large relative to the expected hydrodynamic film thickness in the engine combustion zone area, then film thickness should be maintained at the minimum needed for sufficient lubrication during the low-pressure parts of the cycle.

- If the particles are smaller than hydrodynamic film thickness, then options should be considered for maximizing that thickness.

- If control of the mean contaminant particle size is possible, particles size should be made either much smaller than the typical hydrodynamic film thickness (0.5 μm or less would probably be sufficient), or much larger (3 μm or larger). Of course, common sense dictates that the particles will cause problems in other parts of the engine if they are made too large, so some caution should be used.

It should be noted that the recommendations listed above depend on knowing what the hydrodynamic film thickness is in the critical parts of the cycle where the ring is exposed to high loads and high concentrations of contaminants. It is not obvious, however, exactly what those critical parts of the cycle are. In the bench wear tests conducted here, load and concentration were constant, so hydrodynamic film thickness was simply determined at the mid-stroke where the velocity was at its maximum. In the engine, ring load and concentration of contaminants will vary. Without better knowledge, the best condition at which to calculate film thickness is probably during the compression stroke, at or some time soon after the start of injection.

B. Recommendations on Lubricant Formulation

Because of the the complex interactions that can occur, it is impossible to predict what will happen when various additives (such as the Calcium Sulfonate Detergent) are added to a fully formulated oil, but the results of this program indicate that the abrasive wear can be significantly reduced by the correct formulation. No specific recommendations can be made at this time, however, it does seem apparent that the additive which was able to form a thick coating or film on the cylinder specimen was the most effective in reducing wear. Perhaps the film was effective in excluding particles from the wear zone, or in widening the gap between wearing specimens to the point where contaminant particles were smaller than the size needed to contact both pieces. Further exploration of additive

formulation might be appropriate as the slurry-fueled engine is more completely developed. It is reasonable to expect that the lube-oil formulation would have to be tailored to the properties of the fuel being used (i.e. coal particle size and ash content).

C. Recommendations on Slots in the Cylinder Liner Surface

Slots in the cylinder surface serve to enhance hydrodynamic film thickness, but it has not been proven that they promote any significant mixing or dilution of the contaminant particles on the combustion side of the ring. One thing that has been learned from this program is that, if there are advantages to be gained from slotted surfaces, the slot widths and spacings should be configured so that there is not a significant decrease in load-bearing areas around the slots. Several of the configurations tested here significantly decreased the load-bearing areas, had a corresponding increase in contact pressure on the remaining surfaces, and showed a corresponding increase in wear. Longitudinal slot orientation caused less wear than circumferential orientation, however, it is likely that the longitudinal slots will also result in the most severe blowby problems.

The dripped oil supplies configuration tests described in the previous Task 4 report were a significant step closer to real engine conditions, but the existing Cameron-Plint rig is not capable of simulating the light load conditions and the variation of load conditions that are present in the engine. Since the Cameron-Plint is not really capable of simulating the lubricant flow patterns under these conditions, and since the effectiveness of cylinder slots is highly dependent on lubricant flow at low loads, future testing of slot configurations should probably be done in an apparatus closer to the real engine geometry, where load variations are accurately simulated.

III. CONCLUSIONS

Conclusions presented in this report can be summarized as follows:

- Cylinder surface finish should be held as smooth as possible, and everything possible should be done to promote a tight clearance between the ring and cylinder liner. It is especially critical that the liner asperities be at least an order of magnitude smaller than the contaminant particles.

- If contaminant particle size can be controlled, it would be best to maintain it at a moderate size (at least 3 micrometers). As indicated above, this allows for a surface finish much smaller than the particle size using conventional honing techniques. The model predicts that wear will continue to decrease as particle size increases, however, common sense dictates that there must be a limit at which large particles would begin to cause problems somewhere else in the system.

- The model also predicts that wear can be reduced if the contaminant consists of extremely small particles (much smaller than the hydrodynamic film thickness). This suggests an alternate strategy of attempting to reduce particle size while at the same time increasing hydrodynamic film thickness. In either the case, the idea is to avoid a situation where the film thickness + surface roughness is approximately the same as the mean contaminant particle size.

- If hydrodynamic film thickness can be controlled, it is not obvious how it will affect the wear. In a situation where most of the contaminant particles are much larger than the film thickness + surface finish, a thicker film could allow more abrasive particles into the wear zone. On the other hand, a real engine depends on having some hydrodynamic lubrication at the mid-stroke of the ring.

- Despite Cameron-Plint data indicating there is little advantage to using slots in the cylinder surface, it is still felt that slots in a real engine might play a constructive role in diluting and channeling contaminants away from the wear zone. If slots are to be used, they should be oriented longitudinally, at a relatively wide spacing (at least 0.5 mm) and using a slot width of 0.15 mm.

- Data presented in this program indicates the wear process can be extremely sensitive to lube-oil additive formulation. Because of unknown additive interactions, it cannot be predicted what would happen if similar additives are added to a fully formulated oil, but it seems that the magnitude of wear reductions experienced here warrant some further experimentation. It should be possible to tailor the oil formulation to the coal/water slurry fueled engine application.

APPENDIX E

Task VII - Extended Wear Testing

WEAR MECHANISM AND WEAR PREVENTION IN COAL-FUELED DIESEL ENGINES

TASK VII: EXTENDED WEAR TESTING

U.S. DOE Contract DE-AC21-89MC26044
Southwest Research Institute Project No. 03-2681

Prepared for:

U.S. Department of Energy
Morgantown Energy Technology Center
P.O. Box 880
Morgantown, WV 26507-0880

Prepared by
James F. Wakenell
Steven G. Fritz
James A. Schwalb

Approved:

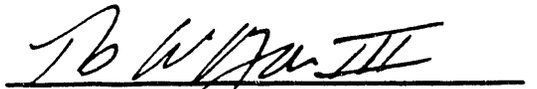

Thomas W. Ryan III, Manager
Combustion Technology
Department of Engine Research

TABLE OF CONTENTS

LIST OF TABLES

LIST OF ILLUSTRATIONS

I. INTRODUCTION

Over the past several years, interest has arisen in the development of coal-fired diesel engines for the purpose of efficiently utilizing the extensive coal reserves in the United States, and therefore reducing dependence on foreign oil. One process which is being considered for use in producing clean coal fuel products involves mild gasification. This process produces by-products which can be further refined and, when blended with neat diesel fuel, used as an engine fuel. The purpose of this task was to test a blend of this coal liquid and diesel fuel (referred to as coal-lite) in an engine, and determine if any detrimental results were observed. This was done by performing a back-to-back performance and emission test of neat diesel fuel and the coal-lite fuel, followed by a 500-hour test of the coal-lite fuel, and completed by a back-to-back performance and emission test of the coal-lite fuel and neat diesel fuel.

II. EXPERIMENTAL APPARATUS AND PROCEDURE

A. Engine Description

The engine chosen as the test bed in this experiment was the two-cylinder version of the Electro-Motive Division of General Motors (EMD) 567 locomotive engine. This engine was chosen specifically because one of the markets for this fuel is the railroad industry. The two-cylinder engine was used, quite simply, because of the lower operating costs and fuel consumption and lower repair costs if detrimental results were observed. The EMD two-cylinder 567 engine was a limited production research engine built by EMD and designed specifically for research use. The engine is a two-stroke cycle, blower-scavenged unit with a displacement of 567 cubic inches per cylinder that produces 215 brake horsepower at 835 rpm. Details of the engine are presented in Table 1.

Table 1. Engine Specifications

	EMD 2-567B
Number of Cylinders	2
Displacement (cu. in./cyl.)	567
Bore and Stroke (in.)	8.5 x 10
Rated Speed (rpm)	835
Rated Brake Horsepower	215
Compression Ratio	16.1
Cycle	2
Injection System	Unit Injector

The 567 series engines were produced and used by the railroad industry in 6, 8-, 12-, and 16-cylinder configurations. The engine is loaded by a DC generator and the power is absorbed by a resistive load grid, water cooled for heat dissipation.

B. Engine Test Cycle

The engine was operated at conditions that simulated the notch operation of a locomotive. Locomotive engines operate only at specified speed/power combinations defined by throttle positions or "notches." Since the power output and speed are constant at each notch position, the fuel consumption rate is also constant and can be defined for each position. EMD engines in locomotive service operate at eight power producing notches. There are also idle and, in some locomotives, low idle operating positions. To facilitate fuel testing, the positions were redefined in terms of speed and load combinations (see Table 2).

Table 2. Engine Speed and Fuel Flowrate Combinations

Notch Position	Engine Speed (RPM)	Fuel Flowrate (kg/hr)	Typical BHP
8*	835	40.8	207
7	755	34.0	178
6	675	27.2	149
5	585	20.4	114
4	515	15.0	77
3	425	9.5	47
2	345	5.4	20
1	285	3.6	8
Idle	285	2.5	0

* Notch 8 of the schedule represents rated speed and load of the engine. All other positions represent part-load conditions.

Fuel rate for the two-cylinder EMD 567 research engine was taken as 1/8 the typical values for the 16-cylinder 567 C with 16:1 compression ratio pistons. Unlike revenue service locomotive engines, the two-cylinder engine is equipped with a

pneumatic governor that permits infinite variations of both speed and load. However, during testing the engine was operated only at the speeds and fuel consumption rates corresponding to the notch schedule presented in Table 2.

Performance data was corrected to standard ambient conditions in all cases. Factors defined by EMD were applied to correct performance to 60° F and 29.9 in-Hg. Engine test data have shown the engine manufacturers recommended factors to provide the best correlation for correction.

C. Engine Instrumentation

The test engine was instrumented to monitor engine speed, power output and pressures and temperatures throughout the lubricating, cooling, intake and exhaust systems. Smoke density was measured using the Bosch method. A Micro-Motion mass flowmeter provided a continuous mass fuel flow rate measurement.

Engine instrumentation was connected to a low-speed data acquisition system. In addition to monitoring pressures and temperatures, the computer system also monitored alternator voltage and amperage output, the Micro-Motion voltage signal and engine speed. A computer averaging routine was employed for all performance measurements. During the performance tests, signals were recorded once every five seconds for approximately 20 minutes to provide a total of 250 data sampling readings. The 250 readings were averaged and the power output, thermal efficiency, mean effective pressure, and brake specific fuel consumption were calculated based on these averages. This procedure accounted for periodic oscillations in power output and fuel consumption rate and resulted in an accurate fuel consumption measurement.

D. Test Procedure

The study began with a tear-down and reassembly of the engine power packs (pistons, rings, and liners) for baseline measurement. Ring and liner measurements were performed using standard measurement instruments. Two new fuel injectors were "pop tested" for conformation of integrity and installed in the engine. Next, a nine hour baseline neat diesel fuel performance, economy, and emission test at all eight throttle notches (and idle) was performed.

Next, in order to evaluate the affects of the test (coal-lite) fuel, the engine was purged with the test fuel and a nine hour performance, economy, and emission test run using the test fuel. Data was recorded at each notch position. Upon completion of the performance test, the 500 hour durability test was performed. This test consists of 250 two-hour cycles at Notch 8, 5, and idle. During the durability test, performance data was recorded at Notch eight only. Emissions measurements were not taken during the durability test. Following the 500 hour test, another nine hour

performance, economy, and emission test using the test fuel was conducted in order to assess any performance loss as a result of engine wear. These results were compared to the pre-500 hour test fuel run.

The final engine test was performed using neat diesel fuel for a comparison to the baseline test.

Upon completion of the engine tests the engine power packs were removed and disassembled for inspection and measurement. Photographs were taken to visually record engine wear and carbon deposition. Engine wear was assessed based on a comparison to the initial measurement and visual inspection. The fuel injectors were again "pop tested" to check for injector dribbling. After which, the injectors were disassembled and inspected and measured.

III. FUELS

The fuels used for this evaluation were neat diesel fuel and the coal-lite liquid. The neat diesel fuel was a commercially available No. 2 diesel. Chemical analysis of the fuels are presented in Table 3.

IV. EXPERIMENTAL RESULTS

A. Performance Tests

The performance test results for all four performance tests are shown in Figures 1 through 5. Basically, there is very little difference between all the fuels. During the tests, horsepower was held constant as indicated in Figure 1. Therefore, there also should not be any differences in BMEP as shown in Figure 2. Because horsepower was held constant, any performance differences encountered as a result of the fuel differences would be detected in fuel consumption, BSFC, and possibly thermal efficiency.

Shown in Figure 3, is a plot of fuel consumption for each notch position. For the most part, fuel consumption was approximately the same for Notches 1 through 5. At the higher notches, fuel consumption varied. At Notch eight, the first coal-lite test fuel consumption was 4 percent greater than the first baseline. This increase in fuel consumption could be a function of two factors. Shown in Figure 4, thermal efficiency at Notch eight for the first coal-lite test was 3 percent less than the first baseline. This is a function of how efficiently the combusted fuel (heat) is converted into work, and partially accounts for the increase in fuel consumption. The other one percent difference is most likely a result of the 1 percent lower heating value of the fuel as shown in Table 3. The combined effect of a lower heat of combustion and reduced thermal efficiency will account for the increased fuel consumption. Notch eight was used as the example here, however the same conclusion can be drawn for the other notches where the difference was significant.

Table 3. Properties of the Engine Test Fuels

Property	Procedure[a]	Neat No. 2 Diesel Fuel	Coal-Lite Fuel
Gravity, °API, 60° F	D1298		29.8
Specific Gravity, 60° F			.8767
Distillation, °F:	D86		
IBP/5[b]		344/394	354/392
10/20		425/461	425/456
30/40		490/508	480/499
50/60		525/540	518/534
70/80		560/578	555/578
90/95		611/636	609/633
EP[c]		660	653
Recovery, %		99.5	
Residue, %		0.5	
Viscosity:			
cSt @ 104° F (40° C)	D445		2.8
SUS @ 104			
Flash Point, °F	D93		154
Elemental Analysis, %	D3178		
Carbon	CEC 240[d]	86.77	86.42
Hydrogen		12.80	12.01
Sulfur	XRF	0.324	0.506
Nitrogen	Chemilumi		0.136
Oxygen (difference)	nescent	0.43	0.92
Hydrocarbon Type, (FIA) %	D1319		
Aromatics			45.5
Olefins			1.2
Saturates			53.3
Heat of Combustion	D240		
Gross, Btu/lb		19405	19023
Gross, MJ/kg		45.133	44.249
Net, Btu/lb		18187	17928
Net, MJ/kg		42.300	41.702
Accelerated Stability, mg/100 ml	D2274		6.2
Carbon Residue, 10% Btms, wt%	D524		0.35
Particulates	D2276		12.6
Metals, ppm in fuel:	ICP[e]		
Vanadium			<1
Potassium			<25
Nickel			<1
Iron			<1

a = Numbers preceded by a D are ASTM
b = IBP is the initial boiling point
c = EP is the end point
d = Instrumental analysis
e = Inductively coupled plasma

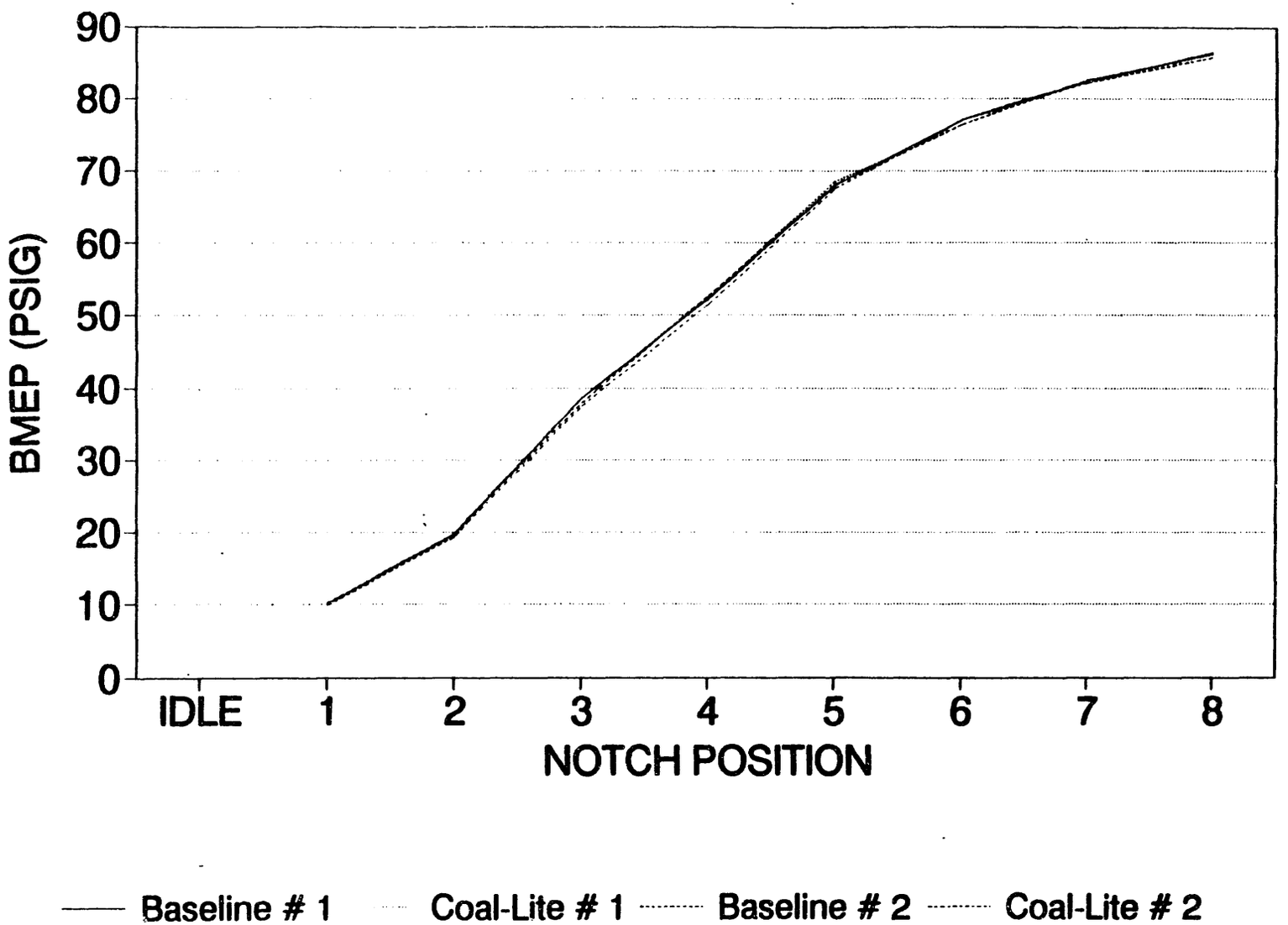

Figure 1. BHP Versus Notch Position

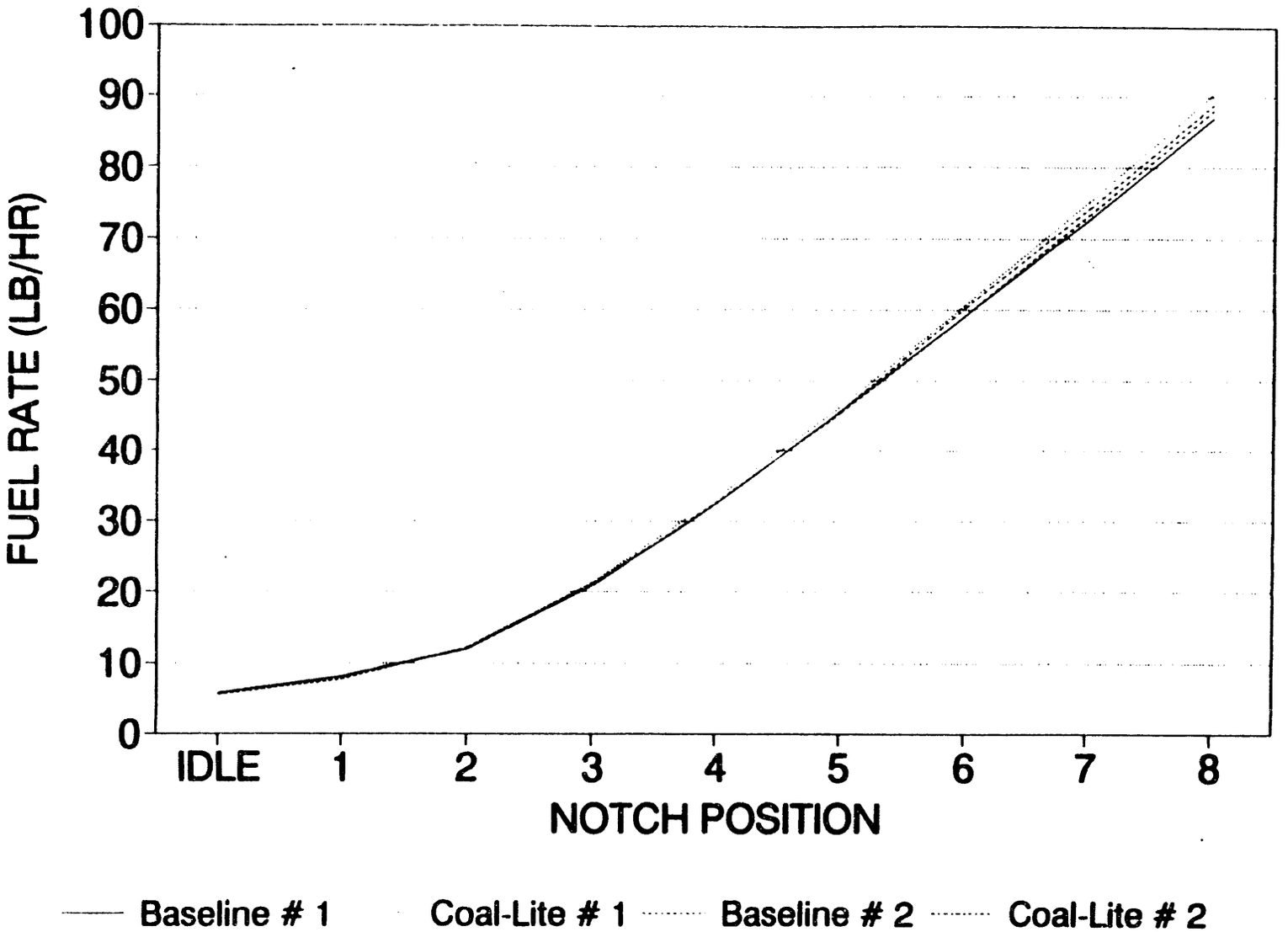

Figure 2. BMEP Versus Notch Position

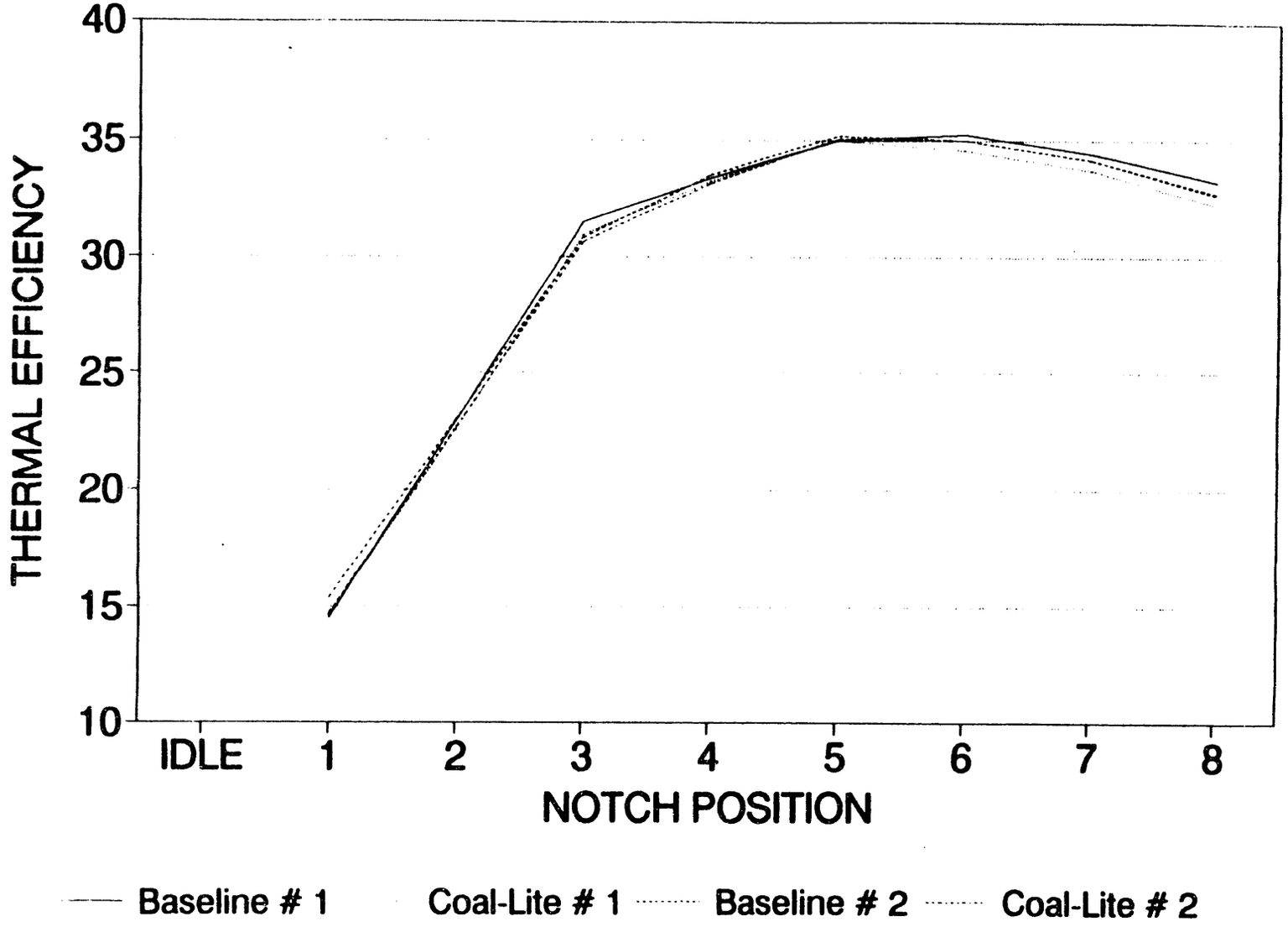

Figure 3. Fuel Rate Versus Notch Position

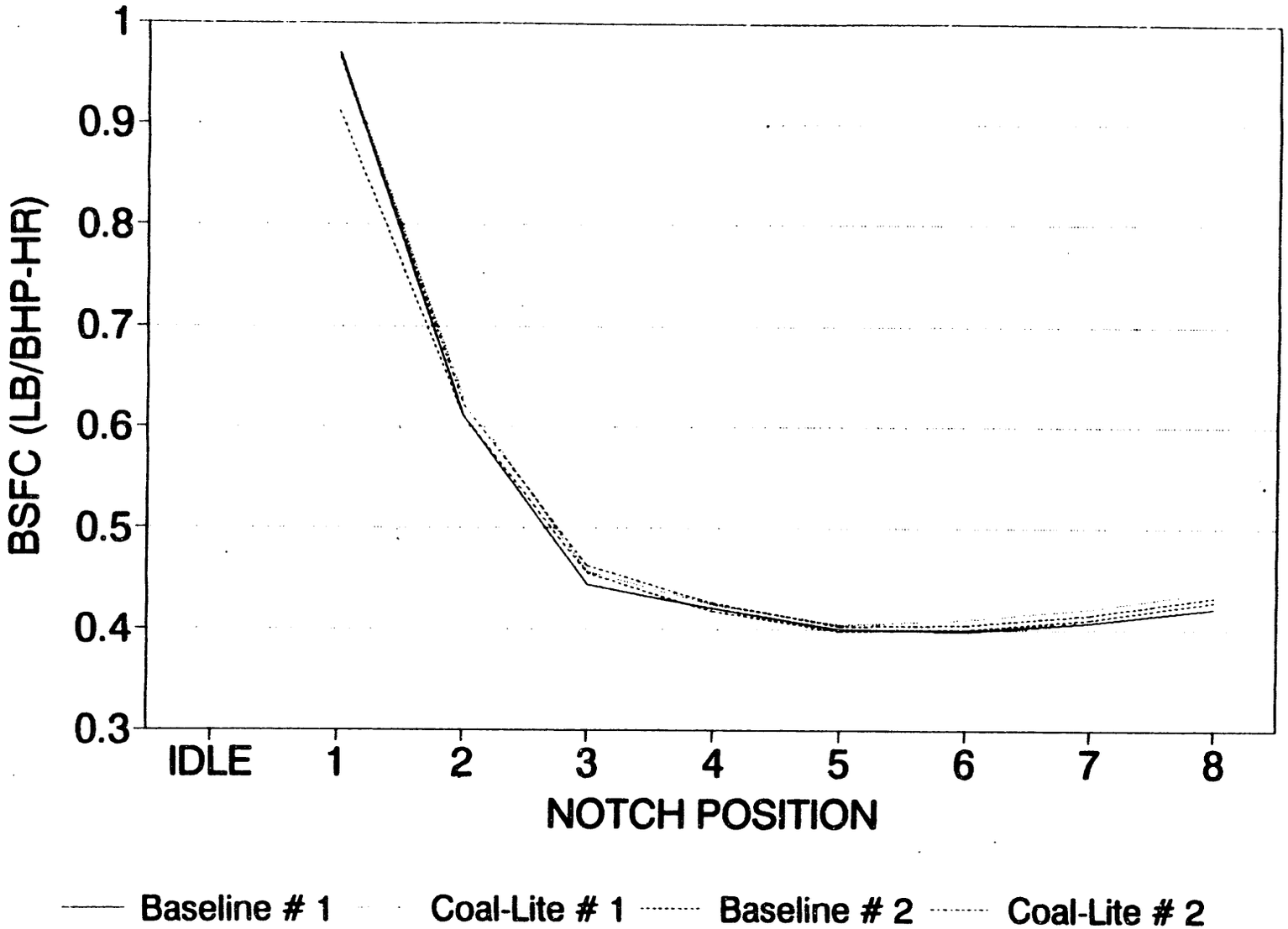

Figure 4. T.E. Versus Notch Position

Also shown at Notch eight (Figure 3), is a roughly 2 percent increase in fuel consumption for the post 500-hour coal-lite test. The immediate question asked is why this differs from the first coal-lite test (4 percent increase). The explanation here is not quite as clear however, it is suspected that throughout the 500-hour test, the engine was continuing to seat in the rings and liners and that motoring friction was higher for the pre 500-hour tests. This would result in greater fuel consumption at the start of test for both fuels when compared to the end of test (500 hours) results, and in fact, that is what was observed.

Finally, shown in Figure 5, is a plot of BSFC verses notch position. BSFC is determined by dividing fuel rate by horsepower. Specific fuel consumption is a comparative parameter that describes how efficiently the engine converts fuel into work. BSFC comparisons are preferred to thermal efficiency because all parameters are measured in standard and accepted units: time, horsepower, and mass. In any case, both thermal efficiency and BSFC indicate how efficiently the engine is working and the trends shown in Figure 5 (BSFC) are the same as those shown in Figure 4 (thermal efficiency).

B. Emissions Tests

The Department of Emissions Research of Southwest Research Institute (SwRI) performed steady-state gaseous and particulate emission tests on the engine using both fuels. The tests were performed before and after the 500-hour engine durability test of the coal-lite fuel. This report section summarizes the emissions test procedure and gives a detailed listing of the emission results as well as a composite emissions factor comparison of the baseline diesel fuel and the coal-lite fuel.

Gaseous Emission Measurement

Gaseous emission measurements during each steady-state test condition were obtained by sampling raw exhaust following procedures detailed in 40 CFR Part 86, Subpart D. Exhaust gases were analyzed for unburned hydrocarbons (HC), carbon monoxide (CO), oxides of nitrogen (NO_x), carbon dioxide (CO_2), and oxygen (O_2). Hydrocarbons were measured by a heated flame ionization detector (HFID) unit built to specifications given in SAE Recommended Practice J215. Carbon monoxide and carbon dioxide were measured by a non-dispersive infrared (NDIR) analyzer in a system that conforms to SAE Recommended Practice J177a. Oxides of nitrogen were measured using a chemiluminescent analyzer.

Sulfur dioxide (SO_2) mass emission rates were also determined for the EMD 2-567B engine. The exhaust of SO_2 in the diesel exhaust was measured as sulfate

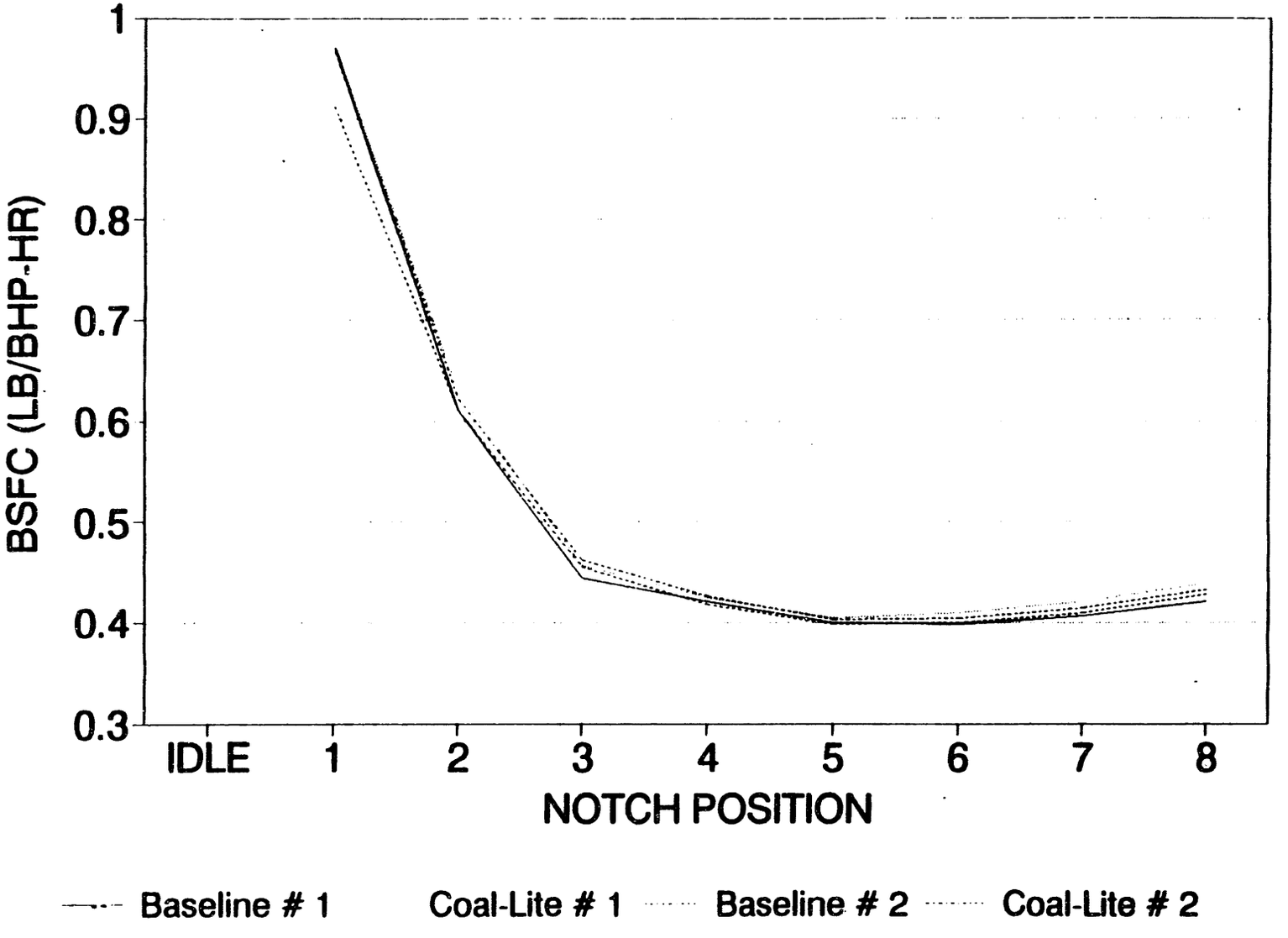

Figure 5. BSFC Versus Notch Position

using an ion chromatograph following EPA procedures[1]. SO_2 exhaust samples were collected in two glass bubblers, each containing 3 percent hydrogen peroxide. The temperature of the absorbing solution was kept at 0°C by means of an ice water bath. The bubbled samples were analyzed on an ion chromatograph and compared to standards of known sulfate concentrations. The measured SO_2 mass concentration in the exhaust were then compiled with the measured engine exhaust flow rates to compute the mass emission rate of SO_2.

Particulate Emission Measurement

Particulate measurements during each steady-state test condition were obtained using a "splitter" dilution system. The splitter system splits off a portion of the total raw exhaust flow and mixes it with dilution air. Mixing occurs in a dilution tunnel prior to sampling the mixture for particulate. The stainless steel dilution tunnel used for this work was 20 centimeters (8 inches) in diameter and approximately 5 meters (15 feet long). Particulate mass samples were collected on dual 47-mm Pallflex T60A20 fluorocarbon-coated glass fiber filters (primary and backup). Dilution air and the split-off portion of the total exhaust were regulated such that the maximum temperature at the filter sample zone was 52°C (125°F). All filters were weighed in a temperature and humidity controlled chamber to ensure consistency of results.

Emission Test Results

Mass emission rates of HC, CO, NO_x, particulates, and SO_2 were computed using the raw gaseous emissions measurements, the particulate tunnel flow data along with the particulate filter weight gain, and the engine air flow, fuel flow, and power output data. For the test performed in this program, the power output (bhp) at each notch position was held constant and observations of the mass flow rate of the fuel were made.

Individual emission test results for each test point are given in Appendices A-D. Included are the baseline pre 500-hour baseline test on diesel fuel (Appendix A), the pre 500-hour test on the coal-lite fuel (Appendix B), the post 500-hour test on the coal-lite fuel (Appendix C), and the final post 500-hour test on the baseline diesel (Appendix D).

A summary of the NO_X mass emission rates are shown in Figure 6. Note that ambient air temperature and humidity are known to affect internal combustion engine exhaust emissions. NO_X is especially sensitive to these factors, and as a result, NOx correction factors are commonly used to adjust observed NO_X results to standard conditions. For this project, SwRI has reported NO_X values corrected to:

---

[1] "Analytical Procedures for Characterizing Unregulated Emissions from Vehicles Using Middle-Distillate Fuels" EPA Interim Report EPA-600/2-80-0068, 1980.

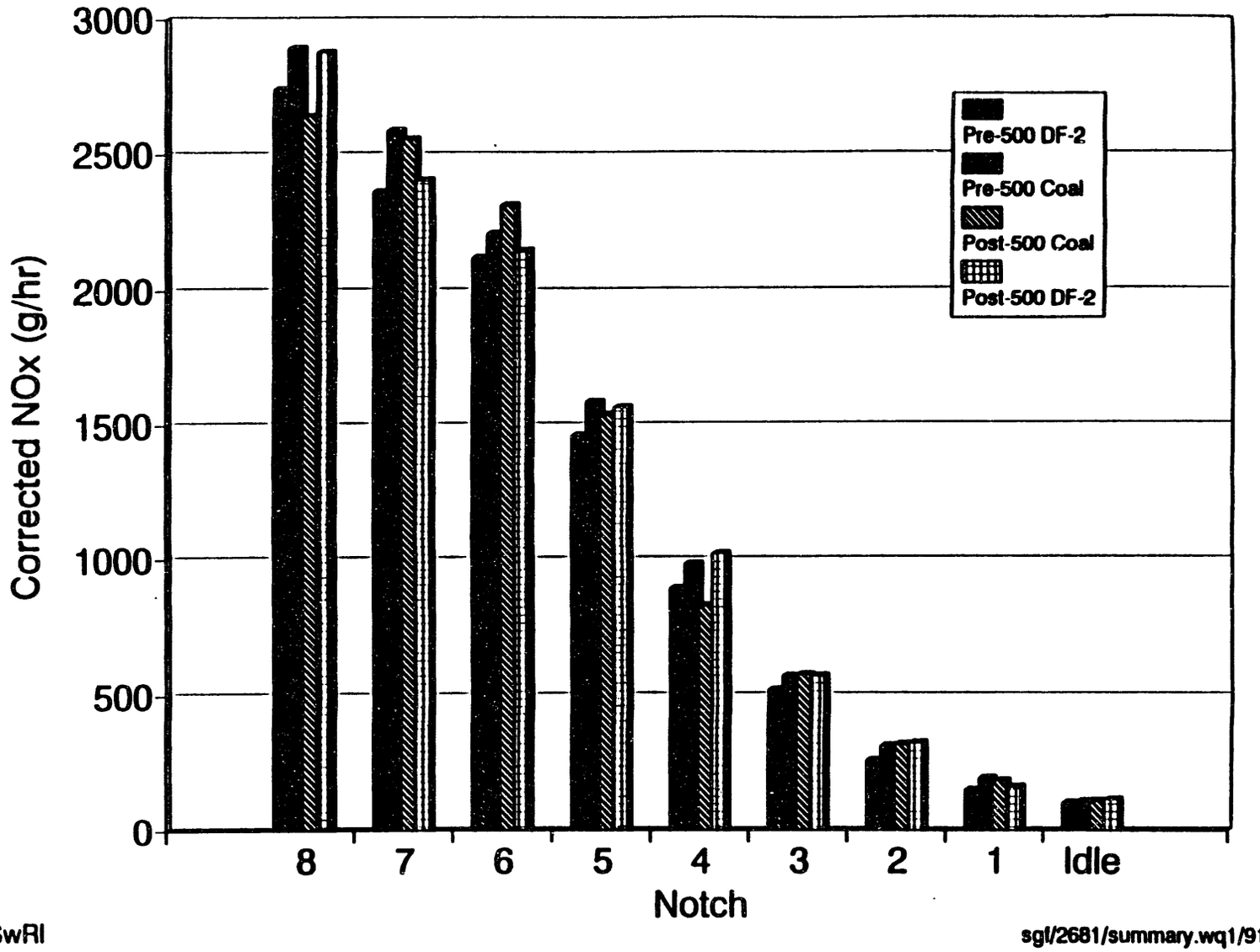

Figure 6. EMD 2-567 Engine Corrected NO_x Mass Emission Rate at Each Notch Position, Before and After a 500-Hour Durability Test, on Both Test Fuels.

1. 85°F engine intake air temperature,

2. 75 grains of water per pound of dry air humidity.

The engine intake air temperature correction factor and humidity correction factor vary with measured fuel/air ratio (i.e. engine load). These correction factors are used for EPA 13-mode steady-state testing and are referenced in 40 CFR, Subpart D 86.345-79. The NO_x values shown in Figure 6 and Appendices A-D are the corrected values.

Figures 7, 8, 9, and 10 give summaries of the measured mass emission rates at each notch position for carbon monoxide, hydrocarbons, particulates, and sulfur dioxide, respectively.

A duty-cycle based weighting procedure was used in determining composite brake specific emissions. The weighting factors used in determining composite brake-specific emissions are typical of a locomotive line-haul duty cycle, and are fairly representative of locomotive operations through out the U.S.; with approximately 10 percent of the time spent at rated conditions (Notch 8) and a significant amount of time (55 percent) at idle. The remainder of the time is spent distributed over the other throttle notch positions. Table 4 shows the un-weighted and weighted emission results, as well as the composite weighted brake specific exhaust emissions expressed in g/bhp-hr.

The composite brake specific emissions for the EMD 2-567B operating on both baseline ASTM 2D diesel and the coal-lite fuel are summarized in Table 5.

C. Wear Results

Engine wear was assessed based on visual inspection and physical wear measurements. Wear measurements were taken according to the standard EMD dimension sheets. Sheets 1 through 26 are presented in Appendix C. Generally, in 500 hours of operation, wear in this class of engine should be at the lower limits of measurable range. Measurable range using classical measurement tools is typically 0.001" or greater. Therefore, wear reported less than 0.001" can be considered beyond the range of measurement accuracy. However, wear greater than 0.001" for this engine can be considered significant.

Of particular interest, when evaluating alternative fuels, is the ring and liner wear. These surfaces are normally the first to show signs of abnormal wear with undesirable fuels. As shown, on dimension sheets 13, 14, and 21, 22, the wear was

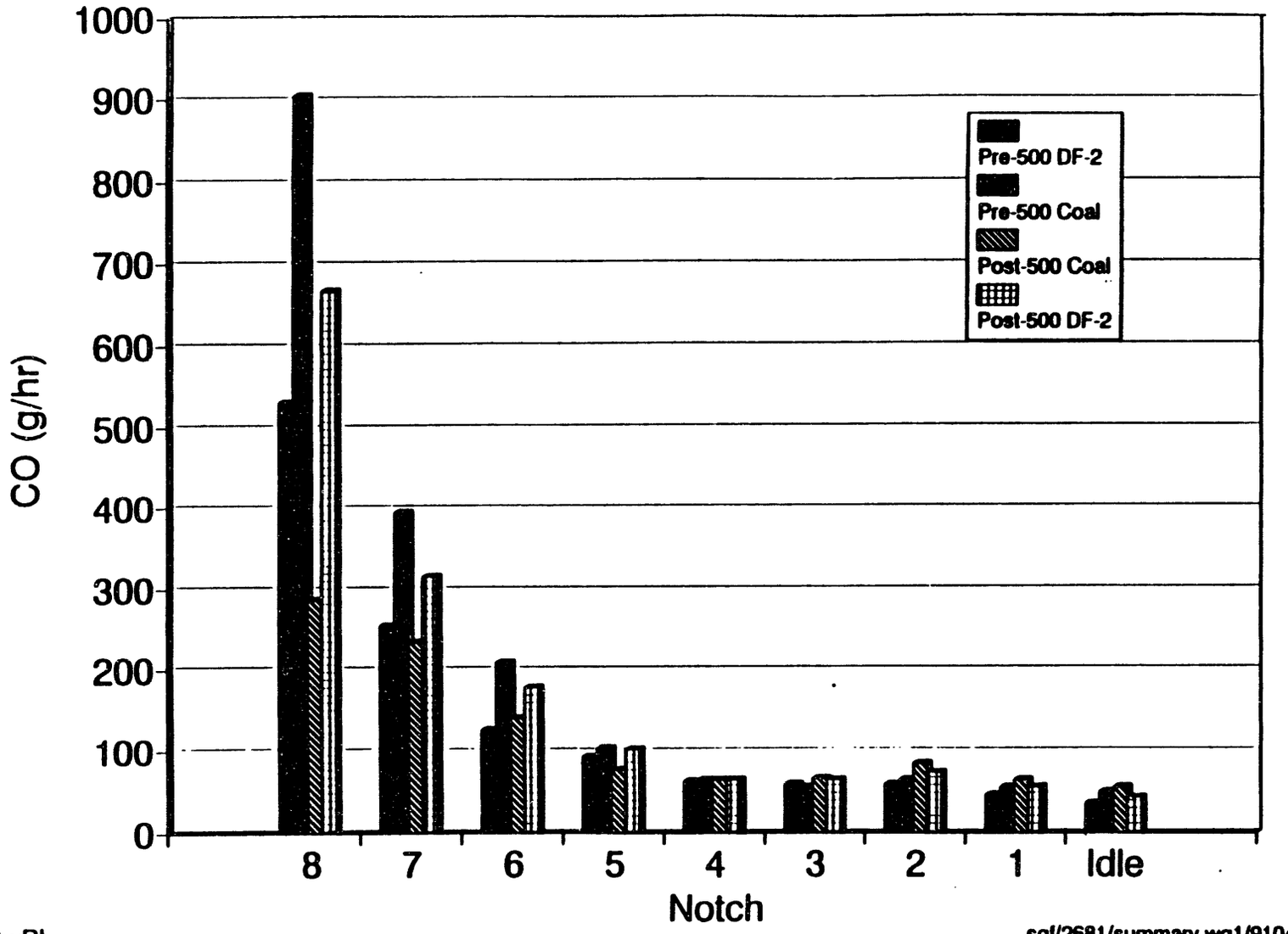

Figure 7. EMD 2-567 Engine Carbon Monoxide Mass Emission Rate at Each Notch Position, Before and After a 500-Hour Durability Test, on Both Test Fuels.

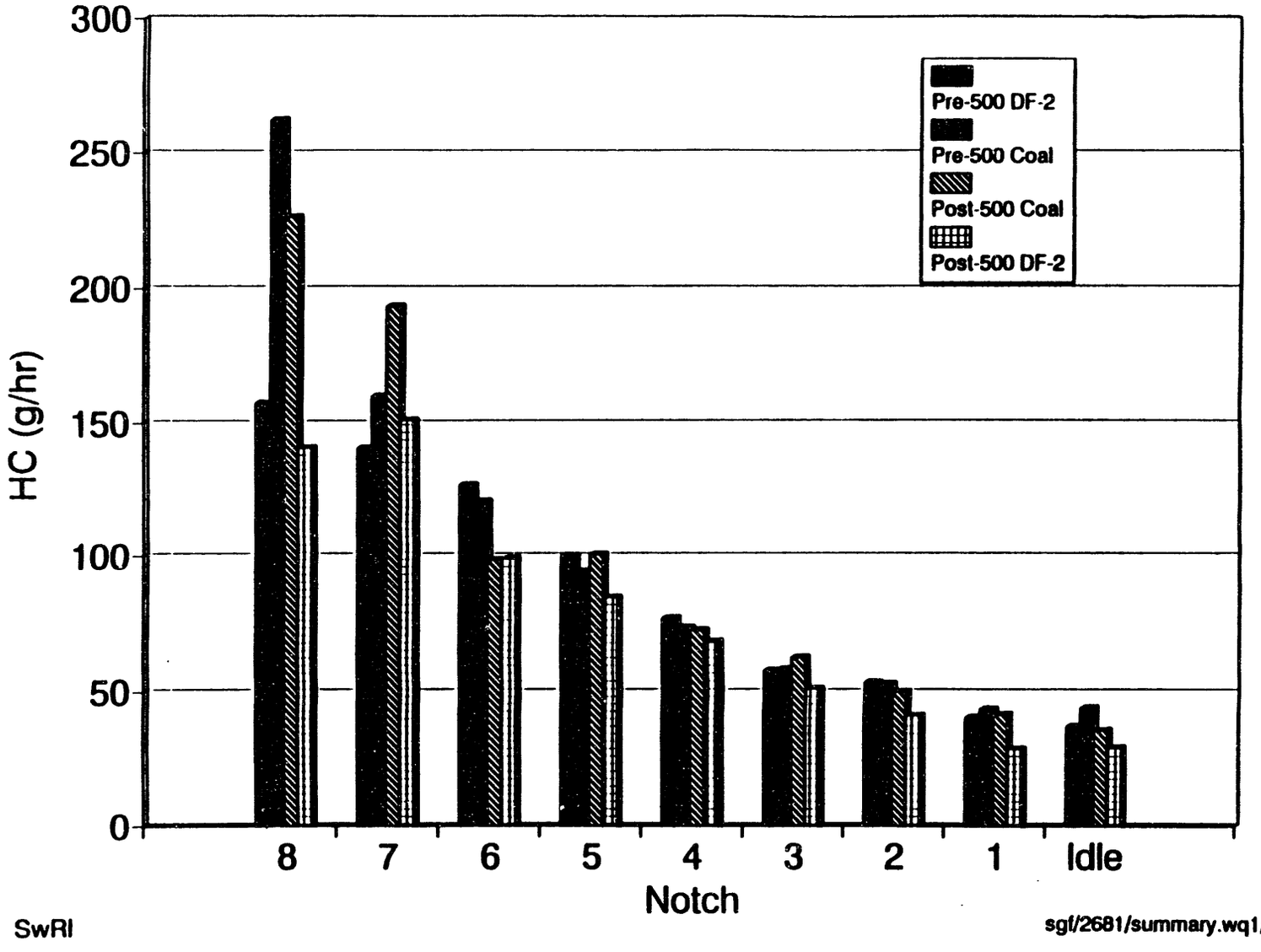

Figure 8. EMD 2-567 Engine Hydrocarbon Mass Emission Rate at Each Notch Position, Before and After a 500-Hour Durability Test, on Both Test Fuels.

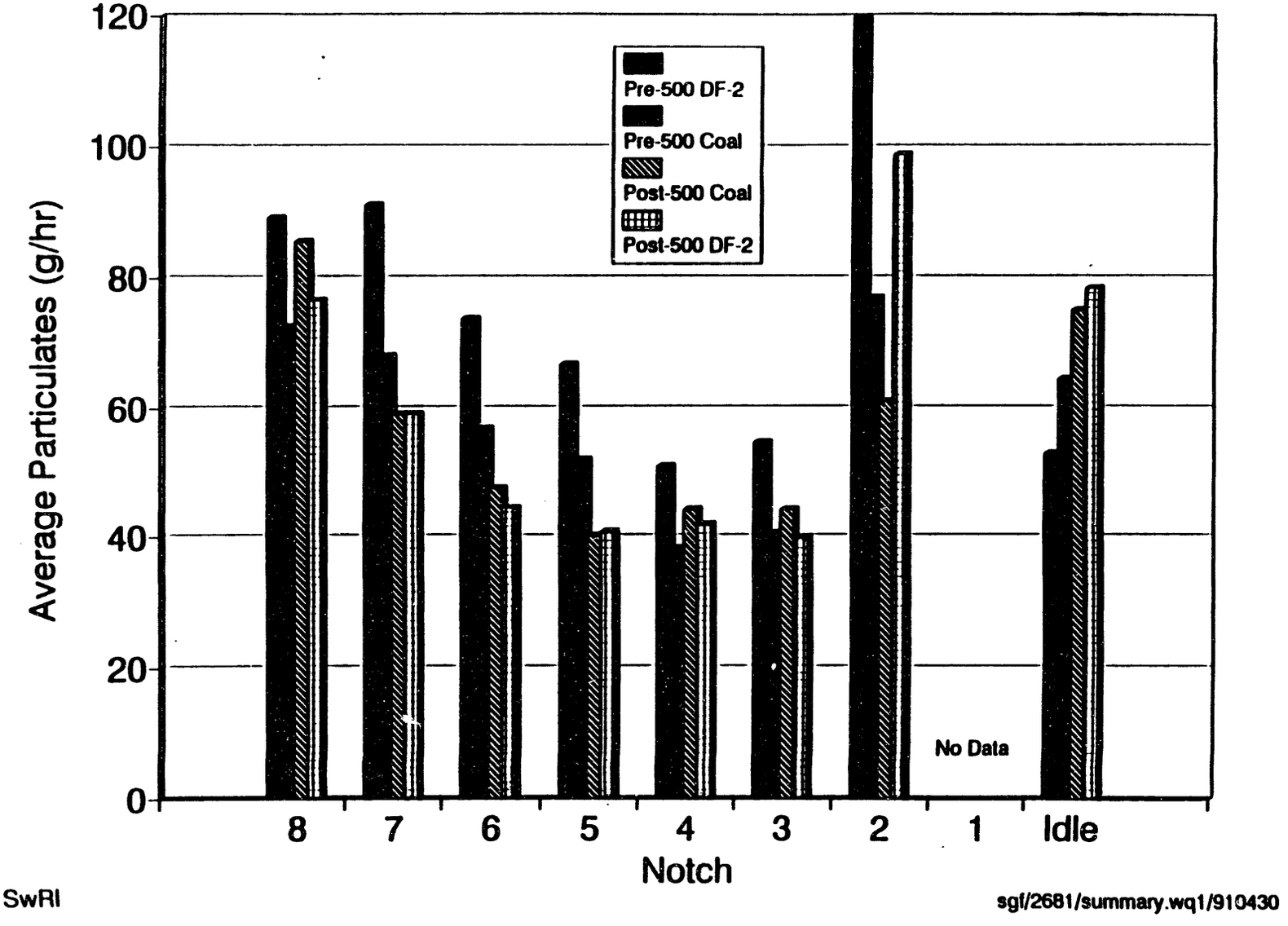

Figure 9. EMD 2-567 Engine Average Particulate Mass Emission Rate at Each Notch Position, Before and After a 500-Hour Durability Test, on Both Fuels.

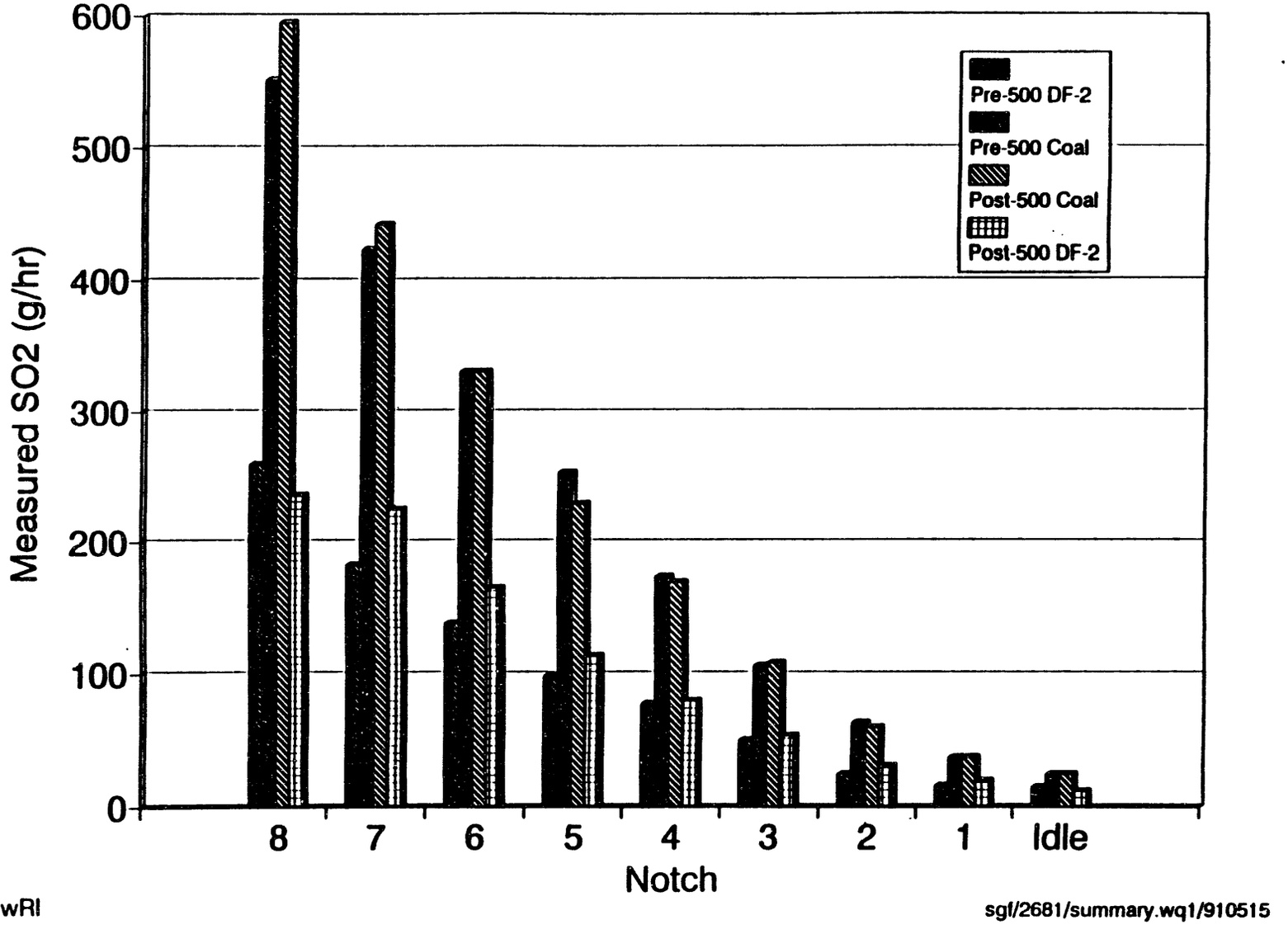

Figure 10. SO_2 EMD 2-567 Engine SO_2 Emission Rate at Each Notch Position, Before and After a 500-Hour Durability Test, on Both Fuels.

Table 4. Summary of Emissions Data for the EMD 2-567 Locomotive Engine

Test Summary 1/31/91				Baseline Diesel					***** Weighted g/hr *****				
Notch	BHP	HC g/hr	CO g/hr	Corr. NO_x g/hr	Avg. Part. g/hr	Meas. SO_2 g/hr	wf	BHP	HC g/hr	CO g/hr	Corr. NO_x g/hr	Avg. Part. g/hr	Meas. SO_2 g/hr
8	207	157	531	2743	89	260	0.10	21	16	53	274	9	26
7	178	140	254	2360	91	183	0.05	9	7	13	118	5	9
6	149	126	127	2121	74	139	0.05	7	6	6	106	4	7
5	114	100	93	1462	67	99	0.05	6	5	5	73	3	5
4	77	77	62	893	51	77	0.05	4	4	3	45	3	4
3	47	57	59	520	55	50	0.05	2	3	3	26	3	3
2	20	53	58	257	120	25	0.05	1	3	3	13	6	1
1	8	40	45	138	nd	15	0.05	0	2	2	7	4	1
idle	0	37	35	100	53	15	0.55	0	20	19	55	29	8
						Sum	1.00	50	66	107	717	65	64
Weighted Composite g/hp-hr =									1.3	2.1	14.2	1.29	1.26

Table 4. Summary of Emissions Data for the EMD 2-567 Locomotive Engine(Continued)

Test Summary 1/31/91				Baseline Diesel					***** Weighted g/hr *****				
Notch	BHP	HC g/hr	CO g/hr	Corr. NO_x g/hr	Avg. Part. g/hr	Meas. SO_2 g/hr	wf	BHP	HC g/hr	CO g/hr	Corr. NO_x g/hr	Avg. Part. g/hr	Meas. SO_2 g/hr
8	206	263	906	2894	73	552	0.10	21	26	91	289	7	55
7	179	160	396	2585	68	424	0.05	9	8	20	129	3	21
6	149	121	210	2210	57	331	0.05	7	6	10	110	3	17
5	115	94	104	1584	52	253	0.05	6	5	5	79	3	13
4	78	73	65	984	38	174	0.05	4	4	3	49	2	9
3	47	58	56	568	41	107	0.05	2	3	3	28	2	5
2	19	53	64	309	77	63	0.05	1	3	3	15	4	3
1	8	43	54	192	nd	37	0.05	0	2	3	10	4	2
idle	0	44	49	107	64	25	0.55	0	24	27	59	35	14
						Sum	1.00	50	81	165	770	63	138
Weighted Composite g/hp-hr =									1.6	3.3	15.3	1.26	2.75

Table 4. Summary of Emissions Data for the EMD 2-567 Locomotive Engine (Continued)

Test Summary 1/31/91				Baseline Diesel					***** Weighted g/hr *****				
Notch	BHP	HC g/hr	CO g/hr	Corr. NO_x g/hr	Avg. Part. g/hr	Meas. SO_2 g/hr	wf	BHP	HC g/hr	CO g/hr	Corr. NO_x g/hr	Avg. Part. g/hr	Meas. SO_2 g/hr
8	206	226	288	2643	86	627	0.10	21	23	29	264	9	63
7	179	193	234	2554	59	483	0.05	9	10	12	128	3	24
6	149	99	142	2313	48	343	0.05	7	5	7	116	2	17
5	113	101	76	1537	40	246	0.05	6	5	4	77	2	12
4	76	73	64	825	44	166	0.05	4	4	3	41	2	8
3	46	62	65	573	44	112	0.05	2	3	3	29	2	6
2	19	50	85	317	61	65	0.05	1	2	4	16	3	3
1	8	41	65	181	nd	42	0.05	0	2	3	9	4	2
idle	0	35	55	108	75	26	0.55	0	19	31	59	41	14
						Sum	1.00	50	73	96	739	69	150
Weighted Composite g/hp-hr =									1.4	1.9	14.7	1.36	2.98

Table 4. Summary of Emissions Data for the EMD 2-567 Locomotive Engine (Continued)

Test Summary 1/31/91				Baseline Diesel					***** Weighted g/hr *****				
Notch	BHP	HC g/hr	CO g/hr	Corr. NO_x g/hr	Avg. Part. g/hr	Meas. SO_2 g/hr	wf	BHP	HC g/hr	CO g/hr	Corr. NO_x g/hr	Avg. Part. g/hr	Meas. SO_2 g/hr
8	206	140	668	2879	77	235	0.10	21	14	67	288	8	24
7	179	151	316	2405	59	459	0.05	9	8	16	120	3	23
6	148	99	179	2147	45	166	0.05	7	5	9	107	2	8
5	114	85	101	1567	41	114	0.05	6	4	5	78	2	6
4	78	68	64	1022	42	79	0.05	4	3	3	51	2	4
3	46	51	64	568	40	26	0.05	2	3	3	28	2	1
2	20	41	74	319	99	31	0.05	1	2	4	16	5	2
1	8	29	55	159	nd	19	0.05	0	1	3	8	4	1
idle	0	29	42	108	78	11	0.55	0	16	23	60	43	6
							Sum	50	56	132	757	71	74
Weighted Composite g/hp-hr =									5.6	2.6	15.0	1.41	1.48

Table 5. Weighted Composite Brake Specific Emissions Summary for the EMD 2-567 Locomotive Engine

	PM	HC	CO	NO_x	SO_2
	Composite (g/bhp-hr)				
Pre 500-Hour : Baseline 2D	1.29	1.3	2.1	14.2	1.3
Pre 500-Hour : Coal-Lite	1.26	1.6	3.3	15.3	2.8
Post 500-Hour : Coal-Lite	1.36	1.4	1.9	14.7	3.0
Post 500-Hour : Baseline 2D	1.41	1.1	2.6	15.0	1.5
EPA Heavy Duty Diesel Std. : 1994	0.1	1.3	15.5	5.0	NA
Proposed Off-Highway California 8 Mode : 1995 : 2000	0.4 0.16	1.0 1.0	N.A. N.A.	6.9 5.8	N.A. N.A.

significant on the piston and liner of the left cylinder. Wear on the piston of 0.002", and on the liner of 0.0057" is considerably greater than normal. Additionally, the wear area was visually detected, as shown in Figure 11.

Although the wear on the left piston and liner was significant, it does not mean that the wear was induced as a result of running the coal-lite fuel. In fact, other evidence indicates that the wear was not fuel related. This is substantiated by examining the right cylinder piston and liner. Wear here was below the measurable range as expected in 500 hours. Additionally, none of the other components measured indicated significant wear as shown on the dimension sheets (Appendix E).

Except for the left cylinder, visual inspection of all engine components did not indicate any abnormal wear condition. Photographs of the components inspected are presented in Appendix F. Visually, varnish deposits were observed on the injector needle assemblies (see photographs Appendix F). In fact, it was somewhat difficult to remove the needle from the bore due to the varnish deposits. The deposits did not inhibit engine operation but were unusual for 500 hours operation.

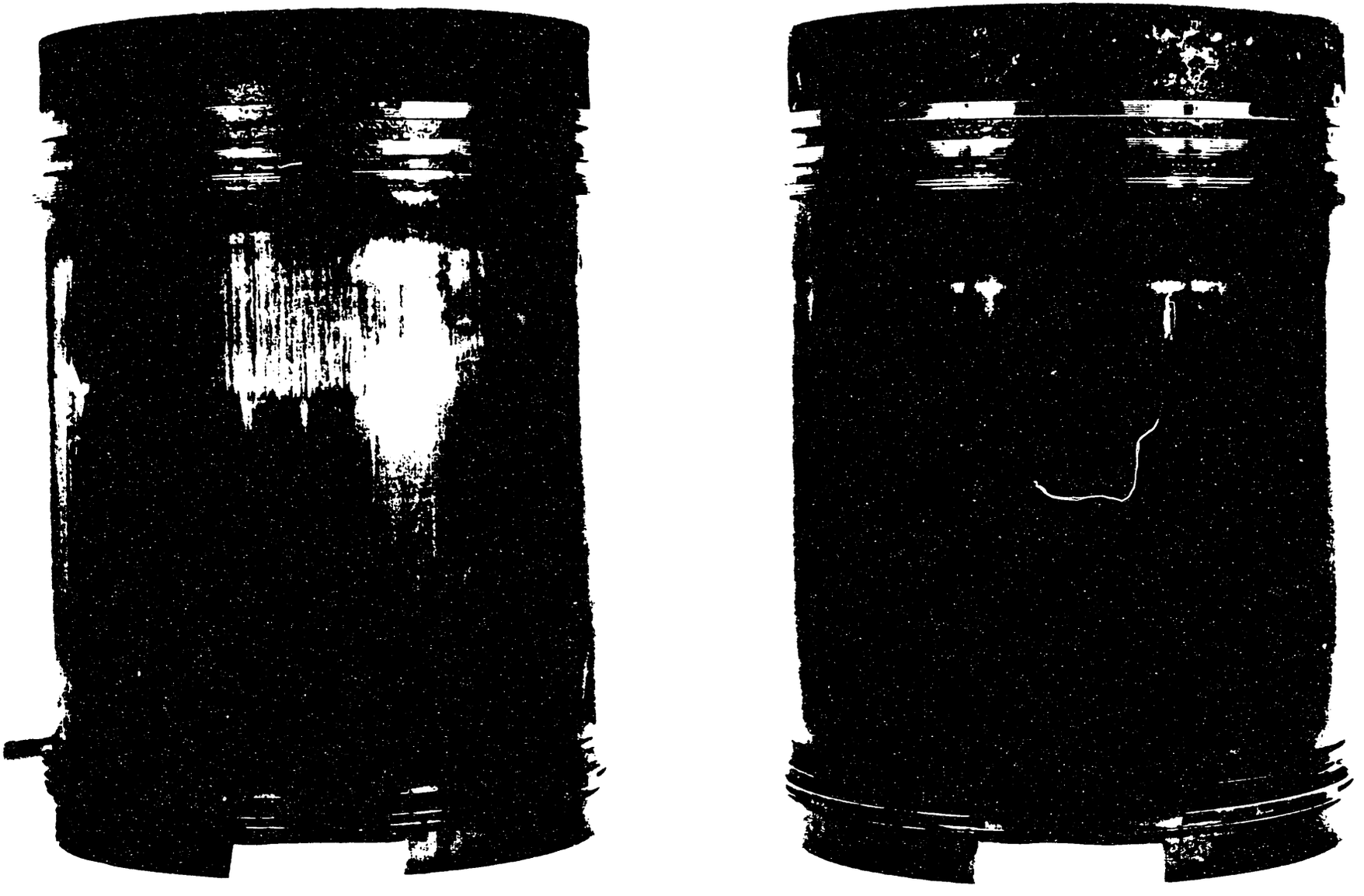

Figure 11. EMD Pistons

V. DISCUSSION

This test was preformed in order to evaluate the performance and emissions of the coal-lite fuel as compared to neat diesel fuel and to determine if any detrimental wear would be observed after 500 hours of operation.

A. Performance Tests

The performance results indicated that, operationally in the medium-speed diesel engine, the fuel functioned well. No problems were encountered with starting, knock, or general engine operation. However, due to the lower heating value of the fuel and lower thermal efficiency observed, a fuel efficiency penalty of approximately 2 to 4 percent can be expected at the higher notch operation (Notches 5 to 8). The thermal efficiency penalty could be a result of a slower burn duration of the coal-lite fuel. Therefore, if this is the case, some of the penalty might be recovered by advancing the injection timing. This would have to be determined experimentally.

B. Wear Tests

In 500 hours of operation on medium-speed diesel engines, wear measurements can only determine if the fuel tested was catastrophic to the engine. Typically, the wear should be undetectable. Therefore, if wear is measured, then it can be assumed that the fuel is unsatisfactory and should not be consumed for fear of subsequent engine destruction. In this case, significant wear was detected in the left cylinder. The level of this wear, if fuel induced, would condemn the fuel for use in this engine. However, since this level of wear was not detected with any other components it can be assumed that the wear was a function of defective components or the rebuild and not a function of the fuel consumed.

Of some concern is the varnish deposits on the fuel injection components. After 500 hours, the injectors were still functioning properly however the needles were stuck in their bores. Some question exists if this would present a problem with unsatisfactory operation after additional hours of operation.

C. Emissions Tests

Based on the limited emissions tests performed on the EMD 2-567B engine, it appears that the coal-lite fuel blend tested did not significantly change the normally regulated exhaust emissions. The only significant difference detected in the measured exhaust emissions was SO_2, where the weighted composite brake specific emissions of SO_2 were approximately two times higher on the coal-lite fuel as compared to the baseline diesel fuel. However, this result was not unexpected, as the fuel sulfur content of the coal-lite fuel blend was approximately twice that of the

baseline diesel fuel. (It should be noted that SO_2 emissions are not regulated for mobile sources.)

In general, locomotive engine emissions are not regulated is the U.S. The only possible exception to this are the various visible smoke standards in several areas. However, the California Air Resources Board has recently began to study locomotive exhaust emissions, and regulations are anticipated within the next few years for engines built before 1990. At the national level, Congress, through the Clean Air Act Amendments of 1990, instructed the EPA to study locomotive exhaust emissions and to promulgate regulations by 1995. Those regulations would apply to new engines built since 1990.

Although the EMD 2-567B engine used in this study is representative of a large number of locomotive engine currently operating in the U.S., the 567 engine design is now two generations old. Significant improvements to the engine design have been incorporated to both significantly improve fuel economy and to reduce exhaust emission levels. Today's state-of-the-art locomotive engines have NO_X levels of approximately 8-10 g/hp-hr and particulate levels on the order of 0.15-0.25 g/hp-hr. Given the promising performance, wear and emission characteristics of the coal-lite in this limited testing on the EMD 2-567B engine, further evaluations may be warranted on full scale locomotive engines. This testing could involve performance and emissions testing on SwRI's 12-cylinder locomotive engines. These engines, an EMD 12-645E3B, and a GE 12-7FDL, are each rated at 2,500 bhp, and are representative of the majority of the existing locomotive fleet in North America. However, these engines are themselves one generation old, and do not incorporate all of the improvements of today's new locomotive engines. In addition to further 12-cylinder locomotive engine tests, a controlled long-term field study of the coal-lite fuel blend may be considered to evaluate the in-service characteristics of the fuel.

VI. CONCLUSIONS

After 500 hours of operation, performance and wear measurements made on the engine as a result of running on coal-lite fuel did not indicate that the fuel was catastrophic. However, varnish deposits on the fuel injectors should be monitored. If used in rail operation, the coal-lite fuel should be used in controlled field tests for one year until longer term results can be observed. The coal-lite fuel did not significantly change the normally regulated exhaust emissions, but did significantly increase SO_2 emissions because of its higher sulfur content.

APPENDIX A

GASEOUS and/or PARTICULATE EMISSIONS

IDLE

PROJECT 03-2681-809 PROGRAM = EMD16B

TEST NO. RUN NO. 9
ENGINE MODEL EMD 2-567B
TEST CELL LOCO LAB
HCR 1.758
BLOWER COUNTS 47666.
OBS. POWER,BHP .0

TEST DATE 1/31/91
DIESEL DF-2
TUNNEL NO. 26
SAMPLE TIME 20x20 .00 MIN.
BLOWER TEMP. DEG. F 59.
FUEL FLOW,LB/MIN .09

BAROMETER 29.55 IN.HG.
HUMIDITY 26.71 GRAINS H2O/LB. AIR
LFE NO. 15 ENG. LFE NO. 0
SAMPLE TIME 47mm 30.00 MIN.
MEAS. EXH. FLOW,LB/MIN 16.34
AIR FLOW,LB/MIN 16.25

LFE INFORMATION			BLOWER INFORMATION		OTHER
INLET TEMP DEG. F	INLET PRESS. IN. H20	DIFF. PRESS. IN. H20	INLET PRESS. IN. H20	DIFF. PRESS. IN. H20	TUNNEL TEMP DEG. F
68.	.53	4.600	11.00	15.00	96.
67.	.53	4.550	11.00	15.00	95.
67.	.53	4.600	11.00	15.00	94.
69.	.53	4.600	11.00	15.00	95.
69.	.53	4.600	11.00	15.00	95.
68.	.53	4.600	11.00	15.00	95.
66.	.53	4.500	11.00	15.00	93.
AVERAGE 68.	.53	4.579	11.00	15.00	95.

LFE VOL, SCF 7230.9 LFE MASS,LB. 543.3
LFE FLOW SCFM 241.02 LFE FLOW LB/MIN 18.11
F/A DRY, MEAS .0058 F/A CALC .0045

BLOWER + 47mm VOL, SCF 7497.0 BLOWER + 47mm MASS,LB 563.3
BLOWER + 47mm FLOW SCFM 249.88 BLOWER + 47mm FLOW LB/MIN 18.78
F/A PCT, MEAS -22.1

FILTER DATA

POSITION	FILTER NUMBER	SAMPLE VOL. STD.CU.FEET	AVG. SAMPLE SYS. TEMP DEG F	WEIGHT GAIN MILLIGRAMS	MG/SCF OF SAMPLE
1	P47-33&34	22.699	59.	3.334	.147
2	P47-35&36	22.719	59.	3.219	.142

PARTICULATE RESULTS

AVG. SAMPLE ZONE TEMP, DEG F 95. DILUTION FACTOR 28.177
SPLIT EXHAUST VOL,SCF (SCM), LB/MIN 266.1 (7.54) , .67

PARTICULATE CONCENTRATION IN EXHAUST FILTER	CONCENTRATION, MG/SCF (MG/SCM)	CONCENTRATION MULTIPLIER	G/HR	G/HP-HR
P47-33&34	4.139 (146.135)	1.2413	54.011	.000
P47-35&36	3.992 (140.970)	1.2402	52.102	.000

EMISSION RESULTS

	G/HR	G/HP-HR	CONC.
HC	37.039	.000	137. PPMC
CO	34.829	.000	64. PPM
NOX	116.333	.000	131. PPM
NOX,CORR	99.721	.000	
CO2		0.	.93 PCT
O2			19.32 PCT
NOX CORRECTION FACTOR	.8572	WET CORRECTION FACTOR	.9909

GASEOUS and/or PARTICULATE EMISSIONS
NOTCH 1
PROJECT 03-2681-809 PROGRAM = EMD16B

TEST NO. RUN NO. 8
ENGINE MODEL EMD 2-567B
TEST CELL LOCO LAB
HCR 1.758
BLOWER COUNTS 47682.
OBS. POWER,BHP 8.3

TEST DATE 1/31/91
DIESEL DF-2
TUNNEL NO. 26
SAMPLE TIME 20x20 .00 MIN.
BLOWER TEMP. DEG. F 61.
FUEL FLOW,LB/MIN .13

BAROMETER 29.55 IN.HG.
HUMIDITY 25.08 GRAINS H2O/LB. AIR
LFE NO. 15 ENG. LFE NO. 0
SAMPLE TIME 47mm 30.00 MIN.
MEAS. EXH. FLOW,LB/MIN 16.36
AIR FLOW,LB/MIN 16.23

LFE INFORMATION			BLOWER INFORMATION		OTHER
INLET TEMP DEG. F	INLET PRESS. IN. H20	DIFF. PRESS. IN. H20	INLET PRESS. IN. H20	DIFF. PRESS. IN. H20	TUNNEL TEMP DEG. F
69.	.55	4.850	11.00	15.00	101.
70.	.55	4.850	11.00	15.00	101.
69.	.55	4.830	11.00	15.00	101.
70.	.53	4.850	11.00	15.00	101.
71.	.55	4.850	11.00	15.00	102.
71.	.55	4.850	11.00	15.00	102.
71.	.55	4.830	11.00	15.00	101.
AVERAGE 70.	.55	4.844	11.00	15.00	101.

LFE VOL, SCF 7567.2 LFE MASS,LB. 568.6 BLOWER + 47mm VOL, SCF 7467.4 BLOWER + 47mm MASS,LB 561.1
LFE FLOW SCFM 252.23 LFE FLOW LB/MIN 18.95 BLOWER + 47mm FLOW SCFM 248.90 BLOWER + 47mm FLOW LB/MIN 18.70
F/A DRY, MEAS .0082 F/A CALC .0066 F/A PCT, MEAS -19.9

FILTER DATA

POSITION	FILTER NUMBER	SAMPLE VOL. STD.CU.FEET	AVG. SAMPLE SYS. TEMP DEG F	WEIGHT GAIN MILLIGRAMS	MG/SCF OF SAMPLE
1	P47-29&30	21.448	64.	6.477	.302
2	P47-31&32	21.478	64.	6.193	.288

PARTICULATE RESULTS

AVG. SAMPLE ZONE TEMP, DEG F 101. DILUTION FACTOR ******
SPLIT EXHAUST VOL,SCF (SCM), LB/MIN ***** (*****) , ****

PARTICULATE CONCENTRATION IN EXHAUST

FILTER	CONCENTRATION, MG/SCF (MG/SCM)	CONCENTRATION MULTIPLIER	G/HR	G/HP-HR
P47-29&30	******* (*******)	*******	*******	*******
P47-31&32	******* (*******)	*******	*******	*******

EMISSION RESULTS

	G/HR	G/HP-HR	CONC.
HC	40.034	4.853	152. PPMC
CO	45.421	5.506	86. PPM
NOX	174.091	21.102	202. PPM
NOX,CORR	148.042	17.944	
CO2		1065.	1.37 PCT
O2			18.44 PCT
NOX CORRECTION FACTOR	.8504	WET CORRECTION FACTOR	.9871

GASEOUS and/or PARTICULATE EMISSIONS
NOTCH 2
PROJECT 03-2681-809 PROGRAM = EMD16B

TEST NO. RUN NO. 7
ENGINE MODEL EMD 2-567B
TEST CELL LOCO LAB
HCR 1.758
BLOWER COUNTS 47674.
OBS. POWER,BHP 20.0

TEST DATE 1/31/91
DIESEL DF-2
TUNNEL NO. 26
SAMPLE TIME 20x20 .00 MIN.
BLOWER TEMP. DEG. F 63.
FUEL FLOW,LB/MIN .20

BAROMETER 29.54 IN.HG.
HUMIDITY 25.56 GRAINS H2O/LB. AIR
LFE NO. 15 ENG. LFE NO. 0
SAMPLE TIME 47mm 30.00 MIN.
MEAS. EXH. FLOW,LB/MIN 21.53
AIR FLOW,LB/MIN 21.33

LFE INFORMATION			BLOWER INFORMATION		OTHER
INLET TEMP DEG. F	INLET PRESS. IN. H20	DIFF. PRESS. IN. H20	INLET PRESS. IN. H20	DIFF. PRESS. IN. H20	TUNNEL TEMP DEG. F
72.	.48	4.590	11.00	15.00	114.
72.	.48	4.590	11.00	15.00	114.
72.	.48	4.590	11.00	15.00	114.
72.	.48	4.590	11.00	15.00	114.
71.	.48	4.570	11.00	15.00	113.
71.	.50	4.550	11.00	15.00	113.
71.	.50	4.550	11.00	15.00	113.
AVERAGE 72.	.49	4.576	11.00	15.00	114.

LFE VOL, SCF 7132.6 LFE MASS,LB. 535.9 BLOWER + 47mm VOL, SCF 7433.9 BLOWER + 47mm MASS,LB 558.6
LFE FLOW SCFM 237.75 LFE FLOW LB/MIN 17.86 BLOWER + 47mm FLOW SCFM 247.80 BLOWER + 47mm FLOW LB/MIN 18.62
F/A DRY, MEAS .0094 F/A CALC .0080 F/A PCT, MEAS -14.6

FILTER DATA

POSITION	FILTER NUMBER	SAMPLE VOL. STD.CU.FEET	AVG. SAMPLE SYS. TEMP DEG F	WEIGHT GAIN MILLIGRAMS	MG/SCF OF SAMPLE
1	P47-25&26	21.422	65.	6.160	.288
2	P47-27&28	21.412	65.	5.949	.278

PARTICULATE RESULTS

AVG. SAMPLE ZONE TEMP, DEG F 114. DILUTION FACTOR 24.675
SPLIT EXHAUST VOL,SCF (SCM), LB/MIN 301.3 (8.53) , .75

PARTICULATE CONCENTRATION IN EXHAUST

FILTER	CONCENTRATION, MG/SCF (MG/SCM)	CONCENTRATION MULTIPLIER	G/HR	G/HP-HR
P47-25&26	7.095 (250.542)	1.1519	121.981	6.099
P47-27&28	6.856 (242.072)	1.1524	117.858	5.893

EMISSION RESULTS

	G/HR	G/HP-HR	CONC.
HC	53.297	2.665	164. PPMC
CO	58.494	2.925	90. PPM
NOX	294.835	14.742	278. PPM
NOX,CORR	257.184	12.859	
CO2		659.	1.67 PCT
O2			18.07 PCT

NOX CORRECTION FACTOR .8723 WET CORRECTION FACTOR .9845

GASEOUS and/or PARTICULATE EMISSIONS
NOTCH 3
PROJECT 03-2681-809 PROGRAM = EMD16B

TEST NO. RUN NO. 6
ENGINE MODEL EMD 2-567
TEST CELL LOCO LAB
HCR 1.758
BLOWER COUNTS 47656.
OBS. POWER,BHP 47.0

TEST DATE 1/31/91
DIESEL DF-2
TUNNEL NO. 26
SAMPLE TIME 20x20 .00 MIN.
BLOWER TEMP. DEG. F 66.
FUEL FLOW,LB/MIN .35

BAROMETER 29.54 IN.HG.
HUMIDITY 29.37 GRAINS H2O/LB. AIR
LFE NO. 15 ENG. LFE NO. 0
SAMPLE TIME 47mm 30.00 MIN.
MEAS. EXH. FLOW,LB/MIN 27.80
AIR FLOW,LB/MIN 27.45

LFE INFORMATION			BLOWER INFORMATION		OTHER
INLET TEMP DEG. F	INLET PRESS. IN. H2O	DIFF. PRESS. IN. H2O	INLET PRESS. IN. H2O	DIFF. PRESS. IN. H2O	TUNNEL TEMP DEG. F
72.	.45	4.300	11.00	15.00	122.
72.	.45	4.300	11.00	15.00	122.
71.	.44	4.300	11.00	15.00	122.
71.	.46	4.300	11.00	15.00	122.
71.	.47	4.300	11.00	15.00	122.
71.	.45	4.280	11.00	15.00	122.
AVERAGE 71.	.45	4.297	11.00	15.00	122.

LFE VOL, SCF 6723.0 LFE MASS,LB. 505.2 BLOWER + 47mm VOL, SCF 7387.3 BLOWER + 47mm MASS,LB 555.1
LFE FLOW SCFM 224.11 LFE FLOW LB/MIN 16.84 BLOWER + 47mm FLOW SCFM 246.26 BLOWER + 47mm FLOW LB/MIN 18.50
F/A DRY, MEAS .0127 F/A CALC .0104 F/A PCT, MEAS -17.9

FILTER DATA

POSITION	FILTER NUMBER	SAMPLE VOL. STD.CU.FEET	AVG. SAMPLE SYS. TEMP DEG F	WEIGHT GAIN MILLIGRAMS	MG/SCF OF SAMPLE
1	P47-21&22	21.533	63.	4.854	.225
2	P47-23&24	21.503	63.	4.697	.218

PARTICULATE RESULTS

AVG. SAMPLE ZONE TEMP, DEG F 122. DILUTION FACTOR 11.120
SPLIT EXHAUST VOL,SCF (SCM), LB/MIN 664.4 (18.81) , 1.66

PARTICULATE CONCENTRATION IN EXHAUST

FILTER	CONCENTRATION, MG/SCF (MG/SCM)	CONCENTRATION MULTIPLIER	G/HR	G/HP-HR
P47-21&22	2.507 (88.507)	.5164	55.635	1.184
P47-23&24	2.429 (85.763)	.5171	53.911	1.147

EMISSION RESULTS

	G/HR	G/HP-HR	CONC.
HC	57.498	1.223	132. PPMC
CO	58.966	1.255	68. PPM
NOX	597.133	12.705	422. PPM
NOX,CORR	520.189	11.068	
CO2		491.	2.19 PCT
O2			17.31 PCT

NOX CORRECTION FACTOR .8711 WET CORRECTION FACTOR .9799

GASEOUS and/or PARTICULATE EMISSIONS
NOTCH 4
PROJECT 03-2681-809 PROGRAM = EMD16B

TEST NO. RUN NO. 5
ENGINE MODEL EMD 2-567B
TEST CELL LOCO LAB
HCR 1.758
BLOWER COUNTS 33964.
OBS. POWER,BHP 77.0

TEST DATE 1/31/91
DIESEL DF-2
TUNNEL NO. 26
SAMPLE TIME 20x20 .00 MIN.
BLOWER TEMP. DEG. F 67.
FUEL FLOW,LB/MIN .54

BAROMETER 29.55 IN.HG.
HUMIDITY 25.54 GRAINS H2O/LB. AIR
LFE NO. 15 ENG. LFE NO. 0
SAMPLE TIME 47mm 21.38 MIN.
MEAS. EXH. FLOW,LB/MIN 34.24
AIR FLOW,LB/MIN 33.70

LFE INFORMATION			BLOWER INFORMATION		OTHER
INLET TEMP DEG. F	INLET PRESS. IN. H20	DIFF. PRESS. IN. H20	INLET PRESS. IN. H20	DIFF. PRESS. IN. H20	TUNNEL TEMP DEG. F
73.	.52	4.080	11.00	15.00	123.
72.	.52	4.080	11.00	15.00	123.
72.	.49	4.130	11.00	15.00	123.
73.	.51	4.130	11.00	15.00	123.
73.	.52	4.150	11.00	15.00	124.
73.	.48	4.200	11.00	15.00	123.
AVERAGE 73.	.51	4.128	11.00	15.00	123.

LFE VOL, SCF 4591.9 LFE MASS,LB. 345.0 BLOWER + 47mm VOL, SCF 5256.2 BLOWER + 47mm MASS,LB 394.9
LFE FLOW SCFM 214.81 LFE FLOW LB/MIN 16.14 BLOWER + 47mm FLOW SCFM 245.88 BLOWER + 47mm FLOW LB/MIN 18.48
F/A DRY, MEAS .0161 F/A CALC .0136 F/A PCT, MEAS -15.6

FILTER DATA

POSITION	FILTER NUMBER	SAMPLE VOL. STD.CU.FEET	AVG. SAMPLE SYS. TEMP DEG F	WEIGHT GAIN MILLIGRAMS	MG/SCF OF SAMPLE
1	P47-17&18	15.154	61.	3.639	.240
2	P47-19&20	15.169	61.	3.505	.231

PARTICULATE RESULTS

AVG. SAMPLE ZONE TEMP, DEG F 123. DILUTION FACTOR 7.913
SPLIT EXHAUST VOL,SCF (SCM), LB/MIN 664.2 (18.81) , 2.33

PARTICULATE CONCENTRATION IN EXHAUST

FILTER	CONCENTRATION, MG/SCF (MG/SCM)	CONCENTRATION MULTIPLIER	G/HR	G/HP-HR
P47-17&18	1.900 (67.099)	.5222	51.957	.675
P47-19&20	1.828 (64.564)	.5217	49.994	.649

EMISSION RESULTS

	G/HR	G/HP-HR	CONC.
HC	76.786	.997	147. PPHC
CO	62.036	.806	60. PPM
NOX	1032.552	13.410	612. PPM
NOX,CORR	892.959	11.597	
CO2		468.	2.87 PCT
O2			16.31 PCT

NOX CORRECTION FACTOR .8648 WET CORRECTION FACTOR .9744

GASEOUS and/or PARTICULATE EMISSIONS
NOTCH 5
PROJECT 03-2681-809 PROGRAM = EMD16B

TEST NO. RUN NO. 4	TEST DATE 1/31/91	BAROMETER 29.60 IN.HG.
ENGINE MODEL EMD 2-567	DIESEL DF-2	HUMIDITY 23.35 GRAINS H2O/LB. AIR
TEST CELL LOCO LAB	TUNNEL NO. 26	LFE NO. 15 ENG. LFE NO. 0
HCR 1.758	SAMPLE TIME 20x20 .00 MIN.	SAMPLE TIME 47mm 20.70 MIN.
BLOWER COUNTS 32889.	BLOWER TEMP. DEG. F 67.	MEAS. EXH. FLOW,LB/MIN 38.26
OBS. POWER,BHP 114.0	FUEL FLOW,LB/MIN .76	AIR FLOW,LB/MIN 37.50

LFE INFORMATION			BLOWER INFORMATION		OTHER
INLET TEMP DEG. F	INLET PRESS. IN. H20	DIFF. PRESS. IN. H20	INLET PRESS. IN. H20	DIFF. PRESS. IN. H20	TUNNEL TEMP DEG. F
72.	.55	4.080	11.00	15.00	123.
72.	.55	4.030	11.00	15.00	123.
72.	.50	4.100	11.00	15.00	122.
72.	.55	4.050	11.00	15.00	123.
72.	.55	4.050	11.00	15.00	123.
AVERAGE 72.	.54	4.062	11.00	15.00	123.

LFE VOL, SCF 4395.6	LFE MASS,LB. 330.3	BLOWER + 47mm VOL, SCF 5098.9	BLOWER + 47mm MASS,LB 383.1
LFE FLOW SCFM 212.32	LFE FLOW LB/MIN 15.95	BLOWER + 47mm FLOW SCFM 246.28	BLOWER + 47mm FLOW LB/MIN 18.51
F/A DRY, MEAS .0203	F/A CALC .0174	F/A PCT, MEAS -14.4	

FILTER DATA

POSITION	FILTER NUMBER	SAMPLE VOL. STD.CU.FEET	AVG. SAMPLE SYS. TEMP DEG F	WEIGHT GAIN MILLIGRAMS	MG/SCF OF SAMPLE
1	P47-13&14	14.616	73.	4.810	.329
2	P47-15&16	14.744	73.	4.028	.273

PARTICULATE RESULTS

AVG. SAMPLE ZONE TEMP, DEG F 123. DILUTION FACTOR 7.251
SPLIT EXHAUST VOL,SCF (SCM), LB/MIN 703.2 (19.92) , 2.55

PARTICULATE CONCENTRATION IN EXHAUST

FILTER	CONCENTRATION, MG/SCF (MG/SCM)	CONCENTRATION MULTIPLIER	G/HR	G/HP-HR
P47-13&14	2.386 (84.251)	.4961	72.895	.639
P47-15&16	1.981 (69.944)	.4918	60.517	.531

EMISSION RESULTS

	G/HR	G/HP-HR	CONC.
HC	100.087	.878	174. PPMC
CO	92.717	.813	82. PPM
NOX	1693.758	14.858	918. PPM
NOX,CORR	1461.542	12.821	
CO2		444.	3.69 PCT
O2			15.30 PCT

NOX CORRECTION FACTOR .8629 WET CORRECTION FACTOR .9676

GASEOUS and/or PARTICULATE EMISSIONS
NOTCH 6
PROJECT 03-2681-809 PROGRAM = EMD16B

TEST NO. RUN NO. 3 | TEST DATE 1/31/91 | BAROMETER 29.62 IN.HG.
ENGINE MODEL EMD 2-567 | DIESEL DF-2 | HUMIDITY 23.31 GRAINS H2O/LB. AIR
TEST CELL LOCO LAB | TUNNEL NO. 26 | LFE NO. 15 ENG. LFE NO. 0
HCR 1.758 | SAMPLE TIME 20x20 .00 MIN. | SAMPLE TIME 47mm 30.01 MIN.
BLOWER COUNTS 47669. | BLOWER TEMP. DEG. F 67. | MEAS. EXH. FLOW,LB/MIN 43.69
OBS. POWER,BHP 149.0 | FUEL FLOW,LB/MIN .99 | AIR FLOW,LB/MIN 42.70

LFE INFORMATION			BLOWER INFORMATION		OTHER
INLET TEMP DEG. F	INLET PRESS. IN. H20	DIFF. PRESS. IN. H20	INLET PRESS. IN. H20	DIFF. PRESS. IN. H20	TUNNEL TEMP DEG. F
70.	.53	4.050	11.00	15.00	123.
71.	.53	4.020	11.00	15.00	123.
71.	.53	4.030	11.00	15.00	124.
71.	.55	4.030	11.00	15.00	124.
71.	.50	4.100	11.00	15.00	124.
71.	.50	4.100	11.00	15.00	124.
71.	.52	4.080	11.00	15.00	124.
AVERAGE 71.	.52	4.059	11.00	15.00	124.

LFE VOL, SCF 6394.1 | LFE MASS,LB. 480.5 | BLOWER + 47mm VOL, SCF 7394.5 | BLOWER + 47mm MASS,LB 555.6
LFE FLOW SCFM 213.10 | LFE FLOW LB/MIN 16.01 | BLOWER + 47mm FLOW SCFM 246.44 | BLOWER + 47mm FLOW LB/MIN 18.52
F/A DRY, MEAS .0232 | F/A CALC .0195 | F/A PCT, MEAS -15.9

FILTER DATA

POSITION	FILTER NUMBER	SAMPLE VOL. STD.CU.FEET	AVG. SAMPLE SYS. TEMP DEG F	WEIGHT GAIN MILLIGRAMS	MG/SCF OF SAMPLE
1	P47-9&10	20.770	71.	5.925	.285
2	P47-11&12	20.642	71.	5.921	.287

PARTICULATE RESULTS

AVG. SAMPLE ZONE TEMP, DEG F 124. DILUTION FACTOR 7.392
SPLIT EXHAUST VOL,SCF (SCM), LB/MIN 1000.4 (28.33) , 2.51

PARTICULATE CONCENTRATION IN EXHAUST

FILTER	CONCENTRATION, MG/SCF (MG/SCM)	CONCENTRATION MULTIPLIER	G/HR	G/HP-HR
P47-9&10	2.109 (74.455)	.3559	73.556	.494
P47-11&12	2.120 (74.866)	.3581	73.962	.496

EMISSION RESULTS

	G/HR	G/HP-HR	CONC.
HC	126.259	.847	189. PPMC
CO	126.891	.852	97. PPM
NOX	2375.859	15.945	1113. PPM
NOX,CORR	2120.927	14.234	
CO2		441.	4.14 PCT
O2			14.55 PCT

NOX CORRECTION FACTOR .8927 WET CORRECTION FACTOR .9639

GASEOUS and/or PARTICULATE EMISSIONS
NOTCH 7
PROJECT 03-2681-809 PROGRAM = EMD16B

TEST NO. RUN NO. 2
ENGINE MODEL EMD 2-567B
TEST CELL LOCO LAB
HCR 1.758
BLOWER COUNTS 47646.
OBS. POWER,BHP 178.0

TEST DATE 1/31/91
DIESEL DF-2
TUNNEL NO. 26
SAMPLE TIME 20x20 .00 MIN.
BLOWER TEMP. DEG. F 66.
FUEL FLOW,LB/MIN 1.21

BAROMETER 29.63 IN.HG.
HUMIDITY 24.93 GRAINS H2O/LB. AIR
LFE NO. 15 ENG. LFE NO. 0
SAMPLE TIME 47mm 30.00 MIN.
MEAS. EXH. FLOW,LB/MIN 49.79
AIR FLOW,LB/MIN 48.58

LFE INFORMATION			BLOWER INFORMATION		OTHER
INLET TEMP DEG. F	INLET PRESS. IN. H20	DIFF. PRESS. IN. H20	INLET PRESS. IN. H20	DIFF. PRESS. IN. H20	TUNNEL TEMP DEG. F
72.	.55	4.100	11.00	15.00	121.
72.	.55	4.100	11.00	15.00	122.
71.	.55	4.100	11.00	15.00	122.
71.	.55	4.050	11.00	15.00	121.
71.	.54	4.000	11.00	15.00	122.
71.	.55	4.100	11.00	15.00	122.
71.	.56	4.050	11.00	15.00	122.
AVERAGE 71.	.55	4.071	11.00	15.00	122.

LFE VOL, SCF 6404.7 LFE MASS,LB. 481.2 BLOWER + 47mm VOL, SCF 7408.1 BLOWER + 47mm MASS,LB 556.6
LFE FLOW SCFM 213.50 LFE FLOW LB/MIN 16.04 BLOWER + 47mm FLOW SCFM 246.95 BLOWER + 47mm FLOW LB/MIN 18.56
F/A DRY, MEAS .0250 F/A CALC .0230 F/A PCT, MEAS -7.8

FILTER DATA

POSITION	FILTER NUMBER	SAMPLE VOL. STD.CU.FEET	AVG. SAMPLE SYS. TEMP DEG F	WEIGHT GAIN MILLIGRAMS	MG/SCF OF SAMPLE
1	P47-5&6	20.767	68.	6.432	.310
2	P47-7&8	20.757	68.	6.474	.312

PARTICULATE RESULTS

AVG. SAMPLE ZONE TEMP, DEG F 122. DILUTION FACTOR 7.383
SPLIT EXHAUST VOL,SCF (SCM), LB/MIN 1003.4 (28.42) , 2.51

PARTICULATE CONCENTRATION IN EXHAUST

FILTER	CONCENTRATION, MG/SCF (MG/SCM)	CONCENTRATION MULTIPLIER	G/HR	G/HP-HR
P47-5&6	2.287 (80.747)	.3555	90.915	.511
P47-7&8	2.303 (81.313)	.3557	91.552	.514

EMISSION RESULTS

	G/HR	G/HP-HR	CONC.
HC	140.413	.789	202. PPMC
CO	254.211	1.428	188. PPM
NOX	2753.695	15.470	1248. PPM
NOX,CORR	2360.537	13.261	
CO2		452.	4.90 PCT
O2			13.79 PCT

NOX CORRECTION FACTOR .8572 WET CORRECTION FACTOR .9576

GASEOUS and/or PARTICULATE EMISSIONS
NOTCH 8
PROJECT 03-2681-809 PROGRAM = EMD16B

TEST NO. RUN NO. 1
ENGINE MODEL EMD 2-567B
TEST CELL LOCO LAB
HCR 1.758
BLOWER COUNTS 47673.
OBS. POWER,BHP 206.8

TEST DATE 1/31/91
DIESEL DF-2
TUNNEL NO. 26
SAMPLE TIME 20x20 .00 MIN.
BLOWER TEMP. DEG. F 67.
FUEL FLOW,LB/MIN 1.45

BAROMETER 29.62 IN.HG.
HUMIDITY 29.21 GRAINS H2O/LB. AIR
LFE NO. 15 ENG. LFE NO. 0
SAMPLE TIME 47mm 30.00 MIN.
MEAS. EXH. FLOW,LB/MIN 55.92
AIR FLOW,LB/MIN 54.47

LFE INFORMATION			BLOWER INFORMATION		OTHER
INLET TEMP DEG. F	INLET PRESS. IN. H2O	DIFF. PRESS. IN. H2O	INLET PRESS. IN. H2O	DIFF. PRESS. IN. H2O	TUNNEL TEMP DEG. F
71.	.65	3.950	11.00	15.00	122.
72.	.65	3.980	11.00	15.00	124.
72.	.65	3.950	11.00	15.00	124.
72.	.65	3.950	11.00	15.00	124.
72.	.67	4.000	11.00	15.00	124.
73.	.66	4.000	11.00	15.00	123.
73.	.65	3.990	11.00	15.00	123.
AVERAGE 72.	.65	3.974	11.00	15.00	123.

LFE VOL, SCF 6237.2 LFE MASS,LB. 468.7
LFE FLOW SCFM 207.91 LFE FLOW LB/MIN 15.62
F/A DRY, MEAS .0267 F/A CALC .0266

BLOWER + 47mm VOL, SCF 7394.7 BLOWER + 47mm MASS,LB 555.6
BLOWER + 47mm FLOW SCFM 246.49 BLOWER + 47mm FLOW LB/MIN 18.52
F/A PCT, MEAS -.6

FILTER DATA

POSITION	FILTER NUMBER	SAMPLE VOL. STD.CU.FEET	AVG. SAMPLE SYS. TEMP DEG F	WEIGHT GAIN MILLIGRAMS	MG/SCF OF SAMPLE
1	P47-1&2	20.444	63.	6.306	.308
2	P47-3&4	20.424	63.	6.473	.317

PARTICULATE RESULTS

AVG. SAMPLE ZONE TEMP, DEG F 123. DILUTION FACTOR 6.389
SPLIT EXHAUST VOL,SCF (SCM), LB/MIN 1157.5 (32.78) , 2.90

PARTICULATE CONCENTRATION IN EXHAUST

FILTER	CONCENTRATION, MG/SCF (MG/SCM)	CONCENTRATION MULTIPLIER	G/HR	G/HP-HR
P47-1&2	1.971 (69.581)	.3125	87.991	.425
P47-3&4	2.025 (71.493)	.3128	90.410	.437

EMISSION RESULTS

	G/HR	G/HP-HR	CONC.
HC	157.423	.761	217. PPMC
CO	531.231	2.569	379. PPM
NOX	3163.238	15.296	1383. PPM
NOX,CORR	2743.229	13.265	
CO2		466.	5.66 PCT
O2			12.79 PCT

NOX CORRECTION FACTOR .8672 WET CORRECTION FACTOR .9511

APPENDIX B

GASEOUS and/or PARTICULATE EMISSIONS

IDLE

PROJECT 03-2681-809 PROGRAM = EMD16B

TEST NO. RUN NO. 9
ENGINE MODEL EMD 2-567B
TEST CELL LOCO LAB
HCR 1.656
BLOWER COUNTS 47620.
OBS. POWER,BHP .0

TEST DATE 2/ 4/91
DIESEL COAL LIQU
TUNNEL NO. 26
SAMPLE TIME 20x20 .00 MIN.
BLOWER TEMP. DEG. F 73.
FUEL FLOW,LB/MIN .09

BAROMETER 29.26 IN.HG.
HUMIDITY 61.20 GRAINS H2O/LB. AIR
LFE NO. 15 ENG. LFE NO. 0
SAMPLE TIME 47mm 30.00 MIN.
MEAS. EXH. FLOW,LB/MIN 16.54
AIR FLOW,LB/MIN 16.45

LFE INFORMATION			BLOWER INFORMATION		OTHER
INLET TEMP DEG. F	INLET PRESS. IN. H2O	DIFF. PRESS. IN. H2O	INLET PRESS. IN. H2O	DIFF. PRESS. IN. H2O	TUNNEL TEMP DEG. F
81.	.60	4.600	10.00	14.00	106.
81.	.60	4.620	10.00	14.00	105.
80.	.60	4.600	10.00	14.00	105.
80.	.60	4.600	10.00	14.00	105.
80.	.60	4.600	10.00	14.00	104.
80.	.60	4.600	10.00	14.00	104.
80.	.60	4.600	10.00	14.00	104.
AVERAGE 80.	.60	4.603	10.00	14.00	105.

LFE VOL, SCF 6902.3 LFE MASS,LB. 518.6
LFE FLOW SCFM 230.08 LFE FLOW LB/MIN 17.29
F/A DRY, MEAS .0057 F/A CALC .0043

BLOWER + 47mm VOL, SCF 7248.5 BLOWER + 47mm MASS,LB 544.6
BLOWER + 47mm FLOW SCFM 241.62 BLOWER + 47mm FLOW LB/MIN 18.15
F/A PCT, MEAS -21.7

FILTER DATA

POSITION	FILTER NUMBER	SAMPLE VOL. STD.CU.FEET	AVG. SAMPLE SYS. TEMP DEG F	WEIGHT GAIN MILLIGRAMS	MG/SCF OF SAMPLE
1	P90-69&70	22.559	68.	5.324	.236
2	P90-71&72	22.549	68.	5.169	.229

PARTICULATE RESULTS

AVG. SAMPLE ZONE TEMP, DEG F 105. DILUTION FACTOR 20.937
SPLIT EXHAUST VOL,SCF (SCM), LB/MIN 346.2 (9.80) , .87

PARTICULATE CONCENTRATION IN EXHAUST

FILTER	CONCENTRATION, MG/SCF (MG/SCM)	CONCENTRATION MULTIPLIER	G/HR	G/HP-HR
P90-69&70	4.941 (174.477)	.9281	65.274	.000
P90-71&72	4.800 (169.471)	.9285	63.401	.000

EMISSION RESULTS

	G/HR	G/HP-HR	CONC.
HC	43.968	.000	157. PPMC
CO	48.824	.000	86. PPM
NOX	112.095	.000	121. PPM
NOX,CORR	106.862	.000	
CO2		0.	.89 PCT
O2			19.20 PCT

NOX CORRECTION FACTOR .9533 WET CORRECTION FACTOR .9904

GASEOUS and/or PARTICULATE EMISSIONS

NOTCH 1

PROJECT 03-2681-809 PROGRAM = EMD16B

TEST NO. RUN NO. 8
ENGINE MODEL EMD 2-567B
TEST CELL LOCO LAB
HCR 1.656
BLOWER COUNTS 45450.
OBS. POWER,BHP 8.3

TEST DATE 2/ 4/91
DIESEL COAL LIQU
TUNNEL NO. 26
SAMPLE TIME 20x20 .00 MIN.
BLOWER TEMP. DEG. F 75.
FUEL FLOW,LB/MIN .13

BAROMETER 29.25 IN.HG.
HUMIDITY 116.95 GRAINS H2O/LB. AIR
LFE NO. 15 ENG. LFE NO. 0
SAMPLE TIME 47mm 28.63 MIN.
MEAS. EXH. FLOW,LB/MIN 16.00
AIR FLOW,LB/MIN 15.87

LFE INFORMATION			BLOWER INFORMATION		OTHER
INLET TEMP DEG. F	INLET PRESS. IN. H20	DIFF. PRESS. IN. H20	INLET PRESS. IN. H20	DIFF. PRESS. IN. H20	TUNNEL TEMP DEG. F
82.	.60	4.800	10.00	14.00	112.
82.	.60	4.800	10.00	14.00	112.
83.	.60	4.800	10.00	14.00	111.
82.	.60	4.800	10.00	14.00	111.
82.	.60	4.800	10.00	14.00	111.
82.	.60	4.800	10.00	14.00	111.
82.	.60	4.800	10.00	14.00	111.
AVERAGE 82.	.60	4.800	10.00	14.00	111.

LFE VOL, SCF 6811.1 LFE MASS,LB. 511.8
LFE FLOW SCFM 237.90 LFE FLOW LB/MIN 17.88
F/A DRY, MEAS .0086 F/A CALC .0068

BLOWER + 47mm VOL, SCF 6885.9 BLOWER + 47mm MASS,LB 517.4
BLOWER + 47mm FLOW SCFM 240.51 BLOWER + 47mm FLOW LB/MIN 18.07
F/A PCT, MEAS -21.2

FILTER DATA

POSITION	FILTER NUMBER	SAMPLE VOL. STD.CU.FEET	AVG. SAMPLE SYS. TEMP DEG F	WEIGHT GAIN MILLIGRAMS	MG/SCF OF SAMPLE
1	P90-65&66	19.964	70.	8.271	.414
2	P90-67&68	19.964	70.	7.930	.397

PARTICULATE RESULTS

AVG. SAMPLE ZONE TEMP, DEG F 111. DILUTION FACTOR ******
SPLIT EXHAUST VOL,SCF (SCM), LB/MIN **** (****) , ***

PARTICULATE CONCENTRATION IN EXHAUST

FILTER	CONCENTRATION, MG/SCF (MG/SCM)	CONCENTRATION MULTIPLIER	G/HR	G/HP-HR
P90-65&66	****** (*******)	******	*******	******
P90-67&68	****** (*******)	******	*******	******

EMISSION RESULTS

	G/HR	G/HP-HR	CONC.
HC	43.466	5.261	169. PPMC
CO	54.393	6.583	105. PPM
NOX	164.835	19.951	195. PPM
NOX,CORR	191.510	23.180	
CO2		1074.	1.41 PCT
O2			18.57 PCT

NOX CORRECTION FACTOR 1.1618 WET CORRECTION FACTOR .9841

GASEOUS and/or PARTICULATE EMISSIONS
NOTCH 2
PROJECT 03-2681-809 PROGRAM = EMD16B

TEST NO. RUN NO. 7
ENGINE MODEL EMD 2-567
TEST CELL LOCO LAB
HCR 1.656
BLOWER COUNTS 44781.
OBS. POWER,BHP 19.3

TEST DATE 2/ 4/91
DIESEL COAL LIQU
TUNNEL NO. 26
SAMPLE TIME 20x20 .00 MIN.
BLOWER TEMP. DEG. F 78.
FUEL FLOW,LB/MIN .20

BAROMETER 29.24 IN.HG.
HUMIDITY 73.16 GRAINS H2O/LB. AIR
LFE NO. 15 ENG. LFE NO. 0
SAMPLE TIME 47mm 28.20 MIN.
MEAS. EXH. FLOW,LB/MIN 21.37
AIR FLOW,LB/MIN 21.17

LFE INFORMATION			BLOWER INFORMATION		OTHER
INLET TEMP DEG. F	INLET PRESS. IN. H20	DIFF. PRESS. IN. H20	INLET PRESS. IN. H20	DIFF. PRESS. IN. H20	TUNNEL TEMP DEG. F
84.	.55	4.480	10.00	14.00	123.
84.	.55	4.500	10.00	14.00	123.
84.	.55	4.470	10.00	14.00	123.
83.	.55	4.430	10.00	14.00	123.
83.	.55	4.430	10.00	14.00	123.
84.	.55	4.460	10.00	14.00	123.
83.	.55	4.480	10.00	14.00	123.
AVERAGE 84.	.55	4.464	10.00	14.00	123.

LFE VOL, SCF 6232.3 LFE MASS,LB. 468.3
LFE FLOW SCFM 220.98 LFE FLOW LB/MIN 16.60
F/A DRY, MEAS .0097 F/A CALC .0080

BLOWER + 47mm VOL, SCF 6744.0 BLOWER + 47mm MASS,LB 506.7
BLOWER + 47mm FLOW SCFM 239.12 BLOWER + 47mm FLOW LB/MIN 17.97
F/A PCT, MEAS -17.6

FILTER DATA

POSITION	FILTER NUMBER	SAMPLE VOL. STD.CU.FEET	AVG. SAMPLE SYS. TEMP DEG F	WEIGHT GAIN MILLIGRAMS	MG/SCF OF SAMPLE
1	P90-61&62	20.084	70.	6.978	.347
2	P90-63&64	20.074	70.	6.768	.337

PARTICULATE RESULTS

AVG. SAMPLE ZONE TEMP, DEG F 123. DILUTION FACTOR 13.181
SPLIT EXHAUST VOL,SCF (SCM), LB/MIN 511.7 (14.49) , 1.36

PARTICULATE CONCENTRATION IN EXHAUST

FILTER	CONCENTRATION, MG/SCF (MG/SCM)	CONCENTRATION MULTIPLIER	G/HR	G/HP-HR
P90-61&62	4.580 (161.704)	.6563	78.154	4.045
P90-63&64	4.444 (156.914)	.6566	75.839	3.925

EMISSION RESULTS

	G/HR	G/HP-HR	CONC.
HC	52.801	2.733	160. PPMC
CO	64.435	3.335	97. PPM
NOX	312.182	16.158	288. PPM
NOX,CORR	308.971	15.991	
CO2		697.	1.67 PCT
O2			18.07 PCT

NOX CORRECTION FACTOR .9897 WET CORRECTION FACTOR .9835

GASEOUS and/or PARTICULATE EMISSIONS

NOTCH 3

PROJECT 03-2681-809 PROGRAM = EMD16B

TEST NO. RUN NO. 6	TEST DATE 2/ 4/91	BAROMETER 29.24 IN.HG.
ENGINE MODEL EMD 2-567B	DIESEL COAL LIQU	HUMIDITY 82.18 GRAINS H2O/LB. AIR
TEST CELL LOCO LAB	TUNNEL NO. 26	LFE NO. 15 ENG. LFE NO. 0
ECR 1.656	SAMPLE TIME 20x20 .00 MIN.	SAMPLE TIME 47mm 30.00 MIN.
BLOWER COUNTS 47621.	BLOWER TEMP. DEG. F 78.	MEAS. EXH. FLOW,LB/MIN 27.83
OBS. POWER,BHP 46.6	FUEL FLOW,LB/MIN .35	AIR FLOW,LB/MIN 27.48

	LFE INFORMATION			BLOWER INFORMATION		OTHER
	INLET TEMP DEG. F	INLET PRESS. IN. H20	DIFF. PRESS. IN. H20	INLET PRESS. IN. H20	DIFF. PRESS. IN. H20	TUNNEL TEMP DEG. F
	85.	.65	4.330	11.00	15.00	122.
	84.	.65	4.330	11.00	15.00	122.
	84.	.65	4.330	11.00	15.00	122.
	84.	.65	4.310	11.00	15.00	122.
	85.	.65	4.320	11.00	15.00	122.
	85.	.65	4.330	11.00	15.00	122.
	85.	.65	4.330	11.00	15.00	122.
AVERAGE	85.	.65	4.326	11.00	15.00	122.

LFE VOL, SCF 6410.6	LFE MASS,LB. 481.7	BLOWER + 47mm VOL, SCF 7133.7	BLOWER + 47mm MASS,LB 536.0
LFE FLOW SCFM 213.69	LFE FLOW LB/MIN 16.06	BLOWER + 47mm FLOW SCFM 237.79	BLOWER + 47mm FLOW LB/MIN 17.87
F/A DRY, MEAS .0130	F/A CALC .0113	F/A PCT, MEAS -13.6	

FILTER DATA

POSITION	FILTER NUMBER	SAMPLE VOL. STD.CU.FEET	AVG. SAMPLE SYS. TEMP DEG F	WEIGHT GAIN MILLIGRAMS	MG/SCF OF SAMPLE
1	P90-57&58	21.520	71.	4.065	.189
2	P90-59&60	21.550	71.	3.917	.182

PARTICULATE RESULTS

AVG. SAMPLE ZONE TEMP, DEG F 122. DILUTION FACTOR 9.866

SPLIT EXHAUST VOL,SCF (SCM), LB/MIN 723.1 (20.48) , 1.81

PARTICULATE CONCENTRATION IN EXHAUST

FILTER	CONCENTRATION, MG/SCF (MG/SCM)	CONCENTRATION MULTIPLIER	G/HR	G/HP-HR
P90-57&58	1.864 (65.802)	.4584	41.419	.890
P90-59&60	1.793 (63.320)	.4578	39.857	.856

EMISSION RESULTS

	G/HR	G/HP-HR	CONC.
HC	58.130	1.249	142. PPMC
CO	55.678	1.196	68. PPM
NOX	557.158	11.967	417. PPM
NOX,CORR	568.159	12.203	
CO2		510.	2.39 PCT
O2			17.19 PCT

NOX CORRECTION FACTOR 1.0197 WET CORRECTION FACTOR .9772

GASEOUS and/or PARTICULATE EMISSIONS
NOTCH 4
PROJECT 03-2681-809 PROGRAM = EMD16B

TEST NO. RUN NO. 5
ENGINE MODEL EMD 2-567B
TEST CELL LOCO LAB
HCR 1.656
BLOWER COUNTS 25849.
OBS. POWER,BHP 77.9

TEST DATE 2/ 4/91
DIESEL COAL LIQU
TUNNEL NO. 26
SAMPLE TIME 20x20 .00 MIN.
BLOWER TEMP. DEG. F 78.
FUEL FLOW,LB/MIN .55

BAROMETER 29.24 IN.HG.
HUMIDITY 78.45 GRAINS H2O/LB. AIR
LFE NO. 15 ENG. LFE NO. 0
SAMPLE TIME 47mm 16.29 MIN.
MEAS. EXH. FLOW,LB/MIN 34.42
AIR FLOW,LB/MIN 33.87

LFE INFORMATION			BLOWER INFORMATION		OTHER
INLET TEMP DEG. F	INLET PRESS. IN. H20	DIFF. PRESS. IN. H20	INLET PRESS. IN. H20	DIFF. PRESS. IN. H20	TUNNEL TEMP DEG. F
85.	.67	4.090	11.00	15.00	123.
85.	.67	4.090	11.00	15.00	124.
85.	.67	4.100	11.00	15.00	123.
85.	.67	4.100	11.00	15.00	123.
84.	.67	4.100	11.00	15.00	123.
AVERAGE 85.	.67	4.096	11.00	15.00	123.

LFE VOL, SCF 3300.8 LFE MASS,LB. 248.0 BLOWER + 47mm VOL, SCF 3872.7 BLOWER + 47mm MASS,LB 291.0
LFE FLOW SCFM 202.67 LFE FLOW LB/MIN 15.23 BLOWER + 47mm FLOW SCFM 237.79 BLOWER + 47mm FLOW LB/MIN 17.87
F/A DRY, MEAS .0165 F/A CALC .0142 F/A PCT, MEAS -13.7

FILTER DATA

POSITION	FILTER NUMBER	SAMPLE VOL. STD.CU.FEET	AVG. SAMPLE SYS. TEMP DEG F	WEIGHT GAIN MILLIGRAMS	MG/SCF OF SAMPLE
1	P90-53&54	12.006	71.	2.491	.207
2	P90-55&66	11.958	71.	2.451	.205

PARTICULATE RESULTS

AVG. SAMPLE ZONE TEMP, DEG F 123. DILUTION FACTOR 6.772
SPLIT EXHAUST VOL,SCF (SCM), LB/MIN 571.9 (16.20) , 2.64

PARTICULATE CONCENTRATION IN EXHAUST

FILTER	CONCENTRATION, MG/SCF (MG/SCM)	CONCENTRATION MULTIPLIER	G/HR	G/HP-HR
P90-53&54	1.405 (49.609)	.5640	38.617	.496
P90-55&66	1.388 (49.010)	.5663	38.151	.490

EMISSION RESULTS

	G/HR	G/HP-HR	CONC.
HC	73.457	.943	145. PPMC
CO	64.526	.829	64. PPM
NOX	973.960	12.509	592. PPM
NOX,CORR	984.411	12.644	
CO2		476.	3.03 PCT
O2			16.18 PCT

NOX CORRECTION FACTOR 1.0107 WET CORRECTION FACTOR .9724

GASEOUS and/or PARTICULATE EMISSIONS
NOTCH 5
PROJECT 03-2681-809 PROGRAM = EMD16B

TEST NO. RUN NO. 4
ENGINE MODEL EMD 2-567B
TEST CELL LOCO LAB
HCR 1.656
BLOWER COUNTS 39095.
OBS. POWER,BHP 114.7

TEST DATE 2/ 4/91
DIESEL COAL LIQU
TUNNEL NO. 26
SAMPLE TIME 20x20 .00 MIN.
BLOWER TEMP. DEG. F 78.
FUEL FLOW,LB/MIN .77

BAROMETER 29.26 IN.HG.
HUMIDITY 78.38 GRAINS H2O/LB. AIR
LFE NO. 15 ENG. LFE NO. 0
SAMPLE TIME 47mm 24.63 MIN.
MEAS. EXH. FLOW,LB/MIN 39.57
AIR FLOW,LB/MIN 38.80

LFE INFORMATION			BLOWER INFORMATION		OTHER
INLET TEMP DEG. F	INLET PRESS. IN. H20	DIFF. PRESS. IN. H20	INLET PRESS. IN. H20	DIFF. PRESS. IN. H20	TUNNEL TEMP DEG. F
84.	.70	4.110	11.00	15.00	122.
83.	.70	4.130	11.00	15.00	122.
81.	.70	4.100	11.00	15.00	121.
82.	.70	4.100	11.00	15.00	122.
84.	.70	4.130	11.00	15.00	123.
85.	.70	4.180	11.00	15.00	123.
AVERAGE 83.	.70	4.125	11.00	15.00	122.

LFE VOL, SCF 5055.7 LFE MASS,LB. 379.9
LFE FLOW SCFM 205.25 LFE FLOW LB/MIN 15.42
F/A DRY, MEAS .0201 F/A CALC .0182

BLOWER + 47mm VOL, SCF 5862.2 BLOWER + 47mm MASS,LB 440.5
BLOWER + 47mm FLOW SCFM 238.00 BLOWER + 47mm FLOW LB/MIN 17.88
F/A PCT, MEAS -9.8

FILTER DATA

POSITION	FILTER NUMBER	SAMPLE VOL. STD.CU.FEET	AVG. SAMPLE SYS. TEMP DEG F	WEIGHT GAIN MILLIGRAMS	MG/SCF OF SAMPLE
1	P90-49&50	18.432	66.	4.235	.230
2	P90-51&52	18.471	66.	4.131	.224

PARTICULATE RESULTS

AVG. SAMPLE ZONE TEMP, DEG F 122. DILUTION FACTOR 7.269
SPLIT EXHAUST VOL,SCF (SCM), LB/MIN 806.5 (22.84) , 2.46

PARTICULATE CONCENTRATION IN EXHAUST FILTER	CONCENTRATION, MG/SCF (MG/SCM)	CONCENTRATION MULTIPLIER	G/HR	G/HP-HR
P90-49&50	1.670 (58.971)	.3944	52.773	.460
P90-51&52	1.626 (57.400)	.3935	51.367	.448

EMISSION RESULTS

	G/HR	G/HP-HR	CONC.
HC	94.162	.821	169. PPMC
CO	103.507	.902	94. PPM
NOX	1563.241	13.630	870. PPM
NOX,CORR	1583.536	13.807	
CO2		452.	3.88 PCT
O2			15.05 PCT

NOX CORRECTION FACTOR 1.0130 WET CORRECTION FACTOR .9656

GASEOUS and/or PARTICULATE EMISSIONS
NOTCH 6
PROJECT 03-2681-809 PROGRAM = EMD16B

TEST NO. RUN NO. 3 | TEST DATE 2/ 4/91 | BAROMETER 29.28 IN.HG.
ENGINE MODEL EMD 2-567B | DIESEL COAL LIQU | HUMIDITY 82.46 GRAINS H2O/LB. AIR
TEST CELL LOCO LAB | TUNNEL NO. 26 | LFE NO. 15 ENG. LFE NO. 0
HCR 1.656 | SAMPLE TIME 20x20 .00 MIN. | SAMPLE TIME 47mm 30.00 MIN.
BLOWER COUNTS 47647. | BLOWER TEMP. DEG. F 78. | MEAS. EXH. FLOW,LB/MIN 47.21
OBS. POWER,BHP 148.6 | FUEL FLOW,LB/MIN 1.01 | AIR FLOW,LB/MIN 46.20

LFE INFORMATION			BLOWER INFORMATION		OTHER
INLET TEMP DEG. F	INLET PRESS. IN. H20	DIFF. PRESS. IN. H20	INLET PRESS. IN. H20	DIFF. PRESS. IN. H20	TUNNEL TEMP DEG. F
89.	.75	4.200	11.00	15.00	121.
90.	.75	4.200	11.00	15.00	122.
89.	.75	4.180	11.00	15.00	122.
89.	.75	4.180	11.00	15.00	122.
89.	.75	4.200	11.00	15.00	122.
89.	.75	4.190	11.00	15.00	122.
89.	.75	4.200	11.00	15.00	122.
AVERAGE 89.	.75	4.193	11.00	15.00	122.

LFE VOL, SCF 6138.2 | LFE MASS,LB. 461.2 | BLOWER + 47mm VOL, SCF 7150.3 | BLOWER + 47mm MASS,LB 537.3
LFE FLOW SCFM 204.61 | LFE FLOW LB/MIN 15.37 | BLOWER + 47mm FLOW SCFM 238.34 | BLOWER + 47mm FLOW LB/MIN 17.91
F/A DRY, MEAS .0221 | F/A CALC .0219 | F/A PCT, MEAS -1.0

FILTER DATA

POSITION	FILTER NUMBER	SAMPLE VOL. STD.CU.FEET	AVG. SAMPLE SYS. TEMP DEG F	WEIGHT GAIN MILLIGRAMS	MG/SCF OF SAMPLE
1	P90-45&46	22.553	77.	4.878	.216
2	P90-47&48	22.611	77.	4.762	.211

PARTICULATE RESULTS

AVG. SAMPLE ZONE TEMP, DEG F 122. DILUTION FACTOR 7.065
SPLIT EXHAUST VOL,SCF (SCM), LB/MIN 1012.1 (28.66) , 2.54

PARTICULATE CONCENTRATION IN EXHAUST

FILTER	CONCENTRATION, MG/SCF (MG/SCM)	CONCENTRATION MULTIPLIER	G/HR	G/HP-HR
P90-45&46	1.528 (53.955)	.3132	57.604	.388
P90-47&48	1.488 (52.537)	.3124	56.090	.377

EMISSION RESULTS

	G/HR	G/HP-HR	CONC.
HC	120.731	.812	199. PPMC
CO	209.547	1.410	176. PPM
NOX	2139.056	14.390	1101. PPM
NOX,CORR	2209.823	14.866	
CO2		456.	4.69 PCT
O2			14.17 PCT

NOX CORRECTION FACTOR 1.0331 WET CORRECTION FACTOR .9588

GASEOUS and/or PARTICULATE EMISSIONS
NOTCH 7
PROJECT 03-2681-809 PROGRAM = EMD16B

TEST NO. RUN NO. 2	TEST DATE 2/ 4/91	BAROMETER 29.30 IN.HG.
ENGINE MODEL EMD 2-567B	DIESEL COAL LIQU	HUMIDITY 76.87 GRAINS H2O/LB. AIR
TEST CELL LOCO LAB	TUNNEL NO. 26	LFE NO. 15 ENG. LFE NO. 0
HCR 1.656	SAMPLE TIME 20x20 .00 MIN.	SAMPLE TIME 47mm 27.53 MIN.
BLOWER COUNTS 43728.	BLOWER TEMP. DEG. F 78.	MEAS. EXH. FLOW,LB/MIN 53.48
OBS. POWER,BHP 178.8	FUEL FLOW,LB/MIN 1.25	AIR FLOW,LB/MIN 52.23

LFE INFORMATION			BLOWER INFORMATION		OTHER
INLET TEMP DEG. F	INLET PRESS. IN. H20	DIFF. PRESS. IN. H20	INLET PRESS. IN. H20	DIFF. PRESS. IN. H20	TUNNEL TEMP DEG. F
89.	.75	4.150	11.00	15.00	123.
89.	.75	4.180	11.00	15.00	123.
89.	.75	4.200	11.00	15.00	123.
89.	.75	4.200	11.00	15.00	123.
89.	.75	4.200	11.00	15.00	123.
89.	.75	4.200	11.00	15.00	123.
89.	.75	4.200	11.00	15.00	123.
AVERAGE 89.	.75	4.190	11.00	15.00	123.

LFE VOL, SCF 5635.6	LFE MASS,LB. 423.5	BLOWER + 47mm VOL, SCF 6566.3	BLOWER + 47mm MASS,LB 493.4
LFE FLOW SCFM 204.71	LFE FLOW LB/MIN 15.38	BLOWER + 47mm FLOW SCFM 238.51	BLOWER + 47mm FLOW LB/MIN 17.92
F/A DRY, MEAS .0242	F/A CALC .0250	F/A PCT, MEAS 3.2	

FILTER DATA

POSITION	FILTER NUMBER	SAMPLE VOL. STD.CU.FEET	AVG. SAMPLE SYS. TEMP DEG F	WEIGHT GAIN MILLIGRAMS	MG/SCF OF SAMPLE
1	P90-41&42	20.356	77.	4.662	.229
2	P90-43&44	20.385	77.	4.551	.223

PARTICULATE RESULTS

AVG. SAMPLE ZONE TEMP, DEG F 123. DILUTION FACTOR 7.055
SPLIT EXHAUST VOL,SCF (SCM), LB/MIN 930.7 (26.36) , 2.54

PARTICULATE CONCENTRATION IN EXHAUST

FILTER	CONCENTRATION, MG/SCF (MG/SCM)	CONCENTRATION MULTIPLIER	G/HR	G/HP-HR
P90-41&42	1.616 (57.053)	.3466	69.002	.386
P90-43&44	1.575 (55.616)	.3461	67.263	.376

EMISSION RESULTS

	G/HR	G/HP-HR	CONC.
HC	159.730	.893	242. PPMC
CO	395.598	2.213	307. PPM
NOX	2546.390	14.243	1211. PPM
NOX,CORR	2585.356	14.461	
CO2		468.	5.35 PCT
O2			13.04 PCT
NOX CORRECTION FACTOR	1.0153	WET CORRECTION FACTOR	.9539

GASEOUS and/or PARTICULATE EMISSIONS
NOTCH 8
PROJECT 03-2681-809 PROGRAM = EMD16B

TEST NO. RUN NO. 1	TEST DATE 2/ 4/91	BAROMETER 29.29 IN.HG.
ENGINE MODEL EMD 2-567B	DIESEL COAL LIQU	HUMIDITY 87.52 GRAINS H2O/LB. AIR
TEST CELL LOCO LAB	TUNNEL NO. 26	LFE NO. 15 ENG. LFE NO. 0
HCR 1.656	SAMPLE TIME 20x20 .00 MIN.	SAMPLE TIME 47mm 20.20 MIN.
BLOWER COUNTS 32104.	BLOWER TEMP. DEG. F 78.	MEAS. EXH. FLOW,LB/MIN 60.01
OBS. POWER,BHP 206.3	FUEL FLOW,LB/MIN 1.51	AIR FLOW,LB/MIN 58.50

LFE INFORMATION			BLOWER INFORMATION		OTHER
INLET TEMP DEG. F	INLET PRESS. IN. H20	DIFF. PRESS. IN. H20	INLET PRESS. IN. H20	DIFF. PRESS. IN. H20	TUNNEL TEMP DEG. F
88.	.75	4.210	11.00	15.00	123.
89.	.75	4.210	11.00	15.00	122.
89.	.75	4.210	11.00	15.00	122.
89.	.75	4.220	11.00	15.00	122.
89.	.75	4.220	11.00	15.00	122.
AVERAGE 89.	.75	4.214	11.00	15.00	122.

LFE VOL, SCF 4159.7	LFE MASS,LB. 312.6	BLOWER + 47mm VOL, SCF 4819.4	BLOWER + 47mm MASS,LB 362.1
LFE FLOW SCFM 205.89	LFE FLOW LB/MIN 15.47	BLOWER + 47mm FLOW SCFM 238.54	BLOWER + 47mm FLOW LB/MIN 17.92
F/A DRY, MEAS .0261	F/A CALC .0300	F/A PCT, MEAS 15.0	

FILTER DATA

POSITION	FILTER NUMBER	SAMPLE VOL. STD.CU.FEET	AVG. SAMPLE SYS. TEMP DEG F	WEIGHT GAIN MILLIGRAMS	MG/SCF OF SAMPLE
1	P90-37&38	15.007	74.	3.124	.208
2	P90-39&40	15.027	74.	3.104	.207

PARTICULATE RESULTS

AVG. SAMPLE ZONE TEMP, DEG F 122. DILUTION FACTOR 7.305
SPLIT EXHAUST VOL,SCF (SCM), LB/MIN 659.7 (18.68) , 2.45

PARTICULATE CONCENTRATION IN EXHAUST

FILTER	CONCENTRATION, MG/SCF (MG/SCM)	CONCENTRATION MULTIPLIER	G/HR	G/HP-HR
P90-37&38	1.521 (53.698)	.4868	72.871	.353
P90-39&40	1.509 (53.285)	.4862	72.311	.351

EMISSION RESULTS

	G/HR	G/HP-HR	CONC.
HC	262.600	1.273	394. PPMC
CO	906.040	4.393	703. PPM
NOX	2778.177	13.469	1321. PPM
NOX,CORR	2893.962	14.030	
CO2		486.	6.41 PCT
O2			11.78 PCT
NOX CORRECTION FACTOR	1.0417	WET CORRECTION FACTOR	.9448

APPENDIX C

GASEOUS and/or PARTICULATE EMISSIONS
IDLE
PROJECT 03-2681-809 PROGRAM = EMD16B

TEST NO. RUN NO. 9
ENGINE MODEL EMD 2-567B
TEST CELL LOCO LAB
HCR 1.656
BLOWER COUNTS 26124.
OBS. POWER,BHP .0

TEST DATE 2/26/91
DIESEL COAL LIQU
TUNNEL NO. 26
SAMPLE TIME 20x20 .00 MIN.
BLOWER TEMP. DEG. F 63.
FUEL FLOW,LB/MIN .09

BAROMETER 29.41 IN.HG.
HUMIDITY 36.66 GRAINS H2O/LB. AIR
LFE NO. 15 ENG. LFE NO. 0
SAMPLE TIME 47mm 17.28 MIN.
MEAS. EXH. FLOW,LB/MIN 17.12
AIR FLOW,LB/MIN 17.03

LFE INFORMATION			BLOWER INFORMATION		OTHER
INLET TEMP DEG. F	INLET PRESS. IN. H20	DIFF. PRESS. IN. H20	INLET PRESS. IN. H20	DIFF. PRESS. IN. H20	TUNNEL TEMP DEG. F
77.	.55	4.470	10.00	14.00	101.
77.	.55	4.470	10.00	14.00	101.
76.	.55	4.470	10.00	14.00	101.
76.	.55	4.470	10.00	14.00	101.
76.	.55	4.470	10.00	14.00	101.
AVERAGE 76.	.55	4.470	10.00	14.00	101.

LFE VOL, SCF 3937.2 LFE MASS,LB. 295.8 BLOWER + 47mm VOL, SCF 4068.4 BLOWER + 47mm MASS,LB 305.7
LFE FLOW SCFM 227.81 LFE FLOW LB/MIN 17.12 BLOWER + 47mm FLOW SCFM 235.39 BLOWER + 47mm FLOW LB/MIN 17.69
F/A DRY, MEAS .0053 F/A CALC .0045 F/A PCT, MEAS -16.0

FILTER DATA

POSITION	FILTER NUMBER	SAMPLE VOL. STD.CU.FEET	AVG. SAMPLE SYS. TEMP DEG F	WEIGHT GAIN MILLIGRAMS	MG/SCF OF SAMPLE
1	P47-105&10	15.725	57.	2.811	.179
2	P47-107&10	15.795	57.	2.766	.175

PARTICULATE RESULTS

AVG. SAMPLE ZONE TEMP, DEG F 101. DILUTION FACTOR 31.019
SPLIT EXHAUST VOL,SCF (SCM), LB/MIN 131.2 (3.71) , .57

PARTICULATE CONCENTRATION IN EXHAUST

FILTER	CONCENTRATION, MG/SCF (MG/SCM)	CONCENTRATION MULTIPLIER	G/HR	G/HP-HR
P47-105&10	5.545 (195.801)	1.9727	75.808	.000
P47-107&10	5.432 (191.810)	1.9639	74.263	.000

EMISSION RESULTS

	G/HR	G/HP-HR	CONC.
HC	35.171	.000	135. PPMC
CO	55.477	.000	105. PPM
NOX	116.391	.000	135. PPM
NOX,CORR	107.717	.000	
CO2		0.	.93 PCT
O2			19.20 PCT

NOX CORRECTION FACTOR .9255 WET CORRECTION FACTOR .9908

GASEOUS and/or PARTICULATE EMISSIONS
NOTCH 1
PROJECT 03-2681-809 PROGRAM = EMD16B

TEST NO. RUN NO. 8
ENGINE MODEL EMD 2-567B
TEST CELL LOCO LAB
HCR 1.656
BLOWER COUNTS 40797.
OBS. POWER,BHP 8.1

TEST DATE 2/26/91
DIESEL COAL LIQU
TUNNEL NO. 26
SAMPLE TIME 20x20 .00 MIN.
BLOWER TEMP. DEG. F 65.
FUEL FLOW,LB/MIN .13

BAROMETER 29.40 IN.HG.
HUMIDITY 40.83 GRAINS H2O/LB. AIR
LFE NO. 15 ENG. LFE NO. 0
SAMPLE TIME 47mm 26.98 MIN.
MEAS. EXH. FLOW,LB/MIN 16.80
AIR FLOW,LB/MIN 16.67

LFE INFORMATION			BLOWER INFORMATION		OTHER
INLET TEMP DEG. F	INLET PRESS. IN. H20	DIFF. PRESS. IN. H20	INLET PRESS. IN. H20	DIFF. PRESS. IN. H20	TUNNEL TEMP DEG. F
80.	.60	4.650	10.00	14.00	108.
79.	.60	4.650	10.00	14.00	108.
79.	.60	4.650	10.00	14.00	108.
78.	.60	4.650	10.00	14.00	108.
78.	.60	4.650	10.00	14.00	107.
78.	.60	4.650	10.00	14.00	107.
AVERAGE 79.	.60	4.650	10.00	14.00	108.

LFE VOL, SCF 6332.1 LFE MASS,LB. 475.8 BLOWER + 47mm VOL, SCF 6322.6 BLOWER + 47mm MASS,LB 475.1
LFE FLOW SCFM 234.67 LFE FLOW LB/MIN 17.63 BLOWER + 47mm FLOW SCFM 234.32 BLOWER + 47mm FLOW LB/MIN 17.61
F/A DRY, MEAS .0079 F/A CALC .0066 F/A PCT, MEAS -16.9

FILTER DATA

POSITION	FILTER NUMBER	SAMPLE VOL. STD.CU.FEET	AVG. SAMPLE SYS. TEMP DEG F	WEIGHT GAIN MILLIGRAMS	MG/SCF OF SAMPLE
1	P47-101&10	22.707	59.	6.676	.294
2	P47-103&10	22.747	59.	6.508	.286

PARTICULATE RESULTS

AVG. SAMPLE ZONE TEMP, DEG F 108. DILUTION FACTOR ******
SPLIT EXHAUST VOL,SCF (SCM), LB/MIN **** (****) , ****

PARTICULATE CONCENTRATION IN EXHAUST

FILTER	CONCENTRATION, MG/SCF (MG/SCM)	CONCENTRATION MULTIPLIER	G/HR	G/HP-HR
P47-101&10	******* (*******)	*******	********	******
P47-103&10	******* (*******)	*******	********	******

EMISSION RESULTS

	G/HR	G/HP-HR	CONC.
HC	41.318	5.076	160. PPMC
CO	64.696	7.948	124. PPM
NOX	194.113	23.847	228. PPM
NOX,CORR	181.456	22.292	
CO2		1066.	1.37 PCT
O2			18.07 PCT

NOX CORRECTION FACTOR .9348 WET CORRECTION FACTOR .9871

GASEOUS and/or PARTICULATE EMISSIONS
NOTCH 2
PROJECT 03-2681-809 PROGRAM = EMD16B

TEST NO. RUN NO. 7
ENGINE MODEL EMD 2-567B
TEST CELL LOCO LAB
HCR 1.656
BLOWER COUNTS 41690.
OBS. POWER,BHP 19.0

TEST DATE 2/26/91
DIESEL COAL LIQU
TUNNEL NO. 26
SAMPLE TIME 20x20 .00 MIN.
BLOWER TEMP. DEG. F 68.
FUEL FLOW,LB/MIN .20

BAROMETER 29.40 IN.HG.
HUMIDITY 32.58 GRAINS H2O/LB. AIR
LFE NO. 15 ENG. LFE NO. 0
SAMPLE TIME 47mm 27.58 MIN.
MEAS. EXH. FLOW,LB/MIN 22.13
AIR FLOW,LB/MIN 21.93

LFE INFORMATION			BLOWER INFORMATION		OTHER
INLET TEMP DEG. F	INLET PRESS. IN. H20	DIFF. PRESS. IN. H20	INLET PRESS. IN. H20	DIFF. PRESS. IN. H20	TUNNEL TEMP DEG. F
82.	.50	4.250	10.00	14.00	120.
82.	.51	4.270	10.00	14.00	121.
81.	.51	4.270	10.00	14.00	121.
81.	.52	4.270	10.00	14.00	122.
81.	.52	4.270	10.00	14.00	122.
81.	.55	4.270	10.00	14.00	122.
81.	.55	4.270	10.00	14.00	121.
AVERAGE 81.	.52	4.267	10.00	14.00	121.

LFE VOL, SCF 5914.5 LFE MASS,LB. 444.4
LFE FLOW SCFM 214.42 LFE FLOW LB/MIN 16.11
F/A DRY, MEAS .0092 F/A CALC .0080

BLOWER + 47mm VOL, SCF 6422.9 BLOWER + 47mm MASS,LB 482.6
BLOWER + 47mm FLOW SCFM 232.85 BLOWER + 47mm FLOW LB/MIN 17.50
F/A PCT, MEAS -13.6

FILTER DATA

POSITION	FILTER NUMBER	SAMPLE VOL. STD.CU.FEET	AVG. SAMPLE SYS. TEMP DEG F	WEIGHT GAIN MILLIGRAMS	MG/SCF OF SAMPLE
1	P47-97&98	23.124	61.	6.306	.273
2	P47-99&100	23.263	61.	2.611	.112

PARTICULATE RESULTS

AVG. SAMPLE ZONE TEMP, DEG F 121. DILUTION FACTOR 12.635
SPLIT EXHAUST VOL,SCF (SCM), LB/MIN 508.4 (14.40) , 1.38

PARTICULATE CONCENTRATION IN EXHAUST

FILTER	CONCENTRATION, MG/SCF (MG/SCM)	CONCENTRATION MULTIPLIER	G/HR	G/HP-HR
P47-97&98	3.446 (121.662)	.5464	60.890	3.205
P47-99&100	1.418 (50.072)	.5431	25.060	1.319

EMISSION RESULTS

	G/HR	G/HP-HR	CONC.
HC	49.792	2.621	152. PPMC
CO	84.529	4.449	128. PPM
NOX	353.457	18.603	328. PPM
NOX,CORR	317.183	16.694	
CO2		705.	1.67 PCT
O2			17.82 PCT

NOX CORRECTION FACTOR .8974 WET CORRECTION FACTOR .9850

GASEOUS and/or PARTICULATE EMISSIONS

NOTCH 3

PROJECT 03-2681-809 PROGRAM = EMD16B

TEST NO. RUN NO. 6
ENGINE MODEL EMD 2-567B
TEST CELL LOCO LAB
HCR 1.656
BLOWER COUNTS 20970.
OBS. POWER,BHP 45.7

TEST DATE 2/26/91
DIESEL COAL LIQU
TUNNEL NO. 26
SAMPLE TIME 20x20 .00 MIN.
BLOWER TEMP. DEG. F 68.
FUEL FLOW,LB/MIN .35

BAROMETER 29.40 IN.HG.
HUMIDITY 27.65 GRAINS H2O/LB. AIR
LFE NO. 15 ENG. LFE NO. 0
SAMPLE TIME 47mm 13.87 MIN.
MEAS. EXH. FLOW,LB/MIN 28.58
AIR FLOW,LB/MIN 28.23

LFE INFORMATION			BLOWER INFORMATION		OTHER
INLET TEMP DEG. F	INLET PRESS. IN. H2O	DIFF. PRESS. IN. H2O	INLET PRESS. IN. H2O	DIFF. PRESS. IN. H2O	TUNNEL TEMP DEG. F
80.	.55	4.050	10.00	14.00	124.
81.	.55	4.050	10.00	14.00	124.
81.	.55	4.050	10.00	14.00	124.
81.	.55	4.050	10.00	14.00	124.
AVERAGE 81.	.55	4.050	10.00	14.00	124.

LFE VOL, SCF 2834.0 LFE MASS,LB. 212.9 BLOWER + 47mm VOL, SCF 3231.1 BLOWER + 47mm MASS,LB 242.8
LFE FLOW SCFM 204.32 LFE FLOW LB/MIN 15.35 BLOWER + 47mm FLOW SCFM 232.96 BLOWER + 47mm FLOW LB/MIN 17.50
F/A DRY, MEAS .0125 F/A CALC .0111 F/A PCT, MEAS -11.7

FILTER DATA

POSITION	FILTER NUMBER	SAMPLE VOL. STD.CU.FEET	AVG. SAMPLE SYS. TEMP DEG F	WEIGHT GAIN MILLIGRAMS	MG/SCF OF SAMPLE
1	P47-93&94	11.845	65.	2.879	.243
2	P47-95&96	11.815	65.	2.774	.235

PARTICULATE RESULTS

AVG. SAMPLE ZONE TEMP, DEG F 124. DILUTION FACTOR 8.136
SPLIT EXHAUST VOL,SCF (SCM), LB/MIN 397.1 (11.25) , 2.15

PARTICULATE CONCENTRATION IN EXHAUST

FILTER	CONCENTRATION, MG/SCF (MG/SCM)	CONCENTRATION MULTIPLIER	G/HR	G/HP-HR
P47-93&94	1.978 (69.826)	.6869	45.133	.988
P47-95&96	1.910 (67.448)	.6886	43.596	.954

EMISSION RESULTS

	G/HR	G/HP-HR	CONC.
HC	62.060	1.358	150. PPMC
CO	65.215	1.427	79. PPM
NOX	639.049	13.987	472. PPM
NOX,CORR	572.945	12.540	
CO2		516.	2.34 PCT
O2			17.06 PCT

NOX CORRECTION FACTOR .8966 WET CORRECTION FACTOR .9798

GASEOUS and/or PARTICULATE EMISSIONS

NOTCH 4

PROJECT 03-2681-809 PROGRAM = EMD16B

TEST NO. RUN NO. 5
ENGINE MODEL EMD 2-567B
TEST CELL LOCO LAB
HCR 1.656
BLOWER COUNTS 18634.
OBS. POWER,BHP 76.0

TEST DATE 2/26/91
DIESEL COAL LIQU
TUNNEL NO. 26
SAMPLE TIME 20x20 .00 MIN.
BLOWER TEMP. DEG. F 68.
FUEL FLOW,LB/MIN .54

BAROMETER 29.39 IN.HG.
HUMIDITY 24.39 GRAINS H2O/LB. AIR
LFE NO. 15 ENG. LFE NO. 0
SAMPLE TIME 47mm 12.33 MIN.
MEAS. EXH. FLOW,LB/MIN 34.79
AIR FLOW,LB/MIN 34.25

LFE INFORMATION			BLOWER INFORMATION		OTHER
INLET TEMP DEG. F	INLET PRESS. IN. H20	DIFF. PRESS. IN. H20	INLET PRESS. IN. H20	DIFF. PRESS. IN. H20	TUNNEL TEMP DEG. F
81.	.59	3.900	10.00	14.00	123.
82.	.60	3.900	10.00	14.00	123.
82.	.60	4.000	10.00	14.00	123.
82.	.60	3.980	10.00	14.00	123.
AVERAGE 82.	.60	3.945	10.00	14.00	123.

LFE VOL, SCF 2447.9 LFE MASS,LB. 183.9 BLOWER + 47mm VOL, SCF 2869.9 BLOWER + 47mm MASS,LB 215.6
LFE FLOW SCFM 198.51 LFE FLOW LB/MIN 14.92 BLOWER + 47mm FLOW SCFM 232.73 BLOWER + 47mm FLOW LB/MIN 17.49
F/A DRY, MEAS .0158 F/A CALC .0140 F/A PCT, MEAS -11.3

FILTER DATA

POSITION	FILTER NUMBER	SAMPLE VOL. STD.CU.FEET	AVG. SAMPLE SYS. TEMP DEG F	WEIGHT GAIN MILLIGRAMS	MG/SCF OF SAMPLE
1	P47-89&90	10.422	67.	2.446	.235
2	P47-91&92	10.540	67.	2.467	.234

PARTICULATE RESULTS

AVG. SAMPLE ZONE TEMP, DEG F 123. DILUTION FACTOR 6.800
SPLIT EXHAUST VOL,SCF (SCM), LB/MIN 422.0 (11.95) , 2.57

PARTICULATE CONCENTRATION IN EXHAUST

FILTER	CONCENTRATION, MG/SCF (MG/SCM)	CONCENTRATION MULTIPLIER	G/HR	G/HP-HR
P47-89&90	1.596 (56.355)	.6525	44.336	.583
P47-91&92	1.592 (56.201)	.6452	44.215	.582

EMISSION RESULTS

	G/HR	G/HP-HR	CONC.
HC	72.697	.957	145. PPMC
CO	64.024	.842	64. PPM
NOX	925.572	12.179	567. PPM
NOX,CORR	824.585	10.850	
CO2		476.	2.98 PCT
O2			16.18 PCT

NOX CORRECTION FACTOR .8909 WET CORRECTION FACTOR .9749

GASEOUS and/or PARTICULATE EMISSIONS

NOTCH 5

PROJECT 03-2681-809 PROGRAM = EMD16B

TEST NO. RUN NO. 4
ENGINE MODEL EMD 2-567B
TEST CELL LOCO LAB
HCR 1.656
BLOWER COUNTS 32237.
OBS. POWER,BHP 113.0

TEST DATE 2/26/91
DIESEL COAL LIQU
TUNNEL NO. 26
SAMPLE TIME 20x20 .00 MIN.
BLOWER TEMP. DEG. F 68.
FUEL FLOW,LB/MIN .76

BAROMETER 29.39 IN.HG.
HUMIDITY 22.80 GRAINS H2O/LB. AIR
LFE NO. 15 ENG. LFE NO. 0
SAMPLE TIME 47mm 21.33 MIN.
MEAS. EXH. FLOW,LB/MIN 40.96
AIR FLOW,LB/MIN 40.20

LFE INFORMATION			BLOWER INFORMATION		OTHER
INLET TEMP DEG. F	INLET PRESS. IN. H20	DIFF. PRESS. IN. H20	INLET PRESS. IN. H20	DIFF. PRESS. IN. H20	TUNNEL TEMP DEG. F
84.	.63	3.900	10.00	14.00	123.
83.	.63	3.920	10.00	14.00	123.
83.	.63	3.900	10.00	14.00	122.
83.	.63	3.900	10.00	14.00	122.
83.	.63	3.900	10.00	14.00	123.
83.	.63	3.900	10.00	14.00	123.
AVERAGE 83.	.63	3.903	10.00	14.00	123.

LFE VOL, SCF 4172.3 LFE MASS,LB. 313.5 BLOWER + 47mm VOL, SCF 4964.3 BLOWER + 47mm MASS,LB 373.0
LFE FLOW SCFM 195.58 LFE FLOW LB/MIN 14.70 BLOWER + 47mm FLOW SCFM 232.70 BLOWER + 47mm FLOW LB/MIN 17.49
F/A DRY, MEAS .0190 F/A CALC .0182 F/A PCT, MEAS -4.3

FILTER DATA

POSITION	FILTER NUMBER	SAMPLE VOL. STD.CU.FEET	AVG. SAMPLE SYS. TEMP DEG F	WEIGHT GAIN MILLIGRAMS	MG/SCF OF SAMPLE
1	P47-85&86	17.715	67.	3.532	.199
2	P47-87&88	17.764	67.	3.436	.193

PARTICULATE RESULTS

AVG. SAMPLE ZONE TEMP, DEG F 123. DILUTION FACTOR 6.269
SPLIT EXHAUST VOL,SCF (SCM), LB/MIN 791.9 (22.43) , 2.79

PARTICULATE CONCENTRATION IN EXHAUST

FILTER	CONCENTRATION, MG/SCF (MG/SCM)	CONCENTRATION MULTIPLIER	G/HR	G/HP-HR
P47-85&86	1.250 (44.132)	.3539	40.879	.362
P47-87&88	1.213 (42.814)	.3529	39.658	.351

EMISSION RESULTS

	G/HR	G/HP-HR	CONC.
HC	100.717	.891	184. PPMC
CO	75.901	.672	70. PPM
NOX	1732.197	15.329	979. PPM
NOX,CORR	1537.138	13.603	
CO2		452.	3.88 PCT
O2			14.93 PCT

NOX CORRECTION FACTOR .8874 WET CORRECTION FACTOR .9678

GASEOUS and/or PARTICULATE EMISSIONS
NOTCH 6
PROJECT 03-2681-809 PROGRAM = EMD16B

TEST NO. RUN NO. 3
ENGINE MODEL EMD 2-567B
TEST CELL LOCO LAB
HCR 1.656
BLOWER COUNTS 45358.
OBS. POWER,BHP 149.0

TEST DATE 2/26/91
DIESEL COAL LIQU
TUNNEL NO. 26
SAMPLE TIME 20x20 .00 MIN.
BLOWER TEMP. DEG. F 67.
FUEL FLOW,LB/MIN 1.00

BAROMETER 29.43 IN.HG.
HUMIDITY 25.10 GRAINS H2O/LB. AIR
LFE NO. 15 ENG. LFE NO. 0
SAMPLE TIME 47mm 30.00 MIN.
MEAS. EXH. FLOW,LB/MIN 48.47
AIR FLOW,LB/MIN 47.47

LFE INFORMATION			BLOWER INFORMATION		OTHER
INLET TEMP DEG. F	INLET PRESS. IN. H20	DIFF. PRESS. IN. H20	INLET PRESS. IN. H20	DIFF. PRESS. IN. H20	TUNNEL TEMP DEG. F
83.	.63	3.900	10.00	14.00	123.
83.	.65	3.930	10.00	14.00	123.
83.	.65	3.950	10.00	14.00	122.
83.	.65	3.950	10.00	14.00	122.
83.	.65	4.000	10.00	14.00	122.
83.	.65	4.000	10.00	14.00	122.
83.	.65	4.000	10.00	14.00	122.
AVERAGE 83.	.65	3.961	10.00	14.00	122.

LFE VOL, SCF 5961.8 LFE MASS,LB. 448.0
LFE FLOW SCFM 198.74 LFE FLOW LB/MIN 14.93
F/A DRY, MEAS .0212 F/A CALC .0212

BLOWER + 47mm VOL, SCF 7009.2 BLOWER + 47mm MASS,LB 526.7
BLOWER + 47mm FLOW SCFM 233.65 BLOWER + 47mm FLOW LB/MIN 17.56
F/A PCT, MEAS .0

FILTER DATA

POSITION	FILTER NUMBER	SAMPLE VOL. STD.CU.FEET	AVG. SAMPLE SYS. TEMP DEG F	WEIGHT GAIN MILLIGRAMS	MG/SCF OF SAMPLE
1	P47-81&82	25.102	66.	4.664	.186
2	P47-83&84	25.092	66.	4.569	.182

PARTICULATE RESULTS

AVG. SAMPLE ZONE TEMP, DEG F 122. DILUTION FACTOR 6.692
SPLIT EXHAUST VOL,SCF (SCM), LB/MIN 1047.4 (29.66) , 2.62

PARTICULATE CONCENTRATION IN EXHAUST

FILTER	CONCENTRATION, MG/SCF (MG/SCM)	CONCENTRATION MULTIPLIER	G/HR	G/HP-HR
P47-81&82	1.243 (43.904)	.2666	48.128	.323
P47-83&84	1.219 (43.027)	.2667	47.166	.317

EMISSION RESULTS

	G/HR	G/HP-HR	CONC.
HC	98.581	.662	159. PPMC
CO	141.681	.951	116. PPM
NOX	2584.987	17.349	1297. PPM
NOX,CORR	2313.237	15.525	
CO2		453.	4.55 PCT
O2			13.92 PCT

NOX CORRECTION FACTOR .8949 WET CORRECTION FACTOR .9625

GASEOUS and/or PARTICULATE EMISSIONS
NOTCH 7
PROJECT 03-2681-809 PROGRAM = EMD16B

TEST NO. RUN NO. 2
ENGINE MODEL EMD 2-567B
TEST CELL LOCO LAB
HCR 1.656
BLOWER COUNTS 45271.
OBS. POWER,BHP 179.0

TEST DATE 2/26/91
DIESEL COAL LIQU
TUNNEL NO. 26
SAMPLE TIME 20x20 .00 MIN.
BLOWER TEMP. DEG. F 70.
FUEL FLOW,LB/MIN 1.23

BAROMETER 29.47 IN.HG.
HUMIDITY 25.84 GRAINS H2O/LB. AIR
LFE NO. 15 ENG. LFE NO. 0
SAMPLE TIME 47mm 30.00 MIN.
MEAS. EXH. FLOW,LB/MIN 55.23
AIR FLOW,LB/MIN 54.00

	LFE INFORMATION			BLOWER INFORMATION		OTHER
	INLET TEMP DEG. F	INLET PRESS. IN. H20	DIFF. PRESS. IN. H20	INLET PRESS. IN. H20	DIFF. PRESS. IN. H20	TUNNEL TEMP DEG. F
	85.	.65	4.030	10.00	14.50	123.
	85.	.65	4.030	10.00	14.50	123.
	85.	.65	4.030	10.00	14.50	123.
	85.	.65	4.030	10.00	14.50	122.
	85.	.65	4.030	10.00	14.50	121.
	85.	.65	4.030	10.00	14.50	121.
	85.	.65	4.040	10.00	14.50	121.
AVERAGE	85.	.65	4.031	10.00	14.50	122.

LFE VOL, SCF 6032.0 LFE MASS,LB. 453.2
LFE FLOW SCFM 201.07 LFE FLOW LB/MIN 15.11
F/A DRY, MEAS .0230 F/A CALC .0250

BLOWER + 47mm VOL, SCF 6953.0 BLOWER + 47mm MASS,LB 522.4
BLOWER + 47mm FLOW SCFM 231.77 BLOWER + 47mm FLOW LB/MIN 17.41
F/A PCT, MEAS 8.7

FILTER DATA

POSITION	FILTER NUMBER	SAMPLE VOL. STD.CU.FEET	AVG. SAMPLE SYS. TEMP DEG F	WEIGHT GAIN MILLIGRAMS	MG/SCF OF SAMPLE
1	P47-77&78	24.548	69.	4.060	.165
2	P47-79&80	24.558	69.	4.636	.189

PARTICULATE RESULTS

AVG. SAMPLE ZONE TEMP, DEG F 122. DILUTION FACTOR 7.549
SPLIT EXHAUST VOL,SCF (SCM), LB/MIN 921.1 (26.08) , 2.31

PARTICULATE CONCENTRATION IN EXHAUST

FILTER	CONCENTRATION, MG/SCF (MG/SCM)	CONCENTRATION MULTIPLIER	G/HR	G/HP-HR
P47-77&78	1.249 (44.085)	.3075	55.066	.308
P47-79&80	1.425 (50.319)	.3074	62.853	.351

EMISSION RESULTS

	G/HR	G/HP-HR	CONC.
HC	193.318	1.080	297. PPMC
CO	234.398	1.309	184. PPM
NOX	2849.965	15.922	1371. PPM
NOX,CORR	2553.586	14.266	
CO2		462.	5.35 PCT
O2			12.66 PCT
NOX CORRECTION FACTOR		.8960	WET CORRECTION FACTOR .9562

GASEOUS and/or PARTICULATE EMISSIONS
NOTCH 8
PROJECT 03-2681-809 PROGRAM = EMD16B

TEST NO. RUN NO. 1
ENGINE MODEL EMD 2-567
TEST CELL LOCO LAB
ECR 1.656
BLOWER COUNTS 45375.
OBS. POWER,BHP 206.0

TEST DATE 2/26/91
DIESEL COAL LIQU
TUNNEL NO. 26
SAMPLE TIME 20x20 .00 MIN.
BLOWER TEMP. DEG. F 66.
FUEL FLOW,LB/MIN 1.48

BAROMETER 29.49 IN.HG.
HUMIDITY 35.93 GRAINS H2O/LB. AIR
LFE NO. 15 ENG. LFE NO. 0
SAMPLE TIME 47mm 30.00 MIN.
MEAS. EXH. FLOW,LB/MIN 62.06
AIR FLOW,LB/MIN 60.58

LFE INFORMATION			BLOWER INFORMATION		OTHER
INLET TEMP DEG. F	INLET PRESS. IN. H20	DIFF. PRESS. IN. H20	INLET PRESS. IN. H20	DIFF. PRESS. IN. H20	TUNNEL TEMP DEG. F
83.	.65	4.100	10.00	14.50	120.
83.	.65	4.100	10.00	14.50	120.
83.	.65	4.100	10.00	14.50	120.
83.	.65	4.100	10.00	14.50	120.
83.	.65	4.100	10.00	14.50	120.
83.	.65	4.100	10.00	14.50	120.
83.	.65	4.100	10.00	14.50	120.
AVERAGE 83.	.65	4.100	10.00	14.50	120.

LFE VOL, SCF 6173.8 LFE MASS,LB. 463.9
LFE FLOW SCFM 205.81 LFE FLOW LB/MIN 15.46
F/A DRY, MEAS .0246 F/A CALC .0294

BLOWER + 47mm VOL, SCF 7029.1 BLOWER + 47mm MASS,LB 528.2
BLOWER + 47mm FLOW SCFM 234.32 BLOWER + 47mm FLOW LB/MIN 17.61
F/A PCT, MEAS 19.3

FILTER DATA

POSITION	FILTER NUMBER	SAMPLE VOL. STD.CU.FEET	AVG. SAMPLE SYS. TEMP DEG F	WEIGHT GAIN MILLIGRAMS	MG/SCF OF SAMPLE
1	P47-73&74	24.048	65.	4.703	.196
2	P47-75&76	24.157	65.	5.429	.225

PARTICULATE RESULTS

AVG. SAMPLE ZONE TEMP, DEG F 120. DILUTION FACTOR 8.218
SPLIT EXHAUST VOL,SCF (SCM), LB/MIN 855.3 (24.22) , 2.14

PARTICULATE CONCENTRATION IN EXHAUST

FILTER	CONCENTRATION, MG/SCF (MG/SCM)	CONCENTRATION MULTIPLIER	G/HR	G/HP-HR
P47-73&74	1.607 (56.752)	.3418	79.653	.387
P47-75&76	1.847 (65.218)	.3402	91.535	.444

EMISSION RESULTS

	G/HR	G/HP-HR	CONC.
HC	226.359	1.099	339. PPMC
CO	287.697	1.397	222. PPM
NOX	2871.758	13.941	1358. PPM
NOX,CORR	2642.882	12.830	
CO2		483.	6.32 PCT
O2			7.98 PCT

NOX CORRECTION FACTOR .9203 WET CORRECTION FACTOR .9482

APPENDIX D

GASEOUS and/or PARTICULATE EMISSIONS
IDLE
PROJECT 03-2681-809 PROGRAM = EMD16B

TEST NO. RUN NO. 9
ENGINE MODEL EMD 2-567B
TEST CELL LOCO LAB
HCR 1.758
BLOWER COUNTS 45069.
OBS. POWER,BHP .0

TEST DATE 2/28/91
DIESEL DF-2
TUNNEL NO. 26
SAMPLE TIME 20x20 .00 MIN.
BLOWER TEMP. DEG. F 71.
FUEL FLOW,LB/MIN .09

BAROMETER 29.01 IN.HG.
HUMIDITY 83.92 GRAINS H2O/LB. AIR
LFE NO. 15 ENG. LFE NO. 0
SAMPLE TIME 47mm 30.00 MIN.
MEAS. EXH. FLOW,LB/MIN 16.94
AIR FLOW,LB/MIN 16.85

LFE INFORMATION			BLOWER INFORMATION		OTHER
INLET TEMP DEG. F	INLET PRESS. IN. H20	DIFF. PRESS. IN. H20	INLET PRESS. IN. H20	DIFF. PRESS. IN. H20	TUNNEL TEMP DEG. F
78.	.53	4.400	10.00	14.00	101.
78.	.53	4.400	10.00	14.00	101.
78.	.53	4.400	10.00	14.00	101.
77.	.53	4.400	10.00	14.00	101.
77.	.53	4.400	10.00	14.00	101.
77.	.53	4.400	10.00	14.00	101.
77.	.53	4.400	10.00	14.00	101.
AVERAGE 77.	.53	4.400	10.00	14.00	101.

LFE VOL, SCF 6618.4 LFE MASS,LB. 497.3 BLOWER + 47mm VOL, SCF 6796.7 BLOWER + 47mm MASS,LB 510.7
LFE FLOW SCFM 220.61 LFE FLOW LB/MIN 16.58 BLOWER + 47mm FLOW SCFM 226.56 BLOWER + 47mm FLOW LB/MIN 17.02
F/A DRY, MEAS .0054 F/A CALC .0046 F/A PCT, MEAS -14.1

FILTER DATA

POSITION	FILTER NUMBER	SAMPLE VOL. STD.CU.FEET	AVG. SAMPLE SYS. TEMP DEG F	WEIGHT GAIN MILLIGRAMS	MG/SCF OF SAMPLE
1	P47-142&14	22.090	65.	3.385	.153
2	P90-144&14	22.081	65.	3.330	.151

PARTICULATE RESULTS

AVG. SAMPLE ZONE TEMP, DEG F 101. DILUTION FACTOR 38.118
SPLIT EXHAUST VOL,SCF (SCM), LB/MIN 178.3 (5.05) , .45

PARTICULATE CONCENTRATION IN EXHAUST

FILTER	CONCENTRATION, MG/SCF (MG/SCM)	CONCENTRATION MULTIPLIER	G/HR	G/HP-HR
P47-142&14	5.841 (206.245)	1.7255	79.009	.000
P90-144&14	5.749 (202.983)	1.7263	77.760	.000

EMISSION RESULTS

	G/HR	G/HP-HR	CONC.
HC	29.001	.000	115. PPMC
CO	41.799	.000	82. PPM
NOX	96.748	.000	117. PPM
NOX,CORR	108.285	.000	
CO2		0.	.96 PCT
O2			18.95 PCT

NOX CORRECTION FACTOR 1.1193 WET CORRECTION FACTOR .9882

GASEOUS and/or PARTICULATE EMISSIONS

NOTCH 1

PROJECT 03-2681-809 PROGRAM = EMD16B

TEST NO. RUN NO. 8
ENGINE MODEL EMD 2-567B
TEST CELL LOCO LAB
HCR 1.758
BLOWER COUNTS 23590.
OBS. POWER,BHP 8.4

TEST DATE 2/28/91
DIESEL DF-2
TUNNEL NO. 26
SAMPLE TIME 20x20 .00 MIN.
BLOWER TEMP. DEG. F 72.
FUEL FLOW,LB/MIN .13

BAROMETER 28.91 IN.HG.
HUMIDITY 89.86 GRAINS H2O/LB. AIR
LFE NO. 15 ENG. LFE NO. 0
SAMPLE TIME 47mm 15.69 MIN.
MEAS. EXH. FLOW,LB/MIN 16.71
AIR FLOW,LB/MIN 16.58

LFE INFORMATION			BLOWER INFORMATION		OTHER
INLET TEMP DEG. F	INLET PRESS. IN. H20	DIFF. PRESS. IN. H20	INLET PRESS. IN. H20	DIFF. PRESS. IN. H20	TUNNEL TEMP DEG. F
82.	.55	4.700	10.00	14.00	111.
82.	.55	4.700	10.00	14.00	112.
82.	.55	4.700	10.00	14.00	111.
80.	.55	4.700	10.00	14.00	110.
AVERAGE 82.	.55	4.700	10.00	14.00	111.

LFE VOL, SCF 3624.2 LFE MASS,LB. 272.3
LFE FLOW SCFM 230.99 LFE FLOW LB/MIN 17.36
F/A DRY, MEAS .0078 F/A CALC .0070

BLOWER + 47mm VOL, SCF 3538.2 BLOWER + 47mm MASS,LB 265.9
BLOWER + 47mm FLOW SCFM 225.51 BLOWER + 47mm FLOW LB/MIN 16.94
F/A PCT, MEAS -10.0

FILTER DATA

POSITION	FILTER NUMBER	SAMPLE VOL. STD.CU.FEET	AVG. SAMPLE SYS. TEMP DEG F	WEIGHT GAIN MILLIGRAMS	MG/SCF OF SAMPLE
1	P47-138&13	11.740	68.	4.228	.360
2	P90-140&14	11.701	68.	4.166	.356

PARTICULATE RESULTS

AVG. SAMPLE ZONE TEMP, DEG F 111. DILUTION FACTOR ******
*SPLIT EXHAUST VOL,SCF (SCM), LB/MIN ***** (*****) , ****

PARTICULATE CONCENTRATION IN EXHAUST

FILTER	CONCENTRATION, MG/SCF (MG/SCM)	CONCENTRATION MULTIPLIER	G/HR	G/HP-HR
P47-138&13	******* (*******)	*******	*******	*******
P90-140&14	******* (*******)	*******	*******	*******

EMISSION RESULTS

	G/HR	G/HP-HR	CONC.
HC	28.571	3.405	120. PPMC
CO	55.374	6.600	116. PPM
NOX	149.600	17.831	193. PPM
NOX,CORR	159.175	18.972	
CO2		1005.	1.46 PCT
O2			18.69 PCT

NOX CORRECTION FACTOR 1.0640 WET CORRECTION FACTOR .9835

GASEOUS and/or PARTICULATE EMISSIONS
NOTCH 2
PROJECT 03-2681-809 PROGRAM = EMD16B

TEST NO. RUN NO. 7
ENGINE MODEL EMD 2-567B
TEST CELL LOCO LAB
HCR 1.758
BLOWER COUNTS 36081.
OBS. POWER,BHP 19.7

TEST DATE 2/28/91
DIESEL DF-2
TUNNEL NO. 26
SAMPLE TIME 20x20 .00 MIN.
BLOWER TEMP. DEG. F 74.
FUEL FLOW,LB/MIN .20

BAROMETER 29.07 IN.HG.
HUMIDITY 87.16 GRAINS H2O/LB. AIR
LFE NO. 15 ENG. LFE NO. 0
SAMPLE TIME 47mm 24.00 MIN.
MEAS. EXH. FLOW,LB/MIN 22.13
AIR FLOW,LB/MIN 21.93

LFE INFORMATION			BLOWER INFORMATION		OTHER
INLET TEMP DEG. F	INLET PRESS. IN. H20	DIFF. PRESS. IN. H20	INLET PRESS. IN. H20	DIFF. PRESS. IN. H20	TUNNEL TEMP DEG. F
79.	.50	4.290	10.00	14.00	120.
79.	.50	4.290	10.00	14.00	120.
79.	.50	4.280	10.00	14.00	120.
79.	.50	4.290	10.00	14.00	120.
79.	.50	4.300	10.00	14.00	120.
79.	.50	4.290	10.00	14.00	120.
AVERAGE 79.	.50	4.290	10.00	14.00	120.

LFE VOL, SCF 5153.3 LFE MASS,LB. 387.2
LFE FLOW SCFM 214.71 LFE FLOW LB/MIN 16.13
F/A DRY, MEAS .0092 F/A CALC .0080

BLOWER + 47mm VOL, SCF 5422.5 BLOWER + 47mm MASS,LB 407.4
BLOWER + 47mm FLOW SCFM 225.92 BLOWER + 47mm FLOW LB/MIN 16.98
F/A PCT, MEAS -13.4

FILTER DATA

POSITION	FILTER NUMBER	SAMPLE VOL. STD.CU.FEET	AVG. SAMPLE SYS. TEMP DEG F	WEIGHT GAIN MILLIGRAMS	MG/SCF OF SAMPLE
1	P47-134&13	18.016	67.	5.051	.280
2	P90-136&13	18.045	67.	4.976	.276

PARTICULATE RESULTS

AVG. SAMPLE ZONE TEMP, DEG F 120. DILUTION FACTOR 20.140
SPLIT EXHAUST VOL,SCF (SCM), LB/MIN 269.2 (7.63) , .84

PARTICULATE CONCENTRATION IN EXHAUST

FILTER	CONCENTRATION, MG/SCF (MG/SCM)	CONCENTRATION MULTIPLIER	G/HR	G/HP-HR
P47-134&13	5.646 (199.377)	1.1179	99.780	5.065
P90-136&13	5.554 (196.098)	1.1161	98.139	4.982

EMISSION RESULTS

	G/HR	G/HP-HR	CONC.
HC	40.811	2.072	125. PPMC
CO	73.537	3.733	113. PPM
NOX	285.514	14.493	268. PPM
NOX,CORR	318.895	16.188	
CO2		672.	1.67 PCT
O2			18.07 PCT

NOX CORRECTION FACTOR 1.1169 WET CORRECTION FACTOR .9819

GASEOUS and/or PARTICULATE EMISSIONS
NOTCH 3
PROJECT 03-2681-809 PROGRAM = EMD16B

TEST NO. RUN NO. 6
ENGINE MODEL EMD 2-567B
TEST CELL LOCO LAB
HCR 1.758
BLOWER COUNTS 45099.
OBS. POWER,BHP 46.0

TEST DATE 2/28/91
DIESEL DF-2
TUNNEL NO. 26
SAMPLE TIME 20x20 .00 MIN.
BLOWER TEMP. DEG. F 74.
FUEL FLOW,LB/MIN .35

BAROMETER 29.07 IN.HG.
HUMIDITY 82.07 GRAINS H2O/LB. AIR
LFE NO. 15 ENG. LFE NO. 0
SAMPLE TIME 47mm 30.00 MIN.
MEAS. EXH. FLOW,LB/MIN 28.22
AIR FLOW,LB/MIN 27.87

LFE INFORMATION			BLOWER INFORMATION		OTHER
INLET TEMP DEG. F	INLET PRESS. IN. H20	DIFF. PRESS. IN. H20	INLET PRESS. IN. H20	DIFF. PRESS. IN. H20	TUNNEL TEMP DEG. F
81.	.55	4.100	10.00	14.00	122.
81.	.55	4.100	10.00	14.00	122.
81.	.55	4.100	10.00	14.00	122.
81.	.55	4.100	10.00	14.00	122.
81.	.55	4.100	10.00	14.00	122.
81.	.55	4.100	10.00	14.00	122.
81.	.55	4.100	10.00	14.00	122.
AVERAGE 81.	.55	4.100	10.00	14.00	122.

LFE VOL, SCF 6128.1 LFE MASS,LB. 460.5 BLOWER + 47mm VOL, SCF 6776.1 BLOWER + 47mm MASS,LB 509.2
LFE FLOW SCFM 204.25 LFE FLOW LB/MIN 15.35 BLOWER + 47mm FLOW SCFM 225.84 BLOWER + 47mm FLOW LB/MIN 16.97
F/A DRY, MEAS .0127 F/A CALC .0116 F/A PCT, MEAS -8.4

FILTER DATA

POSITION	FILTER NUMBER	SAMPLE VOL. STD.CU.FEET	AVG. SAMPLE SYS. TEMP DEG F	WEIGHT GAIN MILLIGRAMS	MG/SCF OF SAMPLE
1	P47-129&13	21.678	68.	3.295	.152
2	P90-131&13	21.701	69.	4.027	.186

PARTICULATE RESULTS

AVG. SAMPLE ZONE TEMP, DEG F 122. DILUTION FACTOR 10.457
SPLIT EXHAUST VOL,SCF (SCM), LB/MIN 648.0 (18.35) , 1.62

PARTICULATE CONCENTRATION IN EXHAUST

FILTER	CONCENTRATION, MG/SCF (MG/SCM)	CONCENTRATION MULTIPLIER	G/HR	G/HP-HR
P47-129&13	1.589 (56.120)	.4824	35.813	.779
P90-131&13	1.940 (68.514)	.4818	43.722	.950

EMISSION RESULTS

	G/HR	G/HP-HR	CONC.
HC	51.213	1.113	130. PPMC
CO	64.460	1.401	82. PPM
NOX	527.061	11.458	412. PPM
NOX,CORR	568.413	12.357	
CO2		504.	2.44 PCT
O2			17.19 PCT

NOX CORRECTION FACTOR 1.0785 WET CORRECTION FACTOR .9755

GASEOUS and/or PARTICULATE EMISSIONS
NOTCH 4
PROJECT 03-2681-809 PROGRAM = EMD16B

TEST NO. RUN NO. 5
ENGINE MODEL EMD 2-567B
TEST CELL LOCO LAB
HCR 1.758
BLOWER COUNTS 28131.
OBS. POWER,BHP 78.0

TEST DATE 2/28/91
DIESEL DF-2
TUNNEL NO. 26
SAMPLE TIME 20x20 .00 MIN.
BLOWER TEMP. DEG. F 75.
FUEL FLOW,LB/MIN .54

BAROMETER 29.08 IN.HG.
HUMIDITY 85.57 GRAINS H2O/LB. AIR
LFE NO. 15 ENG. LFE NO. 0
SAMPLE TIME 47mm 18.72 MIN.
MEAS. EXH. FLOW,LB/MIN 33.87
AIR FLOW,LB/MIN 33.33

LFE INFORMATION			BLOWER INFORMATION		OTHER
INLET TEMP DEG. F	INLET PRESS. IN. H20	DIFF. PRESS. IN. H20	INLET PRESS. IN. H20	DIFF. PRESS. IN. H20	TUNNEL TEMP DEG. F
83.	.59	3.920	10.00	14.00	122.
83.	.59	3.920	10.00	14.00	124.
83.	.59	3.920	10.00	14.00	124.
83.	.59	3.920	10.00	14.00	124.
83.	.59	3.930	10.00	14.00	124.
AVERAGE 83.	.59	3.922	10.00	14.00	124.

LFE VOL, SCF 3640.5 LFE MASS,LB. 273.5 BLOWER + 47mm VOL, SCF 4220.2 BLOWER + 47mm MASS,LB 317.1
LFE FLOW SCFM 194.52 LFE FLOW LB/MIN 14.62 BLOWER + 47mm FLOW SCFM 225.50 BLOWER + 47mm FLOW LB/MIN 16.94
F/A DRY, MEAS .0165 F/A CALC .0149 F/A PCT, MEAS -9.8

FILTER DATA

POSITION	FILTER NUMBER	SAMPLE VOL. STD.CU.FEET	AVG. SAMPLE SYS. TEMP DEG F	WEIGHT GAIN MILLIGRAMS	MG/SCF OF SAMPLE
1	P47-125&12	13.673	69.	2.529	.185
2	P90-127&12	13.605	69.	3.295	.242

PARTICULATE RESULTS

AVG. SAMPLE ZONE TEMP, DEG F 124. DILUTION FACTOR 7.280
SPLIT EXHAUST VOL,SCF (SCM), LB/MIN 579.7 (16.42) , 2.33

PARTICULATE CONCENTRATION IN EXHAUST

FILTER	CONCENTRATION, MG/SCF (MG/SCM)	CONCENTRATION MULTIPLIER	G/HR	G/HP-HR
P47-125&12	1.346 (47.544)	.5324	36.420	.467
P90-127&12	1.763 (62.254)	.5351	47.687	.611

EMISSION RESULTS

	G/HR	G/HP-HR	CONC.
HC	68.298	.876	142. PPMC
CO	63.935	.820	68. PPM
NOX	950.598	12.187	615. PPM
NOX,CORR	1021.883	13.101	
CO2		464.	3.15 PCT
O2			15.93 PCT

NOX CORRECTION FACTOR 1.0750 WET CORRECTION FACTOR .9695

GASEOUS and/or PARTICULATE EMISSIONS
NOTCH 5
PROJECT 03-2681-809 PROGRAM = EMD16B

TEST NO. RUN NO. 4
ENGINE MODEL EMD 2-567B
TEST CELL LOCO LAB
HCR 1.758
BLOWER COUNTS 26164.
OBS. POWER,BHP 114.0

TEST DATE 2/28/91
DIESEL DF-2
TUNNEL NO. 26
SAMPLE TIME 20x20 .00 MIN.
BLOWER TEMP. DEG. F 72.
FUEL FLOW,LB/MIN .76

BAROMETER 29.10 IN.HG.
HUMIDITY 80.42 GRAINS H2O/LB. AIR
LFE NO. 15 ENG. LFE NO. 0
SAMPLE TIME 47mm 17.40 MIN.
MEAS. EXH. FLOW,LB/MIN 40.38
AIR FLOW,LB/MIN 39.62

LFE INFORMATION			BLOWER INFORMATION		OTHER
INLET TEMP DEG. F	INLET PRESS. IN. H2O	DIFF. PRESS. IN. H2O	INLET PRESS. IN. H2O	DIFF. PRESS. IN. H2O	TUNNEL TEMP DEG. F
84.	.60	3.950	10.00	14.00	122.
84.	.60	3.950	10.00	14.00	124.
84.	.60	3.950	10.00	14.00	124.
84.	.60	3.950	10.00	14.00	123.
84.	.62	3.950	10.00	14.00	123.
AVERAGE 84.	.60	3.950	10.00	14.00	123.

LFE VOL, SCF 3398.7 LFE MASS,LB. 255.4
LFE FLOW SCFM 195.35 LFE FLOW LB/MIN 14.68
F/A DRY, MEAS .0194 F/A CALC .0189

BLOWER + 47mm VOL, SCF 3951.1 BLOWER + 47mm MASS,LB 296.9
BLOWER + 47mm FLOW SCFM 227.10 BLOWER + 47mm FLOW LB/MIN 17.06
F/A PCT, MEAS -2.5

FILTER DATA

POSITION	FILTER NUMBER	SAMPLE VOL. STD.CU.FEET	AVG. SAMPLE SYS. TEMP DEG F	WEIGHT GAIN MILLIGRAMS	MG/SCF OF SAMPLE
1	P47-121&12	12.712	69.	2.269	.178
2	P90-123&12	12.693	69.	2.236	.176

PARTICULATE RESULTS

AVG. SAMPLE ZONE TEMP, DEG F 123. DILUTION FACTOR 7.153
SPLIT EXHAUST VOL,SCF (SCM), LB/MIN 552.4 (15.64) , 2.39

PARTICULATE CONCENTRATION IN EXHAUST

FILTER	CONCENTRATION, MG/SCF (MG/SCM)	CONCENTRATION MULTIPLIER	G/HR	G/HP-HR
P47-121&12	1.277 (45.083)	.5627	41.166	.361
P90-123&12	1.260 (44.495)	.5636	40.629	.356

EMISSION RESULTS

	G/HR	G/HP-HR	CONC.
HC	84.711	.743	160. PPMC
CO	101.045	.886	97. PPM
NOX	1494.226	13.107	882. PPM
NOX,CORR	1567.139	13.747	
CO2		443.	4.01 PCT
O2			14.39 PCT

NOX CORRECTION FACTOR 1.0488 WET CORRECTION FACTOR .9623

GASEOUS and/or PARTICULATE EMISSIONS
NOTCH 6
PROJECT 03-2681-809 PROGRAM = EMD16B

TEST NO. RUN NO. 3
ENGINE MODEL EMD 2-567B
TEST CELL LOCO LAB
HCR 1.758
BLOWER COUNTS 45115.
OBS. POWER,BHP 148.0

TEST DATE 2/28/91
DIESEL DF-2
TUNNEL NO. 26
SAMPLE TIME 20x20 .00 MIN.
BLOWER TEMP. DEG. F 71.
FUEL FLOW,LB/MIN .98

BAROMETER 29.14 IN.HG.
HUMIDITY 75.20 GRAINS H2O/LB. AIR
LFE NO. 15 ENG. LFE NO. 0
SAMPLE TIME 47mm. 30.00 MIN.
MEAS. EXH. FLOW,LB/MIN 47.63
AIR FLOW,LB/MIN 46.65

LFE INFORMATION			BLOWER INFORMATION		OTHER
INLET TEMP DEG. F	INLET PRESS. IN. H20	DIFF. PRESS. IN. H20	INLET PRESS. IN. H20	DIFF. PRESS. IN. H20	TUNNEL TEMP DEG. F
86.	.65	4.050	10.00	14.00	121.
86.	.65	4.050	10.00	14.00	121.
86.	.65	4.050	10.00	14.00	121.
86.	.65	4.050	10.00	14.00	122.
86.	.65	4.050	10.00	14.00	122.
86.	.65	4.030	10.00	14.00	122.
86.	.65	4.030	10.00	14.00	121.
AVERAGE 86.	.65	4.044	10.00	14.00	121.

LFE VOL, SCF 5962.9 LFE MASS,LB. 448.0
LFE FLOW SCFM 198.77 LFE FLOW LB/MIN 14.94
F/A DRY, MEAS .0213 F/A CALC .0227

BLOWER + 47mm VOL, SCF 6837.2 BLOWER + 47mm MASS,LB 513.7
BLOWER + 47mm FLOW SCFM 227.92 BLOWER + 47mm FLOW LB/MIN 17.13
F/A PCT, MEAS 6.4

FILTER DATA

POSITION	FILTER NUMBER	SAMPLE VOL. STD.CU.FEET	AVG. SAMPLE SYS. TEMP DEG F	WEIGHT GAIN MILLIGRAMS	MG/SCF OF SAMPLE
1	P47-117&11	22.388	68.	3.392	.152
2	P90-119&12	22.388	68.	3.323	.148

PARTICULATE RESULTS

AVG. SAMPLE ZONE TEMP, DEG F 121. DILUTION FACTOR 7.820
SPLIT EXHAUST VOL,SCF (SCM), LB/MIN 874.3 (24.76) , 2.19

PARTICULATE CONCENTRATION IN EXHAUST FILTER	CONCENTRATION, MG/SCF (MG/SCM)	CONCENTRATION MULTIPLIER	G/HR	G/HP-HR
P47-117&11	1.185 (41.836)	.3493	45.065	.304
P90-119&12	1.161 (40.985)	.3493	44.149	.298

EMISSION RESULTS

	G/HR	G/HP-HR	CONC.
HC	99.012	.669	172. PPMC
CO	178.535	1.206	160. PPM
NOX	2096.816	14.168	1150. PPM
NOX,CORR	2146.632	14.504	
CO2		443.	4.83 PCT
O2			14.42 PCT

NOX CORRECTION FACTOR 1.0238 WET CORRECTION FACTOR .9556

GASEOUS and/or PARTICULATE EMISSIONS
NOTCH 7
PROJECT 03-2681-809 PROGRAM = EMD16B

TEST NO. RUN NO. 2
ENGINE MODEL EMD 2-567B
TEST CELL LOCO LAB
HCR 1.758
BLOWER COUNTS 39775.
OBS. POWER,BHP 179.0

TEST DATE 2/28/91
DIESEL DF-2
TUNNEL NO. 26
SAMPLE TIME 20x20 .00 MIN.
BLOWER TEMP. DEG. F 71.
FUEL FLOW,LB/MIN 1.22

BAROMETER 29.18 IN.HG.
HUMIDITY 59.78 GRAINS H2O/LB. AIR
LFE NO. 15 ENG. LFE NO. 0
SAMPLE TIME 47mm 26.44 MIN.
MEAS. EXH. FLOW,LB/MIN 54.42
AIR FLOW,LB/MIN 53.20

LFE INFORMATION			BLOWER INFORMATION		OTHER
INLET TEMP DEG. F	INLET PRESS. IN. H20	DIFF. PRESS. IN. H20	INLET PRESS. IN. H20	DIFF. PRESS. IN. H20	TUNNEL TEMP DEG. F
88.	.65	4.100	10.00	14.00	123.
88.	.65	4.100	10.00	14.00	123.
88.	.65	4.100	10.00	14.00	124.
88.	.65	4.100	10.00	14.00	124.
88.	.65	4.100	10.00	14.00	124.
88.	.65	4.100	10.00	14.00	124.
88.	.65	4.100	10.00	14.00	124.
AVERAGE 88.	.65	4.100	10.00	14.00	124.

LFE VOL, SCF 5297.2 LFE MASS,LB. 398.0 BLOWER + 47mm VOL, SCF 6035.7 BLOWER + 47mm MASS,LB 453.5
LFE FLOW SCFM 200.37 LFE FLOW LB/MIN 15.06 BLOWER + 47mm FLOW SCFM 228.31 BLOWER + 47mm FLOW LB/MIN 17.16
F/A DRY, MEAS .0231 F/A CALC .0255 F/A PCT, MEAS 10.1

FILTER DATA

POSITION	FILTER NUMBER	SAMPLE VOL. STD.CU.FEET	AVG. SAMPLE SYS. TEMP DEG F	WEIGHT GAIN MILLIGRAMS	MG/SCF OF SAMPLE
1	P47-113&11	19.168	71.	3.121	.163
2	P90-115&11	19.197	71.	3.252	.169

PARTICULATE RESULTS

AVG. SAMPLE ZONE TEMP, DEG F 124. DILUTION FACTOR 8.172
SPLIT EXHAUST VOL,SCF (SCM), LB/MIN 738.6 (20.92) , 2.10

PARTICULATE CONCENTRATION IN EXHAUST

FILTER	CONCENTRATION, MG/SCF (MG/SCM)	CONCENTRATION MULTIPLIER	G/HR	G/HP-HR
P47-113&11	1.331 (46.986)	.4264	57.825	.323
P90-115&11	1.384 (48.884)	.4257	60.161	.336

EMISSION RESULTS

	G/HR	G/HP-HR	CONC.
HC	150.811	.843	237. PPMC
CO	316.210	1.767	257. PPM
NOX	2456.928	13.726	1223. PPM
NOX,CORR	2405.404	13.438	
CO2		453.	5.43 PCT
O2			13.16 PCT

NOX CORRECTION FACTOR .9790 WET CORRECTION FACTOR .9514

GASEOUS and/or PARTICULATE EMISSIONS
NOTCH 8
PROJECT 03-2681-809 PROGRAM = EMD16B

TEST NO. RUN NO. 1
ENGINE MODEL EMD 2-567B
TEST CELL LOCO LAB
HCR 1.758
BLOWER COUNTS 30246.
OBS. POWER,BHP 206.0

TEST DATE 2/28/91
DIESEL DF-2
TUNNEL NO. 26
SAMPLE TIME 20x20 .00 MIN.
BLOWER TEMP. DEG. F 70.
FUEL FLOW,LB/MIN 1.47

BAROMETER 29.00 IN.HG.
HUMIDITY 68.95 GRAINS H2O/LB. AIR
LFE NO. 15 ENG. LFE NO. 0
SAMPLE TIME 47mm 20.10 MIN.
MEAS. EXH. FLOW,LB/MIN 60.20
AIR FLOW,LB/MIN 58.73

LFE INFORMATION			BLOWER INFORMATION		OTHER
INLET TEMP DEG. F	INLET PRESS. IN. H20	DIFF. PRESS. IN. H20	INLET PRESS. IN. H20	DIFF. PRESS. IN. H20	TUNNEL TEMP DEG. F
86.	.65	4.120	10.00	14.00	122.
86.	.65	4.120	10.00	14.00	122.
86.	.65	4.120	10.00	14.00	122.
87.	.65	4.120	10.00	14.00	122.
87.	.65	4.120	10.00	14.00	122.
AVERAGE 86.	.65	4.120	10.00	14.00	122.

LFE VOL, SCF 4042.1 LFE MASS,LB. 303.7 BLOWER + 47mm VOL, SCF 4570.7 BLOWER + 47mm MASS,LB 343.4
LFE FLOW SCFM 201.10 LFE FLOW LB/MIN 15.11 BLOWER + 47mm FLOW SCFM 227.40 BLOWER + 47mm FLOW LB/MIN 17.09
F/A DRY, MEAS .0253 F/A CALC .0296 F/A PCT, MEAS 17.2

FILTER DATA

POSITION	FILTER NUMBER	SAMPLE VOL. STD.CU.FEET	AVG. SAMPLE SYS. TEMP DEG F	WEIGHT GAIN MILLIGRAMS	MG/SCF OF SAMPLE
1	P47-109&11	15.555	66.	2.889	.186
2	P90-111&11	15.604	66.	2.853	.183

PARTICULATE RESULTS

AVG. SAMPLE ZONE TEMP, DEG F 122. DILUTION FACTOR 8.647
SPLIT EXHAUST VOL,SCF (SCM), LB/MIN 528.6 (14.97) , 1.98

PARTICULATE CONCENTRATION IN EXHAUST

FILTER	CONCENTRATION, MG/SCF (MG/SCM)	CONCENTRATION MULTIPLIER	G/HR	G/HP-HR
P47-109&11	1.606 (56.708)	.5559	77.199	.375
P90-111&11	1.581 (55.826)	.5542	76.000	.369

EMISSION RESULTS

	G/HR	G/HP-HR	CONC.
HC	140.373	.681	212. PPMC
CO	668.319	3.244	526. PPM
NOX	2892.032	14.039	1395. PPM
NOX,CORR	2879.349	13.977	
CO2		473.	6.32 PCT
O2			11.90 PCT
NOX CORRECTION FACTOR		.9956	WET CORRECTION FACTOR .9435

APPENDIX E

DIMENSION SHEET 1

	DATE	BEGINNING or END OF TEST	RIGHT SIDE FRONT	RIGHT SIDE REAR	LEFT SIDE FRONT	LEFT SIDE REAR
PISTON TO HEAD CLEARANCE Ref. PAGE 318 LIMIT .068 / .026 NOTE RECORD BOTH BEFORE & AFTER TEST	11-15-90		.065	.057	.051	.056

DIMENSION SHEET 3C

DATE	BORE OF BLADE ROD	PISTON PIN DIAMETER									
		RIGHT 88-H 0060					LEFT 88-G D0438				
		A	A'	B	B'	C	A	A'	B	B'	C
10-24-90	.002	3.6845	3.6845	3.6845	3.6845	3.6845	3.6840	3.6843	3.6839	3.6834	3.6840
3-20-91	.003	3.6848	3.6848	3.6848	3.6848	3.6848	3.6843	3.6843	3.6840	3.6840	3.6843
DIFFERENCE	.001	-0.0003	-0.0003	-0.0003	-0.0003	-0.0003	-0.0003	-0-	-0.0001	-0.0002	-0.0003

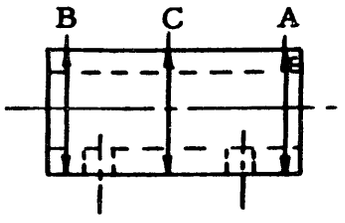

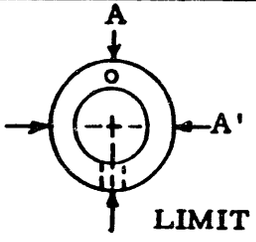

LIMIT $\frac{3.6810}{3.6820}$

DATE	PISTON PIN TO CARRIER CLEARANCE .009 / .012				THRUST WASHER THICKNESS ~~.1860~~ / ~~.1880~~		CLEARANCE BETWEEN SHOULDER ON BLADE ROD AND COUNTERBORE IN FORK ROD PAGE 323 ~~.016~~ / ~~.008~~	CARRIER TO PISTON SNAP RING CLEARANCE .002 / .018	
	RIGHT		LEFT						
	FRONT	REAR	FRONT	REAR	RIGHT	LEFT		RIGHT	LEFT
10-24-90					0.1865	0.1865			
10-26-90	.009	.011	.009	.010				.012	.007
3-20-91	.011	.013	.010	0.12	0.1865	0.1863		.011	.007

SERIAL NO.	DATE	RING THICKNESS A	B	C	GAP IN 8.500 LINER	WIDTH	RING TO LAND CLEARANCE
TOP RING RIGHT SIDE	10-24-90	.3090	.3095	.3115	.039	.2470	
	10-29-90						.004
	3-22-91	.3090	.3095	.3105	.040	.2465	
	3-27-91						.004
	Difference	-0-	-0-	0.001	0.001	0.0001	-0-

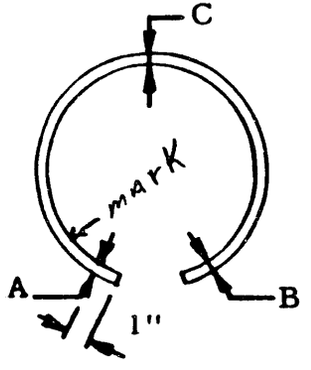

Ref. Page 318

LIMIT GAP .035 / .025

WIDTH .247 / .246

RING TO LAND CLEARANCE (ON ASSEMBLY) .008 / .004

Note: Record Both at Beginning and End of Test

SERIAL NO.	DATE	RING THICKNESS A	B	C	GAP IN 8.500 LINER	WIDTH	RING TO LAND CLEARANCE
TOP RING LEFT SIDE	10-24-90	.3063	.3075	.3028	.035	.2470	
	10-29-90						.004
	3-22-91	.3055	.3065	.3025	.035	.2465	
	3-27-91						.005
	Difference	0.0008	0.001	0.0003	-0-	0.0005	0.001

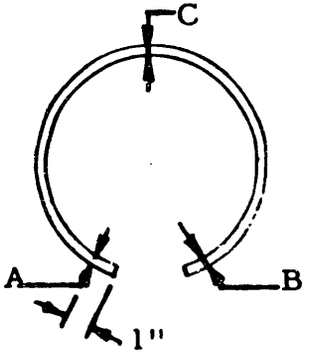

Ref. Page 318

LIMIT GAP $\frac{.035}{.025}$

WIDTH $\frac{.247}{.246}$

RING TO LAND CLEARANCE (ON ASSEMBLY) $\frac{.008}{.004}$

Note: Record Both at Beginning and End of Test

	DATE	RIGHT SIDE RING NO. 2	3	4	5	LEFT SIDE 2	3	4	5
PISTON RING GAP (MEASURE IN 8.500 LINER)	10-24-90	.039	.036	.025	.040	.038	.035	.024	.035
	3-22-91	.039	.037	.031	.038	.036	.041	.030	.035
R ord Both At Beginning and En of Each Test									
	Difference	-0-	0.001	0.006	-0.002	-0.002	0.006	0.006	-0-
LIMIT COMP. RINGS .035 / .025									
OIL RINGS .025 / .015									
REF. PAGE 318									

DIMENSION SHEET

	DATE	RIGHT SIDE				LEFT SIDE			
		RING NO. 2	3	4	5	2	3	4	5
PISTON RING WIDTH	10-24-90	.2430	.2425	.2485	.2485	.2425	.2428	.2485	.2485
Record Both at Beginning & End Of Test	5-25-91	.2435	.2423	.2485	.2485	.2420	.2425	.2485	.2485
LIMITS COMP. RINGS .247 / .246	Difference	-0.0005	0.0002	-0-	-0-	0.0005	0.0003	-0-	-0-
OIL RINGS .249 / .248									
REF. PAGE 318									

DIMENSION SHEET

	DATE	RIGHT SIDE RING NO. 2	3	4	5	LEFT SIDE 2	3	4	5
'ING TO LAND CLEARANCE	10-29-90	.007	.007	.002	.002	.007	.007	.002	.002
	3-27-91	.006	.008	.002	.002	.007	.007	.002	.002
Record Both At Beginning and End of Test									
	Difference	-0.001	0.001	-0-	-0-	-0-	-0-	-0-	-0-
LIMITS COMP. RINGS .008 / .004 OIL RINGS .006 / .002 REF. PAGE 318									

PISTON RING GROOVE WIDTH

RECORD BOTH AT BEGINNING AND END OF EACH TEST. REF. PAGE 315 & 318 LIMIT $\frac{.254}{.251}$

DATE	RIGHT SIDE (PISTON S/N 90H2215) RING NO. 1	2	3	4	5	LEFT SIDE (PISTON S/N 90A1320) 1	2	3	4	5
10-25-90	.252	.252	.251	.251	.251	.252	.251	.251	.251	.251
3-27-91	.253	.252	.253	.252	.253	.253	.252	.252	.252	.253
Difference	0.001	- 0	0.002	0.001	0.002	0.001	0.001	0.001	0.001	0.002

SERIAL NO. 90A1295

Right Hand Piston

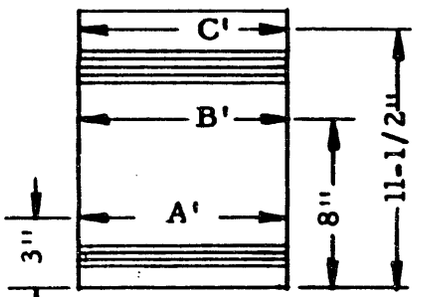

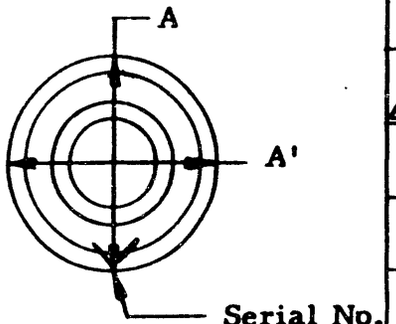

Note: Record at beginning and end of each test.

See Page 318

Limits:
Top Land 8.447-8.452
Skirt 8.488-8.490

Date	Height 3" A	8" B	11-1/2" C	3" A'	8" B'	11-1/2" C'	See Deposit & Wear Bulletin Upper Carrier Pilot Dia.	See Deposit & Wear Bulletin Lower Carrier Pilot Dia.
							36.502 / 6.000	7.491 / 7.488
10-23-90	8.4886	8.4873	8.4568	8.4887	8.4871	8.4563	3.5808	7.4877
3-25-91	8.4985	8.4865	8.4555	8.4893	8.4873	8.4595		
Difference	0.0001	0.0008	0.0013	-0.0006	-0.0002	-0.0032		

DATE	RIGHT CARRIER PILOT DIA. - Female PISTON No. S/N 90A1295				LEFT CARRIER PILOT DIA. — PISTON NO. S/N 90A1320			
	UPPER 3.5650 / 3.5665		LOWER 7.4875 / 7.4890		UPPER 3.5650 / 3.5665		LOWER 7.4875 / 7.4890	
	A	A'	A	A'	A	A'	A	A'
10-25-90	3.5658	~~3.5658~~ 3.5658	7.4882	7.4977	3.5663	3.5663	7.4885	7.4887
3-27-91	3.5660	3.5660	7.4885	7.4875	3.5665	3.5665	7.4885	7.4885

SERIAL NO. 90A1320

Left Hand Piston

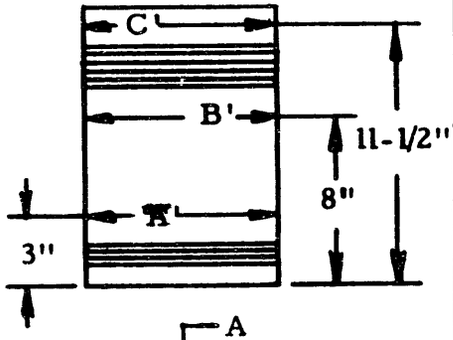

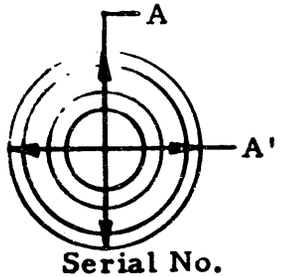

Serial No.

Note: Record at Beginning and End of Each Test

REF. PAGE 318
LIMITS
TOP LAND 8.447 / 8.452
SKIRT 8.488 / 8.490

DATE	HEIGHT 3" A	8" B	11-1/2" C	3" A'	8" B'	11-1/2" C'	See Deposit & Wear Bulletin: Upper Carrier Pilot Dia.	See Deposit & Wear Bulletin: Lower Carrier Pilot Dia.
							6.002 / 6.000	7.491 / 7.488
10-24-90	8.4895	8.4875	8.4558	8.4895	8.4875	8.4565	3.5813	7.4885
3-25-91	8.4885	8.4855	8.4555	8.4890	8.4860	8.4565		
assume	0.001	0.002	0.0003	0.0005	0.0015	-0		

E-84

DATE	RIGHT PISTON PILOT DIA.-CARRIER No. MALE 87B-00373				LEFT PISTON PILOT DIA.-CARRIER No. 87B-00364			
	UPPER 3.5594 / 3.5612		LOWER 7.4820 / 7.4845		UPPER 3.5594 / 3.5612		LOWER 7.4820 / 7.4845	
	LONG.	TRANS.	LONG.	TRANS.	LONG.	TRANS.	LONG.	TRANS.
10-25-90	3.5605	3.5605	7.4818	7.4823	3.5605	3.5605	7.4822	7.4825
5-20-91	3.5605	3.5605	7.4820	7.4825	3.5605	3.5605	7.4825	7.4830

DIMENSION SHEET 15C

DATE	RIGHT CARRIER PIN BEARING - I. D. 3.6930 / 3.6950 CARRIER NO. 87B-00373				LEFT CARRIER BEARING - I. D. 3.6930 / 3.6950 CARRIER NO. 87B-00364			
	PEE END		OTHER END		PEE END		QTHER END	
	VERT.	HORIZ.	VERT.	HORIZ.	VERT.	HORIZ.	VERT.	HORIZ.
10-26-90	3.7065	3.7220	3.7118	3.7225	3.7045	3.7235	3.7070	3.7245
3-20-91	3.7088	3.7225	3.7133	3.7235	3.7065	3.7240	3.7093	3.7235
Difference	0.0023	0.0005	0.0015	0.001	0.002	0.0005	0.0023	-0.001

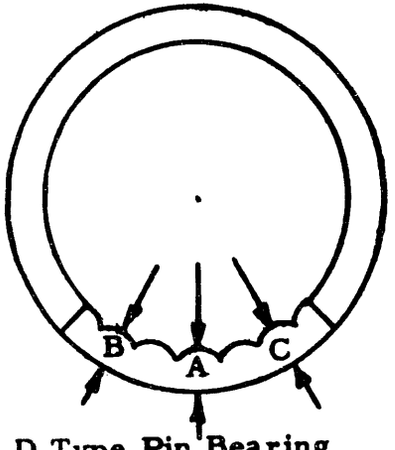

D Type Pin Bearing

The numbered end of the insert will go to the pee hole end of the carrier. The land labeled B at one end will become C at the other end.

RIGHT CARRIER PIN BEARING THICKNESS CARRIER NO. 87B-00373

DATE	PEE END			OTHER END		
	a	b	c	a	b	c
10-24-90	0.150	0.151	0.150	0.150	0.150	0.150
3-20-91	0.150	0.151	0.150	0.150	0.150	0.150

LEFT CARRIER PIN BEARING THICKNESS CARRIER NO. 87B-00364

	PEE END			OTHER END		
	a	b	c	a	b	c
10-24-90	0.150	0.150	0.150	0.150	0.150	0.150
3-20-91	0.150	0.150	0.150	0.150	0.150	0.150

VALVE GUIDE DIAMETER

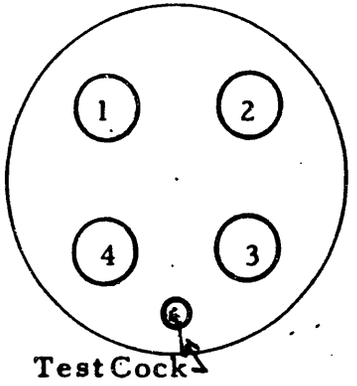

CYLINDER HEAD (BOTTOM VIEW)

Note: Record Largest Dimension ONLY

LIMIT $\frac{.632}{.627}$

MEASUREMENT SHOULD BE MADE 1/2" FROM BOTTOM OF GUIDE.

DATE	RIGHT SIDE CYL. HEAD S/N 81J 4156				LEFT SIDE CYL. HEAD S/N 81J 4135			
	1	2	3	4	1	2	3	4
10-26-90	.6298	.6298	.6315	.6305	.6285	.6283	.6290	.6280
3-28-91	.6298	.6298	.6298	.6298	.6293	.6289	.6294	6285
Difference	-0-	-0.001	-0.0017	-0.0007	0.0008	0.0005	-0.0002	0.0005

	DATE	RIGHT SIDE CYL. HEAD S/N 81J4156				LEFT SIDE CYL. HEAD S/N 81J4135			
		1	2	3	4	1	2	3	4
VALVE STEM DIAMETER									
	10-26-90	.6218	.6218	.6215	.6218	.6223	.6218	.6218	.6220
	3-27-91	.6218	.6218	.6215	.6218	.6220	.6215	.6220	6218
	Difference	-0-	-0-	-0-	-0-	0.0003	0.0003	-0.0002	0.0002

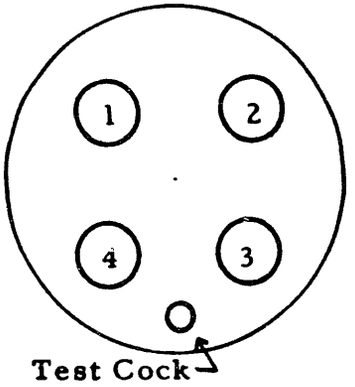

Test Cock

CYLINDER HEAD
(BOTTOM VIEW)

Note: Record Smallest Dimension in Area Worn by Guide

LIMIT

$\frac{.6225}{.620}$

E-89

	DATE	RIGHT SIDE				LEFT SIDE			
		1	2	3	4	1	2	3	4
DEPOSITS ON VALVE STEM	10-26-90	.6218	.6218	.6215	.6218	.6220	.6218	.6218	.6220
	3-20-91	.6255	.6258	.6240	.6238	.6260	.6255	.6238	.6250
	deposit	0.0037	0.0040	0.0025	0.002	0.0040	0.0037	0.0020	0.0030

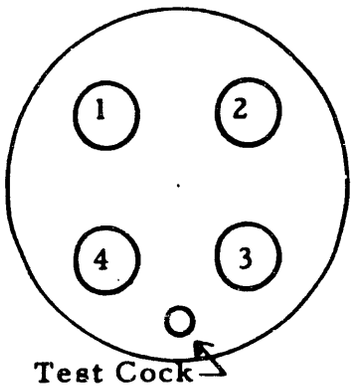

CYLINDER HEAD (BOTTOM VIEW)

REFERENCE: DEPOSIT & WEAR BULLETIN
MEASURE VALVE STEM DIA. OVER DEPOSIT 1/2" BELOW VALVE GUIDE
TRAVEL BEFORE AND AFTER TEST

	DATE	CYL. HEAD S/N RIGHT SIDE 81J 4156				CYL HEAD S/N LEFT SIDE 81J 4135			
		1	2	3	4	1	2	3	4
VALVE SEAT WIDTH ON HEAD	10-29-90	3/32	3/32	3/32	3/32	1/8	1/8	1/8	1/8

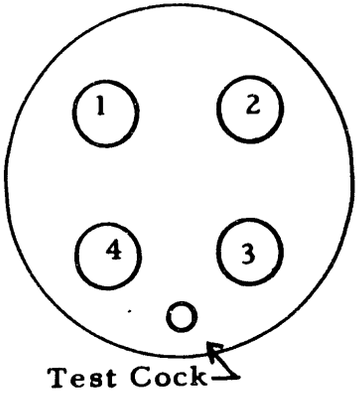

CYLINDER HEAD (BOTTOM VIEW)

MEASURE ON ASSEMBLY ONLY

LIMIT 1/8 $^{+0}_{-1/32}$

REFERENCE PAGE 220

VALVE LEAKCHECK	DATE	CYL HEAD S/N 81J 4156 RIGHT SIDE				CYL HEAD S/N 81J 4135 LEFT SIDE			
		1	2	3	4	1	2	3	4
	10-9-90	2 MIN.	2 MIN.	2 MIN	2 MIN	2 MIN	2 MIN.	2 MIN.	2 MIN

Test Cock

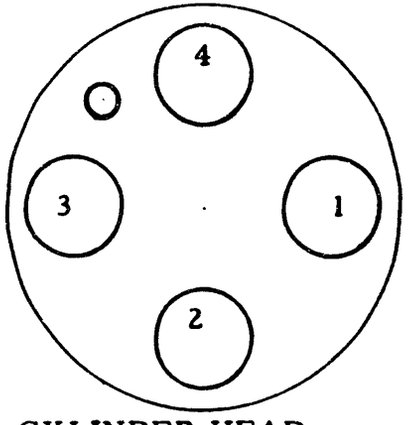

CYLINDER HEAD
(BOTTOM VIEW)

Reference: MEASUREMENT PROCEDURE BULLETIN- TIME TO FILL RUBBER BULB (3" DIAMETER) COMPLETELY COLLAPSED

LIMIT: ~~2~~ 1½ MINUTES MINIMUM
RECORD ON ASSEMBLY ONLY

SERIAL NO. 80C 204D

RIGHT HAND CYLINDER

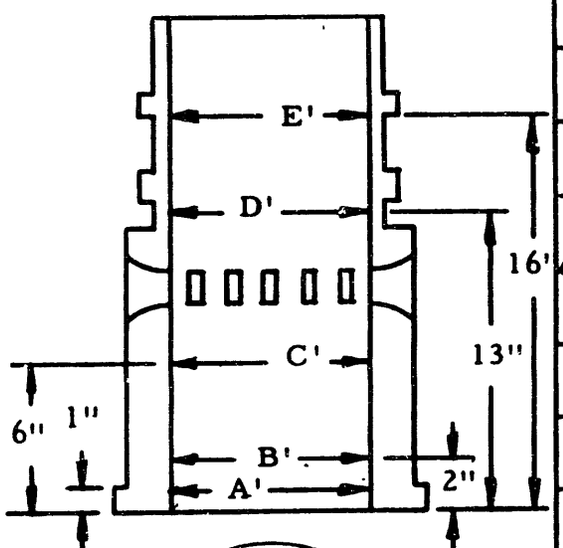

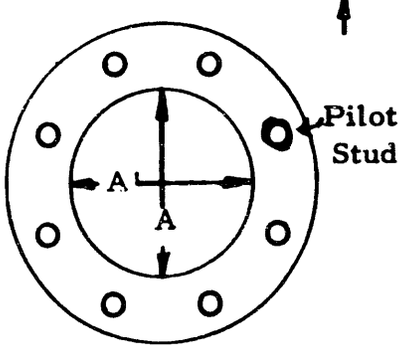

SEE BULLETIN ON MEASUREMENT PROCEDURE. MEASURE BEFORE & AFTER TEST
LIMIT B & B' 8.5~~10~~20 Max.
Rest - 8.504 Max.

DATE	LETTER DIMENSIONS A Depth 1"	B 2"	C 6"	D 13"	E 16"	A' 1"	B' 2"	C' 6"	D' 13"	E' 16"
10-31-90	8.5024	8.5025	8.5017	8.5007	8.4996	8.5027	8.5046	8.5037	8.5008	8.4998
3-28-91	8.5022	8.5025	8.5013	8.5006	8.4994	8.5027	8.5045	8.5039	8.5009	8.4996
Difference	-0.0002	-0-	-0.0004	-0.0001	-0.0002	-0-	-0.0001	0.0002	0.0001	-0.0002

DIMENSION SHEET 22

SERIAL NO. 80F122D

LEFT HAND CYLINDER

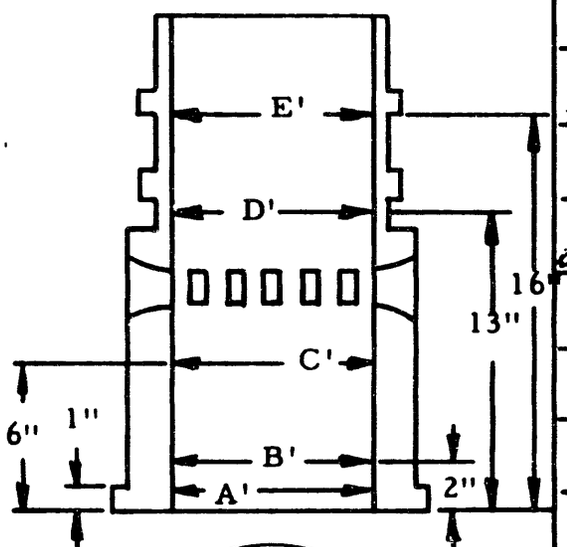

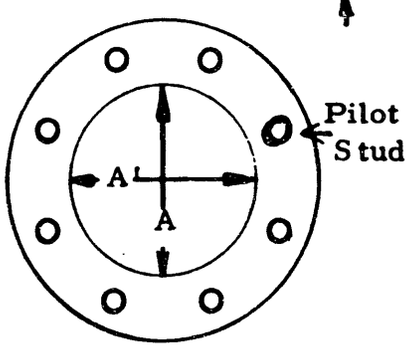

SEE BULLETIN ON MEASUREMENT PROCEDURE. MEASURE BEFORE & AFTER TEST
LIMIT B & B' 8.510 Max.
Rest - 8.504 Max.

DATE	LETTER DIMENSIONS A Depth 1"	B 2"	C 6"	D 13"	E 16"	LETTER DIMENSIONS A' 1"	B' 2"	C' 6"	D' 13"	E' 16"
10-30-90	8.5006	8.5000	8.4998	8.4995	8.4994	8.5008	8.5024	8.5025	8.4996	8.4984
3-28-91	8.5001	8.5002	8.4998	8.4994	8.4983	8.5014	8.5081	8.5078	8.4999	8.4984
Difference	-0.0005	0.0002	-0-	-0.0001	-0.0001	0.0006	0.0057	0.0053	0.0003	-0-

NEW

DIMENSION SHEET 23

DATE	INJECTOR OPENING PRESSURE PSI PAGE 1019 LIMIT ~~1400~~ 600		CLEAN & CHECK INJECTOR TIPS INITIAL WHEN COMPLETE PAGE 1017		PEE-PIPE CHECK INITIAL WHEN COMPLETE PAGE 831		INSTALL NEW LUBE FILTER	AIR FILTER SERVICE	LFE	
	RIGHT	LEFT	RIGHT	LEFT	RIGHT	LEFT	INITIAL	INITIAL		
	SERIAL NO.	SERIAL NO.	✓	✓	✓	✓	✓	✓		

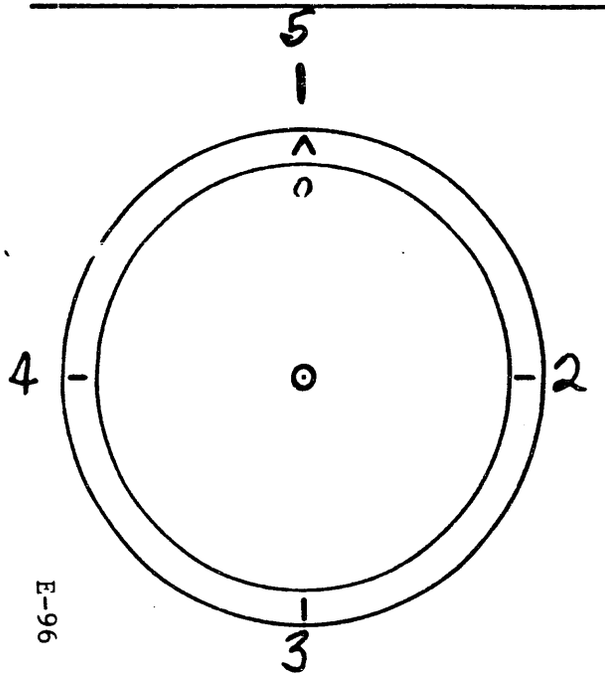

E-96

NOTE: ALL ANGLES START AT THE "V" MARK AND EXTEND CLOCKWISE AROUND THE PISTON CROWN.

#2 L Ring @ 320° from Piston I.D. MARK. ALL OTHER RINGS OK.

#2 R STUCK COMPLETLY ALL OTHER RINGS OK

RING GAP POSITIONS	DATE	RIGHT RING NO. 1	2	3	4	5	LEFT RING NO. 1	2	3	4	5
	11-1-90	0°	90°	180°	270°	0°	0°	90°	180°	270°	0°
	3-18-91	325°	250°	245°	160°	90°	65°	230°	285°	160°	270°
			PISTON					PISTON			
	11-1-90	* INSTALLED		—	0°			* INSTALLED		—	0°
	3-18-91	REMOVED		—	45°			REMOVED		—	160°

* PISTON INSTALLED WITH I.D. MARK FACING TOP OF LINER TOWARDS EXHAUST SIDE.

EMD TEST NO. _____

TEST PART WEIGHTS, GRAMS

Camshaft Bearings

	Date	Right Front	Left Front	Right Rear	Left Rear
0 hours					
300 hours					

Pin Bearings

	Date	Right	Left
0-hours	11-14-90	508.40	509.65
300 hours	3-19-91	507.47	508.60

Thrust Washers

	Date	Right	Left
0 hours	11-14-90	715.62	715.33
300 hours	3-19-91	714.12	712.82

TEST PART DIMENSIONS, INCHES

Piston Pin Diameter (Parallel to Threaded Holes)

		Date	Pee Hole End	Center	Opposite End
Right	0-hours	11-14-90	3.6845	3.6845	3.6845
	300 hours	3-19-91	3.6850	3.6849	3.6849
Left	0-hours	11-14-90	3.6840	3.6840	3.6839
	300 hours	3-19-91	3.6843	3.6843	3.6843

Pin Bearing Clearance in Carrier

		Date	Pee Hole End	Center	Opposite End
Right	0 hours	11-14-90	.010	.013	.016
	300 hours	3-19-91	.009	.013	.016
Left	0-hours	11-14-90	.009	.010	.013
	300 hours	3-19-91	.007	.008	.013

APPENDIX F

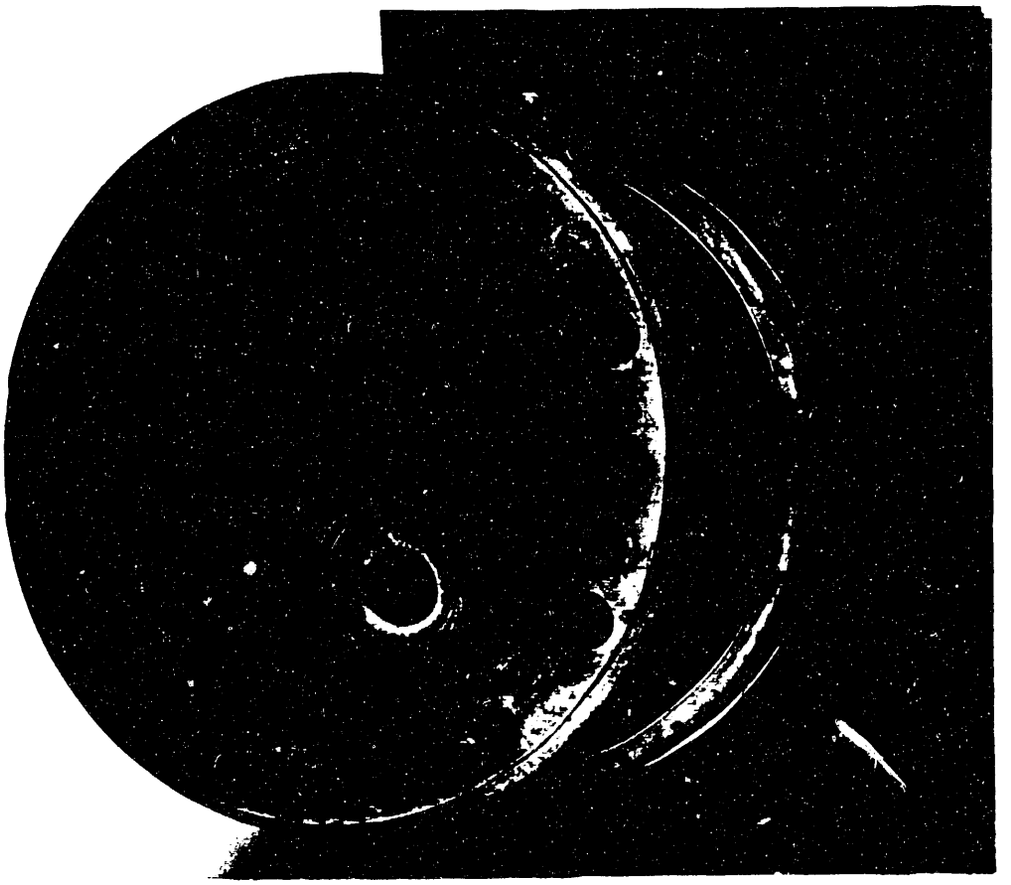

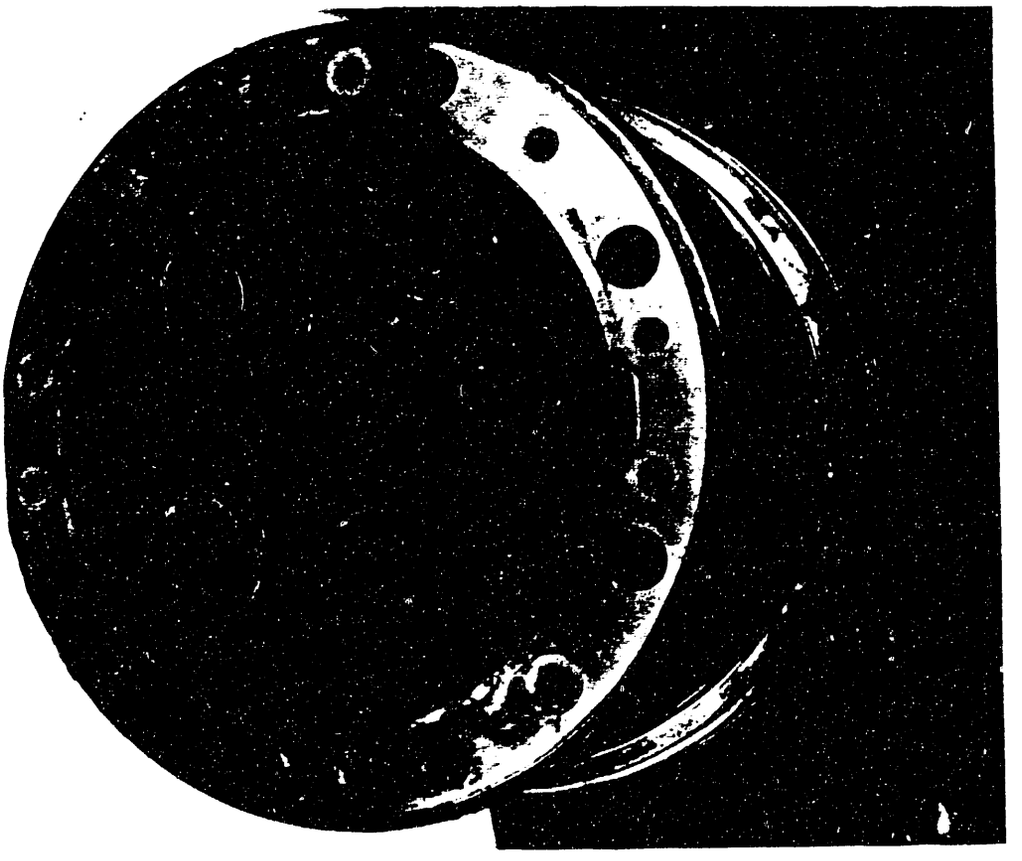

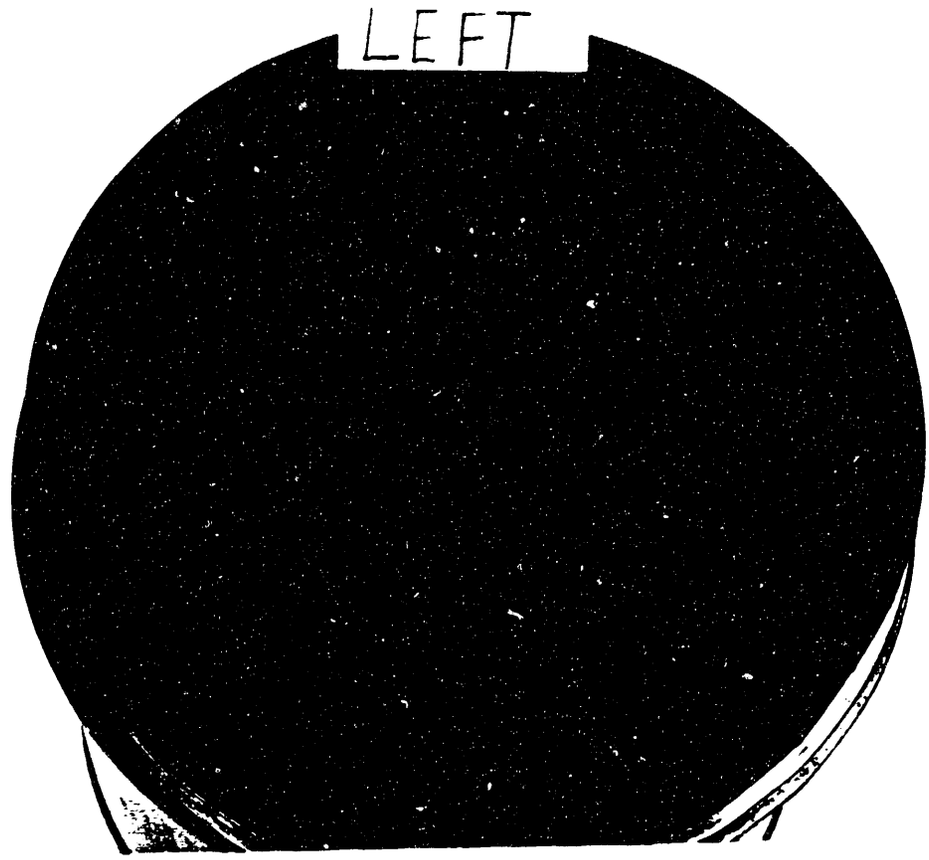
LEFT

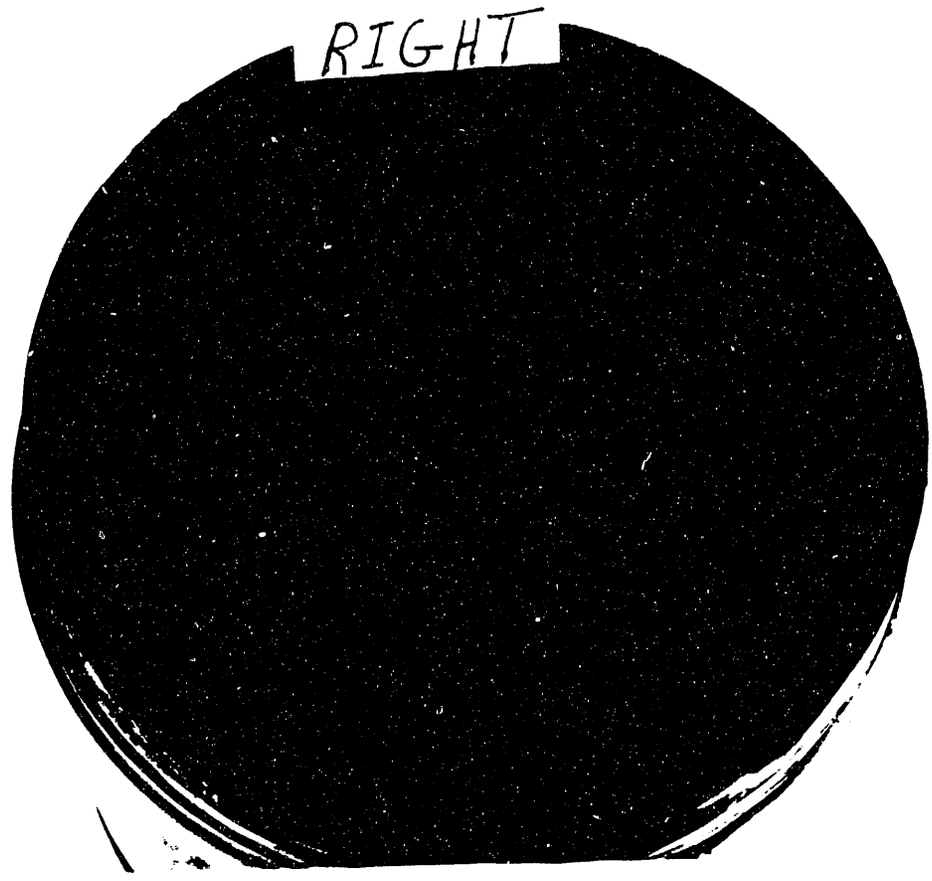
RIGHT

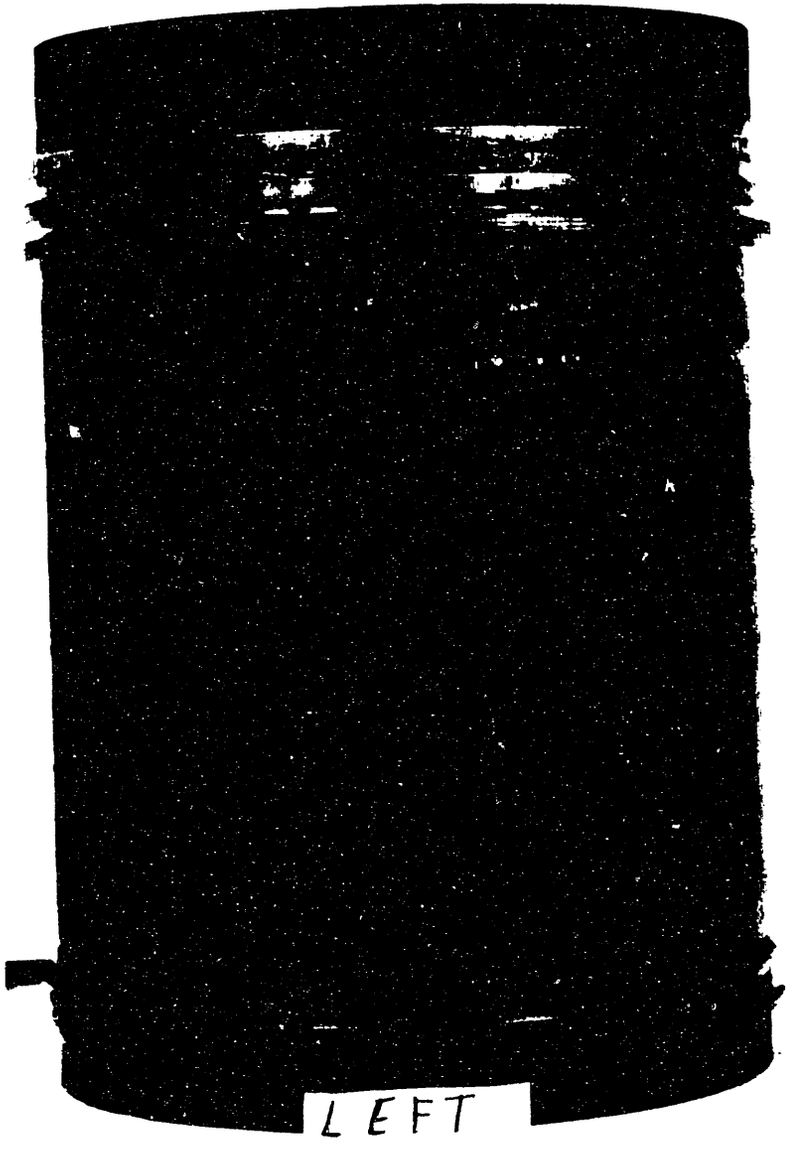
LEFT

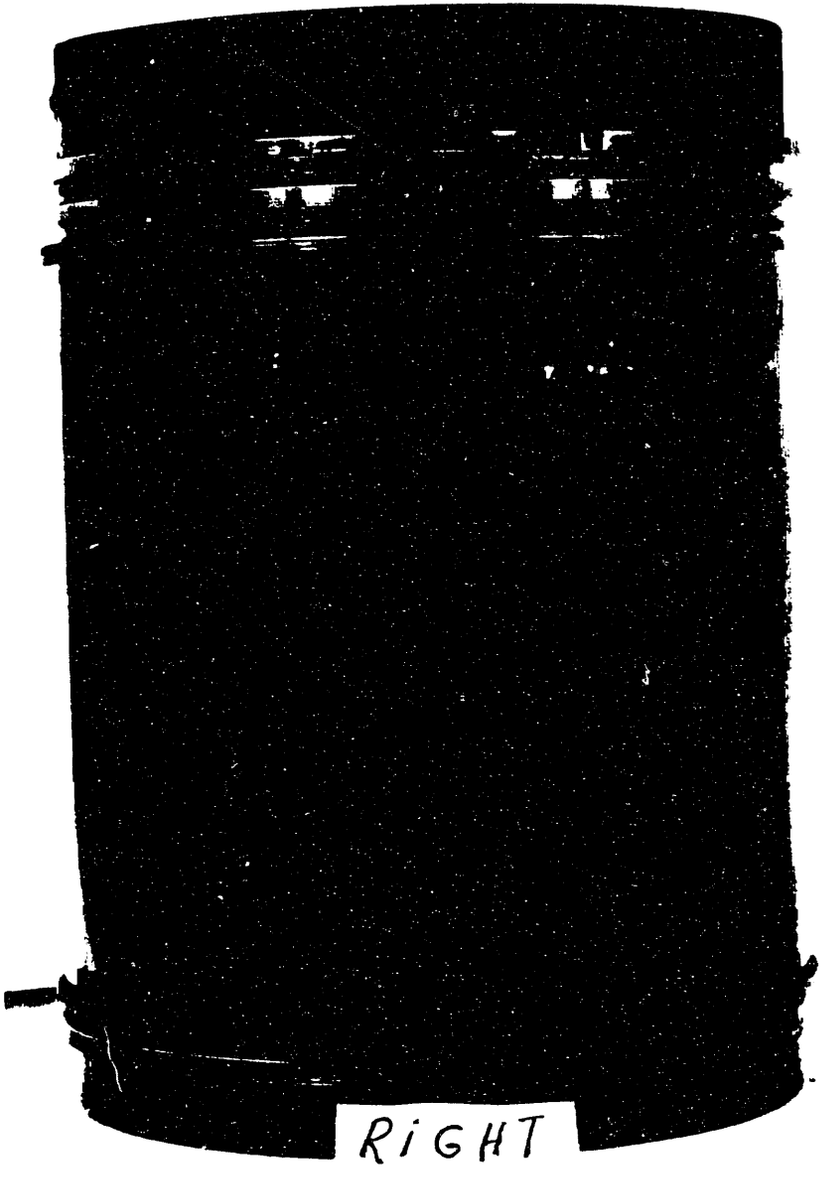
RIGHT

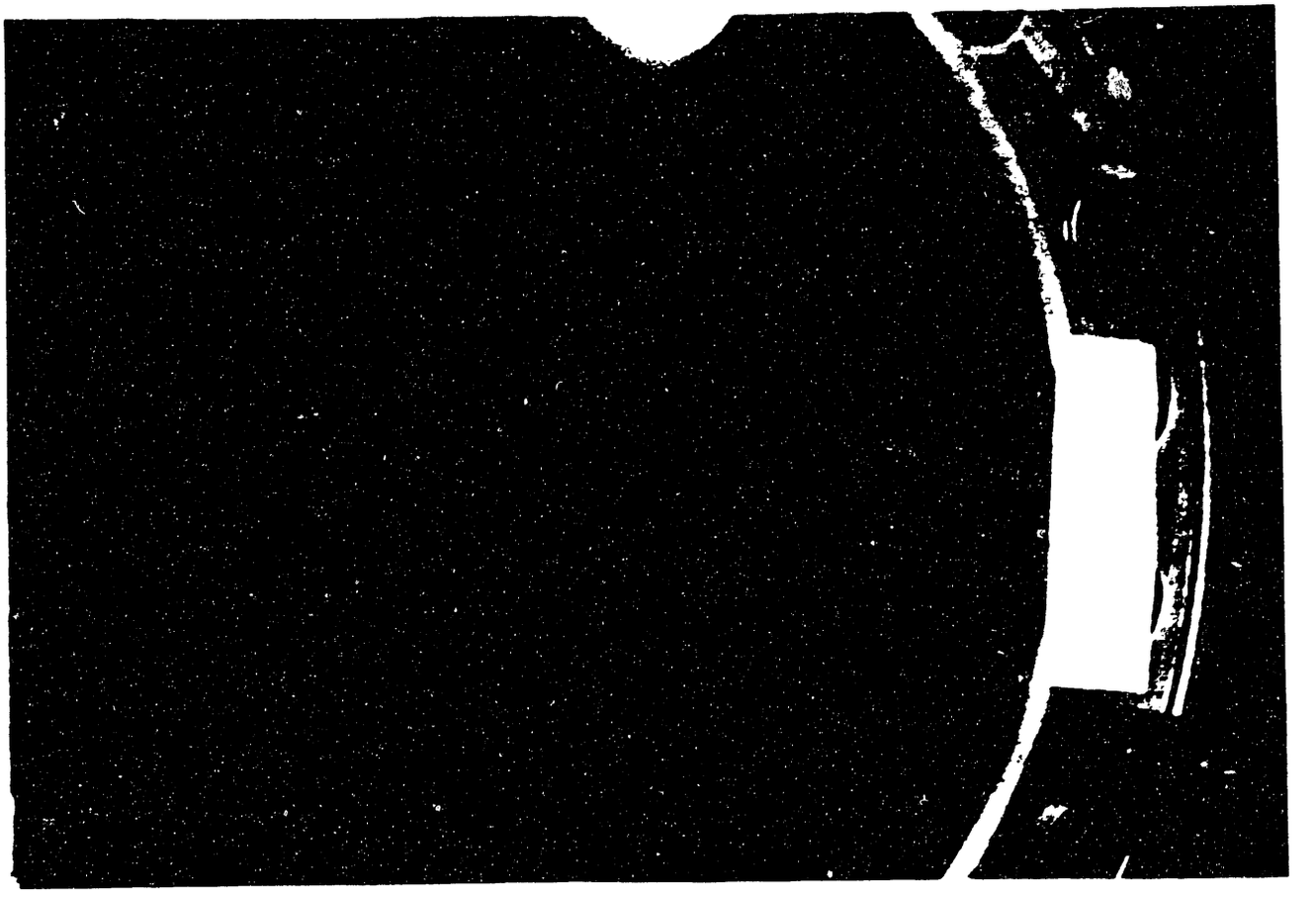

LEFT

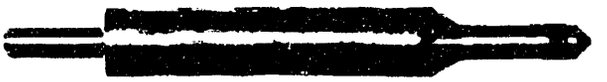

RIGHT

END

DATE
FILMED
5/11/92